Three-Dimensional Displacement Mapping of Carbon Fibre Bicycle Frames using Digital Image Correlation

By

Juan Miguel Celeste Laurea

A thesis submitted for the degree of

Bachelor of Engineering (Mechanical) (Honours), Master of Engineering (Biomedical)

Academic Supervisor: Professor Mark Taylor

Industry Supervisor: Mr. Andrew Warr

Submitted to the College of Science and Engineering in fulfilment of the requirement for the degree of Bachelor of Engineering (Mechanical) (Honours), Master of Engineering (Biomedical) at Flinders University – Adelaide, Australia

Declaration of Originality

I certify that this work does not incorporate without acknowledgment any material previously submitted for a degree or diploma in any university; and that to the best of my knowledge and belief it does not contain any material previously published or written by another person except where due reference is made in the text.

Signed: _____ 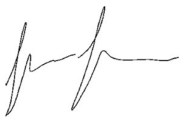 _____ Date: _____04/06/2018_____

Acknowledgements

I would like to acknowledge my two supervisors Professor Mark Taylor from Flinders University, and Mr. Andrew Warr from Cycling Australia for their knowledge and patience throughout this project. Their high technical skills made some aspects of this project a little easier.

Secondly, thank you to Richard Stanley for helping providing feedback and construction aid for the testing rig design. Also, Craig Peacock and Craig Dawson for their helping on aspects within this project.

Finally, I would like to thank my family and friends for their support throughout the span of this project.

Abstract

The investigation of three carbon fibre bicycle frames using Digital Image Correlation (DIC) was conducted to provide a full-field assessment of these structures. Literature research for this project found finite element analysis (FEA) and strain gauges to be common methods of testing bicycle frames, however, the use of DIC was limited. Therefore, using this measurement tool may offer a new approach to obtaining the lateral and vertical displacement values for bicycle frames. Research showed that using DIC enabled a comprehensive measurements of full field displacements on a bicycle frame, which was not easily achieved with strain gauges and FEA required laboratory testing to confirm its findings.

The bicycle frames tested were designed to suit sprint cycling conditions, hence, a testing rig was created to emulate these parameters. The design was mainly inspired from an international standard (ISO 4210-6), however, modifications were made to create to suit static testing conditions. These were to implement multiple crank angles (90^{O} – 180^{O}) during the downstroke phase cycling as this area has the highest loads applied, and applying 266 N.m (Korff et al. 2007; Martin et al. 2006).

A testing and post-processing protocol was developed to obtain the displacement values, consistently. There were several investigations involved; one to find locations of high displacement, the second was to observer if the displacement changed as the crank angle changed, and finally, a comparison between bicycle frame designs.

The results found that vertical displacement for all bicycle frames was the same, regardless of the crank angle, however, the development of these displacements was different along each section of the bicycle frame. All three bicycle frames showed high lateral displacement at the seat tube, down tube, and chain stays near the bottom bracket, as the load increased. As well, it was found that lateral displacement changes as crank angle changes.

Comparison between the left-hand side (LHS) and right-hand side (RHS) of a single bicycle frame design (CA01) showed differences in lateral displacement. Moreover, the comparison of two bicycle frames with the same design (CA01 and CA02) also showed considerable differences. These differences in lateral displacement may have be caused by the manufacturing process. Two bicycle frames with different designs, CA01 and AR01, were compared to observe which bicycle frame was stiffer. It was found that the AR01 design deflected less than the CA01 design during testing. Therefore, the AR01 design may be preferable for sprint cycling based in terms of its stiffness properties. AR01 may be stiffer because of its design, how the carbon fibre was layered, or the curing method (Bie et al. 2017; Chang et al. 2017; Rahmani et al. 2014).

Table of Contents

Table of Figures

Table of Tables

1 Introduction

Elite-level sprint cycling in the Olympic Games requires bicycle frames to have a high stiffness-to-weight ratio. Bicycle frames with low stiffness-to-weight ratios produce unwanted displacement at certain areas along the bicycle frame. This displacement may cause the athlete to be less efficient as they cycle, hence, identifying these areas becomes beneficial for newer designs as improving these sections may improve the efficiency of the athlete. Parts of the bicycle frames are may produce unwanted displacement (Figure 1). Digital image correlation (DIC) was used in this project to measure these unwanted displacements because it has the ability to undergo a full-field assessment of the bicycle frame structure in a laboratory environment.

This thesis presents the structural analyses of three carbon fibre bicycle frames that was tailored for velodrome cycling and aims to identify the areas of unwanted displacement. There are different sprint cycling specialisations contested in the Olympic Games. These are sprint, team sprint, keirin, and omnium cycling (Union Cycliste Internationale 2018). These athletes exert a large amount of power when cycling (Gardner et al. 2007; Dorel et al. 2005). This, in turn, exerts large loads along the bicycle frame and may produce unwanted displacement. Replicating these loading conditions similar to these athletes may identify the areas that experience unwanted displacement. Therefore, a testing rig was created to produce the similar loading conditions these athletes exert onto these bicycle frames.

This project explored previous literature which details the parameters that affect the stiffness for these bicycle frames, derived cycling parameters that were later implemented on the testing rig, previous testing rigs from literature, and different measurement techniques. The following section show the requirements, conceptualisation and final design of the testing rig for this project. The methodology section details the testing and post-processing protocols created to obtain results. The results are then interpreted in the discussion, which includes an interpretation of their meaning and limitations of the project. Lastly, in the conclusion, the major findings of the project are discussed as well as the project's potential direction in the future.

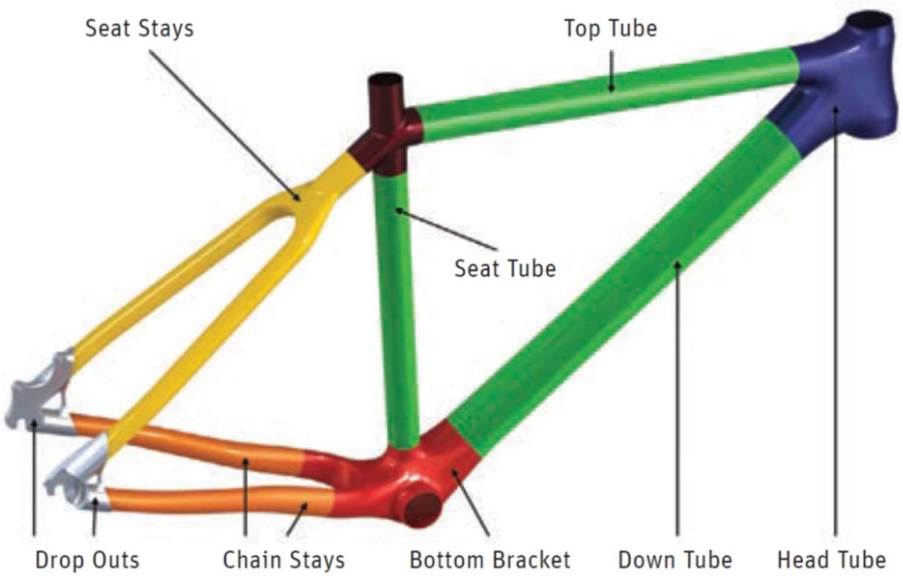

Figure 1: Bicycle Frame Naming Convention of Each Part (Tara 2017)

1.1 Carbon-Fibre Bicycle Frames Tested

There were three carbon-fibre bicycle frames tested for this study which were CA01, CA02, and AR01, and all had the frame size of 57 cm (Figure 2). CA01 and CA02 are the same brand of bicycle frame, which means that they were based on the same design. AR01, however, has a different design compared to the CA design. The whole design of AR01 was different to the CA design, as they are different brands. These three bicycle frames were compared to each other to assess if there were differences in displacement values.

Figure 2: Carbon-Fibre Bicycle Frames CA01, CA02, and AR01. CA01 and CA02 have the Same Design, and AR01 has a Different Design.

2 Literature Review

The intended goal of this project was to measure the displacements of carbon fibre bicycle frames while applying cyclist loads at the bottom bracket. Furthermore, a method of measuring displacement must be used to identify areas of low stiffness in the bicycle frame designs. A review of previous relevant literature is covered in this section and includes topics such as parameters of a bicycle frame that affect stiffness, previous testing rigs used in studies and methods of measuring displacement. Cycling-related parameters such as maximum power and torque outputs, and the relationship between the load and crank angle during cycling were covered to obtain suitable boundary conditions for the testing rig.

2.1 Bicycle Frame Stiffness Parameters

Advancements in bicycle frame designs aim to improve their stiffness-to-weight ratio and focus on the optimisation so that less deflection occurs under sprint cycling conditions. A bicycle frame with an ideal stiffness-to-weight ratio will enable greater power transfer when the cyclist is pedalling (Usamentiaga et al. 2017). There are two parameters that affect the stiffness properties of bicycle frames, and these are the materials that are used and the frame geometry. Materials must have a high stiffness-to-weight ratio. Materials chosen must have high stiffness properties while the design must be optimised to withstand loading exerted by the cyclist. Bicycles, especially the frames, undergo a combination of tension, bending, compression, and torsional loading conditions (Froes et al. 1988; Vandermark 1997). Since bicycle frames rely on the two parameters mentioned above, it can be difficult to determine whether it is the material or the design that causes displacement on different sections of the frame. The following sections (Sections 2.1.1 and Section 2.1.2) further detail which materials are considered, and how the structure affects the overall stiffness of bicycle frames, respectively.

2.1.1 Bicycle Frame Materials

There are a number of materials considered when designing a bicycle frame, but all have one characteristic in common, which is a high stiffness-to-weight ratio. The materials used in bicycle frames are titanium (Section 2.1.1.1), aluminium (Section 2.1.1.2), and carbon-fibre composites (Section 2.1.1.3). Since this study assesses carbon-fibre bicycle frames, this section examines the common materials chosen including carbon-fibre and why they are favourable. The following section covers the materials and a comparison between the three is made based on their properties.

2.1.1.1 Titanium

Titanium alloys are commonly chosen for manufacturing bicycle frames due to their high material stiffness properties. One alloy that is often considered is Ti6Al4V because of its high stiffness and fatigue strength compared to Aluminium Al6061. This titanium alloy has an elastic modulus of 110 GPa and 530-630 MPa compared to aluminium's 69 GPa and 96 MPa (ASM International 2001; Niinomi 1998). Hence, titanium's stiffness-to-weight ratio is higher compared to another commonly-used material aluminium.

Arola et al. (1999) utilised a static test for a bicycle that used Ti6Al4V for the top tube, down tube and seat tube, applying a 910 N vertical load downward from the bottom bracket, however, the crank angle is unknown. Applying a strain rosette on the down tube near the head tube region, they found low strain values with a magnitude of 100 $\mu\varepsilon$.

Since Ti6Al4V has a high elastic modulus, the result obtained was expected. If testing a bicycle frame made of titanium, the displacement when undergoing load would be low because of its high stiffness properties. Compared to aluminium and carbon fibre composites, Ti6Al4V is higher in density at 4.43 g/cm^3 (ASM International 2001). If the same frame design is manufactured using each of the three materials, the titanium frame would be the heaviest. Hence, designing a bicycle frame solely of titanium to improve frame stiffness may not be viable due to the corresponding increase in weight.

2.1.1.2 Aluminium

Aluminium, specifically Al6061, is another common material due to its high stiffness-to-weight ratio and good manufacturability having an elastic modulus of 69 GPa (Rontescu et al. 2015; ASM International 2001; Arola et al. 1999). Moreover, the density of Al6061 is low compared to Ti6Al4V with it being 2.70 g/cm^3, compared to titanium's 4.43 g/cm^3. Aluminium's low density allows good manufacturability of parts, such as bicycle frame tubes. This material can produce a structurally effective tube diameter while higher density materials may be limited (Nelson 2003; ASM International 2001). However, if tube sizes were the same and underwent the same loading conditions, Al6061 will deflect more because of its relatively low stiffness properties compared to titanium Ti6Al4V.

2.1.1.3 Carbon Fibre

Carbon fibre/epoxy resin composite is another material used for bicycle parts but also has a property not shared by Ti6Al4V and Al6061 mentioned above. This material behaves as an anisotropic material, which means the material's stiffness properties differ depending on the direction of loading. For unidirectional carbon fibre, if the force exerted is parallel to the fibre grain (in-plane), then the material

will displace less compared to a force with the same magnitude orthogonal to the fibre grains (out-of-plane) (Minus & Kumar 2005; Hashin 1983).

Bie et al. (2017) showed this behaviour by testing T700 uniaxial carbon fibre/epoxy at ten off-axis angles. These specimens underwent tension tests, and the strain fields were measured using synchrotron x-ray DIC and computerised tomography. The results show that higher off-axis angles (16^{O}-90^{O}) demonstrated remarkably lower stiffness properties compared to ones with lower off-axis angles (4^{O}-13^{O}) (Figure 3).

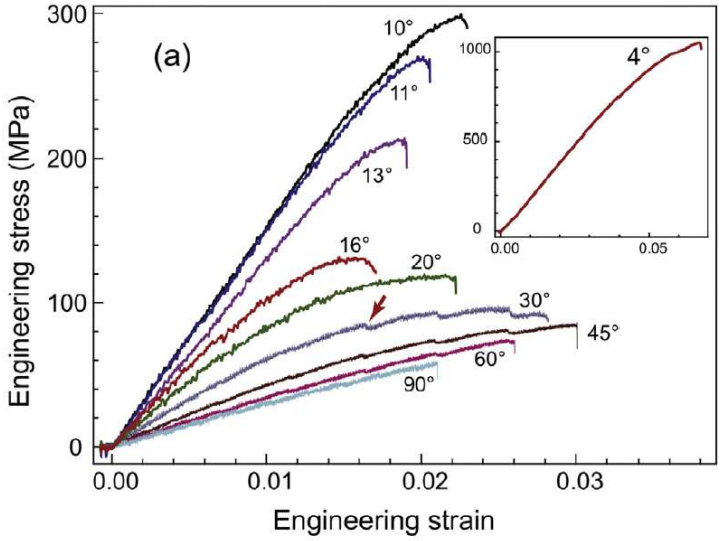

Figure 3: The Change in Uniaxial Carbon fibre/Epoxy Composite Properties When Tested at Off-Axis Angles. As the Angle Increases, Tensile Properties Decrease (Bie et al. 2017)

Regarding using uniaxial carbon fibre as a material for bicycle frames, anisotropy must be kept in mind because of it varying degrees of stiffness which leads to unwanted deflection. However, layering carbon fibre at different orientations improves the stiffness when there are loads applied in different directions and, an example of this is shown in Figure 4 below (Rahmani et al. 2014).

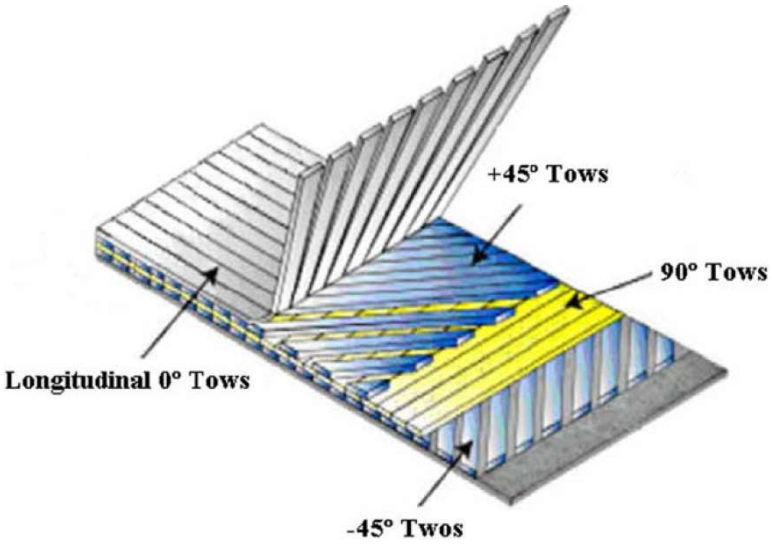

Figure 4: Example of Carbon Fibre Fabric Layering at Different Orientations (Rahmani et al. 2014)

A study on the material properties of layered carbon fibre was conducted by Rahmani et al. (2014) which investigated 14 different combinations (Table 1) that varied in orientation, number of layers, and fibre content. It was noted that all 14 combinations showed higher tensile properties when compared to uniaxial carbon fibre (Table 2), with LY60/4 being the highest elastic modulus and tensile modulus of 2.55 GPa and 135 GPa, respectively. The properties of carbon fibre heavily depend on the fibre content. Samples with 60% fibre content showed superior mechanical properties when compared to those with a 40% fibre content specimens regardless of the orientation and number of layers.

Table 1: Carbon Fibre Composites Tested from Rahmani et al. (2014)

Treatment code	Angle-ply (°)	Number of plies	Fiber content (%)
LY60/1	0,90,0	3	60
LY60/2	0,35,0	3	60
LY60/3	90,45,90	3	60
LY60/4	0,-35,0,+35,0	5	60
LY60/5	+35,-35,0,+35,-35	5	60
LY60/6	+35,-35,0,-35,+35	5	60
LY60/7	0,90,0,90,0	5	60
LY40/1	0,90,0	3	40
LY40/2	0,35,0	3	40
LY40/3	90,45,90	3	40
LY40/4	0,-35,0,+35,0	5	40
LY40/5	+35,-35,0,+35,-35	5	40
LY40/6	+35,-35,0,-35,+35	5	40
LY40/7	0,90,0,90,0	5	40

Table 2: Material Properties of Carbon Fibre Composites from Rahmani et al. (2014)

Sample code	Tensile strength (MPa)	Tensile modulus (GPa)	Elongation at break (%)	Flexural strength (MPa)	Flexural modulus (GPa)	Izod impact strength (J/m)
LY60/1	1117	65.5	1.66	1016	45.7	2.2
	(102)	(6.1)	(0.12)	(69)	(30)	(0/07)
LY60/2	1004	60.6	1.59	822	55.6	3.5
	(62)	(7.5)	(0.10)	(78)	(3.3)	(0.12)
LY60/3	20	6.8	0.32	56	2.4	2.8
	(8)	(2.3)	(0.12)	(18)	(1.0)	(0.71)
LY60/4	1114	87.4	1.35	1084	57.6	9.2
	(61)	(4.3)	(0.22)	(21)	(1.8)	(0.6)
LY60/5	633	46.0	1.92	555	26.6	5.2
	(31)	(4.2)	(0.11)	(71)	(2.4)	(1.0)
LY60/6	575	48.7	1.58	466	26.4	9.73
	(47)	(9.5)	(0.19)	(92)	(3.0)	(0.56)
LY60/7	767	53.9	1.36	754	46.0	6.8
	(62)	(3.2)	(0.12)	(72)	(1.6)	(1.24)
LY40/1	329	27.5	1.04	525	28.5	2/1
	(56)	(2.6)	(0.20)	(103)	(1.1)	(0.4)
LY40/2	1017	73.4	1.25	1110	51.9	2.2
	(82)	(4.8)	(0.15)	(103)	(2.4)	(0.69)
LY40/3	20	6.8	0.29	140	4.1	2.8
	(2)	(0.5)	(0.05)	(94)	(2.8)	(0.28)
LY40/4	1059	79.5	1.33	996	48.0	5.5
	(90)	(3.1)	(0.11)	(107)	(1.3)	(0.36)
LY40/5	518	45.7	1.49	535	22.6	4.5
	(44)	(5.9)	(0.12)	(84)	(3.1)	(1.05)
LY40/6	544	46.7	1.71	118	23.6	6.8
	(264)	(4.3)	(0.16)	(62)	(1.4)	(0.24)
LY40/7	1058	59.0	1.63	769	40.4	5.2
	(23)	(2.8)	(0.03)	(61)	(1.7)	(0.19)

Numbers in the parentheses are standard deviations.

The curing process of carbon fibre also affects the material properties, with one common process being autoclaving, which is the application of a certain temperature and pressure to the layered sheets of carbon fibre and epoxy. The material properties of these composites depend on the curing cycle, and if it is poorly cured, voids between the sheets can occur which decreases the inter-laminar shear strength (ILSS). Autoclaving at high pressures can decrease the number of voids which increases the ILSS (Chang et al. 2017; Ho, Sasayama & Yanagimoto 2017).

Carbon fibre composites are a favourable material for bicycle frames because as layering sheets provides a level of customisability. Since this study examines three carbon-fibre bicycle frames in a laboratory testing environment, layering and curing of the carbon fibre for the CA and AR design may be different The ability of layering sections differently offers more choice compared to the metallic options mentioned above. This material allows for the removal of sections that experience low or negligible loads and added to areas experiencing high loads, keeping the weight at a constant while improving the stiffness properties. Hence, carbon-fibre may be used in sprint cycling because of its high level of customisability.

2.1.2 Bicycle Frame Structure

Although stiffness relies on the material chosen, it is also dependant on the structure of the bicycle frame. When improving the stiffness of the bicycle frame design, the frame must withstand the loading produced by the cyclist which is a combination of tension, compression, bending, and torsional loading along the whole structure (Froes et al. 1988). Therefore, an appropriate design of the bicycle frame is required to prevent unwanted deflection (Covill et al. 2015, 2014; Baumgart & Cordey 2001). Two parameters must be factored in for bicycle frame designs, the lateral stiffness and vertical compliance. The main area of interest in this study was to investigate these displacements on the tube sections linked to the bottom bracket, and the bottom bracket itself.

Bicycle frame designs with high lateral stiffness can transfer the power more efficiently from the athlete compared to another design with lower lateral stiffness. Having a torsionally stiff bottom bracket and head tube is favourable. Moreover, having reasonable vertical compliance offers athletes a comfortable ride (Covill et al. 2014; Lessard, Nemes & Lizotte 1995). Covill et al. (2014) have done a parametric study on how top tube and seat tube lengths affect the lateral and vertical displacement (Figure 5). It was found that longer length tubes produced higher lateral displacement and lower vertical displacement. This is a disadvantage to longer-limbed athletes because a bicycle frame made for their stature may deflect more laterally; and therefore, having a bicycle that is less efficient when cycling.

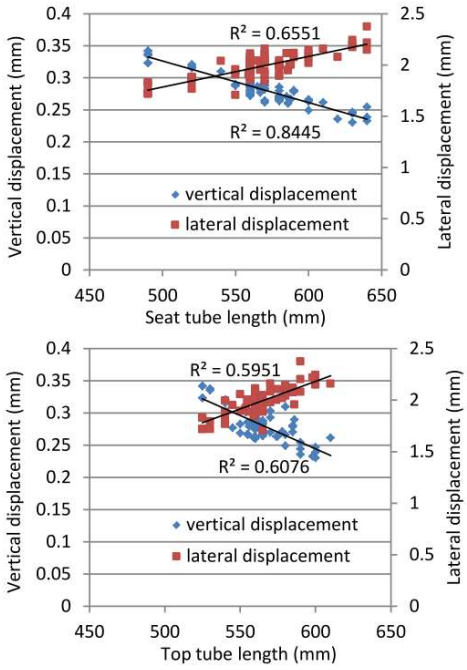

Figure 5: Vertical and Lateral Displacement of Seat Tube and Down Tube. As the Length of the Seat Tube and Top Tube Increases, Lateral Displacement Increases while Vertical Displacement Decreases (Covill et al. 2014)

Another factor that affects lateral stiffness and vertical compliance are tube sizes at different sections of bicycle frames. Covill et al. (2015) tested bicycle frame tube sizes utilising similar load cases by Maestrelli and Falsini (2008). It was found that tubes with a higher second moment of area (in mm^4), both the lateral and vertical displacement lowered with the top tube, down tube and seat stay improving the most (Figure 6). Since this study mainly focuses on applying load onto the bottom bracket, the down tube will be closely investigated when testing because of it being attached to the bottom bracket.

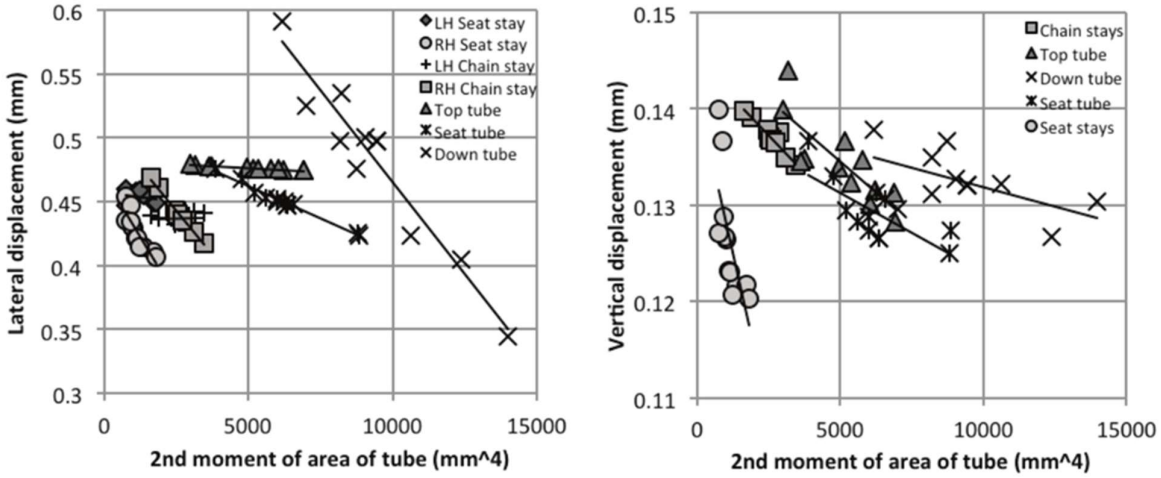

Figure 6: Lateral Displacement (Left) and Vertical Displacement (Right) vs. Second Moment of Area. Both Properties Decrease as the Second Moment of Area Increases (Covill et al. 2015)

Further research showed common sections of the bicycle frame that show high areas of stress (or strain) near the bottom bracket when emulating cycling. The seat tube, down tube, and chain stay near the bottom bracket are areas of high stress / strain (Covill et al. 2016; Manolova & Bertucci 2011). Using finite element analysis (FEA), Covill et al. (2016) found these areas mentioned above to have high stress values when utilising boundary conditions that emulate climbing and out of the saddle. Manolova & Bertucci (2011) also found similar results but through experimental analysis using a laboratory test simulating cycling torques. Maestrelli and Falsini (2008) had similar testing conditions as Covill et al. (2016), but measured lateral and vertical displacement. The highest lateral displacement (change in the z-direction) was found on the bottom bracket (red) while cycling out of the saddle (Figure 7).

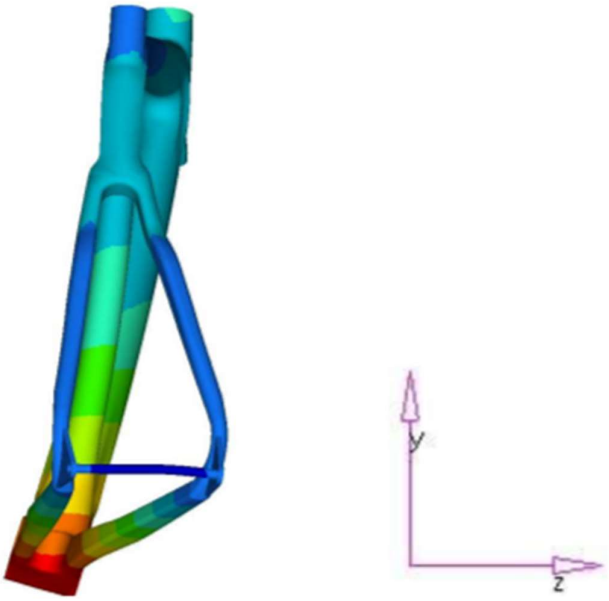

Figure 7: Lateral Deformation Profile with the Bottom Bracket Showing the Highest Lateral Displacement (z-axis) (Maestrelli & Falsini 2008)

The lateral displacement and vertical compliance of bicycle frames rely on the tube length, and its second moment of area (Covill et al. 2015, 2014). Increasing the length of the tubes improve the comfort of the ride, however, lowers the lateral displacement and affects the efficiency of the bicycle frame (Covill et al. 2014). Increasing the second moment of area lowers both lateral and vertical displacement, which can improve the efficiency of the athlete (Covill et al. 2015). However, more material or changing the geometry of the tube is required to increase the second moment of area, which may increase the weight or complexity of the design. Furthermore, altering the length and second moment of area may be limited as the geometry of the rider must be taken to consideration. Hence, altering the tube length and geometry affects the displacement values, however, these two properties may be limited in modification as the geometry of the athlete and the weight of the bicycle frame must be considered.

For this study, the investigation of lateral and vertical displacement of the whole bicycle frame while emulating cyclist loads on the bottom bracket. This study aims to find the lateral and vertical displacement of whole bicycle frames emulating cycling conditions. At the time of this study, there was limited literature on investigating the lateral and vertical displacement for whole bicycle frames, therefore, limiting comparisons with literature. However, common areas of high stress / strain was shown to be at the seat tube, down tube, and chain stays, near the bottom bracket. Furthermore, Maestrelli and Falsini (2008) found high lateral displacement when applying cyclist loads near the bottom bracket. Therefore, applying the load on the bottom bracket may cause the bottom bracket to deflect.

2.2 Bicycle Frame Loading Parameters Based on Cyclist Biomechanics

The purpose of the testing rig created for this project was to emulate the similar loading conditions as sprint cyclists, specifically, the forces applied on the bottom bracket. A set of parameters were identified such as the magnitude of crank torque relative to the crank angle in Section 2.2.1, and high torque output in Section 2.2.2. These parameters were later considered when designing the testing rig. Identifying which crank angles were producing the highest loads and the highest torque produced by sprint cycling athletes was imperative to the testing rig design.

2.2.1 Relationship Between Crank Torque and Crank Angle

During cycling, there is a change in crank torque depending on the crank angle. Korff et al. (2007) show that the highest torques produced, regardless of the pedalling conditions, is during the downstroke, which is from 0^O – 180^O crank angles (Figure 8). Bini & Carpes (2014) and Dorel et al. (2010) both show similar profiles but measured effective force rather than crank torque. The effective force, which is the force that is tangential to the bicycle crank, is the load that is translated as velocity on the wheels. This force is a fraction of the total force applied to the crankset only being 40% – 60 % (Bini & Carpes 2014). The effective force can be converted into crank torque if the crank length is known.

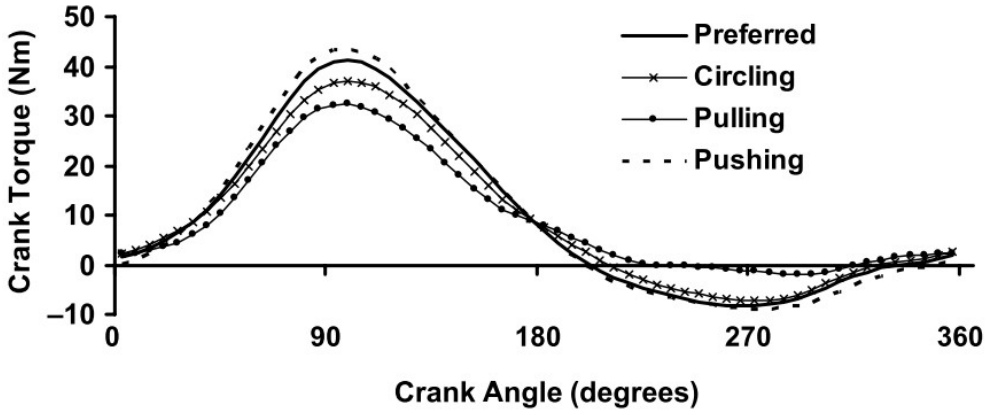

Figure 8: Torque Profiles For Different Pedalling Conditions. The Downstroke Phase (0^O – 180^O) has the highest loads applied to the Crankset (Korff et al. 2007)

As found in previous literature (Section 2.2.1), the downstroke phase during cycling produces the highest loads ranging from 0^O – 180^O. Hence, the highest crank torques are produced within this range, and this parameter later became a part of the specification for the testing rig.

2.2.2 Elite Velodrome Cyclist Power and Torque Outputs

Cycling is an exercise that translates the effort from the lower limb muscles applied to the crank to generate movement. For elite velodrome sprint cyclists, the anaerobic system of metabolism is more dominant because of its short interval of time. This type of exercise consumes muscle and liver glycogen to generate power without the need for oxygen (Katch, McArdle & Katch 2013; Jeukendrup, Craig & Hawley 2000).

On average, the maximal power output from cyclists range from 1600W – 1792W and strongly correlates to cycling torque (Gardner et al. 2007; Dorel et al. 2005). Therefore, higher production of power will produce higher torque as shown in (Figure 9) below. Hence, the torque range that correlates with the previously stated power range is from 266 N.m – 235.7 N.m (Gardner et al. 2007; Dorel et al. 2005).

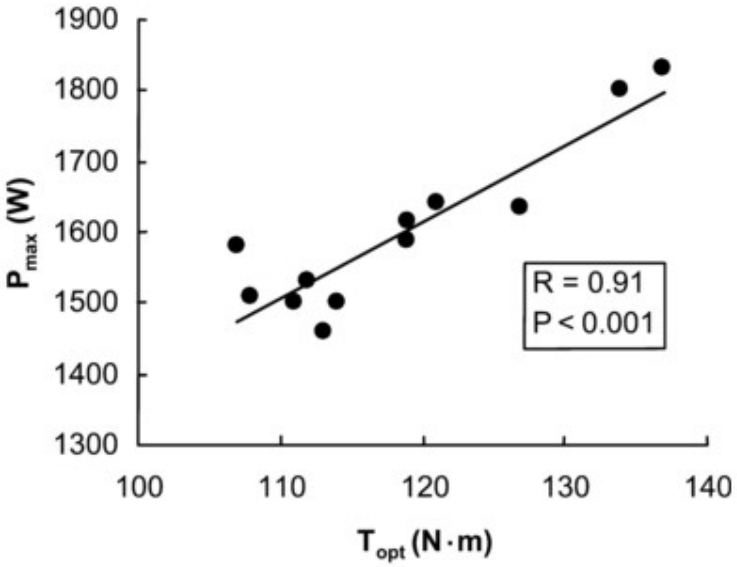

Figure 9: Maximum Power- Optimum Torque Relationship. As Power Increases, the Torque Output Increases (Dorel et al. 2005)

If the peak torque is applied to the bottom bracket at the angles that relate to the downstroke, this will produce the 'worst case' scenario and may display the areas of high displacement testing the carbon fibre bicycle frame. Therefore, 266 N.m was chosen as a design requirement for the testing rig design.

2.3 Testing Rig Inspirations

For this project, a testing rig was required to apply loads similar to what elite sprint cyclists apply. This section covers testing rigs from literature and one standard that inspired the testing rig design (Section 3).

2.3.1 ISO 4210-6 'Fatigue Test with Pedalling Forces'

ISO 4210 -6 is standard that describes a testing rig used for fatigue testing of bicycle frames. The force F_1, which is 1100 N for racing bicycles, is applied dynamically at a 7.5^O angle, which simulates pedalling forces. Shown in Figure 10 below, is the provided diagram of the standard (International Organization for Standardization 2015). This design from ISO 4210-6 aims to closely emulate dynamic cycling conditions. However, this testing rig is designed to test fatigue life of bicycle frames, which makes this design advantageous compared to the other testing rig designs mentioned later. Furthermore, implementing the design parameters mentioned above (Section 2.2) may be simpler as small modifications are required compared to the Bar System or Bicycle Frame Test Fixture. However, there was potential risk of overcomplicating the testing rig system. Hence, this risk must be accounted when creating this testing rig.

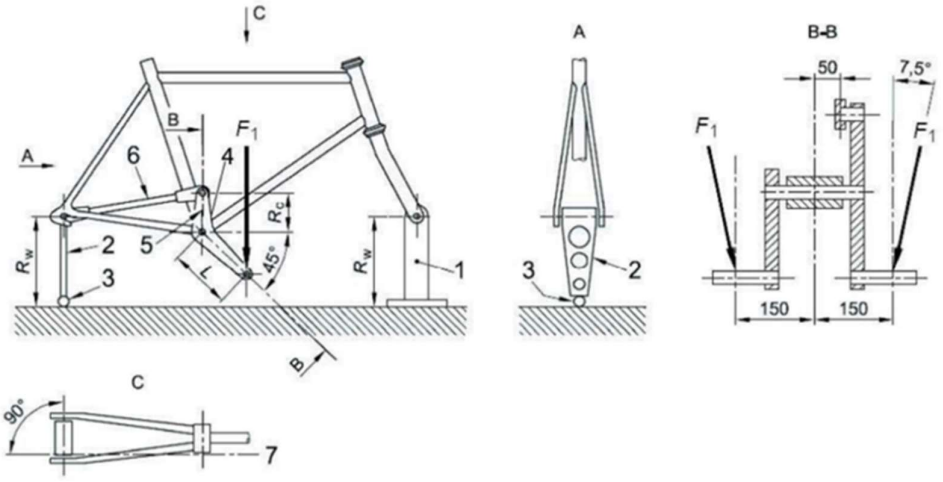

Figure 10: Testing Rig Setup for Fatigue Testing with Pedalling Forces (International Organization for Standardization 2015)

2.3.2 'Bar System'

Manolova et al. (2015) and Manolova and Bertucci (2011) used a testing rig that simulates pedalling forces. The 'Bar System' used two steel bars welded together to simulate the crank arm and pedal as shown in Figure 11 below. These two bars are long in order to amplify the moment produced when using low weight and simulated forces from 40 N - 880 N only using 1-18 kg weights. (Manolova et al. 2015; Manolova & Bertucci 2011). The advantage of using this system is it has long moment arms and small weights can produce high-magnitude moments, however, the long bars can be a disadvantage as there may be limited space when in a laboratory. Furthermore, modifications of this design may be difficult to implement the cycling parameters (Section 2.2). Therefore, this system requires modifications to implement cycling parameters, however, the large bars may cause problems when testing.

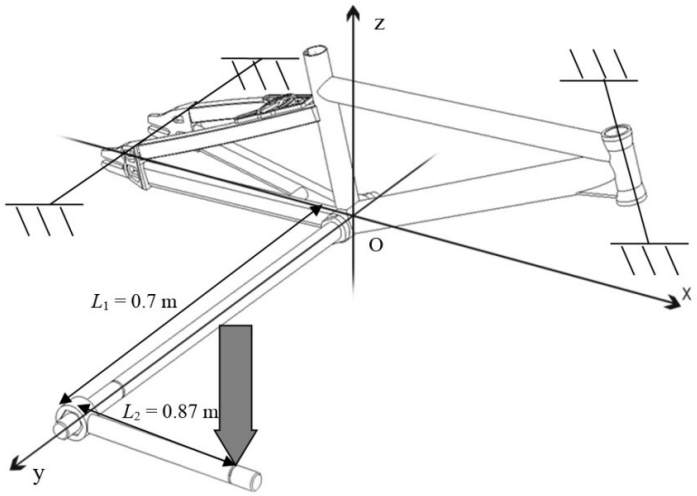

Figure 11: 'Bar System' Simulating Pedalling Forces (Manolova et al. 2015; Manolova & Bertucci 2011)

2.3.3 Bicycle Frame Test Fixture

Hull & Davis (1981) created a testing rig that applies weight to the crank arm. They have used brittle coat paint as well as applying strain gauges to onto the bicycle frame to obtain stress concentrations. This testing rig is similar to the testing rig presented in ISO 4210-6 (Section 2.3.1), but applied a static load on the crank arm. Although this testing rig applies static loading, modifying to emulate the cycling parameters may be difficult as large weights were required for testing. Modifying this testing rig to emulate the downstroke phase may be difficult because of the large weights applied.

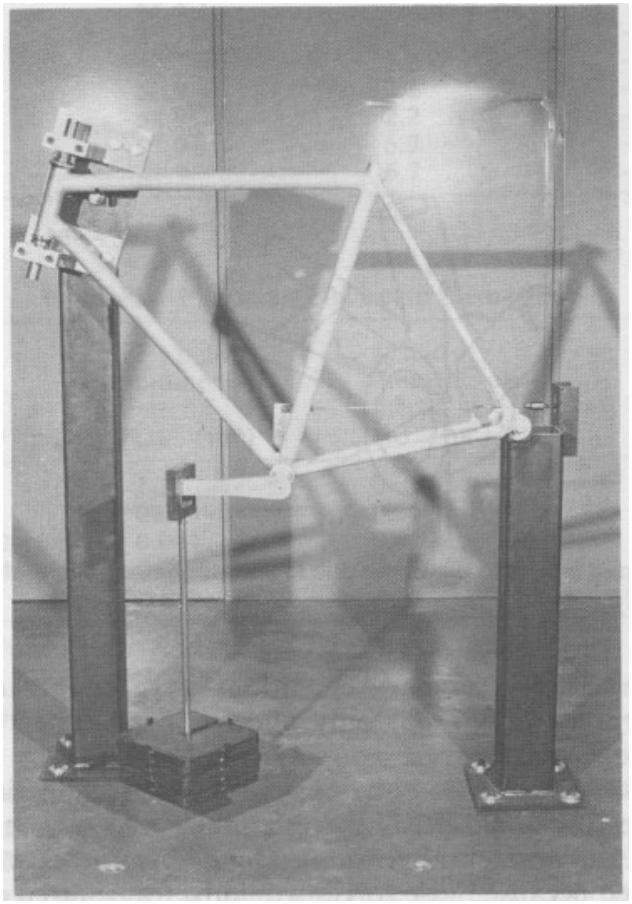

Figure 12: Bicycle Frame Test Fixture (Hull & Davis 1981)

All three testing rigs in this section aims to emulate cycling conditions, however, there were advantages and disadvantages to all three. ISO 4210-6 tests for the life cycle of the bicycle frame, but only slight modifications were required. However, a risk of possible overcomplication of the design may be present. The 'Bar System' uses long lever arms to emulate the crank torque, therefore, only requiring light weights to create high-magnitude moments, however, this can be limited depending on the amount of space in a laboratory environment and modifications of this design may be difficult to implement. Finally, Bicycle Frame Test Fixture resembles ISO 4210-6 and modified to apply static loads, however, the weights used were large and modifying this testing rig to emulate the downstroke may be difficult. Therefore, the design in ISO 4210-6 was chosen because of only requiring slight modifications in the design compared to the other two testing rigs.

2.4 Displacement Measurement Techniques

There are three types of analytical displacement measurement methods that can be used to obtain results for this project. Two of the methods are laboratory-based testing which are strain gauges and Digital Image Correlation (DIC), and another which is computational FEA. Each method may provide unique insight when used to obtain outputs when testing a bicycle frame, with each having advantages and disadvantages. These methods are further discussed in the following sections, to determine which will best suit this project.

2.4.1 Strain Gauges

Strain gauges can be used to measure the displacement of the bicycle frame and one commonly used is the bonded metallic strain gauge. This type of strain gauge has a thin wire oriented into a grid which is attached to a specimen, and an example of this is shown in Figure 13 below. If the specimen is undergoing displacement caused by a load, the strain gauge will displace as well. The strain gauge displacement can then be quantitively translated due to the change in electrical resistance that occurs as the wire reduces in diameter.

Strain gauges are typically configured into a Wheatstone bridge circuit to reduce the changes in wire resistance due to the difference in temperature. The connections of the Wheatstone bridge are usually two or four, otherwise known as half-bridge or full-bridge circuits. These circuit layouts improve the sensitivity of the strain gauge as it can cancel output voltage when the displacement value is zero as well as reducing thermal drift (National Instruments 2014).

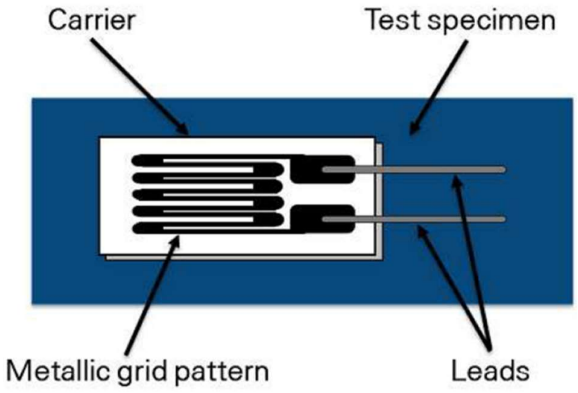

Figure 13: Strain Gauge (National Instruments 2014)

Strain gauges as a method of measurement are commonly used in literature (Covill et al. 2016; Dorel et al. 2005, 2010; Huang & Young 1995; Koellner, Cameron & Battley 2014; Manolova et al. 2015; Manolova & Bertucci 2011; Wang et al. 2010). Manolova et al. (2015) used eight strain gauges at different locations on a BMX bicycle frame. Two strain gauges were paired and applied to each location of interest. One was oriented in-line with a tube and another 45^{O} out-of-plane, which measures the axial and torsional strains experienced by each tube. Koellner, Cameron and Battley (2014) created a system to be implemented on bicycle frames for field tests. The system they have created in this study used 24 strain gauges and four accelerometers, which offered reliable data on strain and acceleration measurements. They have stated the data obtained from this system can aid in the optimisation of new bicycle frame designs.

Strain gauges offer reliable values when testing bicycle frames. However, these transducers are only effective on one axis because of their high sensitivity in one direction. Also, instrumentation of bicycle frames at certain regions may be difficult if it experiences more than one type of loading. If testing more than one type of loading at a certain location of interest, more strain gauges are required, which may not be feasible. A major advantage of using strain gauges shown in literature is that the sensor can be used during static or in-field (dynamic) testing. Therefore, the measuring technique has high versatility (Manolova et al. 2015; Koellner, Cameron & Battley 2014).

2.4.2 Finite Element Analysis

Finite element analysis is a software tool that is applied to structural designs. The modelling process of this analytical tool sections large structures into smaller geometries called ‘finite elements’. Governing equations generated from said finite elements can then be used to calculate the structural load distribution (Logan 2011). FEA is a suitable method for testing bicycle frames as it provides accurate information about load distribution on the structure similar to that of laboratory testing. In literature, it is observed that FEA results showed high accuracy when analysing structures and it correlates well with the laboratory testing (Baldissera & Delprete 2014; Giagopoulos & Arailopoulos 2017; Kelly & Costello 2004).

Parametric studies of bicycle frames have been conducted using FEA to analyse the influence of certain aspects of the structure (Covill et al. 2016, 2015, 2014; Rontescu et al. 2015). Hence, the use of FEA to obtain displacement values of a bicycle frame is suitable and can provide rapid parametric studies. However, it still requires validation from physical testing to verify that the outputted results are correct (Rontescu et al. 2015).

2.4.3 Digital Image Correlation

Digital Image Correlation (DIC) is a method of measuring displacement by capturing pictures and comparing all images to a reference photograph. An area of interest (AOI) must be selected on the reference photograph beforehand, which the DIC software focuses on obtaining displacement values at the specified area. The AOI pixels are grouped, often known as subsets, and the subset size can be changed based on the number of pixels grouped. Displacement measured by DIC is the average displacement of the pixels inside the subset compared to the reference photograph (Pan et al. 2008; Lecompte et al. 2006). A speckle pattern, which is a random pattern of contrasting colour to the specimen, must be applied before testing. Applying an appropriate pattern is crucial as it can affect the accuracy of the displacement values measured (Lecompte et al. 2006). Figure 14 below shows examples of typical speckle patterns.

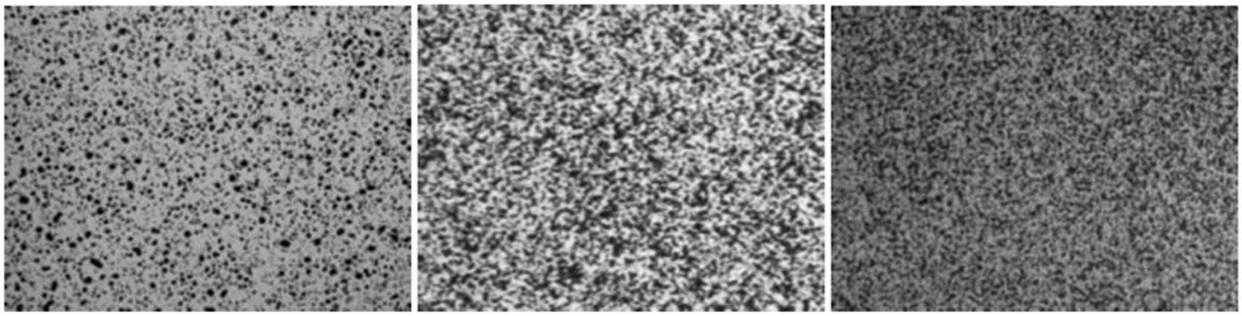

Figure 14: Speckle Pattern Examples (Schreier, Orteu & Sutton 2009)

Pan et al. (2008) found that speckle patterns of high contrast that have unique and identifiable features obtained the most accurate displacement values. Park et al. (2017) found an inverse relationship between the speckle pattern quality and average error values if the subset size is 41 pixels or greater. Hence, a high-quality speckle pattern, with identifiable features, must be applied to the bicycle frame with to obtain accurate outputs. Furthermore, several image artefacts can alter the results such as dust, water spots, imperfections on the specimen, or reflections which can provide an inaccurate portrayal of displacement when measured (Schreier, Orteu & Sutton 2009).

There is another branch of DIC that enables the measurement of depth on the z-axis, which is three-dimensional (3D) DIC. Two-dimensional (2D) DIC only measures in-plane displacements (x-axis and y-axis) (Reu 2012). 3D DIC uses a two-camera system that are focused on the specimen. For a single-

camera system, 3D depth is infinite and multiple points can align to one projection of the image shown in Figure 15a. However, using a two-camera system, the projection point captured by the first camera is no longer infinite shown in Figure 15b. The image from the second camera captures projections as well. If the projections from the second image (*q'* and *r')* intersect with the projection from the first (*p), t*hese intersections create distinct points in the image (*Q* and *R*). Therefore, creating depth as it limits the points aligned with the projections. This correspondence creates unique 3D points of two images from different cameras taken simultaneously (Schreier, Orteu & Sutton 2009).

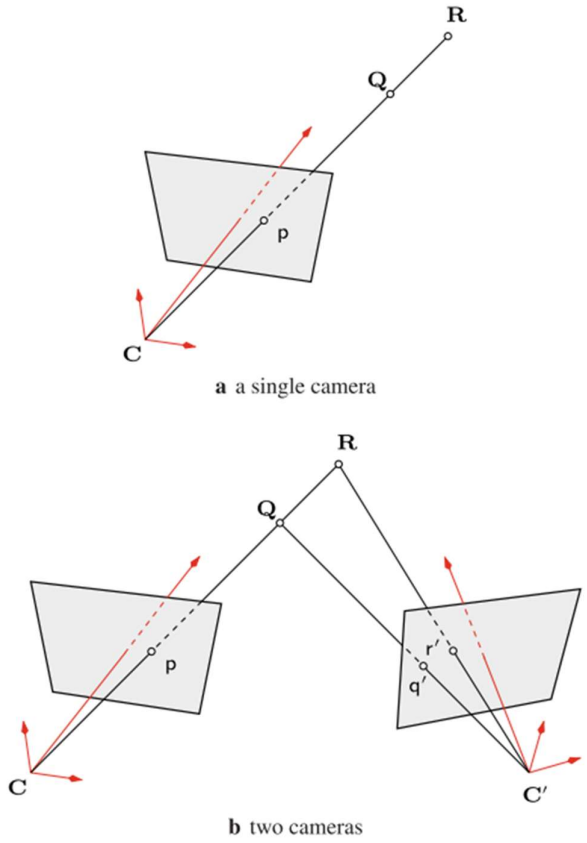

Figure 15: 2D and 3D Camera Systems (Schreier, Orteu & Sutton 2009)

Applying 3D DIC requires calibration before testing. One method is capturing images of a grid or dot pattern target oriented at unknown, arbitrary out-of-plane and in-plane rotations and translations when the image is captured. Altering the focal length and positions of the cameras, after completing calibration, will lower the quality of the measurement and must be recalibrated (Schreier, Orteu & Sutton 2009).

A comparison between strain gauges, FEA and DIC were investigated by Ramos et al. (2015) and Ramault et al. (2011). Both found a high correlation when obtaining values using strain gauges, FEA and DIC. The advantage of DIC as stated in literature is the method's capability of doing full-field assessments when compared to strain gauges. Simulation modelling such as FEA can do full-field assessments but requires validation with physical testing. Therefore, the use of DIC may provide a more suitable method of obtaining full-field displacement and is an experimental technique of testing.

2.5 Gap Statement

From the literature found, it is clear that there are proven methods of measuring bicycle frame displacements. Finite element analysis and strain gauges both presented strong abilities to complete the task, however, they had drawbacks (Covill et al. 2014, 2015, 2016, Dorel et al. 2005, 2010; Huang & Young 1995; Koellner, Cameron & Battley 2014; Manolova et al. 2015; Manolova & Bertucci 2011; Rontescu et al. 2015; Wang et al. 2010). The scope of this project requires the assessment of the entire bicycle frame, and strain gauges do not feasibly meet these requirements. While FEA can show the displacements for the entire bicycle frames, however, in terms of the data obtained, this method still requires experimental results to validate it, similar to what is expected from this study. 3D DIC has not been used widely in this field and exploring this method to capture displacements experienced by bicycle frames may be useful. Testing rigs for bicycle frames have been explored in both literature and international standards. This information shows many feasible designs for a testing rig, but a gap lies in the use of a testing rig and 3D DIC to measure displacements. This has directly impacted the aim of this study.

2.5.1 Project Aim

Using both strain gauges and FEA have been widely used to analyse the structure of bicycle frames. However, the literature review identified the limited use of DIC. Therefore, this project aims to find the lateral and vertical displacement of three bicycle frames using DIC.

2.5.2 Project Deliverables

To obtain the lateral and vertical displacement, a set of deliverables had to be met. Firstly, designing and constructing a testing rig that emulates sprint cycling loads derived from literature in Sections 2.2 and Section 2.3. Secondly, create a testing protocol that utilised both the testing rig and the 3D DIC equipment. Thirdly, investigate the linearity and repeatability of the protocol created, and finally, test all three bicycle frames and compare the results. Figure 16 below shows the three bicycle frames and are labelled as CA01, CA02, and AR01.

Figure 16 CA01, CA02 and AR18 Bicycle Frame Designs

2.5.3 Project Stages

A project plan was created for this project. Two major stages were identified in the beginning. Stage one was creating the testing rig that emulates sprint cycling conditions. The requirements were mainly derived from literature, detailed in Section 2.2. Stage two required a testing protocol, confirming the linearity and reproducibility of the system created, and comparing the lateral and vertical displacement data for all three bicycle frames. With the short project timespan, these stages were broken down into equal timeframes. Refer to Appendix A for a detailed timeline of the project.

3 Testing Rig Design and Construction

Stage one of the project required the design and construction of a testing rig, emulating elite sprint cyclist loads on the bottom bracket. This testing rig also needed to coincide with the camera system used in DIC. Therefore, the design of the testing rig had to expose the full bicycle frame structure with no obstructions. Application of static loads at certain increments shows the development of the displacement fields for the test cases chosen, which were derived from literature. This section covers the requirements, conceptualisation, and the development of the testing rig.

3.1 Design Requirements

Before conceptualising the testing rig, a set of requirements were identified and needed to be considered in the design. The following requirements were considered:

- Applying the load on the bottom bracket to simulate elite sprint cycling loads;
- Must be able to test multiple crank angles emulating the downstroke phase of cycling;
- The testing rig must be able to house the bicycle frame without obstructing the DIC camera system;
- The testing rig must apply static loading and must withstand the highest crank torque applied; and
- House multiple bicycle frames to suit different bicycle frame dimensions.

3.1.1 Justifications of these Requirements

Emulating elite sprint cyclist loads was a requirement because it was to observe lateral and vertical displacements. The parameters used to emulate these loads was using 266 N.m and applying this load on the downstroke phase of cycling, which is 0^{O} – 180^{O} crank angles. The testing rig must withstand this load because this would be the highest load applied to the bottom bracket (Gardner et al. 2007). There were previous testing rigs found in literature and standards mentioned (Section 2.3), but only one crank angle was considered. Therefore, the investigation of multiple angles along the downstroke phase may show more insight than just one crank angle. Since the projects required a full-field assessment of bicycle frames, obstructions between testing rig components and the DIC camera system would obstruct what was captured by the cameras. Furthermore, the choice of using static loading rather than dynamic loading was done because of the limitation of the DIC software used which only takes photographs. These requirements were used to conceptualise the following section.

3.2 Design Conceptualisation

The main inspiration of the testing rig concept comes from an international standard, which was ISO 4210 – 6 'Fatigue Test with Pedalling Forces'(International Organization for Standardization 2015). However, modifications of the testing rig from this standard were made to allow application of static loads at different crank angles during the downstroke. Although the downstroke crank angle range is from 0^O – 180^O, the testing rig concept was limited to 90^O – 180^O to lower the complexity of manufacturing and material cost. Figure 20 - Figure 21 below shows some of the concept drawing made for this project, and more are available in Appendix B.

The crank angle range was made into seven "load cases" shown in Figure 17 below. The testing rig design inspired from ISO 4210-6 required force values, however, the maximum load found in literature was a torque value. Therefore, the crank angle formula in Equation 1 was used to derive the highest force values (Serway 2004).

$$T = rFsin\phi \text{ (Serway 2004)} \quad \text{Equation 1}$$

T = 266 N.m (Gardner et al. 2007)

ϕ = 90^O (Korff et al. 2007)

$r = L$ = 175mm = 0.175m

Rearranging Equation 1 in terms of force, F:

$$\therefore F = \frac{T}{rsin\phi} \quad \text{Equation 2}$$

ISO 4210-6 recommends a crank length L which is 175mm and becomes a factor when calculating force (International Organization for Standardization 2015). Since the highest load applied during the downstroke occurs at approximately 90^O (Korff et al. 2007) and using 266 N.m (Gardner et al. 2007) as the highest torque applied, the derived force was 1520 N. This derived force value became the highest static load applied for testing for all of the crank angle load cases. However, this force was rounded into 1500 N for simplicity when testing the bicycle frames because an additional 20 N may not significantly impact the results. Using Equation 2 the force derived was:

$$F = \frac{266\ [N.m]}{0.175\ [m].\sin(90)} \cong 1520\ [N]$$

A fixture was required to attach the loading plate onto the bottom bracket. A condition that was considered was its interchangeability being able to fix on the left-hand side (LHS) and right-hand side (RHS) of the bicycle frame. Therefore, the fixture concept shown in Figure 18 below shows a rod that can attach to the loading disk using two M10 grub screws, shown in Figure 19 below.

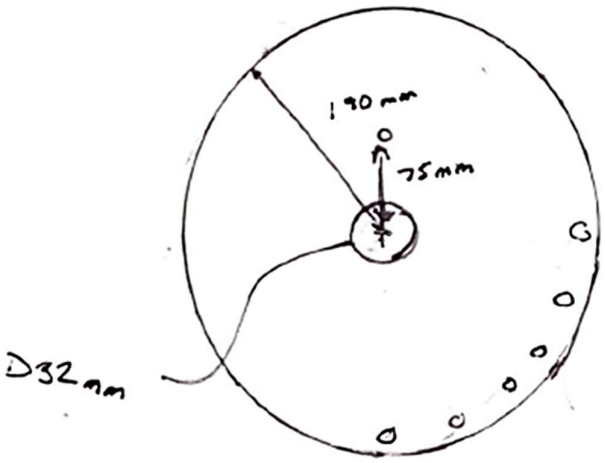

Figure 17: Loading Disk with Crank Angles

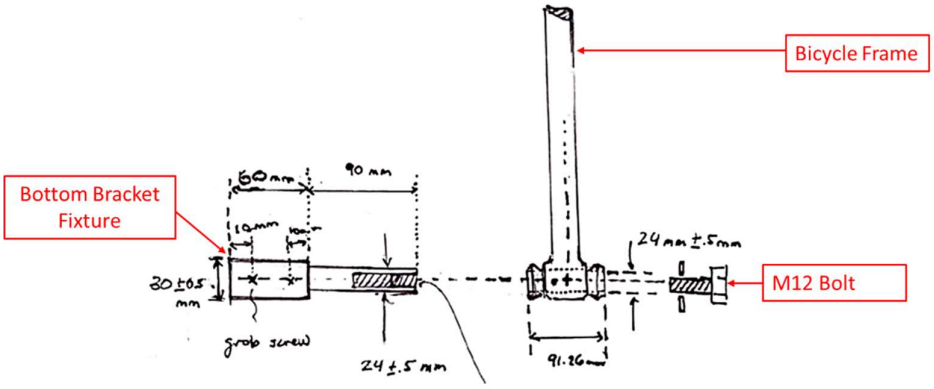

Figure 18: Bottom Bracket Fixture

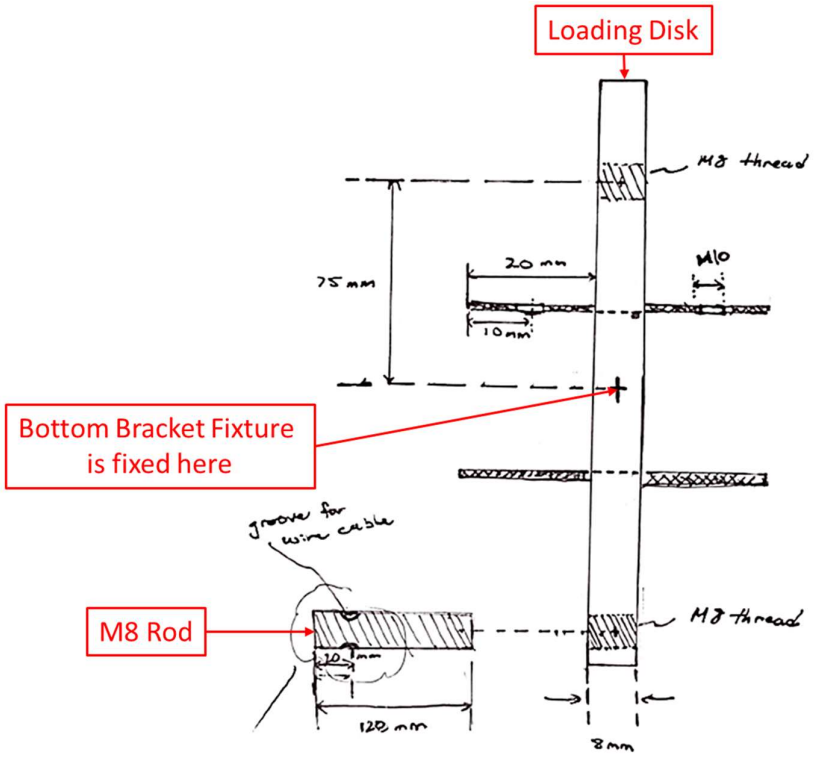

Figure 19: Loading Disk Top-Down View

The testing rig required a reaction frame that fixes the bicycle frame and did not deflect or break when 1500 N was being applied. Furthermore, the ability to adjust the testing rig to suit different bicycle frame dimensions was considered as there are different designs tested in this project. Hence, a suitable material was required for the frame and must be able to withstand high forces. The chosen material was 40mm T-slot aluminium extrusion, shown in Figure 20 below. This was chosen because T-slot aluminium was easy to manufacture and the material suitable mechanical stiffness properties (ASM International 2001). Figure 21 below shows the general outline and the dimensions of the reaction frame concept as the length of the aluminium extrusions must be long enough to provide adjustability.

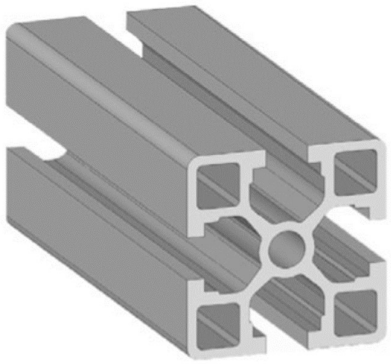

Figure 20: T-Slot Aluminium (Profilium 2017)

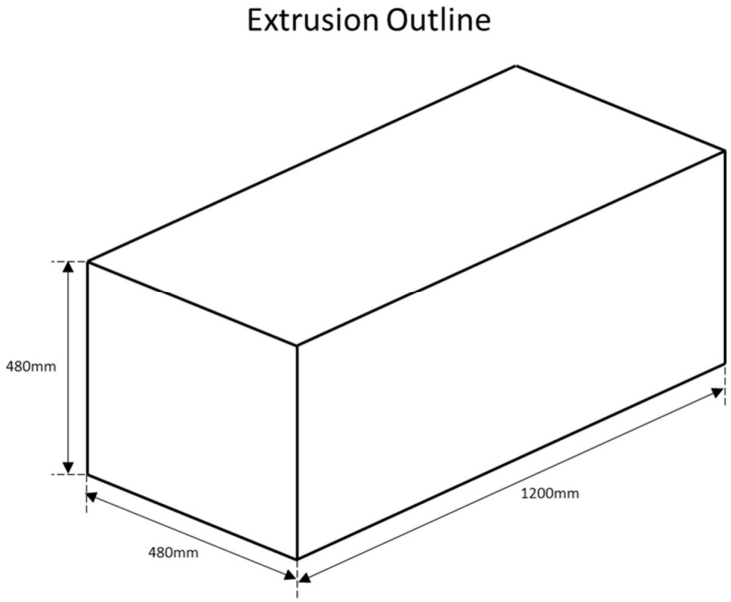

Figure 21: Reaction Frame Aluminium Extrusion Outline

A drawing of the testing rig concept is shown in Figure 22 below. When comparing to the testing rig to ISO 4210-6, the design is similar, but the crank angle varies as it has seven load cases to emulate the downstroke. The head tube attachment fixes onto the head tube of the bicycle frame. Aluminium was chosen as the material for the head tube because of its manufacturability. The vertical link attaches to the rear dropouts of the bicycle frame and must be able to rotate on the x-axis. A turnbuckle was used as the tie rod for the design, which connects the vertical link to the loading disk. Once the design concept was finished, refinement of the design was done, detailed in the following section.

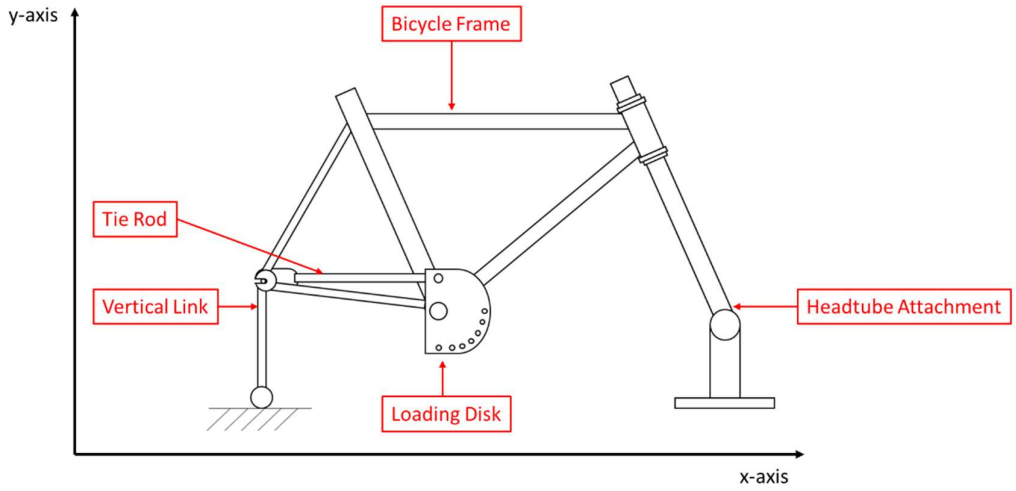

Figure 22: Testing Rig Concept

3.3 Final Design and Constructed Testing Rig

Computer-aided design (CAD) was used to create the final design for the reaction frame and loading disk, shown in Figure 23 below. Since there were multiple bicycle frames tested for this project, the testing rig had to be adjustable to suit these dimensions. The description and the adjustable sections are shown in Figure 24 below. The head tube attachment and parts of the aluminium reaction frame were required to be adjustable because of the varying angles of the head tube. Parts of the aluminium frame, including the aluminium extrusion that fixes onto the head tube attachment, and the position of the reaction bar had to be adjustable due to the varying lengths of the bicycle frame.

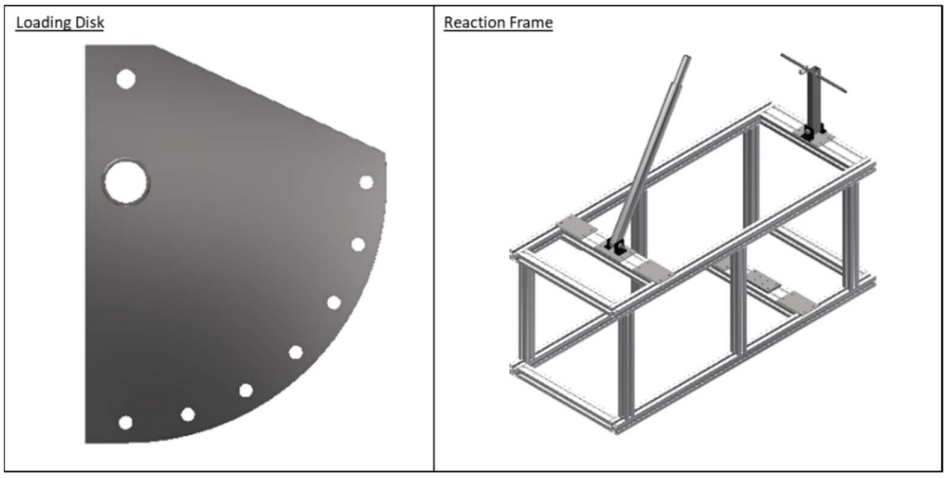

Figure 23: Bicycle Frame Testing Rig Final Design

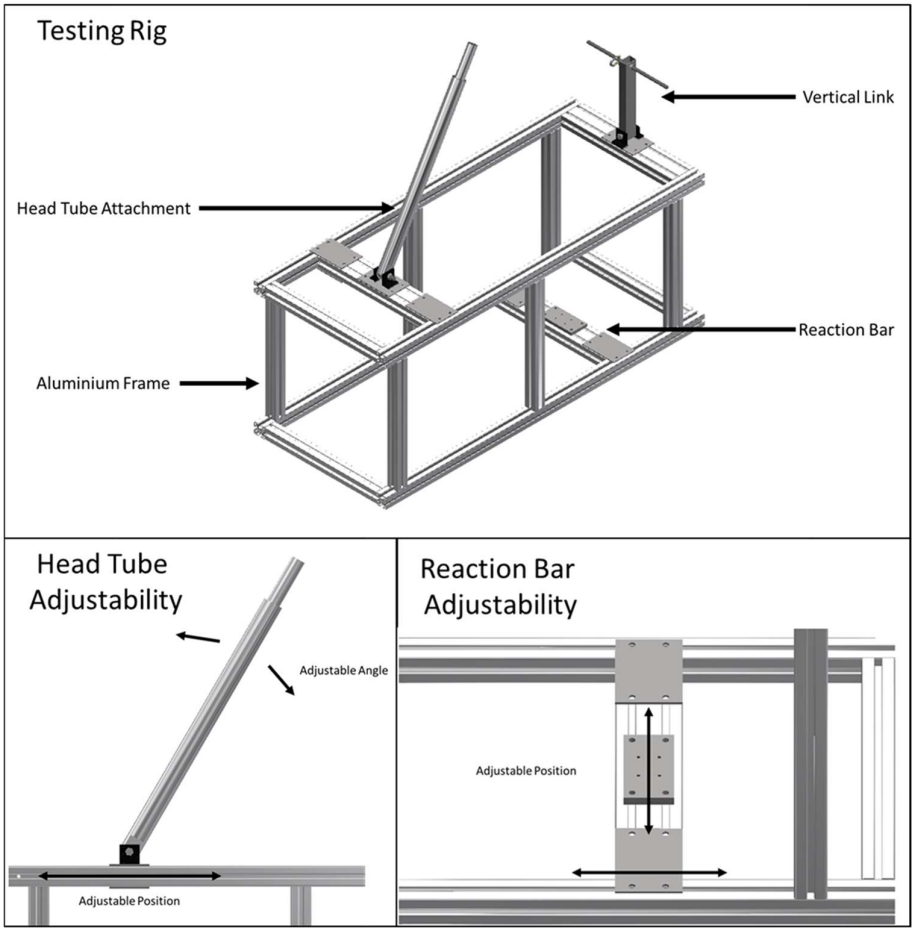

Figure 24: Reaction Frame Description

There were multiple iterations of the reaction frame design to and analysis of these assembled frames were done to find a design that had low deflection when applying 1500 N. These iterations of the reaction frame all have undergone finite element analysis with similar point loads applied at regions that house the bicycle frame such as the head tube attachment and vertical link attachment. Figure 25 shows the reaction frame chosen. The maximum deflection was of this reaction frame was 0.39mm, which was less compared to the other designs analysed (Appendix C). After the design was finalised, the next stage of the project was to construct the testing rig. Once the design had been finalised, engineering drawings were produced (Appendix D) and then the components were manufactured, shown in Figure 26.

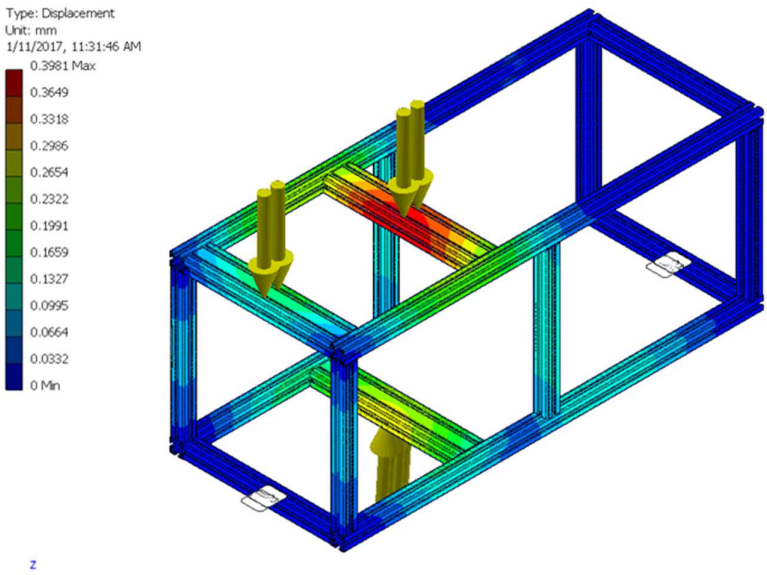

Figure 25: Finite Element Analysis of Aluminium Frame

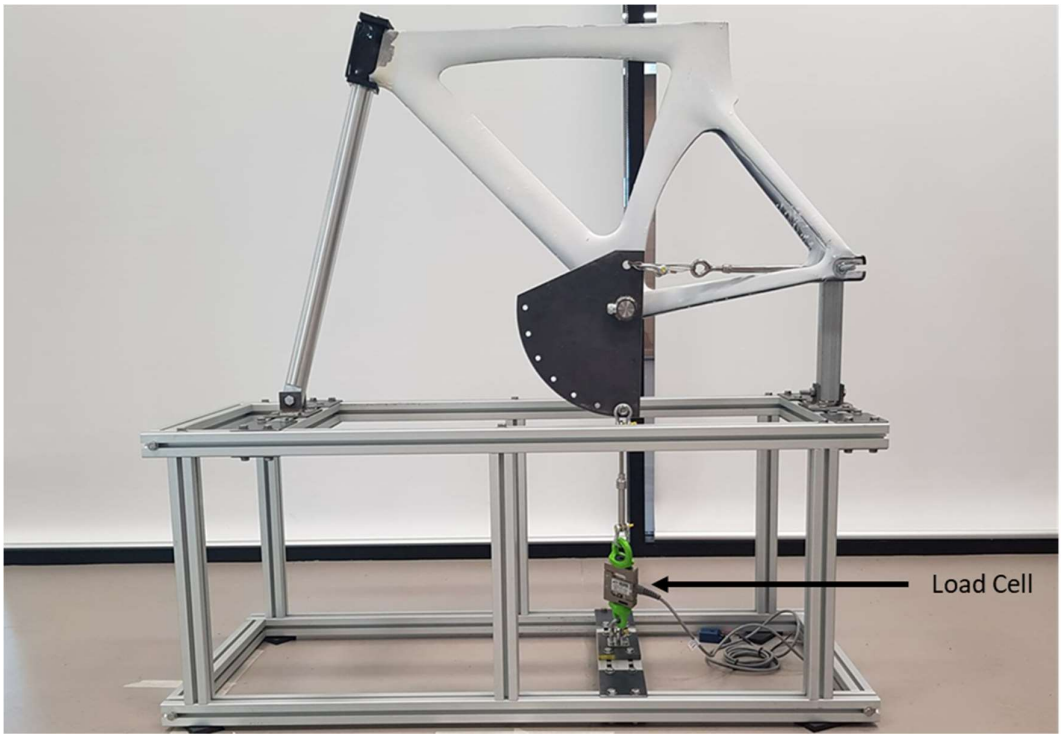

Figure 26: Constructed Testing Rig with Bicycle Frame Attached

The created testing rig applies a tension load onto the bottom bracket using the loading plate at different crank angle test cases. A load cell was used to measure the applied tension force; it is attached to the reaction bar and the loading disk via a link and tension was applied using a turnbuckle.

4 Methodology

From literature, the maximum power varies from 1600W – 1792W, which correlate to 266 N.m – 235.7 N.m of cycling torque (Gardner et al. 2007; Dorel et al. 2005). The relationship between the crank angle and cycling torque was also found which was during the downstroke phase of cycling from 0^O – 180^O (Korff et al. 2007). However, the range between 90^O – 180^O was considered as the test parameters for this project. This is because the 90^O crank angle is the location where the crank torque begins to peak and 180^O is where the downstroke ends.

Four bicycle frame tests were undergone and compared for this project. These were CA01 LHS, CA01 RHS, CA02 RHS, and AR01 RHS. The tests were compared to one another to observe if there were differences in displacement. Testing the LHS and RHS of CA01 was done to observe if there were any differences of one bicycle frame when undergoing similar testing conditions. The deflections felt by the athlete may be only from one side of the bicycle frame. This deflection might be caused by the manufacturing quality of the bicycle frame which relies on the void content, differences in curing, amount of material, or direction of uniaxial carbon fibre (Bie et al. 2017; Chang et al. 2017; Rahmani et al. 2014). A comparison between CA01 RHS and CA02 RHS were undertaken to observe if there are differences between bicycle frames of the same design. Although these bicycle frames are of the same design, there may be differences in deflections which may be felt by one athlete and not by another due to variations in the manufacturing process. Lastly, observation of displacement values between two bicycle frames with different designs, CA01 RHS and AR01 RHS, were made to observe which bicycle frame had higher lateral and vertical stiffness.

4.1 Preparation and Calibration

Before testing the bicycle frame, a speckle pattern must be applied to the specimen. Firstly, white peel coat paint was sprayed on the bicycle frame and was set for 24 hours to let the paint dry completely. After this, a speckle pattern was applied using a speckle pattern roller with a predefined pattern and was left to dry for 15 minutes. The ink for the speckle pattern was black and is a contrasting colour to the white paint applied. Contrasting colour to the white peel coat paint was used because Lecompte et al. (2006) found contrasting colours improve the quality of DIC measurements.

Centre points were marked on the bicycle frame after speckling to provide consistent locations when measuring lateral and vertical displacement. The first centre point was marked 50mm above the bottom bracket. This became the reference location for the dashed lines that are marked in-line to the head tube and seat tube, and the centre points for these sections were marked 50mm apart with the furthest being

250mm. A dashed line was marked parallel to the chain stays with the bottom bracket as the reference location. Three centre points are marked on the chain stay and were 50mm apart from the reference point with the furthest being 150mm. All the points are shown in Figure 27 below.

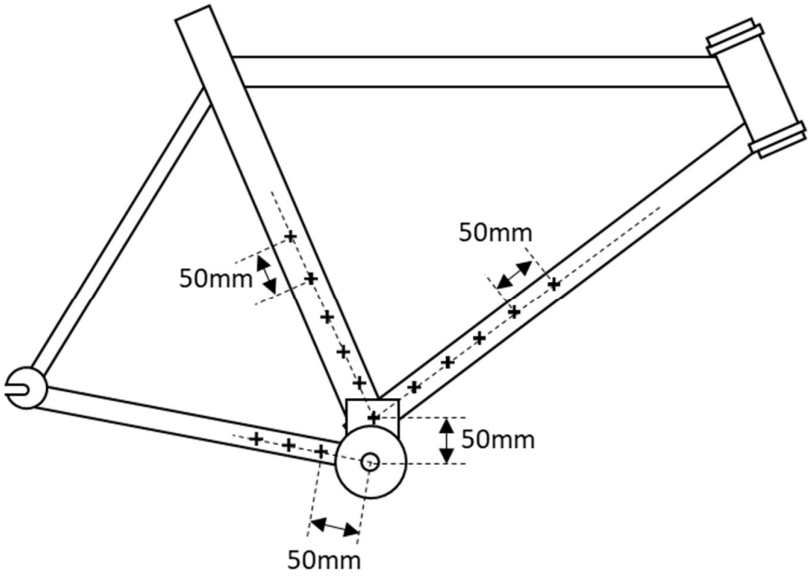

Figure 27: Bicycle Frame Points

The bicycle frames were then fixed to the testing rig as per Figure 28 below. The two cameras were stationed and positioned at a location that captured the speckled areas on the bicycle frame similar to the example shown in Figure 29 below. After positioning the cameras, the aperture of both cameras was changed until the bicycle frame was in focus. This provides high-quality images of the speckle pattern when undergoing post-processing.

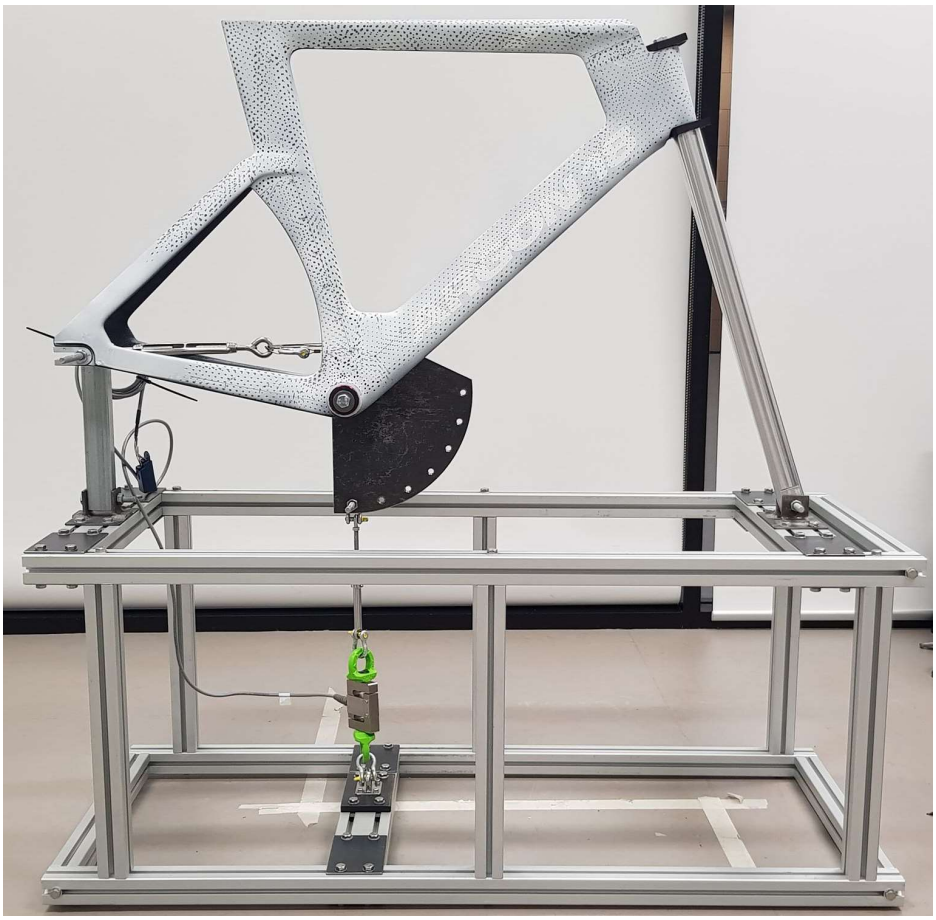

Figure 28: Testing Rig Setup housing the AR01 Bicycle Frame

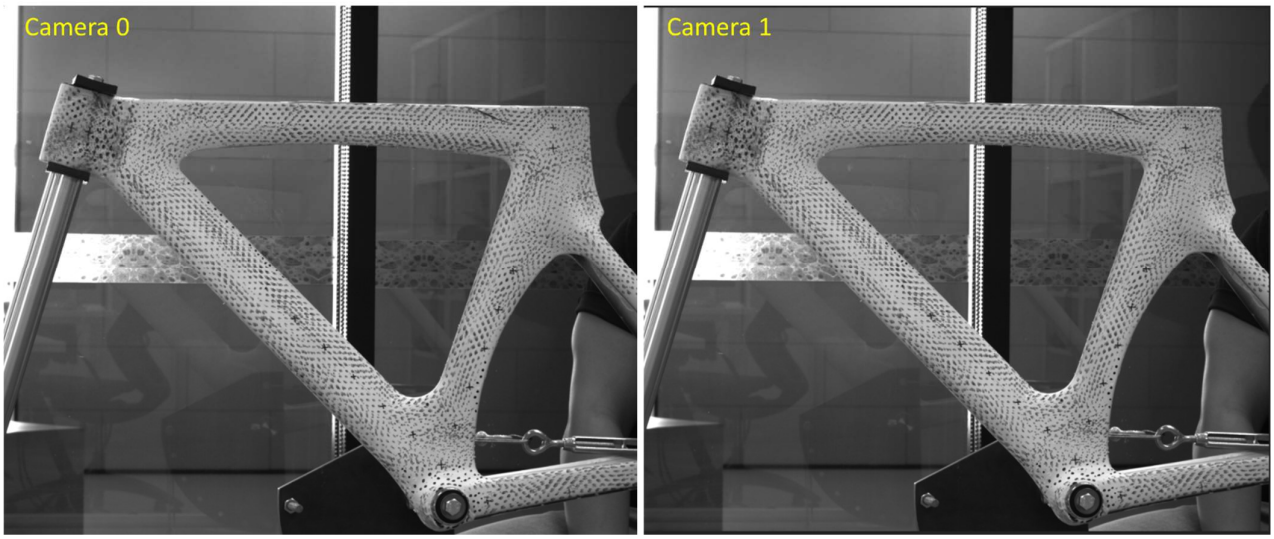

Figure 29: Example Photographs of CA01 Camera Positions

To keep the pictures of the bicycle frame in focus when changing the loading condition during testing, tape was applied at one edge of the testing rig shown in Figure 30 below. Placing this tape also helped

during calibration because the tape acted as a guideline where the cameras were in focus. Afterwards, calibration photographs were taken. VIC-3D requires calibration tiles for these cameras with a grid pattern. For this project, a 28mm grid pattern calibration tile was used, shown in Figure 31 below. Twenty photographs were taken at arbitrary rotations and positions which is one of the methods of calibration. However, changing the aperture and position alters the displacement values mentioned by Schreier, Orteu & Sutton (2009) and recalibration must be performed.

Figure 30: Tape Applied on Ground to Show Where the Cameras Were in Focus

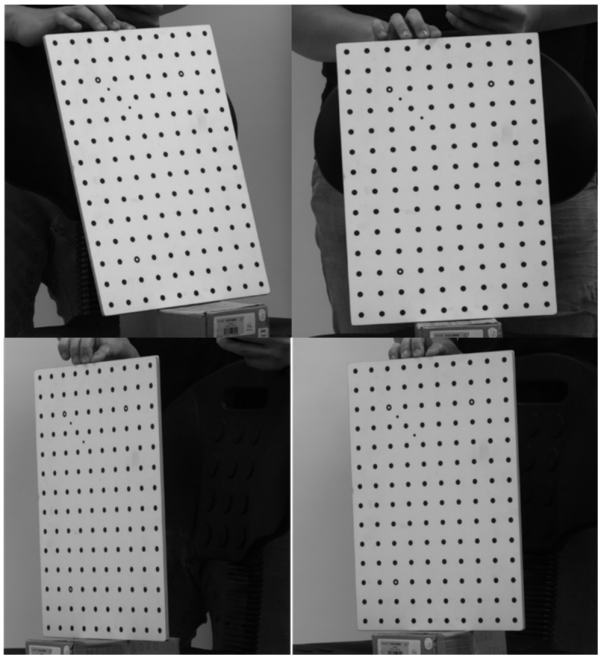

Figure 31: Example of the 28mm Calibration Tile in Arbitrary Locations During Calibration

4.2 Testing Protocol

The software used, VIC-3D, required photographs to process the displacement field as video processing capability is not available. There are seven test cases for each bicycle frame that emulate the downstroke phase ranging from 90^{O} – 180^{O} crank angles and are broken down into 15^{O} intervals. The first test undertaken by these bicycle frames was the 90^{O} test case, and the crank angle was progressively increased up to the final test case angle of 180^{O}. The first photograph taken for each test case is when there is no tension force applied to the loading disk. This photograph becomes the reference image when post-processing. Each test applied a vertical tension load up to 1500 N and unloaded down to 0 N. This is shown in Figure 32 below.

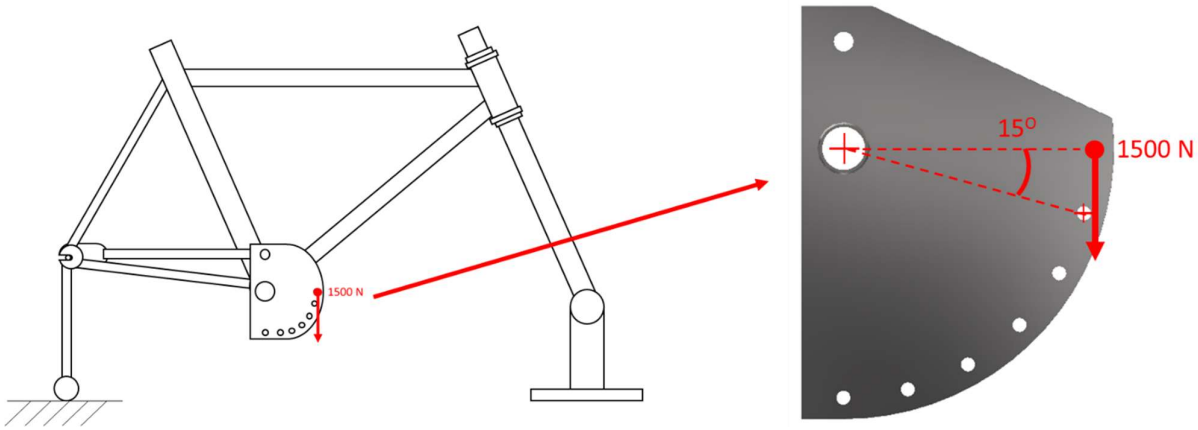

Figure 32: Bicycle Frame Test Case Example

A photograph was taken at 300 N intervals when loading and unloading tension. These images taken shows the development of the displacement field when processing the photographs. The recorded data from the load cell was tabulated to correlate the photographs taken. Table 3 show the picture ID, intended load and recorded tension (denoted as actual load). Once all of the test cases were finished for one bicycle frame, post-processing of all the calibration and bicycle frame images was done, and the details are shown in Section 4.3 below.

Table 3: Example of Loading Condition Tracker for Every Test. It Tracked the Picture ID, the Intended Load, and Actual Load Recorded

Picture ID	Intended Load [N]	Actual load [N]
0	0	0
1	300	307
2	600	605
3	900	900
4	1200	1200
5	1500	1503
6	1200	1200
7	900	900
8	600	600
9	300	301
10	0	0

4.3 Digital Image Correlation Post-Processing Protocol

VIC-3D DIC, the software used, processes the calibration and speckled bicycle frame images. Firstly, the calibration images taken for each test were uploaded and processed. After processing the calibration images, the loaded and unloaded photographs of the bicycle frame were uploaded. An area of interest was selected on the reference photograph before running the software. Figure 33 below shows the area of interest selected for each test case. The subset size chosen was 75 pixels per subset for all test cases which showed unique patterns inside the subset. After the subset size was chosen, the software calculated the displacement values.

Figure 33: Area of Interest Selected for Bicycle Frames

The displacement analysed by VIC-3D was broken down into three parameters, U[mm], V[mm] and W[mm]. U[mm] is the displacement along the x-axis, V[mm] is the displacement along the y-axis, and W[mm] is the displacement along the z-axis. The displacement calculated is direction dependent and based on the positive axes denoted by the software which, shown in Figure 34 below. Hence, if measured displacement obtained by the software was found to be negative, it is moving along in the opposite direction relative to the positive axes.

Since the project aims to obtain the lateral and vertical displacement of the bicycle frames, the displacements that correspond to the values obtained from VIC-3D are W[mm] and V[mm] respectively. Moreover, displacement along the x-axis and was ignored because it did not relate to lateral and vertical displacement because the tension force was applied vertically down. Appendix E show the individual datasets for V[mm] and W[mm].

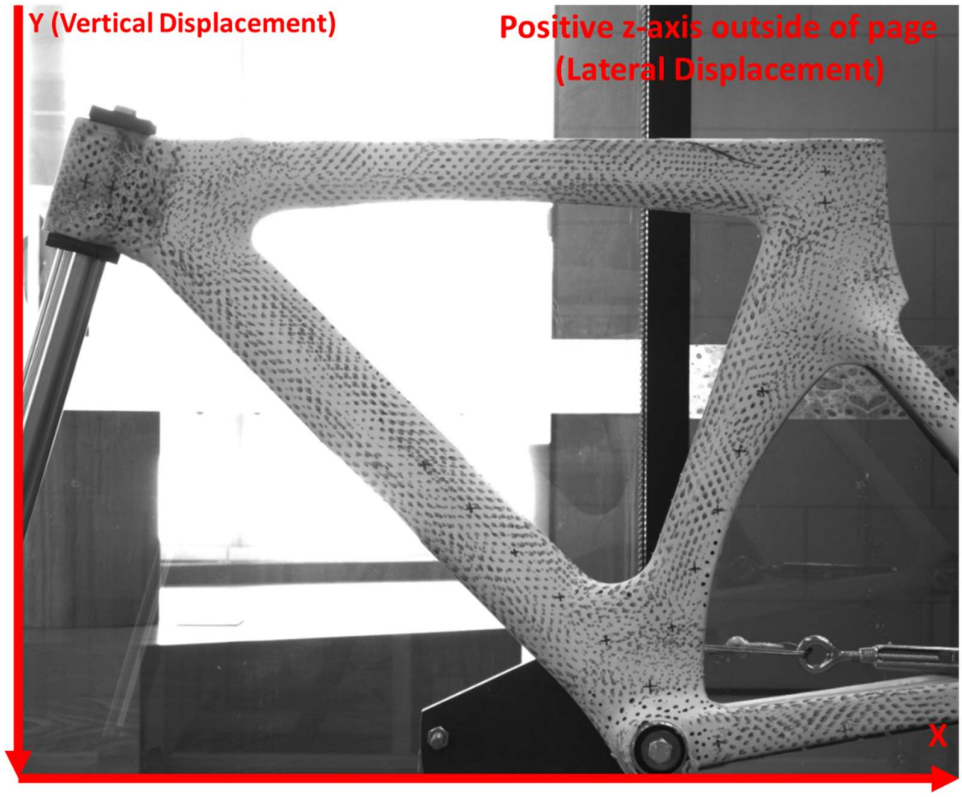

Figure 34: Positive Axis of VIC-3D DIC Software

The first test results were found to have rigid body motion when processing the data from VIC-3D which show a high a rotational component along the top tube, however, there was is no load applied along the z-axis at this section of the bicycle frame. Therefore, using the average transformation tool in VIC-3D was used to remove all displacements caused by rigid body motion. However, using this transformation show displacements along the top tube being equivalent in magnitude to the bottom bracket. As mentioned above, there were no forces applied near the top tube. Therefore, the mapping of displacement using this transformation is not accurate. Figure 35 below shows one of these displacement maps when using the average transform tool.

In the reference manual, the average transform tool uses all the data points inside the area of interest and inverts the photograph to recalculate all components of displacement. This caused the displacement map to be inaccurate because it does not have a stationary position selected. However, this tool can assign a stationary position at the area of interest and recalibrates the displacement values relative to the stationary point selected (Correlated Solutions Inc. 2016). Only one part of the testing rig that remains fixed is the head tube attachment. Hence, the head tube was selected as the stationary position, and average transform was repeated to recalculate the displacements being relative to the head tube.

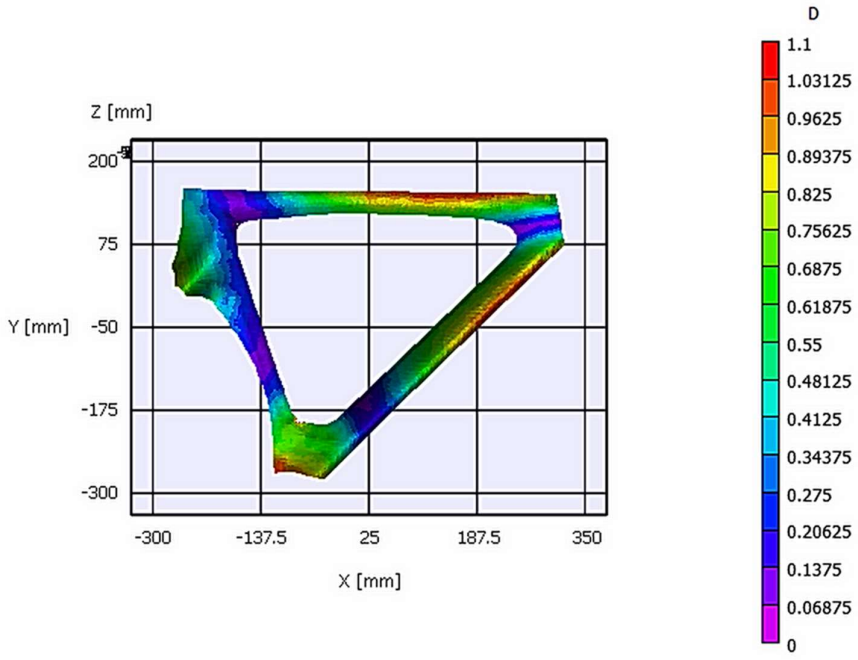

Figure 35: Rigid Body Removal Using Average Body Transform Without Fixed Reference Point

Once the displacement values have been transformed and now relative to the head tube, a set of circle markers were applied at the area of interest. Placement of these markers corresponding to the centre points marked on the bicycle frame mentioned in Section 4.1 (Figure 36). Extraction of V[mm] and W[mm] was done for every test case for each bicycle frame and was paired with the recorded tension force applied to them when testing.

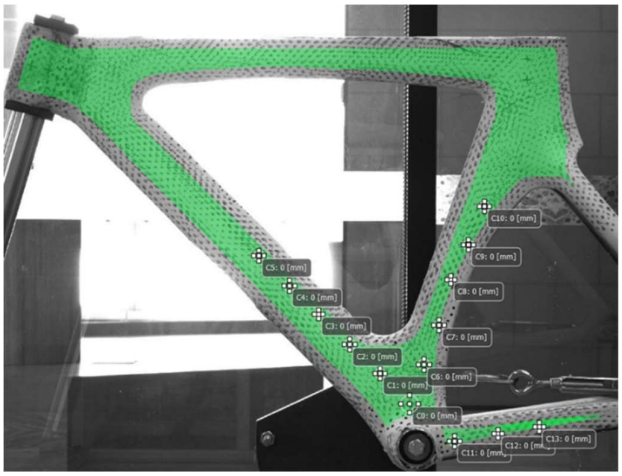

Figure 36: Circle Markers C0 – C13 on Bicycle Frame. C0 was a Circle Point 50mm above the Bottom Bracket, C1 – C5 were Circle Markers Along the Down Tube 50mm Apart, C6 – C10 were Circle Markers Along the Seat Tube 50mm Apart, and C11 – C12 Were Circle Markers Along the Chain Stays 50mm Apart.

4.4 Pilot Test Protocol

Before obtaining the results for all three bicycle frames, an investigation to check the linearity and reproducibility was conducted. The pilot test protocol deviated from two protocols mentioned in Section 4.2 and Section 4.3 because these tests were investigating the linearity of the system and the repeatability between tests. Therefore, the loading conditions from the testing protocol (Section 4.2) and DIC post-processing (Section 4.3) were modified to confirm these two parameters.

4.4.1 Deviations from the Testing Protocol

There were four tests done; two were incremented at 50 N, and the other two were incremented at 100 N with the highest load applied to be 1500 N and at a crank angle of 90^{O}. This deviated from the protocol in Section 4.2 as it tested all seven crank angles at 300 N increments. Maintaining the crank angle load case at 90^{O} was done to observe the repeatability of the system when measuring lateral and vertical displacement values. If the displacement data obtained from these tests were inconsistent, then the system and the protocols created would need to be reassessed. Furthermore, the choice of testing at two different increments aimed to observe if there were differences in the displacement values obtained when changing the incremented load. If there were differences in displacement values obtained when changing the magnitude of the incremented load, the values obtained becomes dependant on the incremented load.

4.4.2 Deviations from the Post-Processing Protocol

Most of the post-processing protocol in Section 4.3 was followed. However, the circle marker placement was different as there were no markers placed along the chain stay and one less marker along the seat tube, shown in Figure 37. Furthermore, the naming convention for these circle marker data were named as “PXX” rather than “CXX” to distinguish the pilot tests from the other tests conducted. Therefore, the circle marker was P0 was 50mm above the bottom bracket, P1 – P5 were circle markers along the downtube 50mm apart, and P6 – P9 were circle markers along the seat tube. The tension load applied for all pilot tests were recorded and plotted against the data recorded by the markers. Once the lateral and vertical displacement data was plotted against the recorded, linear regression was done to see if the system outputted linear results. The lateral and vertical displacement data were compared for all pilot test to observe if the testing protocols had reproducible data. The results obtained from these tests are shown in Section 5.1.

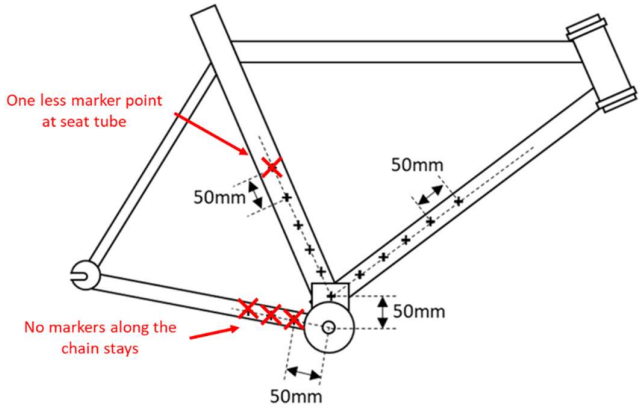

Figure 37: Pilot Test Marker Placement

4.5 Protocol Evaluation

The testing and post-processing protocol created were to obtain the lateral and vertical displacement for the project. Since three bicycle frames were tested, adjustability at certain sections of the testing rig was required to suit the project and detailed (Section 3). Housing the three bicycle frames showed no problems because all the requirements for the testing rig design were carefully considered.

Once the cameras were calibrated and a bicycle frame housed, testing of all specified load cases were done starting at 90^{O} and ending at 180^{O} to emulate the downstroke segment when cycling. Vertical tension was applied up to 1500 N for all test cases and a photo was taken at 300 N to show the development of the displacement values. However, the load applied for all the tests was less than intended because of the value conversion from kilogram-force to Newtons. Hence, the recorded displacement values were lower because of this limitation. This was because the load cell used for this project measures tension in kilogram-force and no conversion procedure was done beforehand to convert to Newtons. Therefore, conversion from kgf to Newtons were done during post-processing.

Post-processing the data required an AOI selected and a subset size to be chosen. The whole structure of the bicycle frame was selected as an AOI and the subset size was kept at 75 pixels. VIC-3D separate the displacement values to the three principle axes (x,y,z). However, there are only two parameters that are considered, and they are V[mm] and W[mm] which represent vertical and lateral displacement respectively. These two parameters show the displacement of the bicycle frame along the y-axis and z-axis caused by the tension load applied. The displacement maps and marker data for these parameters are detailed in the following section.

5 Results

The results obtained using DIC is shown in this section below. Mentioned in Section 4.3 above, there are three components of displacement that VIC-3D processes. However, V[mm] and W[mm] were the only two considered as it represented lateral and vertical displacement respectively. Before testing the bicycle frames, pilot testing was conducted at one load case to check if results found show linearity and reproducibility of these tests. Once linearity and reproducibility were confirmed, testing of the other load cases and bicycle frames was done and the results found is shown in this section.

5.1 Pilot Test Results – Linearity and Reproducibility Tests

Initial testing of the system was done before the actual tests were undergone. The two aims for the pilot tests were to investigate the linearity and reproducibility of these tests. Four tests were conducted with the same bicycle frame, and the test case was kept at a constant 90^{O}. Section 4.4 details the pilot test protocol as this had minor differences compared to the testing protocol and post-processing protocol in Section 4.2 and Section 4.3, respectively. This section details the results found from the pilot tests undertaken.

5.1.1 Linearity Check

The data obtained from the pilot test for all markers recorded (P0-P9) were plotted against the applied tension load. Figure 38 and Figure 39 show the lateral displacement and vertical displacement for Test 1, respectively. Vertical displacement market points appear to have high correlation when plotted against the tension load. However, for lateral displacement, markers P0-P7 presented high correlation, but points P8 and P9 showed very low correlation. All the pilot tests experienced this phenomenon when plotting the lateral displacement marker data, shown Table 4 - Table 7 below. The coefficient of determination data showed inconsistencies for markers P8 and P9 when pilot tests were compared. Further investigation into these two points shows that the displacement values are relatively low and more sporadic compared to the other marker values.

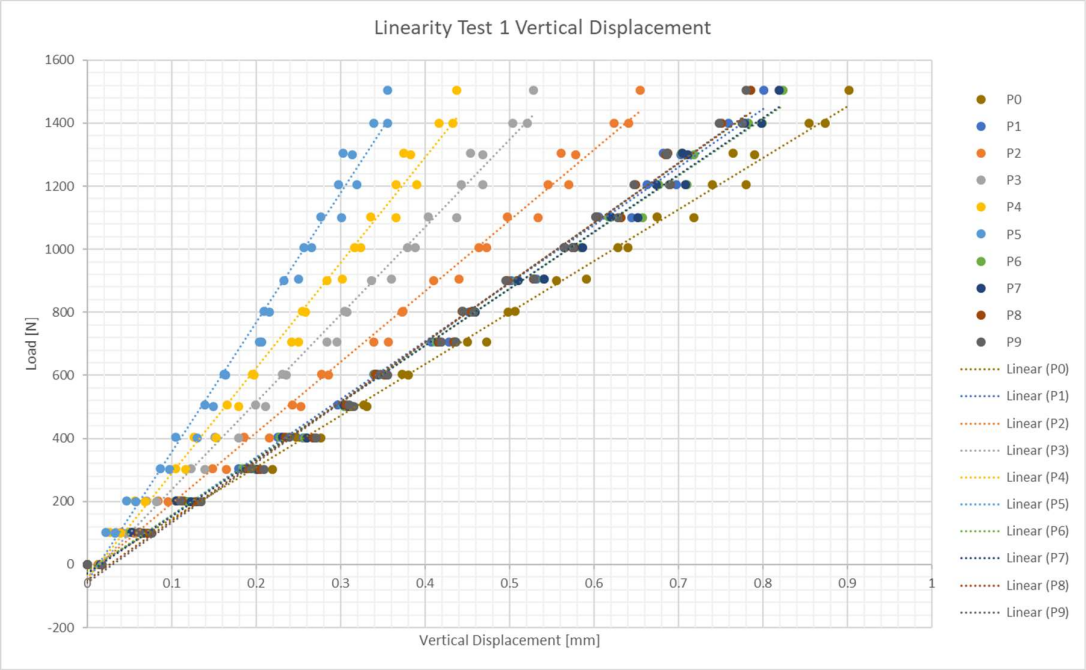

Figure 38: Test 1 - Vertical Displacement

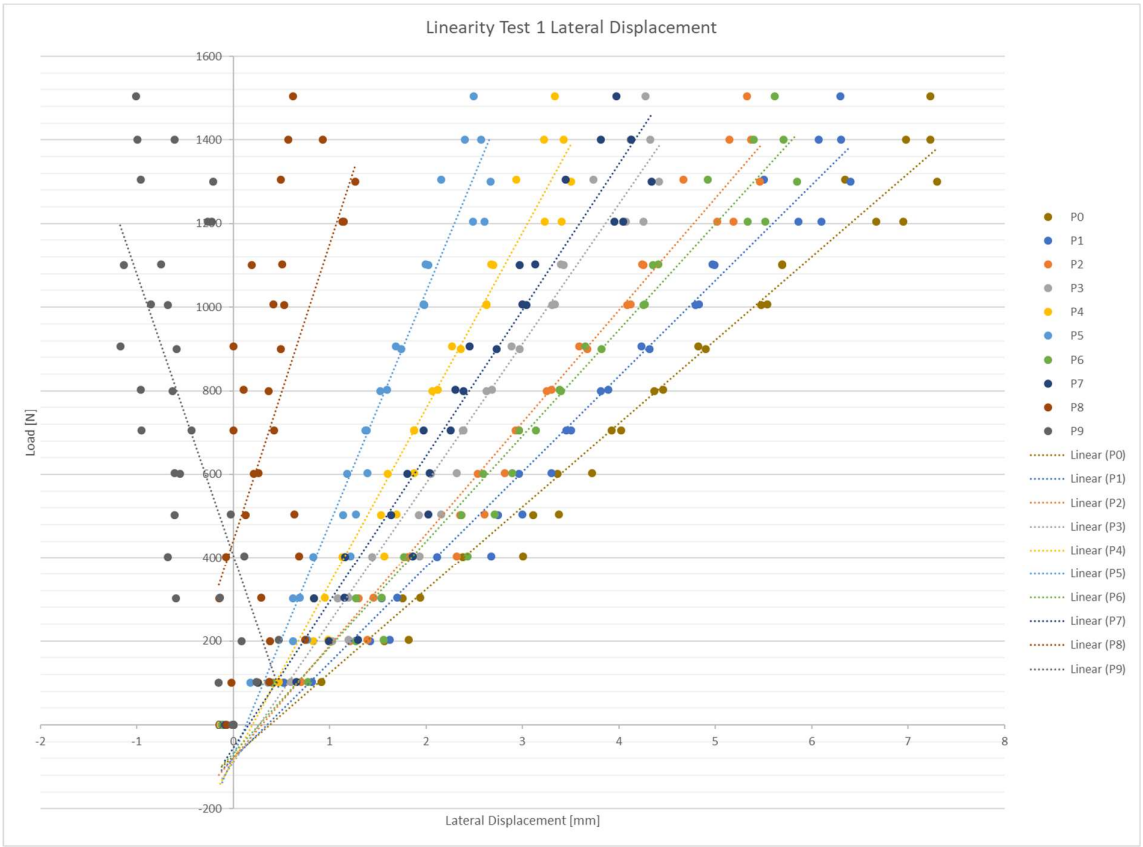

Figure 39: Test 1 - Lateral Displacement

Table 4: Test 1 Vertical and Lateral Displacement R^2

Data Point	Vertical Displacement R^2	Lateral Displacement R^2
0	0.9957	0.98
1	0.9948	0.9775
2	0.9938	0.9749
3	0.9916	0.9694
4	0.9889	0.963
5	0.9857	0.9549
6	0.9958	0.9722
7	0.9955	0.9508
8	0.9937	0.3385
9	0.993	0.416

Table 5: Test 2 Vertical and Lateral Displacement R^2

Data Point	Vertical Displacement R^2	Lateral Displacement R^2
0	0.9974	0.9839
1	0.9969	0.9823
2	0.9962	0.9805
3	0.9945	0.9774
4	0.9929	0.9733
5	0.9908	0.9694
6	0.9971	0.9782
7	0.9971	0.9613
8	0.9962	0.2669
9	0.9958	0.5381

Table 6: Test 3 Vertical and Lateral Displacement R^2

Data Point	Vertical Displacement R^2	Lateral Displacement R^2
0	0.9974	0.9887
1	0.9963	0.9874
2	0.9954	0.9864
3	0.9934	0.9844
4	0.9924	0.983
5	0.99	0.982
6	0.9964	0.9879
7	0.9961	0.9847
8	0.9953	0.88
9	0.9948	0.0628

Table 7: Test 4 Vertical and Lateral Displacement R^2

Data Point	Vertical Displacement R^2	Lateral Displacement R^2
0	0.9755	0.9638
1	0.9751	0.9626
2	0.9733	0.9611
3	0.9707	0.9565
4	0.9706	0.9507
5	0.97	0.9484
6	0.9732	0.9586
7	0.9716	0.941
8	0.9678	0.2239
9	0.9654	0.6543

5.1.2 Reproducibility

The investigation of reproducibility was also conducted to observe if the protocols created were consistent when obtaining displacement data. Comparing the data obtained from these pilot tests showed high precision for lateral and vertical displacement. Intraclass Correlation (ICC) was used to assess the reliability of all lateral and vertical displacement data points obtained from the pilot tests. Table 8 below shows the ICC values of the data points for all four tests. All data points for vertical displacement has shown high reliability with the maximum being 0.937 and lowest 0.879. Hence, the vertical displacement data were reproducible for during the pilot test stage. Lateral displacement has also shown high reliability, however, data points P8 and P9 shows poor reliability. This means that the displacements measured around this region shos inconsistent and unreliable data.

Observing the data has shown low differences between marker sets and an example can be shown in P0 at 1500 N (Table 9). The vertical displacement showed low differences with the highest difference being Linear T1 and Linear T3 having a 0.2mm difference at peak tension load. Lateral displacement also showed very load difference with the highest difference being Linear T1 and Linear T3 having a 0.16mm difference. Therefore, the displacement data were reproducible. However, the lateral displacement marker data for P8 and P9 show inconsistencies for this test as well. This means that the displacements measured around this region shos inconsistent and unreliable data. Hence, validates the ICC values that were conducted. The complete pilot test results are shown in Appendix F.

Table 8: Vertical and Lateral Displacement Intraclass Correlation Values for All Pilot Tests

Intraclass Correlation Values for Pilot Test Data Points		
Data Point	V[mm]	W[mm]
0	0.937	0.991
1	0.930	0.990
2	0.918	0.990
3	0.886	0.986
4	0.899	0.982
5	0.887	0.982
6	0.919	0.983
7	0.910	0.963
8	0.888	0.452
9	0.879	0.559
Max	**0.937**	**0.991**
Min	**0.879**	**0.452**

Table 9: P0 at 1500N Showing Low Differences for Lateral and Vertical Displacement

P0 at 1500 N	
Linear T1	
Vertical Displacement [mm]	Lateral Displacement [mm]
0.902575	7.23384
Linear T2	
Vertical Displacement [mm]	Lateral Displacement [mm]
0.884761	7.3409
Linear T3	
Vertical Displacement [mm]	Lateral Displacement [mm]
0.715982	7.39755
Linear T4	
Vertical Displacement [mm]	Lateral Displacement [mm]
0.860124	7.32738

5.1.3 Pilot Test Discussion

The pilot test data showed high linearity and showed high reproducibility. Correlation between the marker data and the tension applied were high, therefore, this system provides reliable data. Comparing the displacements at peak load showed very little difference with only 0.2mm difference for vertical displacement data and 0.16mm for lateral displacement. Therefore, there was error present when testing but not enough to re-evaluate the protocols created.

There was poor correlation with markers P8 and P9 in terms of linearity and consistency in the data. An explanation for these markers not showing a high degree of correlation was that they are near the area of varying inflection along the seat tube. A section of the seat tube near the saddle deflects negatively and deflect positively near the bottom bracket, which is shown in the displacement map in Figure 40 below. This deflection occurs along the seat tube because the vertical link that fixes the dropouts has a rotational degree of freedom along the x-axis(Figure 41).

The phenomena along the seat tube created a point of inflection along at the middle. This area may have changed from each test or as the tension load was increasing, hence, the point of inflection was not a fixed position. This explains the marker data from P8 and P9, placed at the middle of the seat tube, outputting inconsistent and unreliable data. Therefore, the data from the markers at the middle of the seat tube was not concidered at it was reliable near the headtube. The down tube, chain stays, and seat tube near the bottom bracket were still reliable data, hence, the comparison of CA01 LHS, CA01 RHS, CA02 RHS, and AR01 RHS was done and results are shown in the section below.

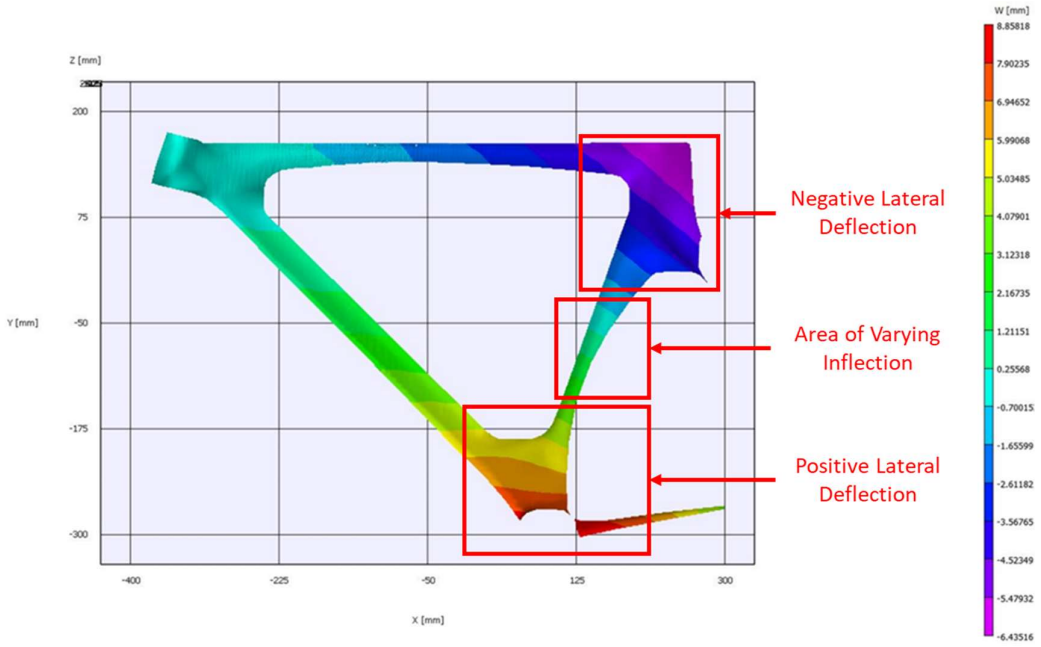

Figure 40: Pilot Test Displacement Map at 1500 N

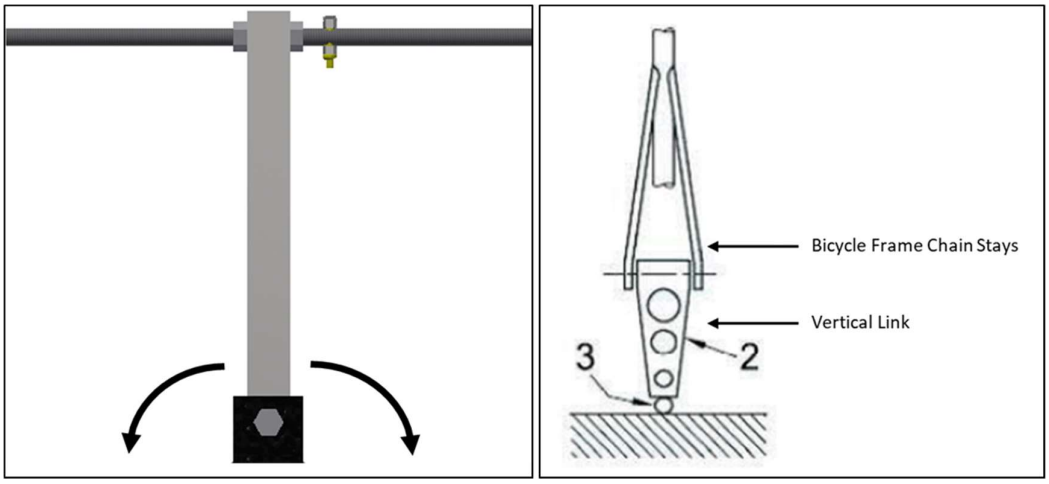

Figure 41: Vertical Link Design (Left) and Vertical Link from ISO 4210-6 (Right)

5.2 Bicycle Frame Structure Analysis

This section details the results obtained for CA01 LHS, CA01 RHS, CA02 RHS, and AR01 RHS undergoing the seven test cases (Section 4.2). Since DIC is capable of full-field investigations, lateral and vertical displacement of all bicycle frames was observed as the tension increases for the seven crank angle tests. The full-field investigations and recorded displacement data as tension increases are shown in this section. However, from the results found in Section 5.1, marker points at the middle of the seat tube are unreliable, therefore, marker data near this region (C8-C10) was not considered.

5.2.1 Displacement Maps

The displacement maps that were obtained from DIC show the development of lateral and vertical displacement for every section of the bicycle frame when testing the seven crank angles. Figure 42 and Figure 43 showed the lateral and vertical displacements for CA01 LHS when the load along the bottom bracket was increased at the 90^{O} crank angle. As tension increased, the lateral and vertical displacement increases along the down tube, seat tube, and chain stay near the bottom bracket. The chain stay section develops displacement faster compared to the other sections. However, the locations of the peak displacement values were different for lateral and vertical displacements. The section of the chain stay near the bottom bracket developed high lateral displacement, while vertical displacement was shown to develop away from the bottom bracket. The lateral displacement of the chain stay deflects 8.7mm (out-of- page) and vertical displacement deflect 2mm downward.

Lateral displacement of the chain stay, observed near the bottom bracket, was caused by the load applied along the bottom bracket. However, vertical displacement of the chain stay deflected away from the bottom bracket because of the lever arm created by the vertical link and bottom bracket. These areas of high displacements are found in all bicycle frame displacement maps and crank angle load cases. The bicycle displacement fields are shown in Appendix G.

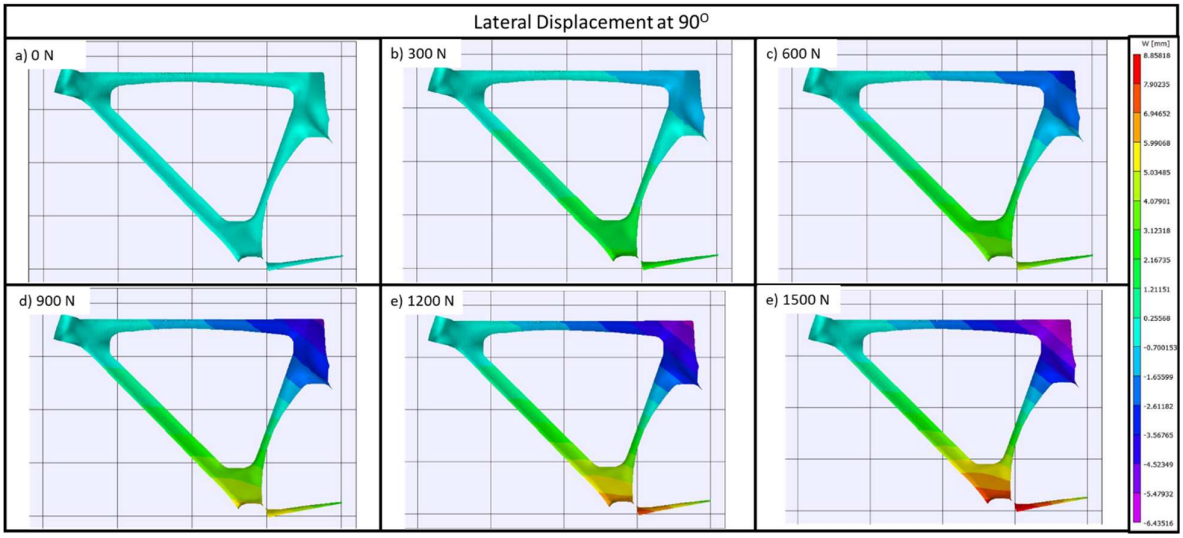

Figure 42: CA01 LHS at 90^{O} - Lateral Displacement Development from 0 N – 150 N

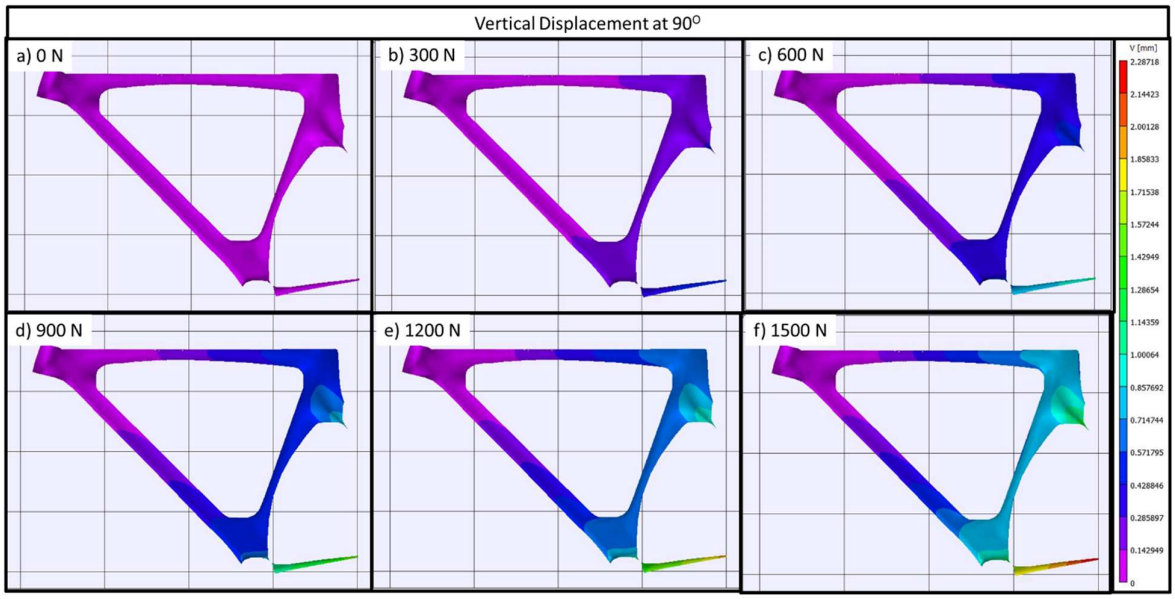

Figure 43: CA01 LHS at 90^{O} - Vertical Displacement Development from 0 N – 1500 N

An investigation into changing the crank angle was conducted to see if the displacement values changed. Observing the lateral displacement maps showed the bottom bracket increase in magnitude as the crank angle changes from 90^{O} – 180^{O}, shown in Figure 44 below. The vertical displacement maps in Figure 45 show that the seat tube and chain stay displacement decreases as crank angle increases while the down tube, stay relatively the same. Table 10 and Table 11 below show the difference between vertical and lateral displacement marker values with the 90^{O} crank angle is compared to the other angles.

The vertical displacement data (Table 10) showed relatively low variation when comparing the difference between crank angles. However, the difference in vertical displacement data could be subject to error caused by the system. The pilot test data (Section 5.1.2) showed a 0.2mm difference in vertical displacement. The vertical displacement data for the crank angle tests are within range. Although there were vertical displacement markers data greater than 0.2mm, they were minor with the highest at 0.38mm. Therefore, the vertical stiffness only changes slightly as the crank angle increases. This case was also the same for the rest of the bicycle frames tested, shown in Appendix E.

When observing the lateral displacement data for all bicycle frames, some sections experienced changes in displacement as the crank angle changes. Some differences in the lateral displacement data were out of the range in error documented in the pilot tests (Section 5.1.2). One significant difference was found was in CA01 LHS (Table 11) when comparing 90^{O} and 120^{O}. Marker placed near the bottom bracket displaced approximately 1mm. There were other considerable differences observed in the other bicycle frames.

- CA01 RHS had differences as high as 0.83mm in CA01 RHS along the chain stay as the crank angle increases from 90^{O} – 180^{O}.
- CA02 is having a difference of 0.9mm along the chain stay on the 180^{O} crank angle load case.
- AR01 is having differences in lateral displacement from 150^{O} – 180^{O} as high as 1.87mm.

The displacement maps and the marker data for the other bicycle frames are shown in Appendix E and Appendix G, respectively.

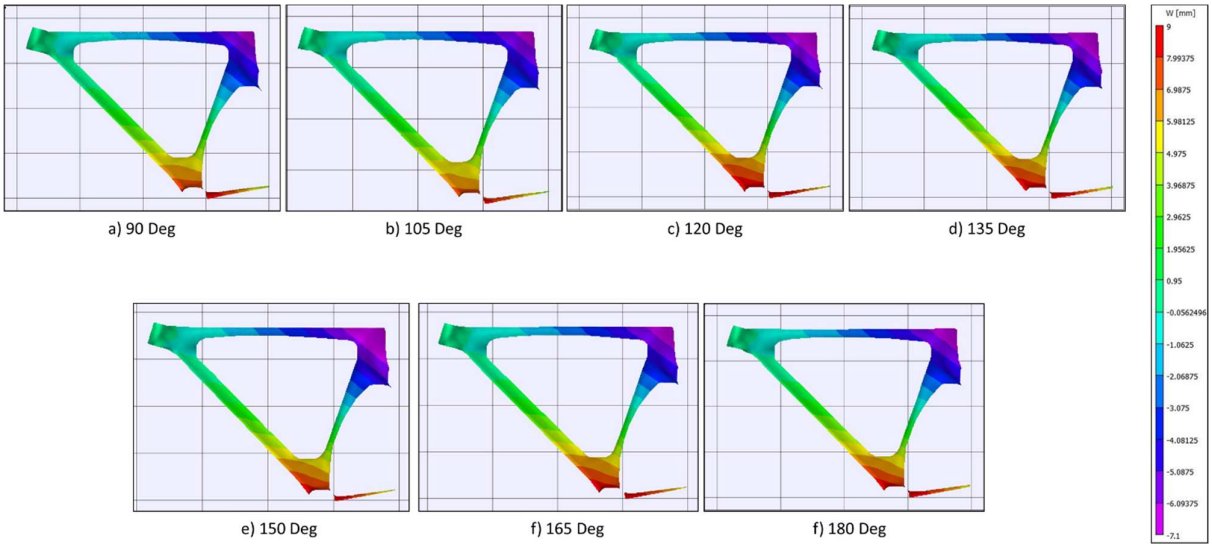

Figure 44: CA01 LHS Lateral Displacement Map at Different Crank Angles at 1500 N

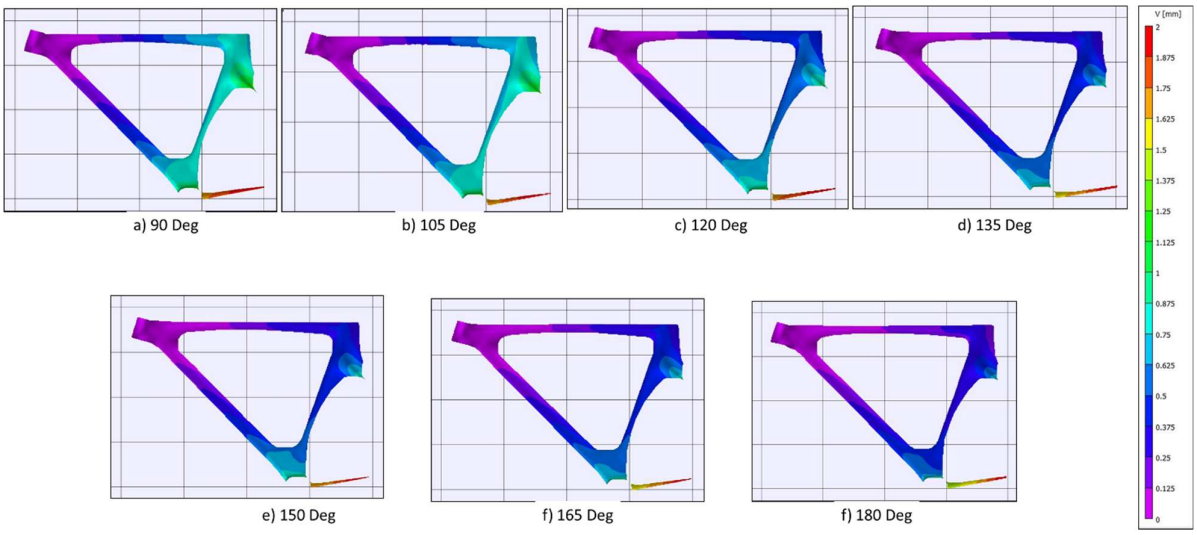

Figure 45: CA01 LHS Vertical Displacement Maps at Different Crank Angles at 1500 N

Table 10: Difference Between Crank Angles for CA01 LHS Vertical Displacement at 1500 N

Compare	C0	C1	C2	C3	C4	C5	C6	C7	C11	C12	C13
Angle 1 – Angle 2	V [mm]	V [mm]	V [mm]	V [mm]	V [mm]	V [mm]	V [mm]	V [mm]	V [mm]	V [mm]	V [mm]
90-105	0.01	0.01	0.01	0.00	-0.01	-0.01	0.01	0.01	0.03	0.04	0.04
90-120	0.08	0.07	0.05	0.05	0.03	0.02	0.13	0.15	0.00	0.02	0.01
90-135	0.18	0.17	0.14	0.11	0.10	0.08	0.24	0.28	0.16	0.17	0.17
90-150	0.14	0.12	0.09	0.07	0.06	0.03	0.20	0.24	0.06	0.08	0.08
90-165	0.20	0.18	0.16	0.13	0.10	0.08	0.26	0.29	0.17	0.17	0.16
90-180	0.29	0.25	0.20	0.16	0.13	0.09	0.35	0.38	0.25	0.26	0.25
	Bottom Bracket	Downtube					Seat Tube		Chain Stays		

Table 11: Difference Between Crank Angles for CA01 LHS Lateral Displacement at 1500 N

Compare	C0	C1	C2	C3	C4	C5	C6	C7	C11	C12	C13
Angle 1 – Angle 2	W [mm]	W [mm]	W [mm]	W [mm]	W [mm]	W [mm]	W [mm]	W [mm]	W [mm]	W [mm]	W [mm]
90-105	0.36	0.31	0.30	0.23	0.21	0.18	0.35	0.34	0.53	0.50	0.40
90-120	-1.06	-0.97	-0.95	-0.81	-0.69	-0.61	-0.67	-0.43	-0.94	-0.73	-0.66
90-135	-0.85	-0.78	-0.79	-0.74	-0.56	-0.51	-0.44	-0.10	-0.52	-0.50	-0.54
90-150	-0.40	-0.43	-0.48	-0.45	-0.44	-0.30	-0.02	0.25	-0.28	-0.06	0.00
90-165	-0.68	-0.72	-0.61	-0.59	-0.55	-0.49	-0.33	-0.16	-0.36	-0.16	-0.57
90-180	-0.44	-0.49	-0.53	-0.53	-0.50	-0.46	-0.10	0.17	-0.27	-0.17	-0.53
	Bottom Bracket	Downtube					Seat Tube		Chain Stays		

5.2.2 Comparison Between CA01 LHS, CA01 RHS, CA02 RHS, and AR01 RHS

The circle marker data and displacement maps for CA01 LHS, CA01 RHS, CA02 RHS, and AR01 RHS are compared in this section. CA01 RHS was chosen as a reference frame when comparing against the other bicycle frames. There are three comparison groups shown in this section, CA01 LHS vs. CA01 RHS, CA01 RHS vs. CA02 RHS, and CA01 RHS vs. AR01 RHS.

Figure 46 shows the development of lateral and vertical displacement maps for CA01 LHS and CA01 RHS. The displacement maps for both LHS and RHS developed similarly. Comparing the marker data shown in Table 13 and Table 14 below confirms this observation as the majority of the compared data had negligible differences for vertical displacement, however, lateral displacement was different. The vertical displacement for both bicycle frames were similar, and no major differences were found. The majority of the compared data fits within the error found in the pilot tests (Section 5.1.2). Therefore, the vertical displacement is similar between bicycle frames.

There were differences in lateral displacement between the LHS and RHS. The major difference was found at 105^{O}, where RHS displacement was considerably more than the LHS. Other marker data at different crank angles showed differences as well, such as, the RHS deflecting higher along the chain stays compared to the LHS at the 150^{O} crank angle. The marker data values used to compare these two tests are shown in Appendix I.

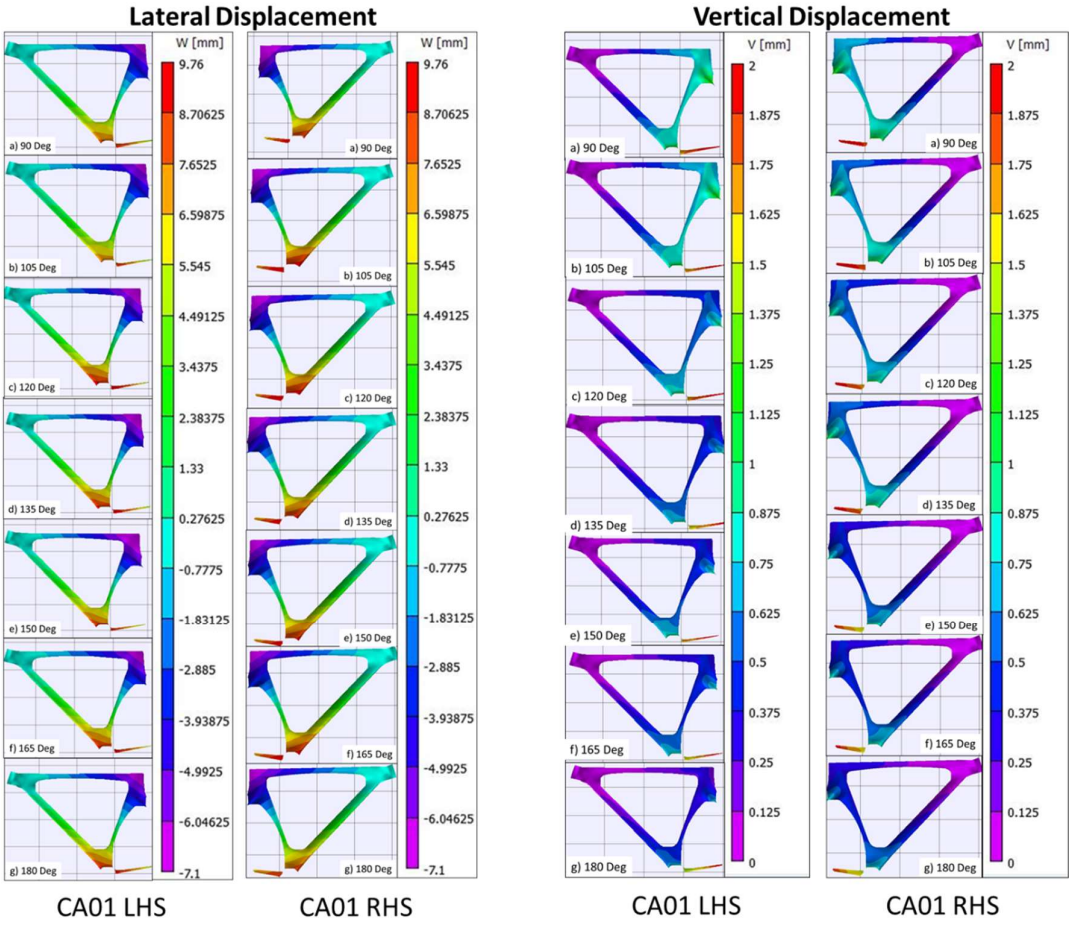

Figure 46: CA01 LHS and CA01 RHS Lateral (Left) and Vertical Displacement (Right) Maps at 1500 N During Downstroke

Table 12: Difference Between CA01 LHS and CA01 RHS Vertical Displacements at 1500 N

CA01 LHS - CA01 RHS											
Angle (Deg)	**C0**	**C1**	**C2**	**C3**	**C4**	**C5**	**C6**	**C7**	**C11**	**C12**	**C13**
	V [mm]	V [mm]	V [mm]	V [mm]	V [mm]	V [mm]	V [mm]	V [mm]	V [mm]	V [mm]	V [mm]
90	-0.02	-0.05	-0.02	-0.01	-0.01	-0.01	-0.04	0.00	-0.13	-0.14	-0.15
105	0.02	-0.02	0.00	0.01	0.03	0.02	0.55	0.00	-0.15	-0.15	-0.17
120	0.04	-0.01	0.03	0.03	0.04	0.04	-0.03	-0.01	-0.02	-0.03	-0.05
135	-0.09	-0.14	-0.09	-0.08	-0.06	-0.06	-0.17	-0.17	-0.18	-0.20	-0.23
150	0.08	0.03	0.06	0.05	0.05	0.05	0.03	0.03	0.07	0.06	0.05
165	0.02	-0.03	-0.02	-0.02	0.00	0.00	-0.04	-0.02	-0.05	-0.06	-0.08
180	-0.01	-0.05	-0.03	-0.01	-0.01	-0.01	-0.07	-0.06	-0.04	-0.05	-0.08
Sections	**BB**	**Down Tube**					**Seat Tube**		**Chain Stays**		

Table 13: Difference Between CA01 LHS and CA01 RHS Lateral Displacement at 1500 N

CA01 LHS - CA01 RHS											
Angle (Deg)	**C0**	**C1**	**C2**	**C3**	**C4**	**C5**	**C6**	**C7**	**C11**	**C12**	**C13**
	W [mm]	W [mm]	W [mm]	W [mm]	W [mm]	W [mm]	W [mm]	W [mm]	W [mm]	W [mm]	W [mm]
90	-0.28	-0.34	-0.24	-0.11	-0.05	-0.01	-0.10	0.09	-0.43	-0.28	-0.20
105	-1.26	-1.27	-1.05	-0.82	-0.68	-0.57	-1.08	-0.80	-1.73	-1.43	-1.22
120	0.18	0.03	0.17	0.28	0.18	0.26	-0.03	0.03	-0.28	-0.33	-0.27
135	0.38	0.18	0.31	0.32	0.22	0.20	0.11	-0.01	-0.20	-0.08	-0.14
150	-0.09	-0.19	-0.10	-0.03	0.09	-0.02	-0.34	-0.40	-0.44	-0.62	-0.88
165	0.17	-0.01	0.00	0.08	0.08	0.12	-0.01	0.02	-0.42	-0.61	-0.46
180	0.62	0.45	0.48	0.50	0.45	0.40	0.38	0.23	0.32	0.10	-0.04
Sections	**BB**	**Down Tube**					**Seat Tube**		**Chain Stays**		

Investigation of the CA designs was undertaken to observe if there were differences in stiffness between the two bicycle frames. Since CA01 and CA02 are the same design, the lateral and vertical displacement for these two bicycle frames were compared to observe if there are differences between bicycle frames of the same design. The RHS of both bicycle frames were tested and compared. Similar to the comparison before, the development of the displacement maps for both bicycle frames were similar, shown in Figure 47. For vertical displacement, the marker data (Table 14) confirms this as it showed very low differences in displacement, however, lateral displacement data (Table 15) showed considerable differences. There were large differences in lateral displacement along the chain stays at 150^{O} – 180^{O} crank angles, with CA02 deflecting higher than CA01.

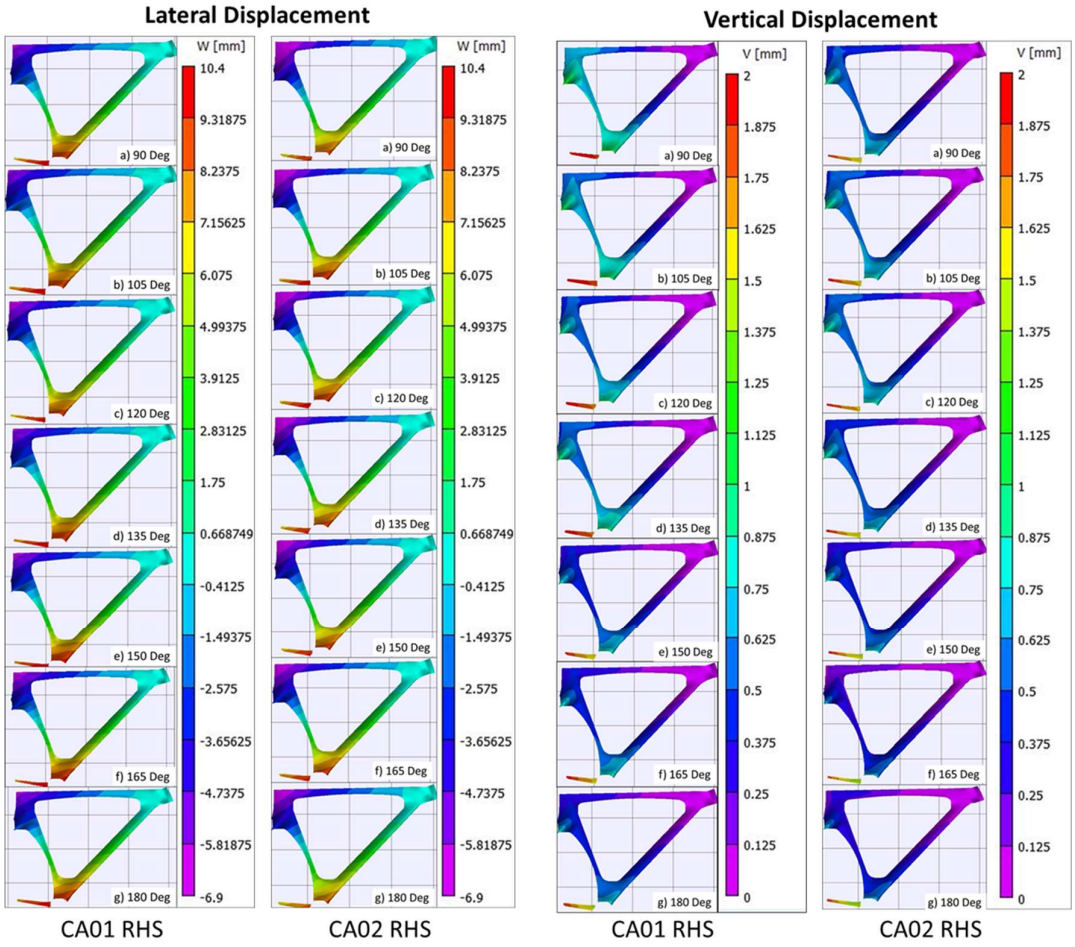

Figure 47: CA01 LHS and CA02 RHS Lateral (Left) and Vertical Displacement (Right) Maps at 1500 N During Downstroke

Table 14: Difference Between CA01 RHS and CA02 RHS Vertical Displacements at 1500 N

CA01 RHS - CA02RHS											
Angle (Deg)	**C0**	**C1**	**C2**	**C3**	**C4**	**C5**	**C6**	**C7**	**C11**	**C12**	**C13**
	V [mm]	V [mm]	V [mm]	V [mm]	V [mm]	V [mm]	V [mm]	V [mm]	V [mm]	V [mm]	V [mm]
90	0.26	0.28	0.24	0.19	0.16	0.14	0.24	0.20	0.28	0.31	0.34
105	0.18	0.21	0.19	0.14	0.10	0.08	-0.40	0.15	0.22	0.22	0.25
120	0.11	0.14	0.13	0.07	0.06	0.05	0.07	0.03	0.13	0.14	0.16
135	0.19	0.22	0.18	0.15	0.12	0.11	0.15	0.12	0.20	0.21	0.22
150	0.11	0.14	0.13	0.09	0.07	0.06	0.08	0.05	0.07	0.06	0.05
165	0.20	0.22	0.19	0.14	0.10	0.08	0.19	0.16	0.18	0.19	0.19
180	0.14	0.16	0.15	0.10	0.08	0.07	0.13	0.09	0.10	0.09	0.08
Sections	**BB**	**Down Tube**					**Seat Tube**		**Chain Stays**		

Table 15: Difference Between CA01 RHS vs. CA02 RHS Lateral Displacements at 1500 N

CA01 RHS - CA02RHS										
Angle (Deg)	**C0**	**C1**	**C2**	**C3**	**C4**	**C5**	**C6**	**C7**	**C12**	**C13**
	W [mm]	W [mm]	W [mm]	W [mm]	W [mm]	W [mm]	W [mm]	W [mm]	W [mm]	W [mm]
90	-0.33	-0.27	-0.08	-0.16	-0.22	-0.20	-0.51	-0.50	-0.86	-0.87
105	0.30	0.38	0.51	0.37	0.29	0.22	0.05	-0.03	-0.44	-0.59
120	0.53	0.53	0.64	0.39	0.37	0.22	0.35	0.36	0.10	-0.01
135	-0.29	-0.13	-0.04	-0.04	-0.09	-0.04	-0.39	-0.43	-0.88	-0.91
150	-0.42	-0.30	-0.11	-0.14	-0.23	-0.18	-0.44	-0.36	-0.98	-1.13
165	-0.41	-0.25	-0.18	-0.20	-0.20	-0.18	-0.39	-0.23	-0.82	-1.01
180	-0.84	-0.70	-0.51	-0.55	-0.50	-0.42	-0.81	-0.73	-1.32	-1.42
Sections	**BB**	**Down Tube**					**Seat Tube**		**Chain Stays**	

A comparison between CA01 and AR01 designs was conducted to observe which design was stiffer when undergoing similar loading conditions. The testing rig aims to emulate the cycling loads of sprint cyclists at maximum effort during the downstroke phase. Hence, comparing these two bicycle frames may show which design offers high lateral stiffness and good vertical compliance. Observing the vertical displacement maps in Figure 48 showed that AR01 RHS deflects higher at the bottom bracket and seat tube compared to CA01 RHS for both displacement values. However, the marker data in Table 16 showed high similarity between the vertical displacements for both frames. Although the development for both bicycle frames develops differently, the marker data displayed a high similarity between the bicycle frames. Therefore, the vertical displacement of both bicycle frames were similar when applying the loading conditions.

The lateral displacement maps of both bicycle frames show the same deflections profile as the crank increases, where the down tube, seat tube and chain stay near the bottom bracket appear to have the higher deflections. However, differences in the displacement maps for CA01 RHS showed higher displacement values developing at the down tube compared to the AR01 RHS design. Comparing the difference in lateral displacement marker data (Table 17) validates this observation as CA01 RHS down tube markers, C1 – C5, deflects higher compared to AR01 RHS. The lateral displacement for CA01 RHS at the chain stays (C11 – C13) were also higher compared to AR01. Therefore, the AR01 design is stiffer laterally when compared to the CA01 design.

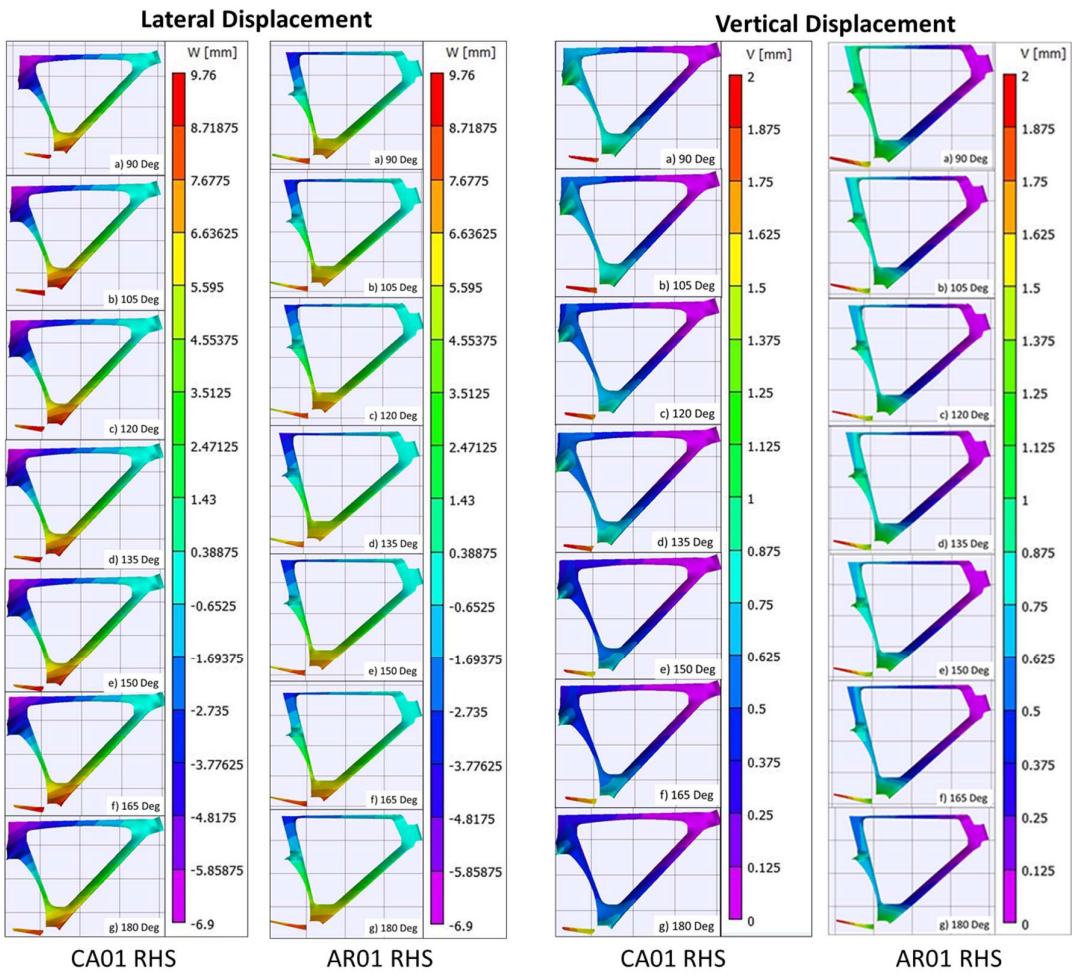

Figure 48: CA01 RHS and AR01 RHS Lateral (Left) and Vertical Displacement (Right) Maps at 1500 N During Downstroke

Table 16: Difference Between CA01 RHS and AR01 RHS Vertical Displacements at 1500 N

CA01 RHS - AR01 RHS											
Angle (Deg)	**C0**	**C1**	**C2**	**C3**	**C4**	**C5**	**C6**	**C7**	**C11**	**C12**	**C13**
	V [mm]	V [mm]	V [mm]	V [mm]	V [mm]	V [mm]	V [mm]	V [mm]	V [mm]	V [mm]	V [mm]
90	-0.21	0.06	0.19	0.16	0.12	0.11	-0.13	-0.16	0.26	0.13	0.07
105	-0.17	0.11	0.21	0.17	0.13	0.11	-0.62	-0.06	0.31	0.20	0.15
120	-0.24	0.04	0.15	0.11	0.08	0.07	-0.14	-0.17	0.25	0.15	0.11
135	-0.21	0.07	0.16	0.14	0.10	0.09	-0.09	-0.12	0.25	0.14	0.09
150	-0.35	-0.06	0.06	0.04	0.02	0.02	-0.24	-0.28	0.08	-0.04	-0.10
165	-0.26	0.01	0.13	0.10	0.07	0.06	-0.14	-0.17	0.18	0.08	0.03
180	-0.31	-0.02	0.11	0.07	0.06	0.06	-0.16	-0.20	0.11	0.00	-0.05
Sections	**BB**	**Down Tube**					**Seat Tube**		**Chain Stays**		

Table 17: Difference Between CA01 RHS and AR01 RHS Lateral Displacements at 1500 N

CA01 RHS - AR01 RHS											
Angle (Deg)	**C0**	**C1**	**C2**	**C3**	**C4**	**C5**	**C6**	**C7**	**C11**	**C12**	**C13**
	W [mm]	W [mm]	W [mm]	W [mm]	W [mm]	W [mm]	W [mm]	W [mm]	W [mm]	W [mm]	W [mm]
90	0.84	0.93	1.25	0.90	0.69	0.49	0.20	-0.31	0.82	0.96	0.95
105	1.61	1.74	1.81	1.39	1.13	0.86	0.98	0.31	1.90	1.73	1.63
120	1.34	1.41	1.51	1.07	0.94	0.69	0.74	0.08	1.56	1.49	1.15
135	1.12	1.22	1.23	0.94	0.69	0.48	0.69	0.06	1.18	0.88	0.49
150	1.15	1.24	1.33	1.00	0.70	0.49	0.72	0.09	1.18	0.97	0.70
165	0.95	1.07	1.11	0.78	0.61	0.37	0.56	-0.11	0.84	0.46	-0.05
180	0.55	0.63	0.81	0.48	0.34	0.27	0.29	-0.26	0.31	-0.09	-0.56
Sections	**BB**	**Down Tube**					**Seat Tube**		**Chain Stays**		

6 Discussion

An investigation of three bicycle frames was conducted to observe the structural stiffness of each design while using DIC to provide a full-field assessment of these structures. Since the bicycle frames investigated are used by elite velodrome sprint cyclists, this study aimed to implement loads along the bottom bracket similar to the loads generated by these athletes. A testing rig was created to apply 266 N.m of cycling torque during the downstroke phase, which ranges from 0^{O}-180^{O} (Korff et al. 2007; Martin et al. 2006). However, the design was limited to 90^{O} – 180^{O} as to avoid design complexity of the testing rig. Observing the displacement map as tension increases showed the development of vertical and lateral stiffness on the bicycle frame. As tension increased, the lateral displacement of the down tube, seat tube and chain stay near the bottom bracket began to increase.

The use of 3D-DIC for this study to measure displacement yielded full-field assessments of these structures. However, some factors must be considered when using this type of measuring technique. Speckle pattern quality, calibration, and image artefacts affect the displacements measured and must be removed to obtain high-quality measurements (Park et al. 2017; Schreier, Orteu & Sutton 2009; Pan et al. 2008; Lecompte et al. 2006). The lateral displacement maps found correlate to the displacement map found in Maestrelli and Falsini (2008), however, the results found were different as this study normalised the data. A comparison to the data found from this paper cannot be not done because the loading conditions were different compared to this study. Hence, the magnitude of the displacement were different but the displacement maps are similar. Moreover, the vertical displacement for all bicycle frames tested had very similar values with no variation between crank angle test cases, which means the vertical compliance for all the bicycles were the same. Therefore, the results found in this study may show another method of measuring displacement on bicycle frame structures.

An investigation of the downstroke phase affecting the magnitude of lateral and vertical displacement was also done to find areas of low stiffness as the crank angle increases. It was found that lateral and vertical displacement maps showed an increase in magnitude at sections along the down tube, seat tube, and chain stays as the crank angle increases. Vertical displacement values for all comparison tests show similar results, however, there were considerable differences in lateral displacement. CA01 LHS showed the highest difference at the 120^{O} crank angle with displacements being high near the bottom bracket. Therefore, there could be less material near the bottom bracket, or the direction of the carbon fibre direction was not optimised at this crank angle. Furthermore, there were notable differences found on the other bicycle frames. CA02 RHS had high lateral displacement along the chain stays, CA01 RHS had high lateral displacement along the chain stay at the 180^{O} loading case, and AR01 having high differences along the chain stays. Therefore, there were differences in stiffness as the crank angle changes. These differences in displacement might be caused by the manufacturing process, which relies on parameters such as void content, differences in curing, amount of material, or direction of uniaxial carbon fibre (Bie et al. 2017; Chang et al. 2017; Rahmani et al. 2014).

Structural analyses of four tests were compared to investigate if there were differences between each design. It was found that the CA design showed very similar vertical displacement, however, the lateral displacements found were different. The LHS and RHS comparison showed large differences in lateral displacement as the crank angle changed. CA01 and CA02 showed large differences in lateral displacement as well, with the chain stay being the highest difference found. Therefore, the differences in lateral displacement may be caused by the manufacturing process for this bicycle frame design.

When comparing the different designs, CA01 and AR01, showed AR01 had slightly lower lateral displacement values when both are undergoing the same loading conditions. Since the lateral displacement values affect the performance of the athlete, the AR01 is slightly more efficient than CA01. Since the testing conditions aimed to emulate the sprint cycling conditions, the AR01 design translates the mechanical output of the cyclists more efficiently than the CA01 design. Hence, making the AR01 design stiffer under sprint cyclist conditions.

6.1 Limitations

Although this project has reached its aims, there were unavoidable limitations. Firstly, image artefacts such as dust, water spots, imperfections on the specimen, or reflections may have affected the images captured. All of these image artefacts were considered while testing the bicycle frame but may have altered the results slightly as these artefacts can only be reduced and not eliminated. The impact of the results may have only been minor as the linearity and reproducibility results shows high reliability.

Secondly, a limitation of this study was the direction of the tension force applied while testing. Tension was applied vertically for all tests and may not represent real cycling conditions as the direction of the force must be tangential to the crank. Applying the forces tangential to the to the crank could have shown different results either in the magnitude of the displacement values or the displacement maps. Furthermore, the testing rig design created for this project created this limitation because this was not identified as a requirement and the current design did not have the range to create tangential forces. Therefore, these tests may not be accurate to real cycling. Thirdly, the methods and techniques developed for this study that new and the number of bicycle frames tested were small. This small sample size affects the validation of this study as statistical error may be present. Therefore, increasing the number of bicycle frames tested and comparing them may validate these techniques. Lastly, a secondary measurement device was not used to provide a concrete measurement such as using strain gauges or dial gauges. Digital image correlation can be subjected to image artefacts and error, therefore, using these measurement tool could have verified the accuracy of the measurements.

7 Conclusion

Digital image correlation was used to assess the structural stiffness of three carbon fibre bicycle frames, two with the same design (CA01 and CA02), and one that is different (AR01). This measurement technique was able to assess the full structure of the bicycle frame and showed areas of vertical and lateral displacement. There are two testing protocols used to obtain the results. The testing protocol tested seven crank angle test cases to investigate the displacement as the crank angle changes during the downstroke phase at maximal effort. However, the lateral and vertical displacement marker data found had no major differences as the crank angle increased. The post-processing protocol obtained the displacement maps to show the regions of high displacement and marker data was extracted to attain quantitative information on the tube sections.

Displacement maps were very helpful as they showed the regions of lateral displacement. For all bicycle frames, it was found that the seat tube, down tube and chain stays near the bottom bracket that had high lateral displacement values. Therefore, this area lowers the efficiency of the athlete because of this area deflecting at a high amount. Moreover, the vertical displacement maps and marker data showed very similar displacement values for all bicycle frames.

The comparison between the four tests displayed very interesting results. The CA design was investigated closely as there are three tests dedicated to this design. These comparison tests showed a high difference between the LHS and RHS of one bicycle frame and between two bicycle frames with the same design. Hence, there may be imperfections present when manufacturing this design. However, when compared to the AR design, the CA design deflected slightly higher along the seat tube, down tube and chain stays near the bottom bracket. Therefore, making the AR design more efficient in transferring mechanical output.

7.1 Future Work

There are areas of future work that can arise from the results found. Firstly, increasing the number of bicycle frames tested of the same model and comparing the results found could strengthen the amount the results obtained, and validate the new techniques created in this study. Secondly, comparing the results obtained from analytical modelling such as FEA with the results found from DIC for a bicycle frame design. Comparing these two methods may show differences between the CAD model and the constructed bicycle frame. Thirdly, create a testing rig design that fixes the bicycle frame that is able to apply tension forces tangential to the crank angle. Improving the testing rig design may emulate actual cycling more closely than what was done in this study. Applying the these tangential forces may show different lateral and vertical displacement values and displacement maps. Lastly, applying a higher quality speckle pattern in future tests must be investigated to improve the results obtained and may reduce error.

8 References

Arola, D, Reinhall, PG, Jenkins, MG & Iverson, SC 1999, 'Experimental analysis of a hybrid bicycle frame', *Experimental Techniques*, vol. 23, no. 3, pp. 21–24.

ASM International 2001, *ASM Handbook Volume 2 Properties and Selection: Nonferrous Alloys and Special -Purpose Materials*, *Technology*, vol. 2.

Baldissera, P & Delprete, C 2014, 'Structural design of a composite bicycle fork', *Materials and Design*, vol. 60, pp. 102–107.

Baumgart, F & Cordey, J 2001, 'Stiffness - An unknown world of mechanical science?', *Injury*, vol. 32, pp. 14–23.

Bie, BX, Huang, JY, Fan, D, Sun, T, Fezzaa, K, Xiao, XH, Qi, ML & Luo, SN 2017, 'Orientation-dependent tensile deformation and damage of a T700 carbon fiber/epoxy composite: A synchrotron-based study', *Carbon*, vol. 121, pp. 127–133.

Bini, RR & Carpes, FP 2014, *Biomechanics of cycling*, *Biomechanics of Cycling*.

Chang, T, Zhan, L, Tan, W & Li, S 2017, 'Void content and interfacial properties of composite laminates under different autoclave cure pressure', *Composite Interfaces*, vol. 24, Taylor & Francis, no. 5, pp. 529–540.

Correlated Solutions Inc. 2016, *Vic-3d V7 Reference Manual*, pp. 1–111.

Covill, D, Allard, P, Drouet, JM & Emerson, N 2016, 'An Assessment of Bicycle Frame Behaviour under Various Load Conditions Using Numerical Simulations', *Procedia Engineering*, vol. 147, Elsevier B.V., pp. 665–670.

Covill, D, Begg, S, Elton, E, Milne, M, Morris, R & Katz, T 2014, 'Parametric finite element analysis of bicycle frame geometries', *Procedia Engineering*, vol. 72, Elsevier B.V., pp. 441–446.

Covill, D, Blayden, A, Coren, D & Begg, S 2015, 'Parametric finite element analysis of steel bicycle frames: The influence of tube selection on frame stiffness', *Procedia Engineering*, vol. 112, Elsevier B.V., pp. 34–39.

Dorel, S, Couturier, A, Lacour, JR, Vandewalle, H, Hautier, C & Hug, F 2010, 'Force-velocity relationship in cycling revisited: Benefit of two-dimensional pedal forces analysis', *Medicine and Science in Sports and Exercise*, vol. 42, no. 6, pp. 1174–1183.

Dorel, S, Hautier, CA, Rambaud, O, Rouffet, D, Van Praagh, E, Lacour, JR & Bourdin, M 2005, 'Torque and power-velocity relationships in cycling: Relevance to track sprint performance in world-class cyclists', *International Journal of Sports Medicine*, vol. 26, no. 9, pp. 739–746.

Froes, F., Haake, S, Fagg, S, Tabeshfar, K & Velay, X 1988, 'Materials for Sports', pp. 6–11.

Gardner, AS, Martin, JC, Martin, DT, Barras, M & Jenkins, DG 2007, 'Maximal torque- and power-pedaling rate relationships for elite sprint cyclists in laboratory and field tests', *European Journal of Applied Physiology*, vol. 101, no. 3, pp. 287–292.

Giagopoulos, D & Arailopoulos, A 2017, 'Computational framework for model updating of large scale linear and nonlinear finite element models using state of the art evolution strategy', *Computers & Structures*, vol. 192, Elsevier Ltd, pp. 210–232.

Hashin, Z 1983, 'Analysis of Composite Materials—A Survey', *Journal of Applied Mechanics*, vol. 50, no. 3, p. 481.

Ho, YC, Sasayama, H & Yanagimoto, J 2017, 'Mechanical properties and drawing process of multilayer carbon-fiber-reinforced plastic sheets with various prepreg thicknesses', *Advances in Mechanical Engineering*, vol. 9, no. 3, pp. 1–12.

Huang, Y & Young, RJ 1995, 'Interfacial behaviour in high temperature cured carbon fibre/epoxy resin model composite', *Composites*, vol. 26, no. 8, pp. 541–550.

Hull, ML & Davis, R 1981, 'Design of Aluminium Bicycle Frames', *Journal of Mechanical Design*, vol. 103, no. October 1981, pp. 901–907.

International Organization for Standardization 2015, 'ISO 4210-6:2015 - Cycles -- Safety requirements for bicycles -- Part 6: Frame and fork test methods', *2015-09-01*.

Jeukendrup, AE, Craig, NP & Hawley, JA 2000, 'The bioenergetics of world class cycling', *Journal of Science and Medicine in Sport*, vol. 3, no. 4, pp. 414–433.

Katch, VL, McArdle, WD & Katch, FI 2013, *Essentials of exercise physiology: Fourth edition*, *Essentials of Exercise Physiology: Fourth Edition*.

Kelly, B & Costello, C 2004, 'FEA modelling of setting and mechanical testing of aluminum blind rivets', *Journal of Materials Processing Technology*, vol. 153–154, no. 1–3, pp. 74–79.

Koellner, A, Cameron, CJ & Battley, MA 2014, 'Measurement and analysis system for bicycle field test studies', *Procedia Engineering*, vol. 72, Elsevier B.V., no. 0, pp. 350–355.

Korff, T, Romer, LM, Mayhew, I & Martin, JC 2007, 'Effect of pedaling technique on mechanical effectiveness and efficiency in cyclists', *Medicine and Science in Sports and Exercise*, vol. 39, no. 6, pp. 991–995.

Lecompte, D, Smits, A, Bossuyt, S, Sol, H, Vantomme, J, Van Hemelrijck, D & Habraken, AM 2006, 'Quality assessment of speckle patterns for digital image correlation', *Optics and Lasers in Engineering*, vol. 44, no. 11, pp. 1132–1145.

Lessard, L, Nemes, J & Lizotte, PL 1995, 'Utilization of FEA in the design of composite bicycle frames', *Composites*, vol. 26, no. 1, pp. 72–74.

Logan, DL 2011, *First Course in Finite Element Methods*, R Adams, H Gowans & T Altieri (eds), Fifth, Global Engineering, Stamford CT.

Maestrelli, L & Falsini, A 2008, 'Bicycle Frame Optimization By Means of an Advanced Gradient Method Algorithm', *Htc*.

Manolova, a. V. & Bertucci, W 2011, 'Measurements of strain in bicycle frame through different conditions of test', *Computer Methods in Biomechanics and Biomedical Engineering*, vol. 14, pp. 57–59.

Manolova, A V, Crequy, S, Lestriez, P, Debraux, P & Bertucci, WM 2015, 'Relationship between the Pedaling Biomechanics and Strain of Bicycle Frame during Submaximal Tests', *Sports*, vol. 3, pp. 87–102.

Martin, JC, Gardner, AS, Barras, M & Martin, DT 2006, 'Modeling sprint cycling using field-derived parameters and forward integration', *Medicine and Science in Sports and Exercise*, vol. 38, no. 3, pp. 592–597.

Minus, ML & Kumar, S 2005, 'The processing, properties, and structure of carbon fibers', *Journal of the Minerals, Metals and Materials Society*, vol. 57, pp. 52–58.

National Instruments 2014, *Measuring Straing with Strain Gauges*, National Instruments, p. 9.

Nelson, R 2003, 'Bike frame races carbon consumer goods forward', *Nelson, R, Composites, C & Oclv, T 2003, 'Bike frame races carbon consumer goods forward', Reinforced Plastics, vol. 47, no. 7, pp. 36–40.Reinforced Plastics*, vol. 47, no. 7, pp. 36–40.

Niinomi, M 1998, *Mechanical properties of biomedical titanium alloys*, *Materials Science and Engineering: A*, vol. 243, no. 1–2, pp. 231–236.

Pan, B, Xie, H, Wang, Z, Qian, K & Wang, Z 2008, 'Study on subset size selection in digital image correlation for speckle patterns', *Optics Express*, vol. 16, no. 10, p. 7037.

Park, J, Yoon, S, Kwon, TH & Park, K 2017, 'Assessment of speckle-pattern quality in digital image correlation based on gray intensity and speckle morphology', *Optics and Lasers in Engineering*, vol. 91, Elsevier, no. February 2016, pp. 62–72.

Profilium 2017, *PROFILE 40×40 – 4 SLOT*.

Rahmani, H, Najafi, SHM, Saffarzadeh-Matin, S & Ashori, A 2014, 'Mechanical properties of carbon fiber/epoxy composites: Effects of number of plies, fiber contents, and angle-ply Layers', *Polymer Engineering and Science*, vol. 54, no. 11, pp. 2676–2682.

Ramault, C, Makris, A, Van Hemelrijck, D, Lamkanfi, E & Van Paepegem, W 2011, 'Comparison of different techniques for strain monitoring of a biaxially loaded cruciform specimen', *Strain*, vol. 47, no. SUPPL. 2, pp. 210–217.

Ramos, T, Braga, DFO, Eslami, S, Tavares, PJ & Moreira, PMGP 2015, 'Comparison between Finite Element Method Simulation, Digital Image Correlation and Strain Gauges Measurements in a 3-Point Bending Flexural Test', in *Procedia Engineering*, vol. 114, pp. 232–239.

Reu, P 2012, 'Introduction to Digital Image Correlation: Best Practices and Applications', *Experimental Techniques*, vol. 36, no. 1, pp. 3–4.

Rontescu, C, Cicic, TD, Amza, CG, Chivu, O & Dobrotă, D 2015, 'Choosing the Optimum Material for Making a Bicycle Frame', *Metalurgija*, vol. 54, no. 4, pp. 679–682.

Schreier, H, Orteu, JJ & Sutton, MA 2009, *Image correlation for shape, motion and deformation measurements: Basic concepts, theory and applications*, *Image Correlation for Shape, Motion and Deformation Measurements: Basic Concepts,Theory and Applications*.

Serway, J 2004, *Physics for Scientists and Engineers*, *Journal of College Science Teaching*, no. 6.

Tara, R 2017, *How to Design the Lightest Possible Bike - And Still Sleep at Night*.

Union Cycliste Internationale 2018, 'Part 11 Olympic Games', *UCI Cyling Regulations*.

Usamentiaga, R, Ibarra-Castanedo, C, Klein, M, Maldague, X, Peeters, J & Sanchez-Beato, A 2017, 'Nondestructive Evaluation of Carbon Fiber Bicycle Frames Using Infrared Thermography', *Sensors*, vol. 17, no. 11, p. 2679.

Vandermark, R 1997, 'Opportunities for the titanium industry in bicycles and wheelchairs', *JOM*, vol.

49, no. 6, pp. 24–27.

Wang, JH, Zhao, JN, Zhao, YS, Wang, Z & Guo, DL 2010, 'Simulation about Sports Bicycle Frame Based on the Experiments', *Applied Mechanics and Materials*, vol. 37–38, pp. 1142–1147.

9 Appendix A – Project Timeline

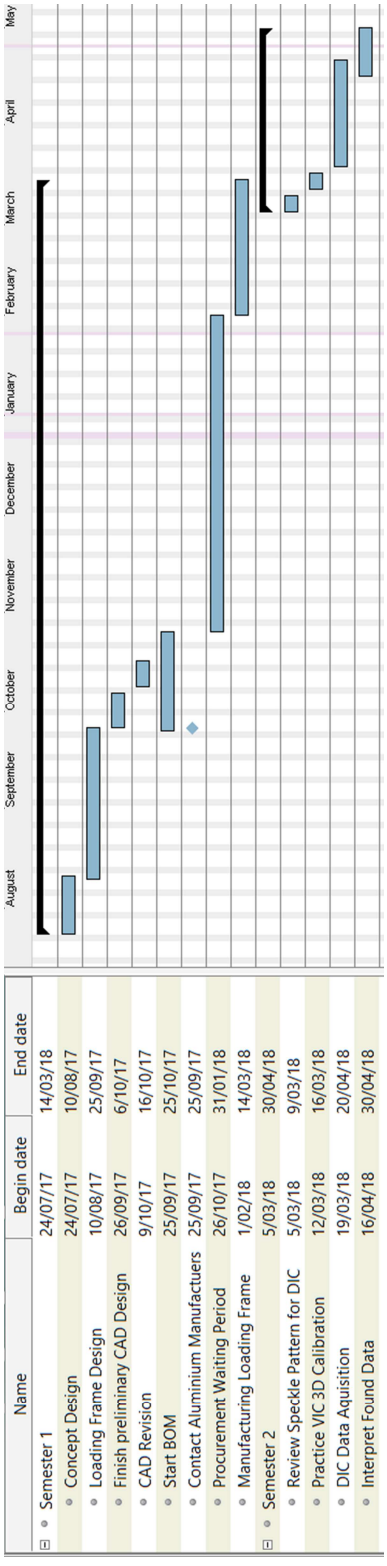

Name	Begin date	End date
Semester 1	24/07/17	14/03/18
Concept Design	24/07/17	10/08/17
Loading Frame Design	10/08/17	25/09/17
Finish preliminary CAD Design	26/09/17	6/10/17
CAD Revision	9/10/17	16/10/17
Start BOM	25/09/17	25/10/17
Contact Aluminium Manufactuers	25/09/17	25/09/17
Procurement Waiting Period	26/10/17	31/01/18
Manufacturing Loading Frame	1/02/18	14/03/18
Semester 2	5/03/18	30/04/18
Review Speckle Pattern for DIC	5/03/18	9/03/18
Practice VIC 3D Calibration	12/03/18	16/03/18
DIC Data Aquisition	19/03/18	20/04/18
Interpret Found Data	16/04/18	30/04/18

10 Appendix B – Concept Drawings

Below show the concept drawings.

ALUMINIUM EXTRUSION PROFILE : USING 4040 & 8040 T SLOT PROFILES.

1:20 scale

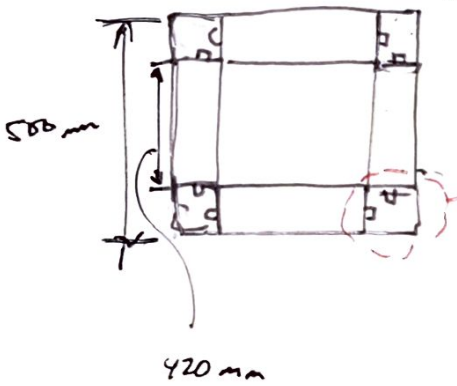

Half slot : Angled.

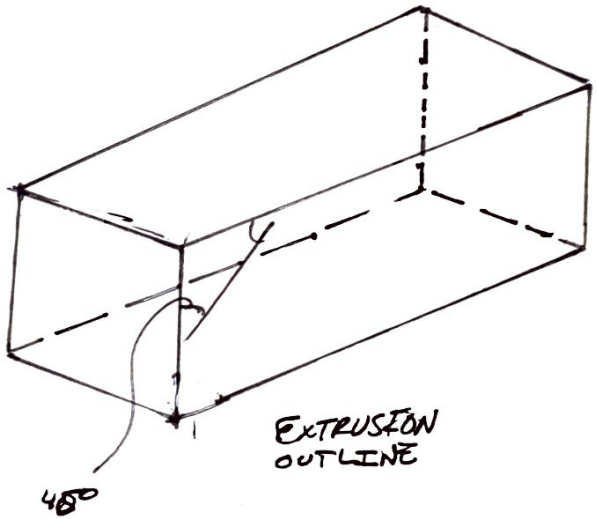

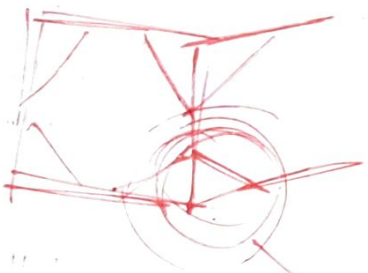

Joint angle 45° 40x80

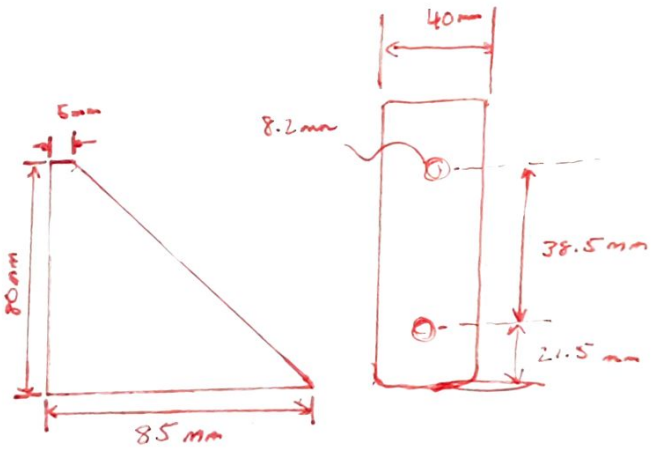

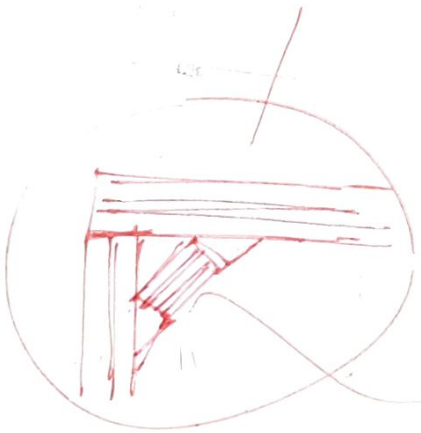

8040 EXTRUSION

Circle fixed bracket dimensions:

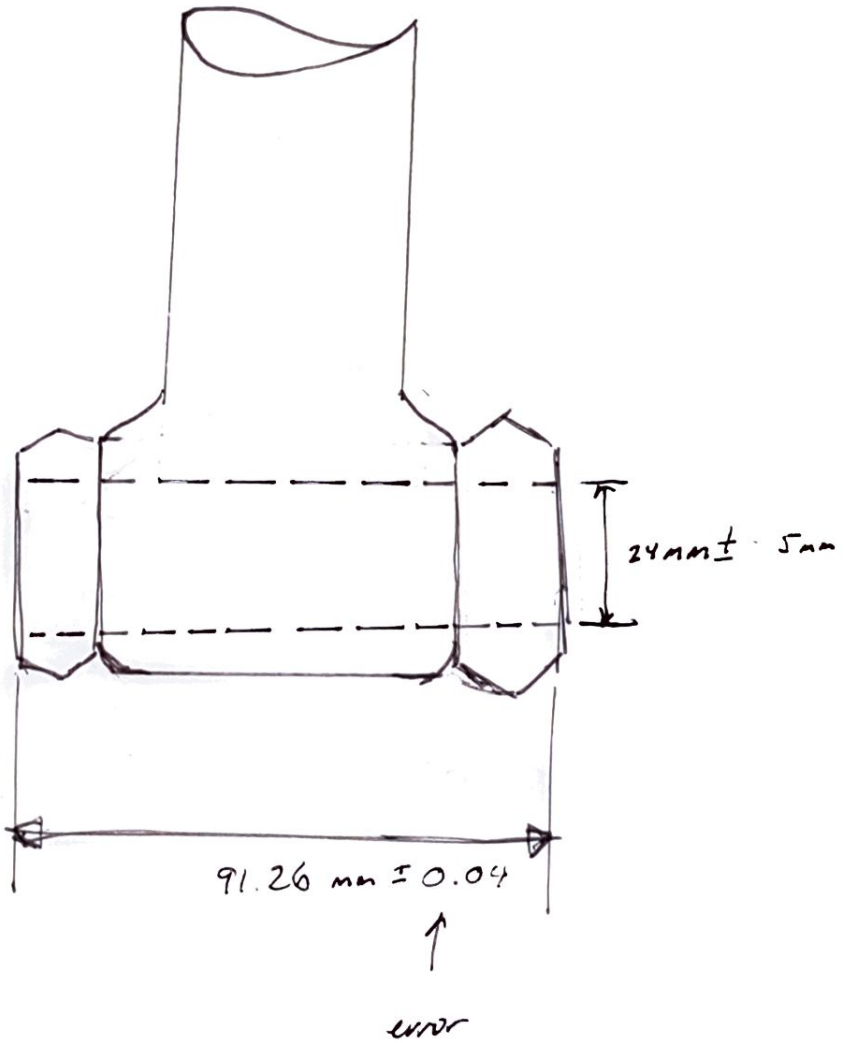

- 65 = 23mm

Fixed bracket design:

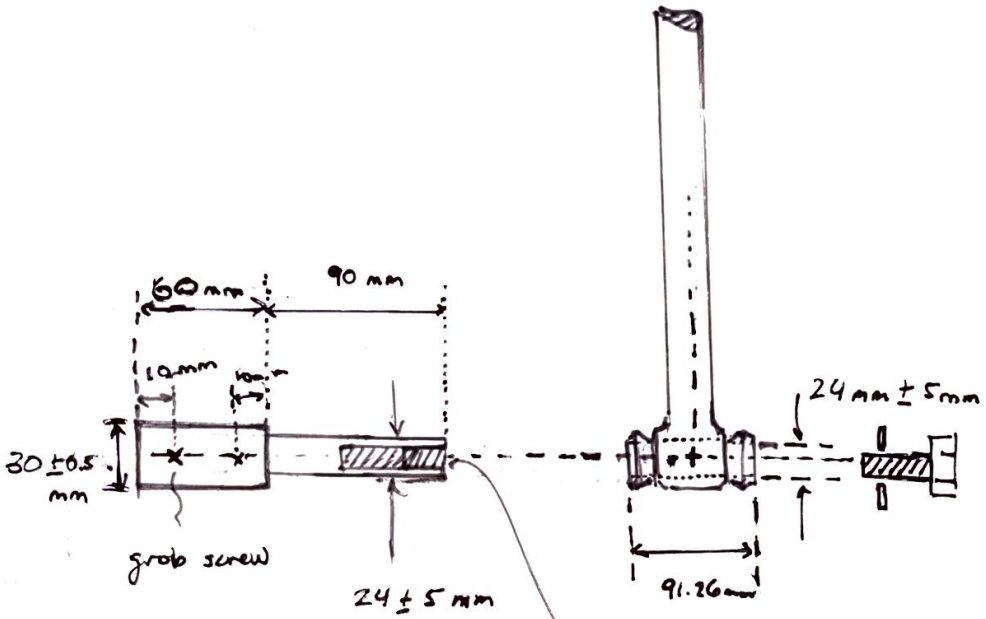

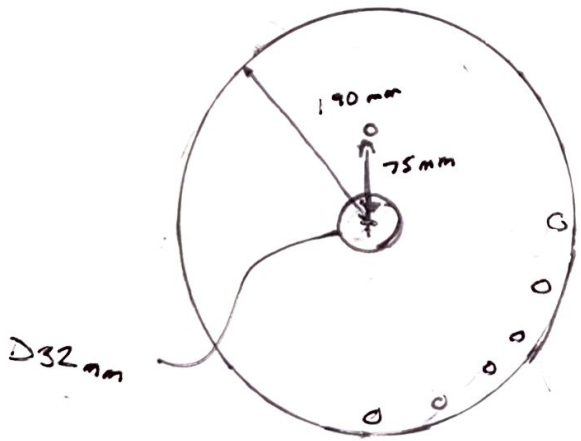

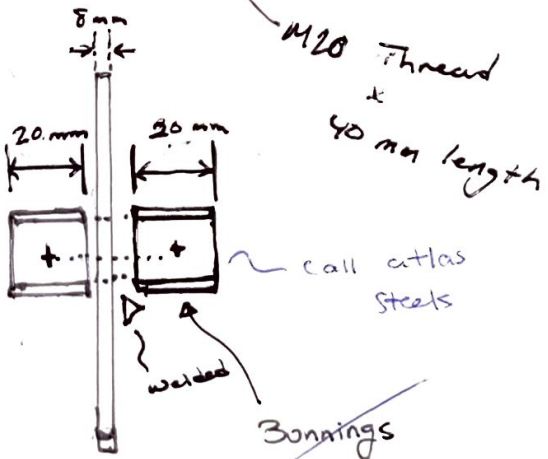

M20 Thread
+
40 mm length

call atlas steels

Bonnings
- Metal Mate
' 31.8 x 1.2m
Galvanised Steel
Round tube'

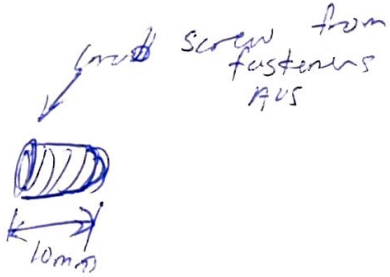

Fasteners Australia:

2x M20 Hex bolts (galv)
4.50 each + gst

2x 20mm Washers
0.70 each (galv)

BOTTOM BRACKET IDEAS:

Keeping 7° ± 0.5° of Force applied into consideration

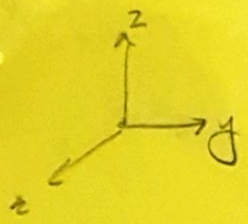

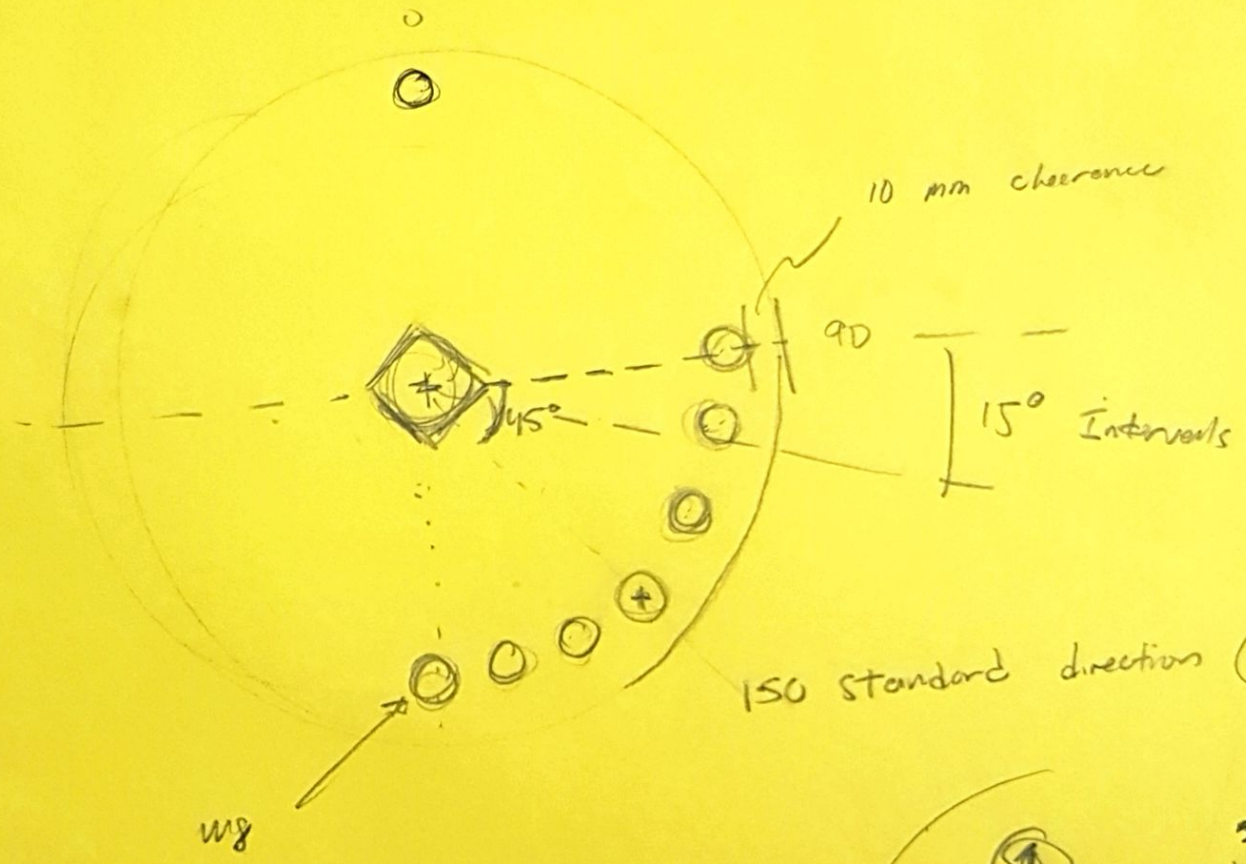

Boundary is 90-180

150 standard direction (125°)

- Keeps the tie rod the in same location

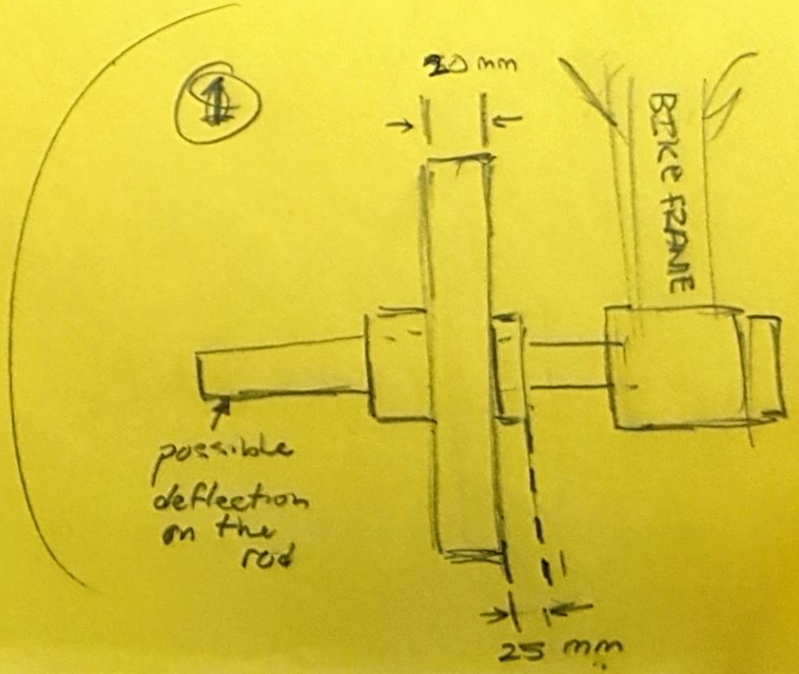

DESIGN 1

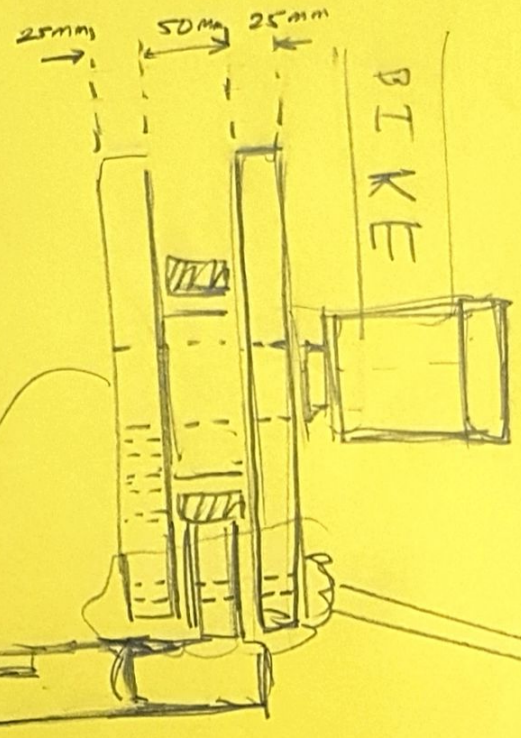

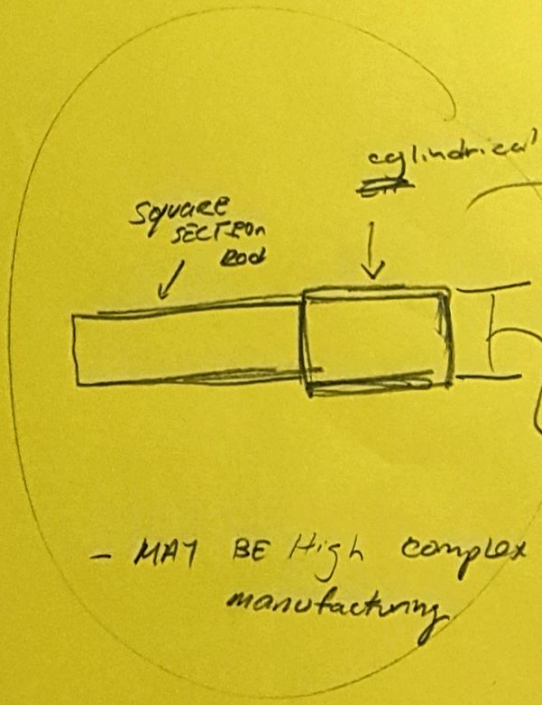

OD = BOTTOM BRACKET ID

- MAY BE High complex manufacturing

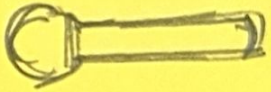

sits flush at furthest hole

HEADTUBE

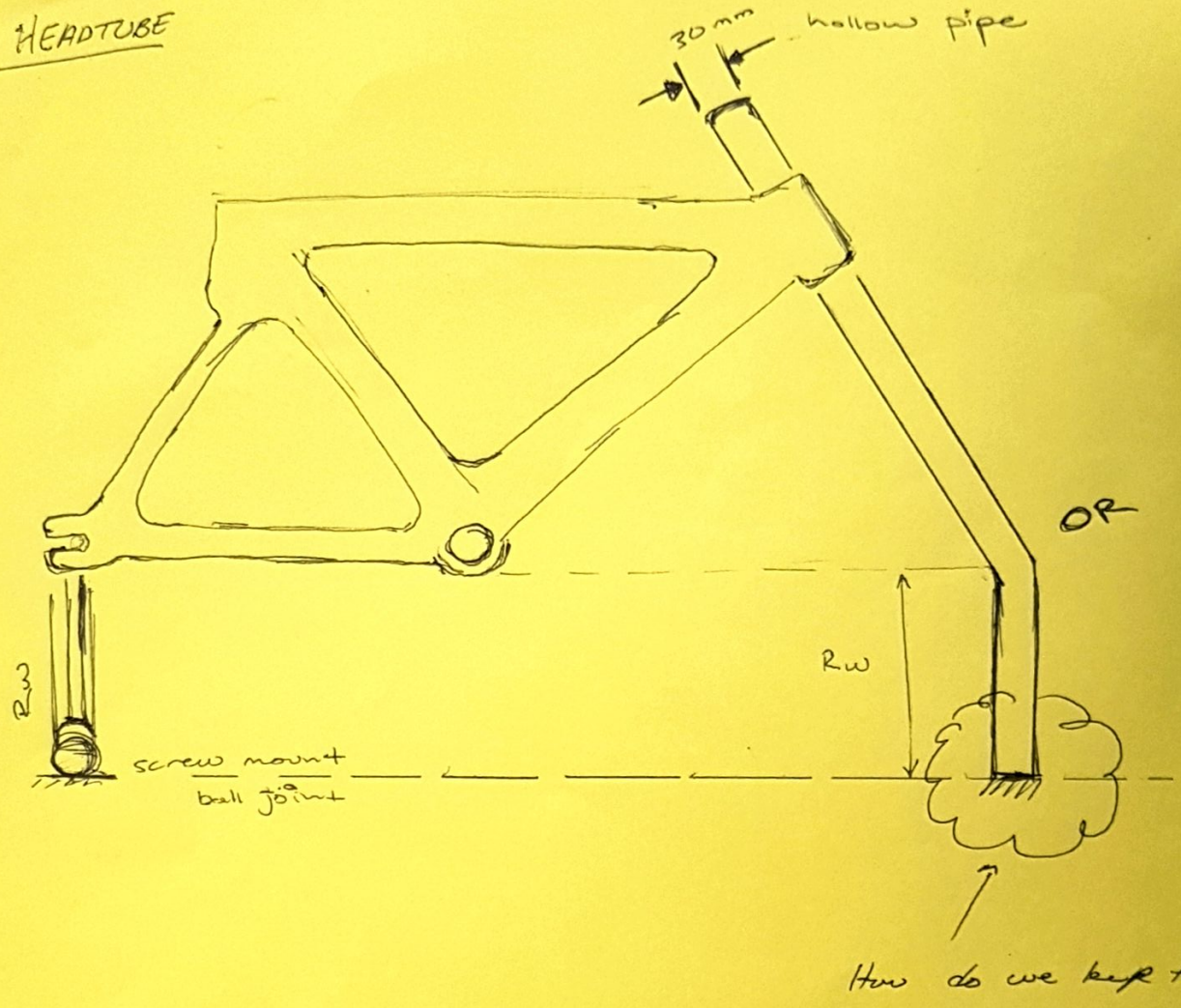
30 mm
hollow pipe
OR
It can be a straight rod
how to hold?
Rw
R3
screw mount
ball joint
How do we keep this fixed?

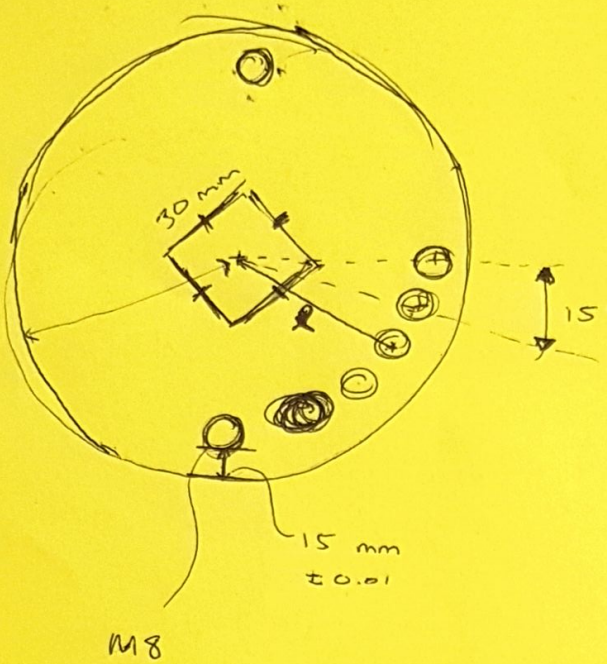

R = 175 mm

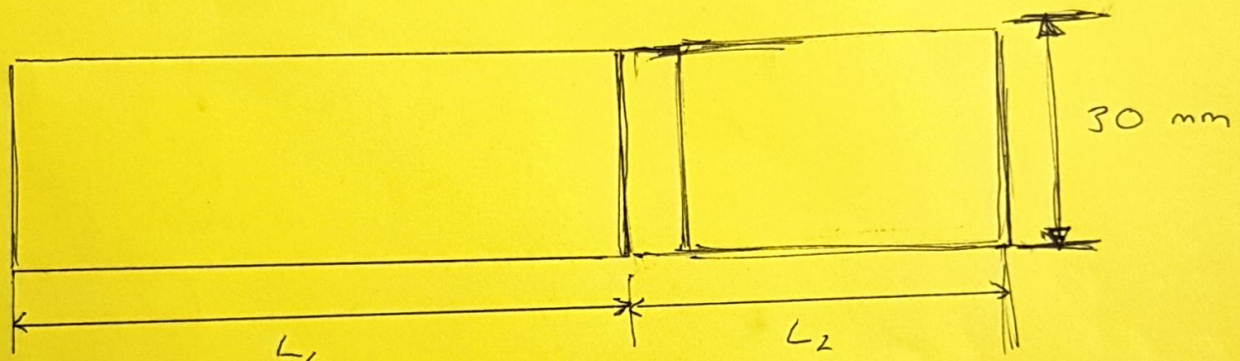

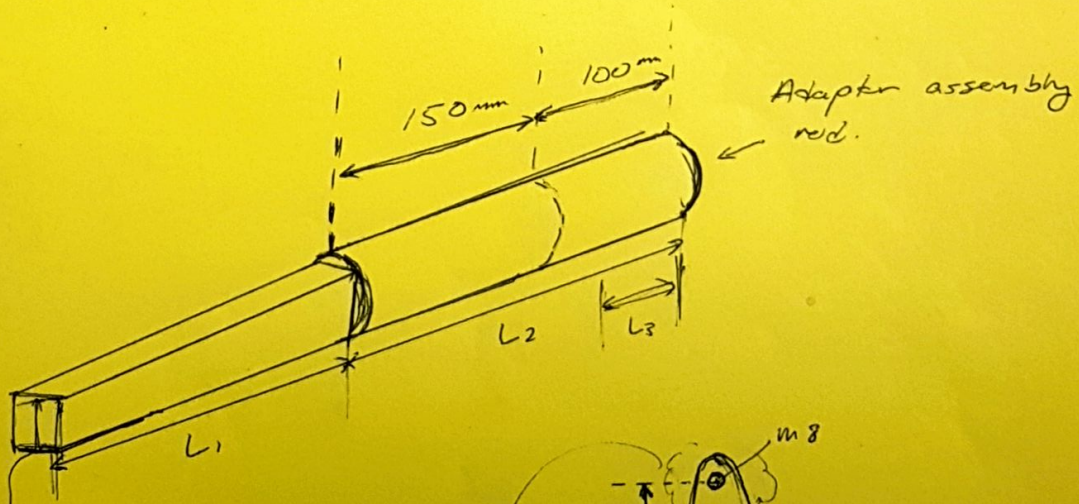

L_1 → varies, could be modular

L_2 = 250 mm

L_3 =

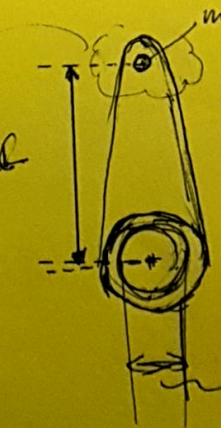

SCA Scissor Jack -- Super Cheap Auto

load cell needed

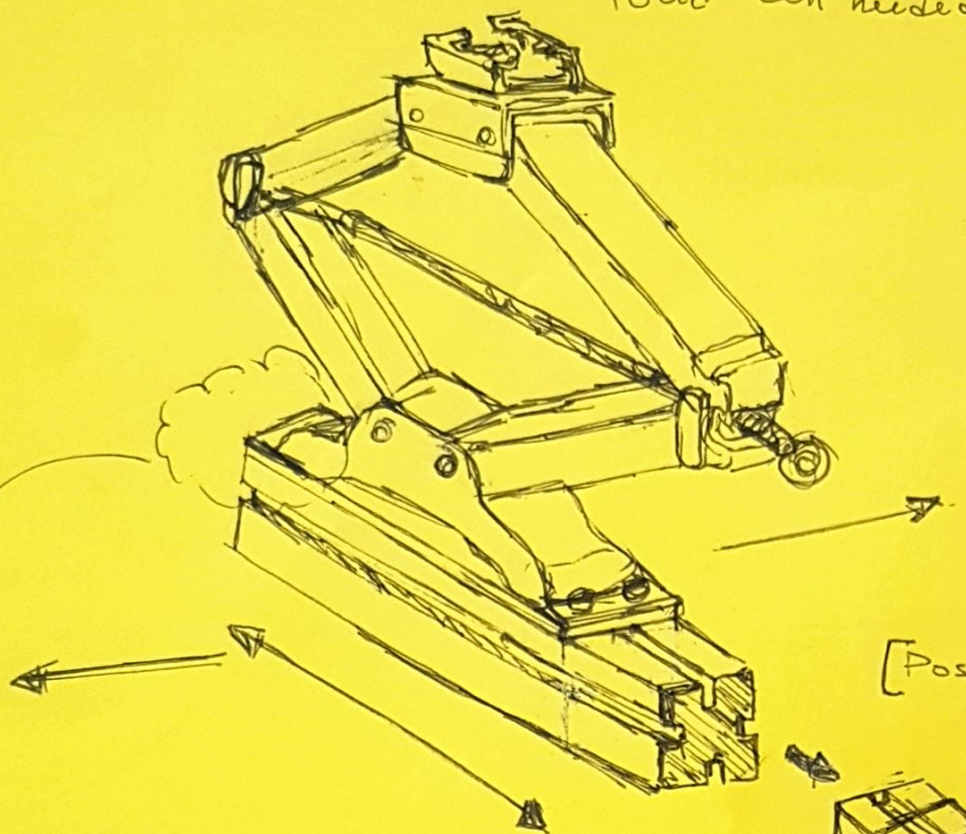

Working height range
115 - 405 mm

[Possible option]

Slides on other side of frame

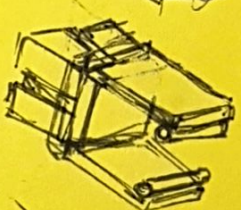

This provides

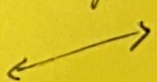

It'd be better to keep it @150 mm from ISO4210-6

UPSIDE down

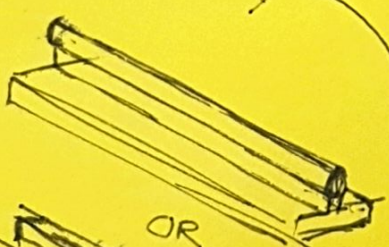

OR

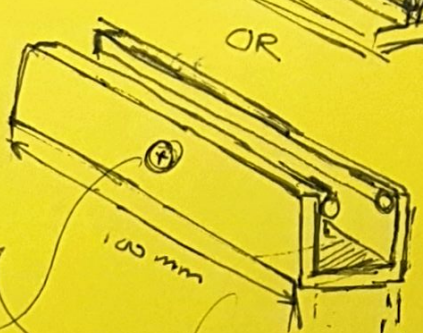

Steel ?

SCREWS TO FIX

USE T-SLOT NUTS ME

Possibly heavy duty

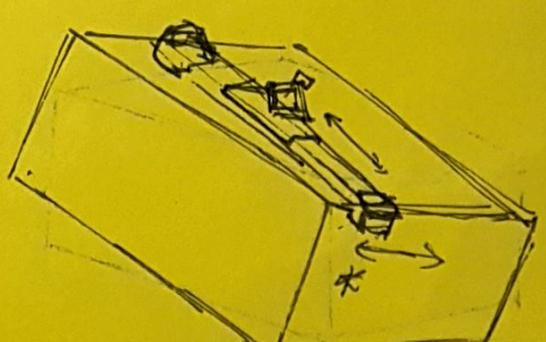

* Possibly just keep it stationary

MATERIAL :

- EXTRUDED ALUMINIUM.

T SLOT 8020..?

40 x 40 mm

40 40

dimensions?

x - ~~2000 mm~~ 1200 mm

y - ~~1000 mm~~ 500 mm

z - ~~1000 mm~~ 500 mm

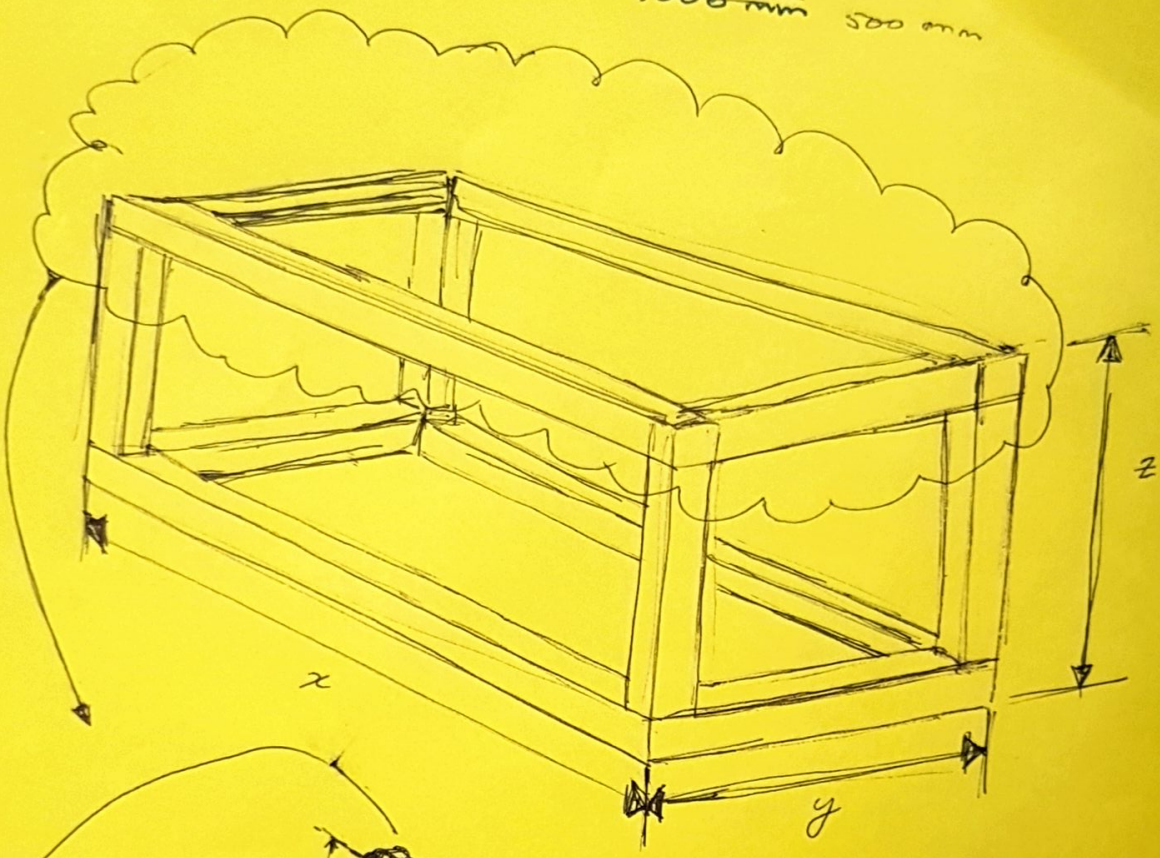

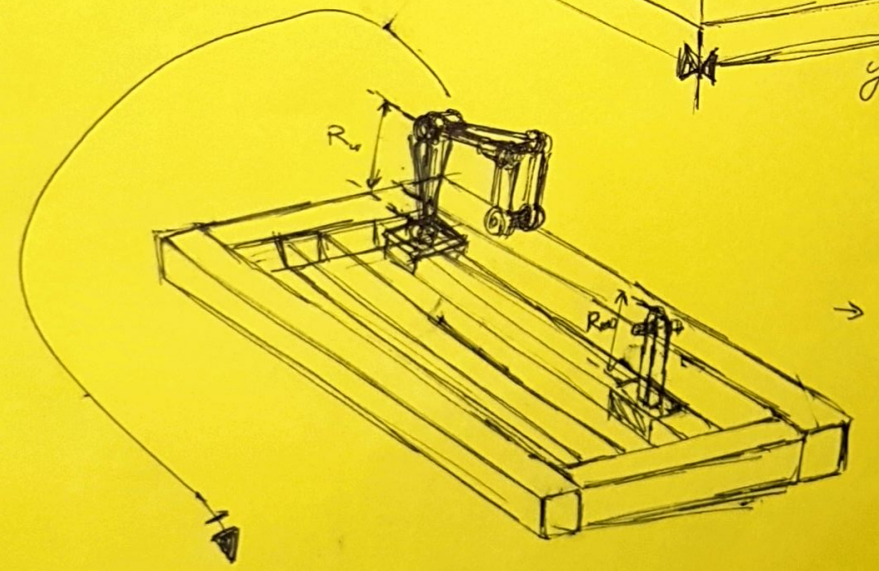

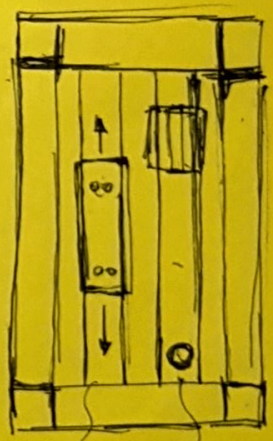

SCISSOR JIG

Seat

Bike frame

Seat

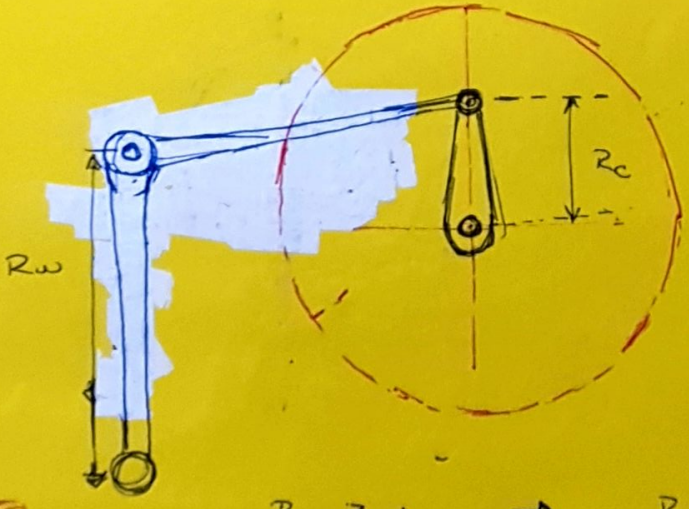

$R_w > L \rightarrow R_w > 175$ mm

Circle Fixed Bracket / Circle:

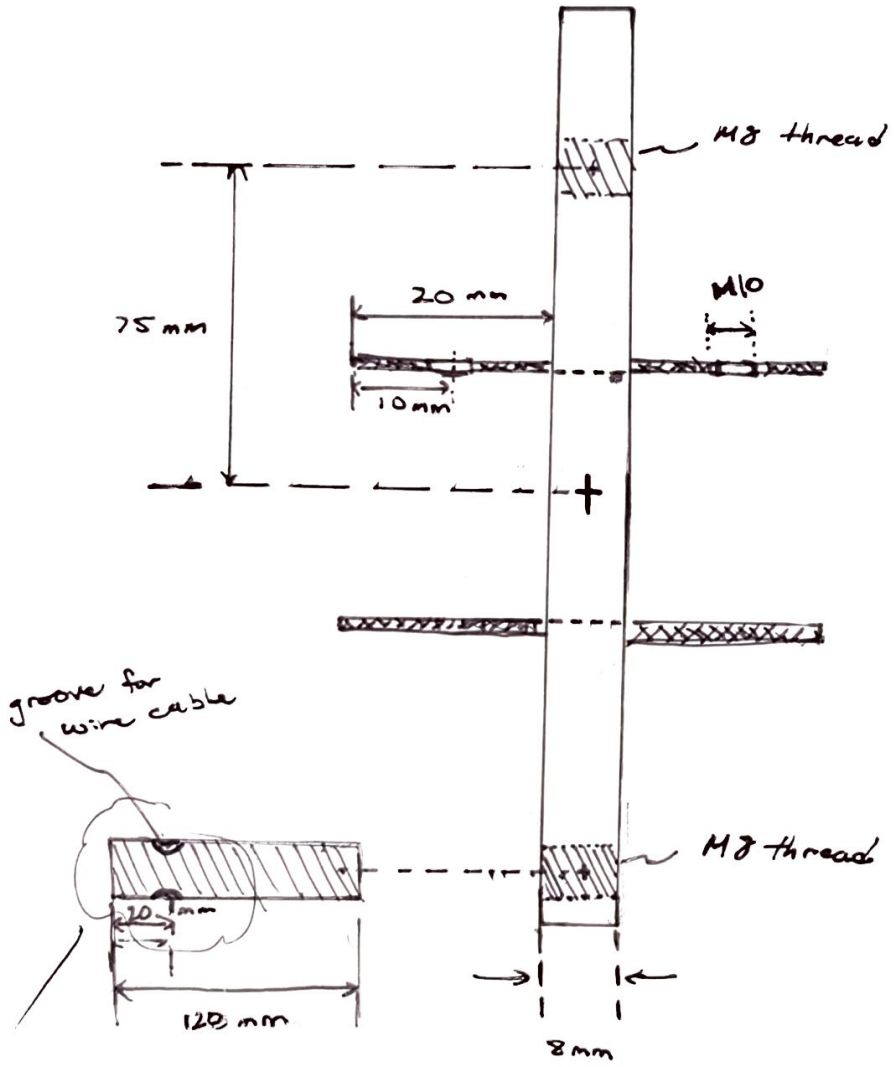

Bigger and hole instead of groove.

ALUMINIUM EXTRUSION PROFILE: USING 4040 & 8040 T SLOT PROFILES.

1:20 scale

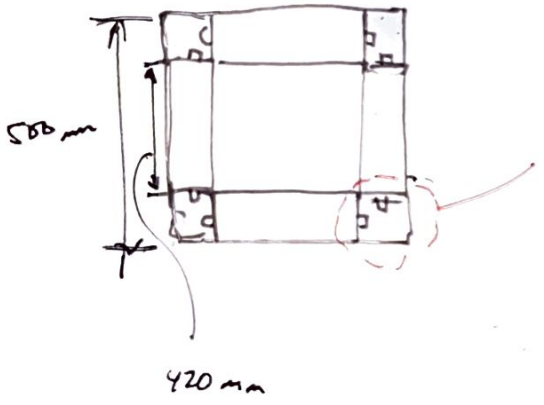

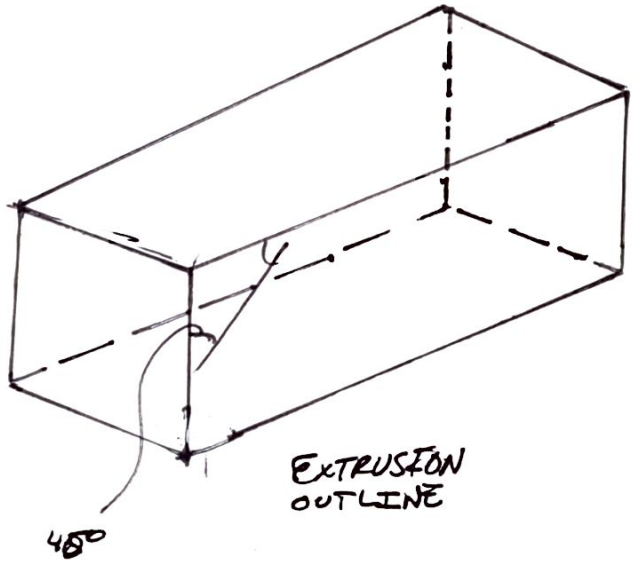

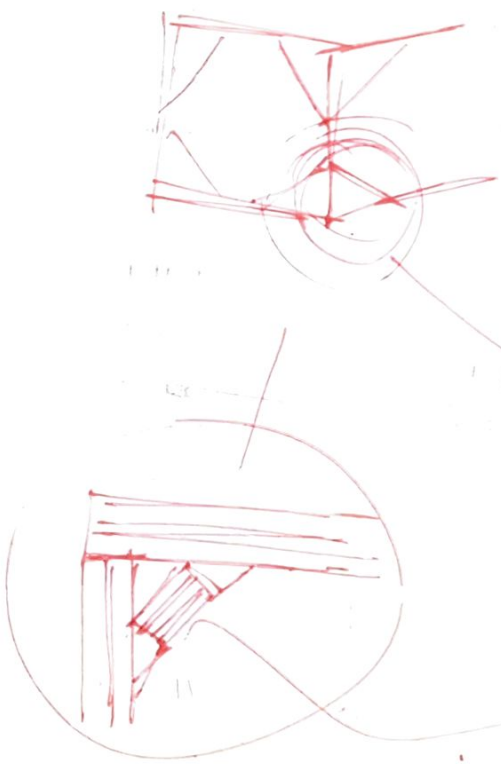

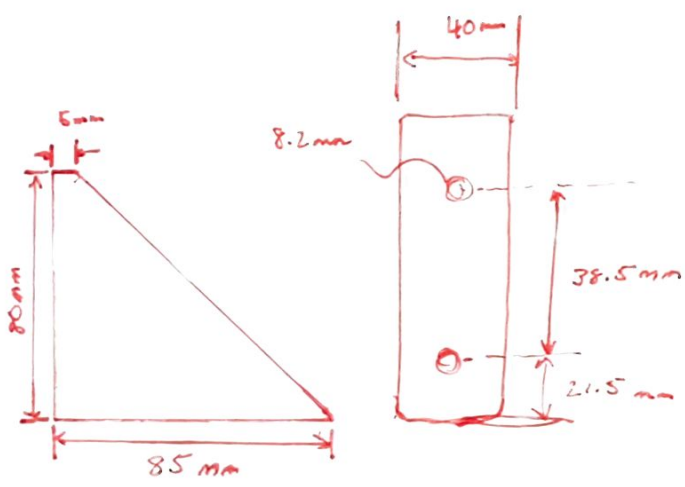

11/10/2017

Ronstar CS311-12E Loading capacity:

External bottom bracket ~ 30mm ID] This will suit for bottom bracket.
↑ Buy one ↓ 24mm ID

Meeting w/ ESG -- Richard S: 2:30 pm E: 3:30 pm

o vertical link -- Rigid — talk to MARK 14 hours.

→ To round

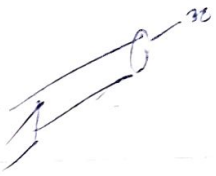

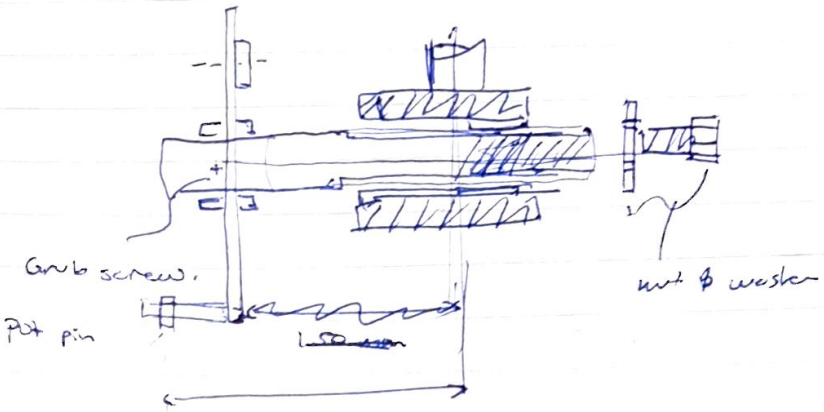

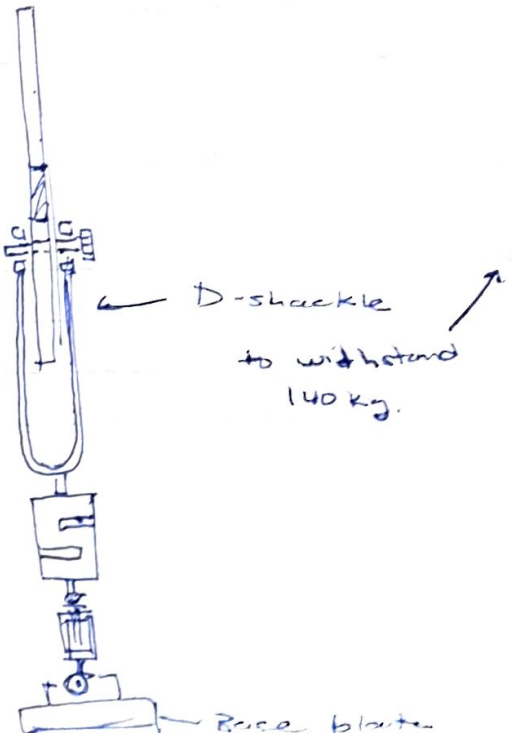

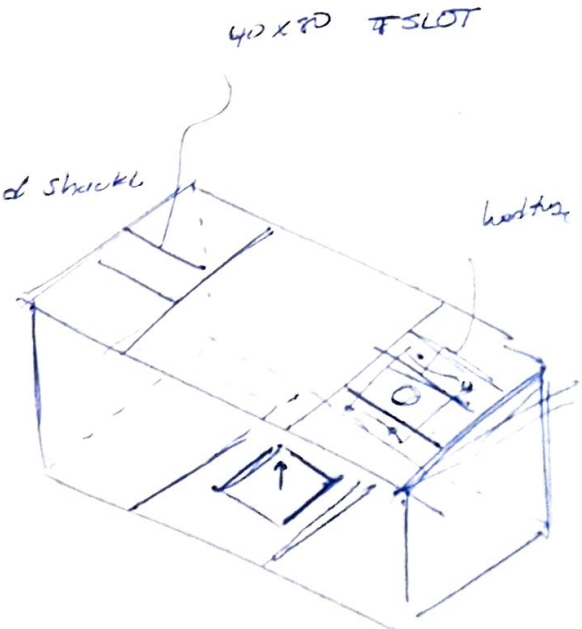

22/10/17

Al extrusion tolerance for tensile strength at grooves

Normal - 5000 ~~kg~~ N → 500 kg

Light - 2500 N → 250 kg

E - 1,750 N → ~~kg~~

This would be the safest & cheapest compared to others.

Change frame design

call modular components.

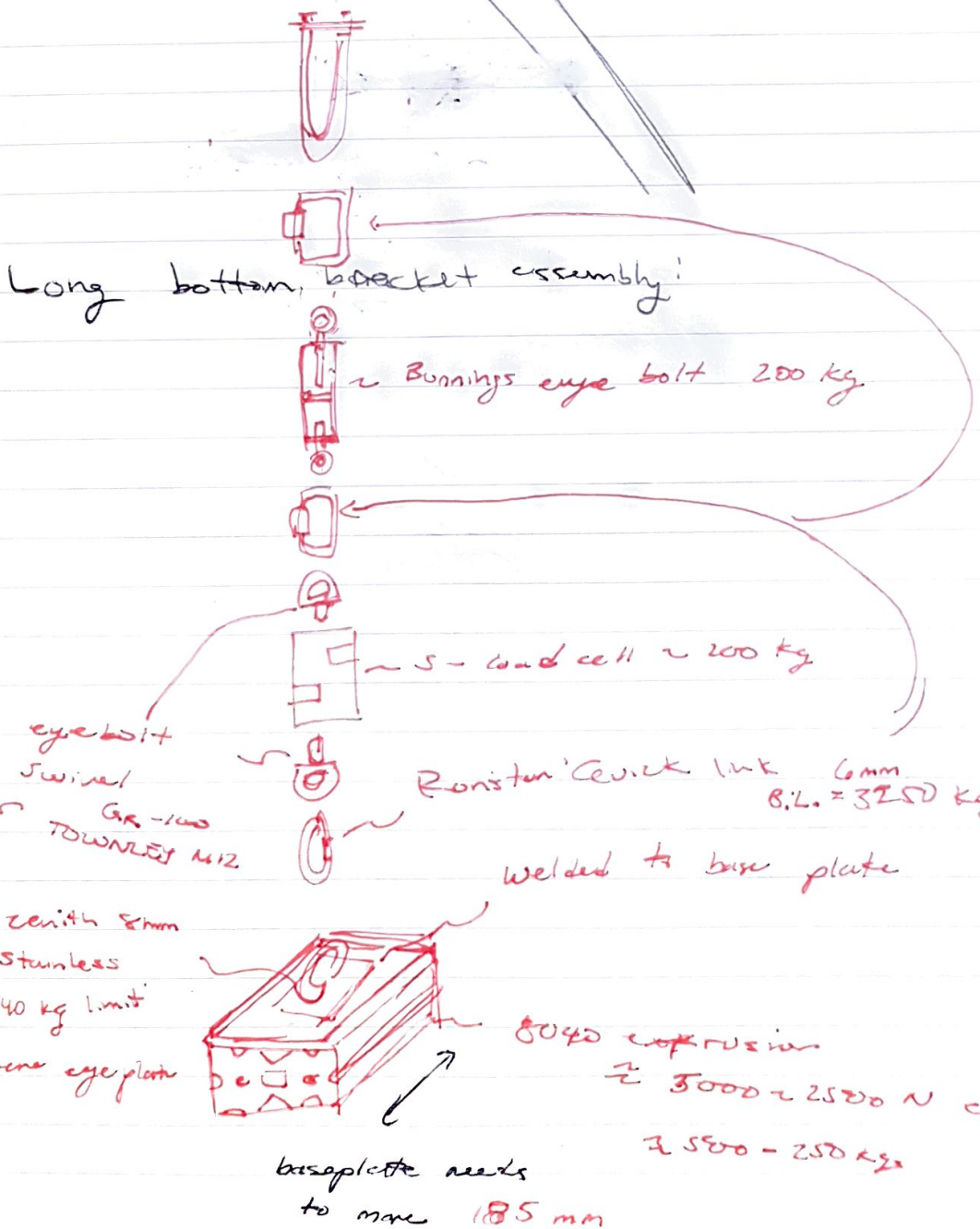

31/10/17

FOUND ~~CLAMP ANGLE~~ FOUND JOINT ANGLE FOR 40 40 extrusion

1/11/17

VERTICAL LINK DESIGN

PIN JOINT

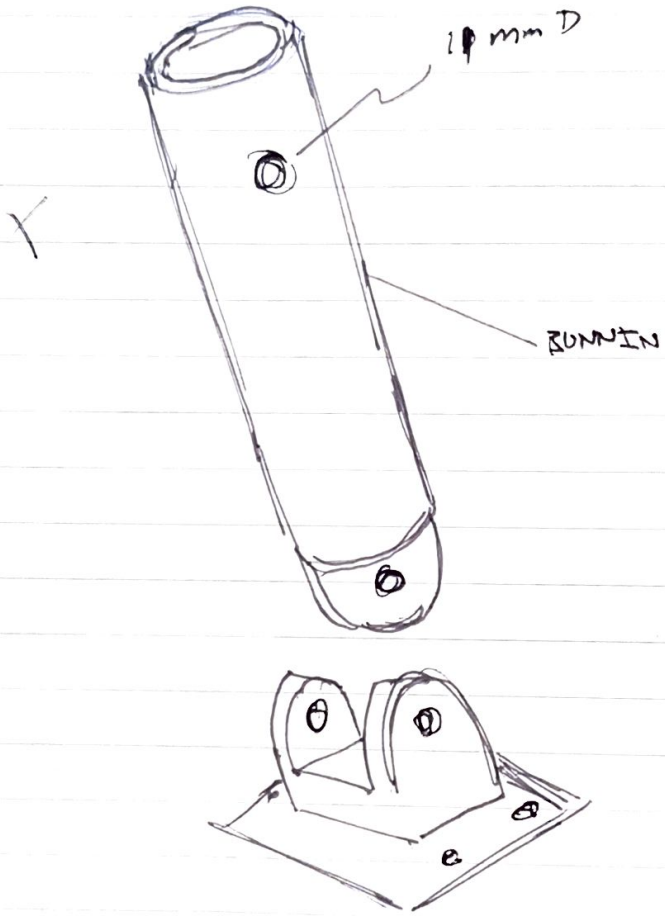

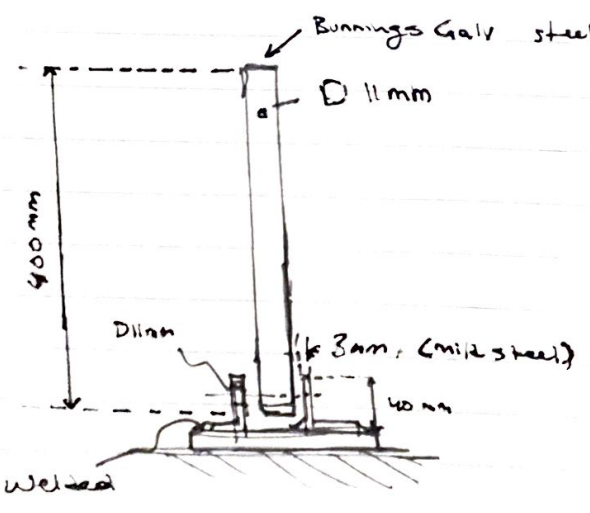

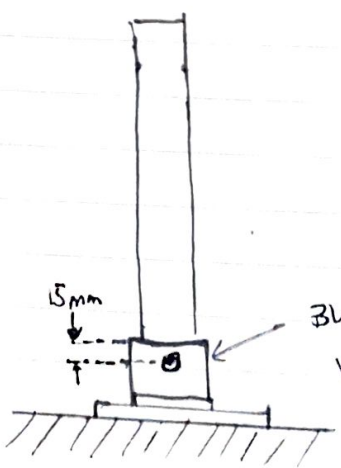

Bus Eyelet plate 12/02/18

Ø6mm holes x suitable for M5 screws

3mm thick steel plate.

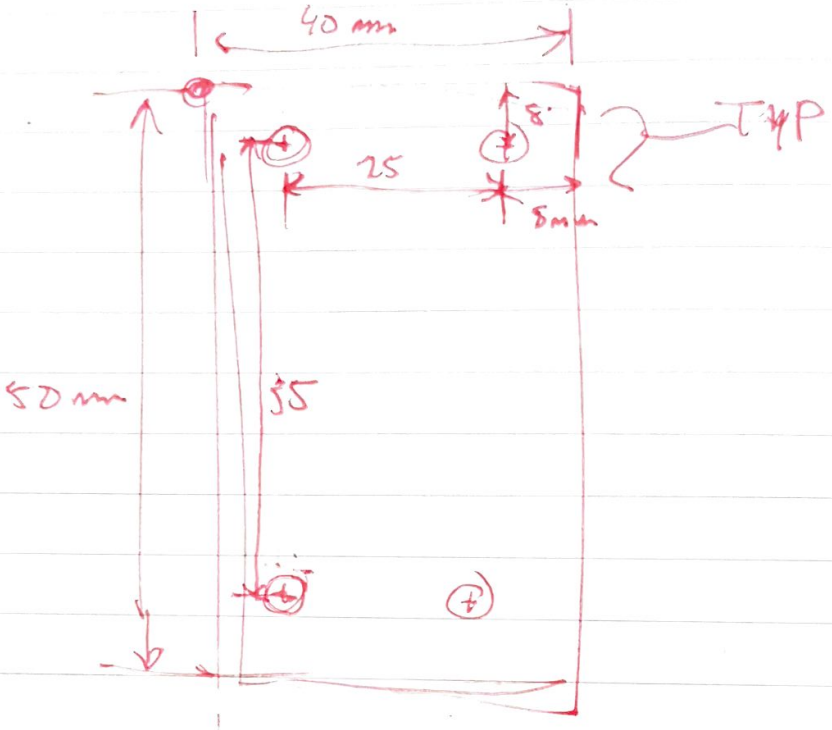

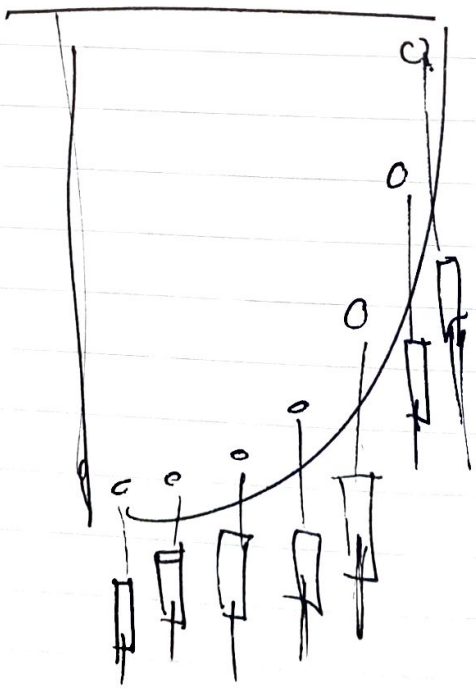

11 Appendix C – Reaction Frame FEA

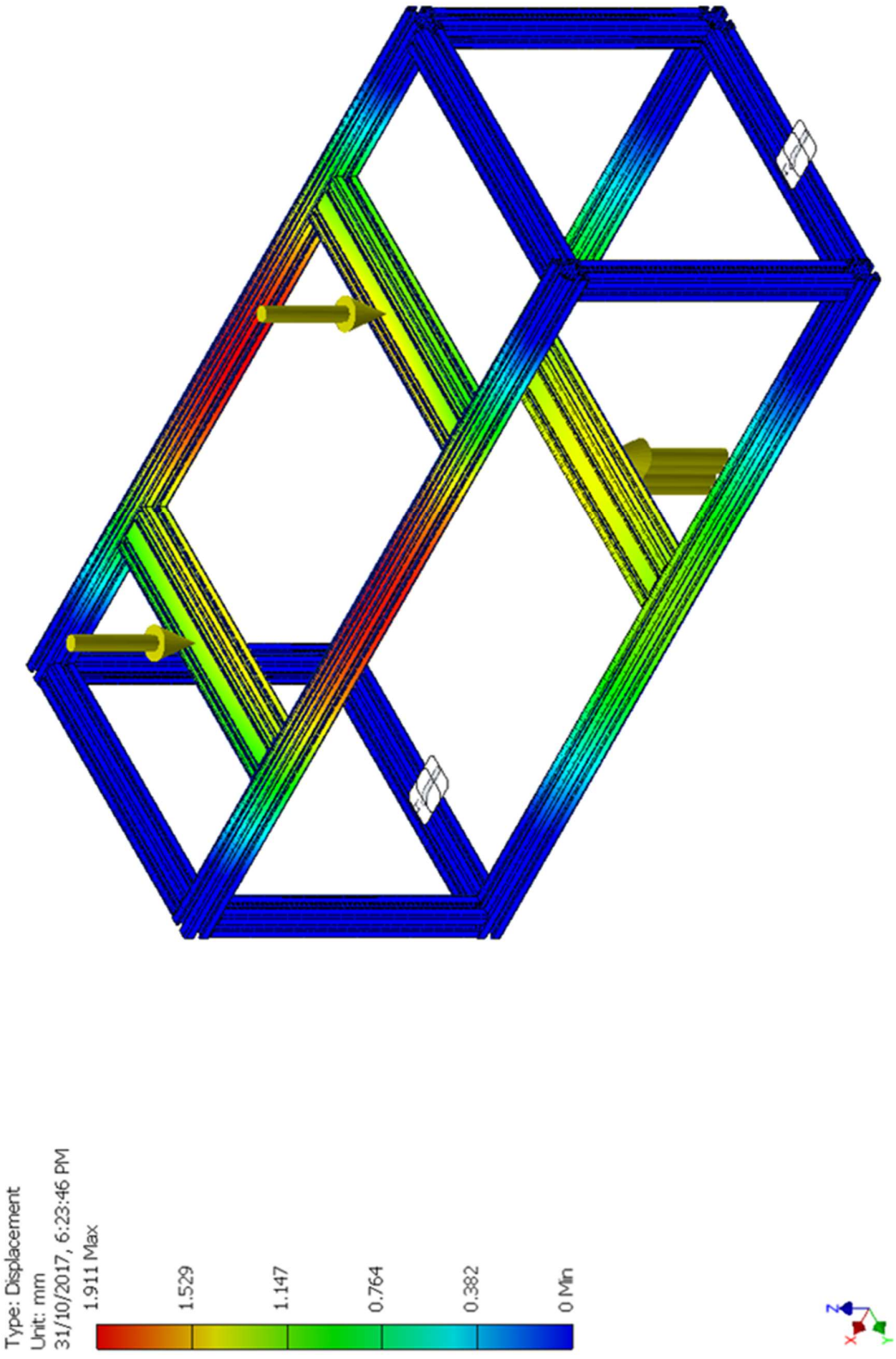

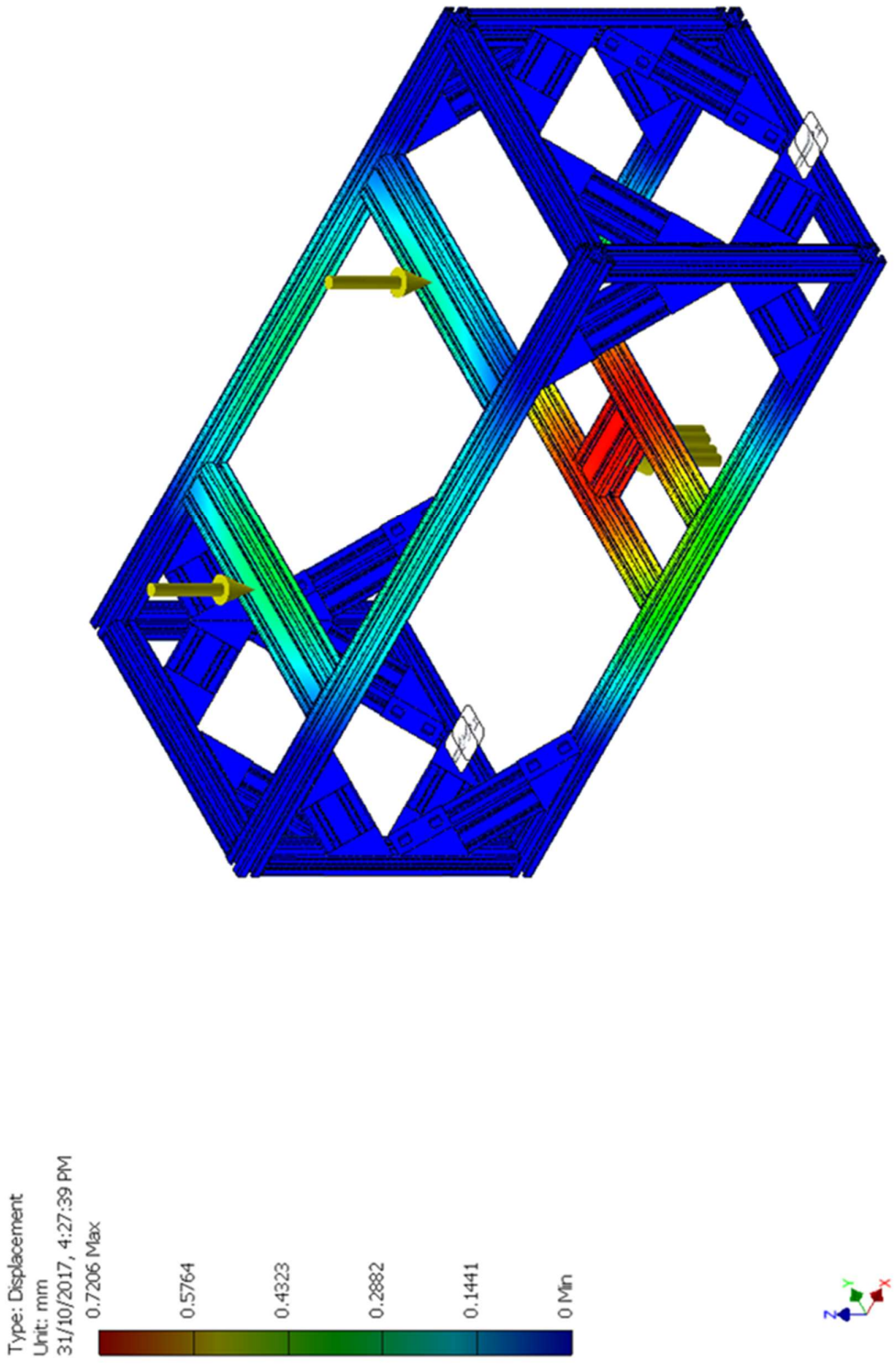
Type: Displacement
Unit: mm
31/10/2017, 4:27:39 PM
0.7206 Max
0.5764
0.4323
0.2882
0.1441
0 Min

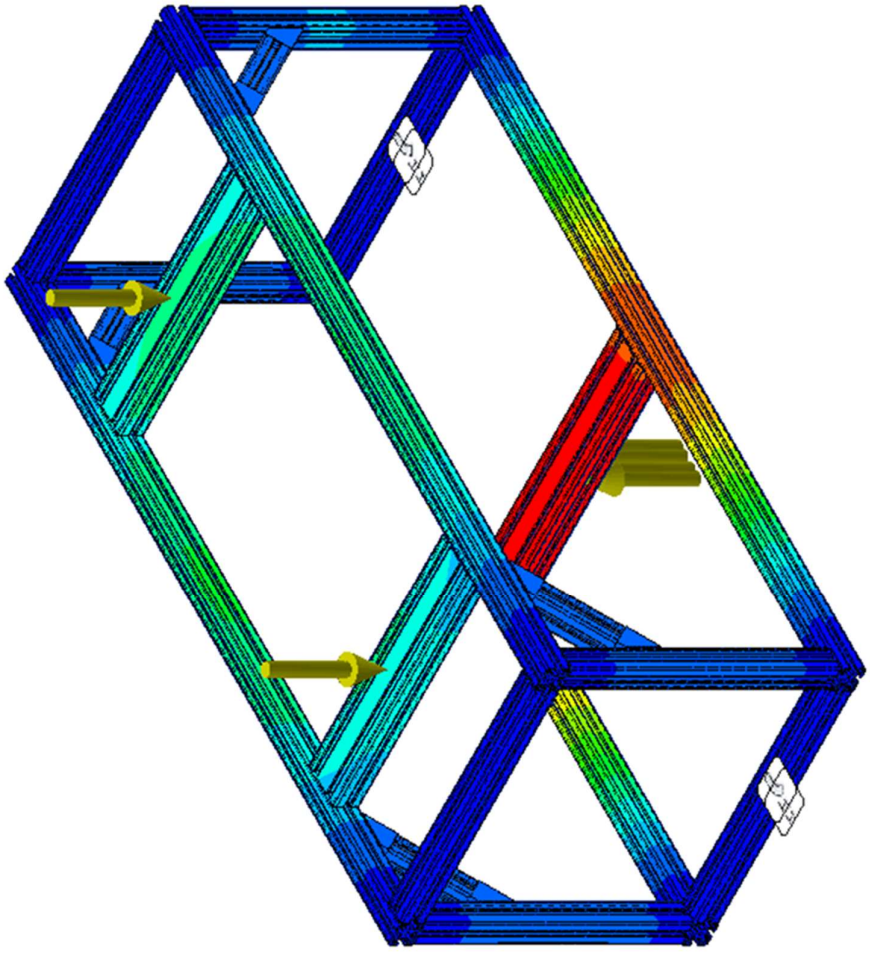

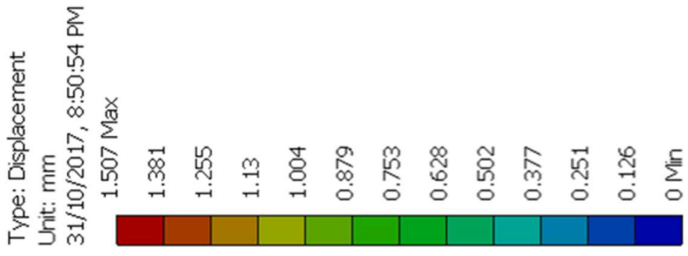
Type: Displacement
Unit: mm
31/10/2017, 8:50:54 PM
1.507 Max
1.381
1.255
1.13
1.004
0.879
0.753
0.628
0.502
0.377
0.251
0.126
0 Min


Y
Z
X

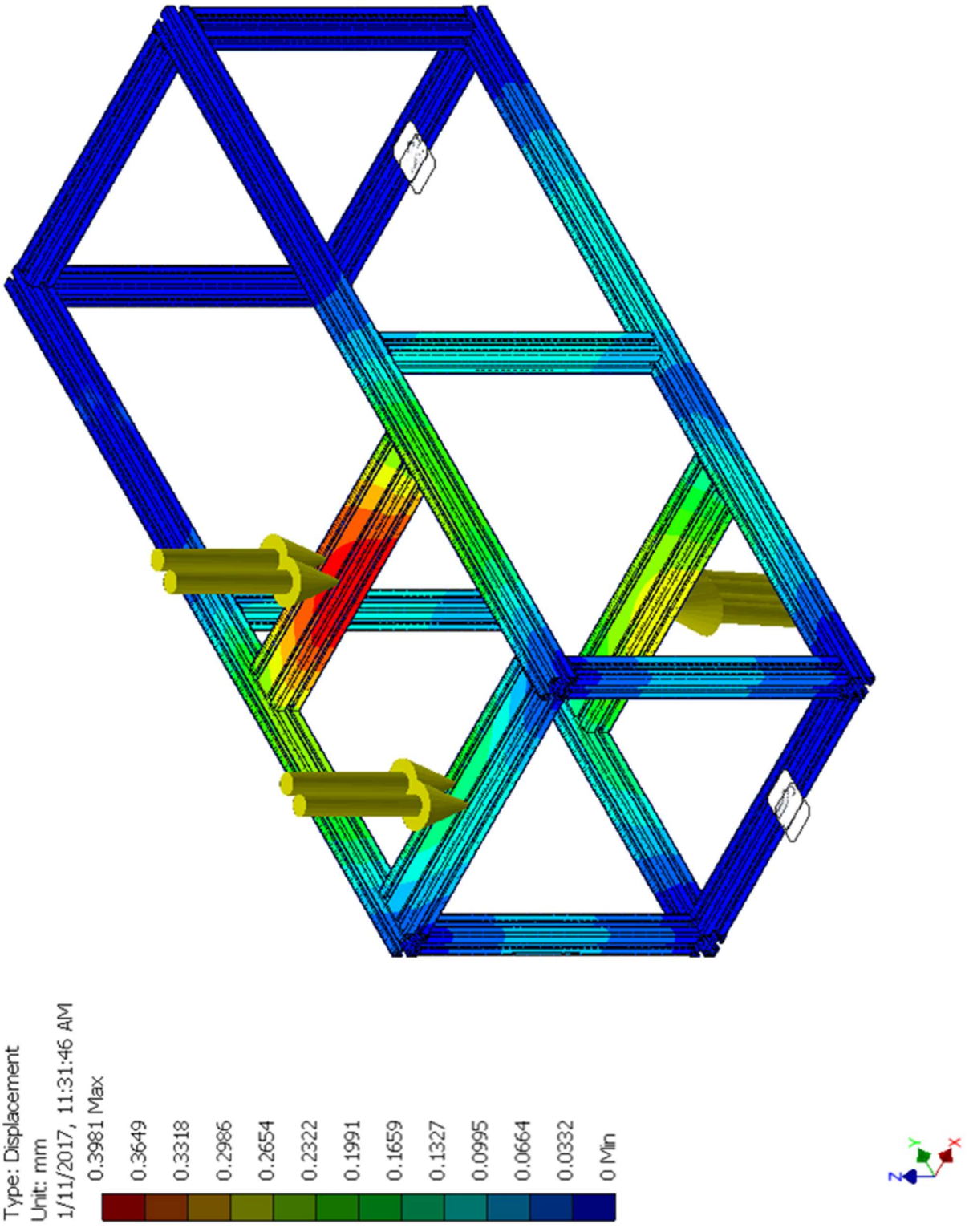
Type: Displacement
Unit: mm
1/11/2017, 11:31:46 AM
0.3981 Max
0.3649
0.3318
0.2986
0.2654
0.2322
0.1991
0.1659
0.1327
0.0995
0.0664
0.0332
0 Min

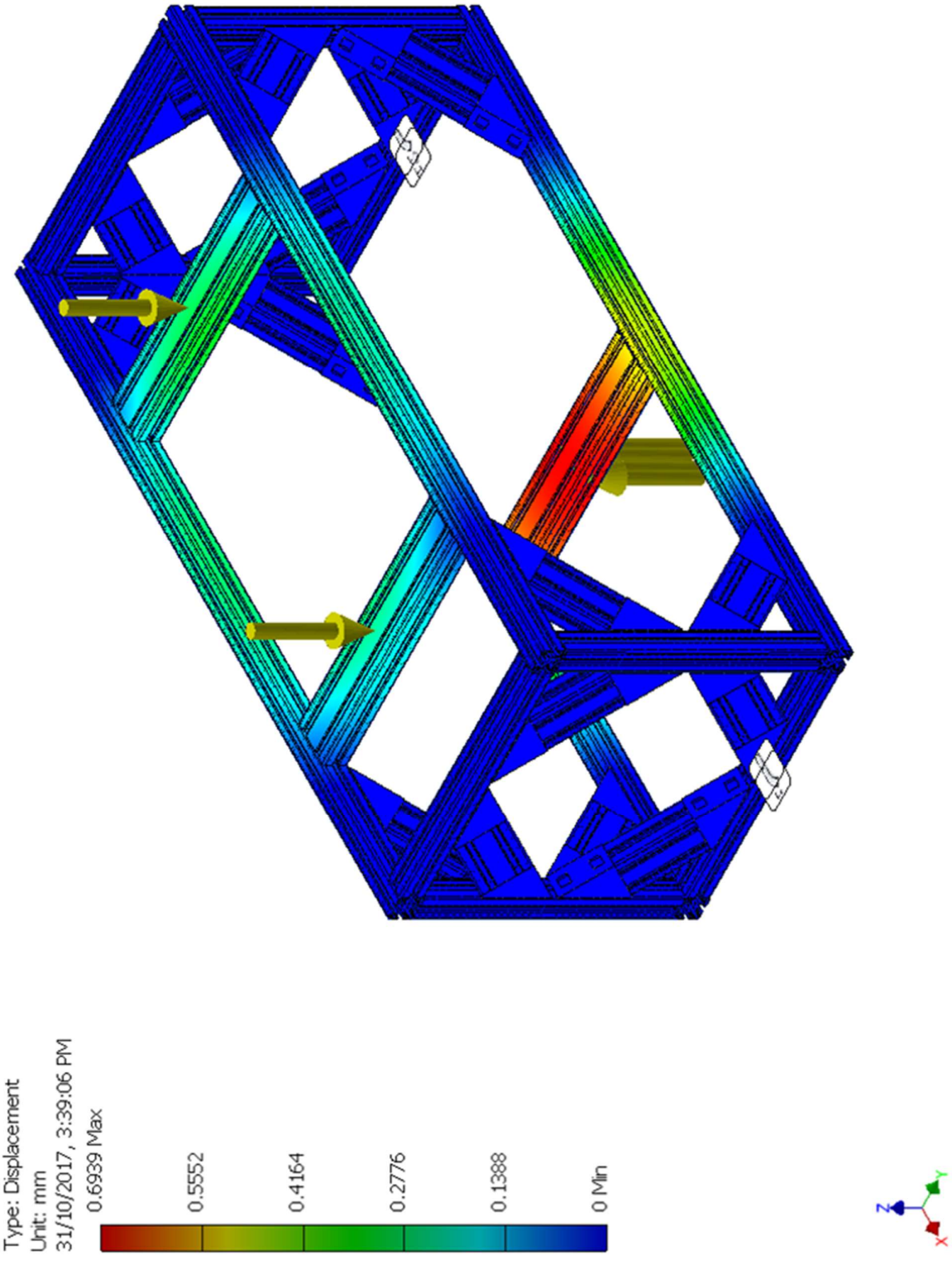
Type: Displacement
Unit: mm
31/10/2017, 3:39:06 PM
0.6939 Max
0.5552
0.4164
0.2776
0.1388
0 Min
Y
Z
X

12 Appendix D – Computer Aided Design Drawings

Below show the CAD drawings used for construction.

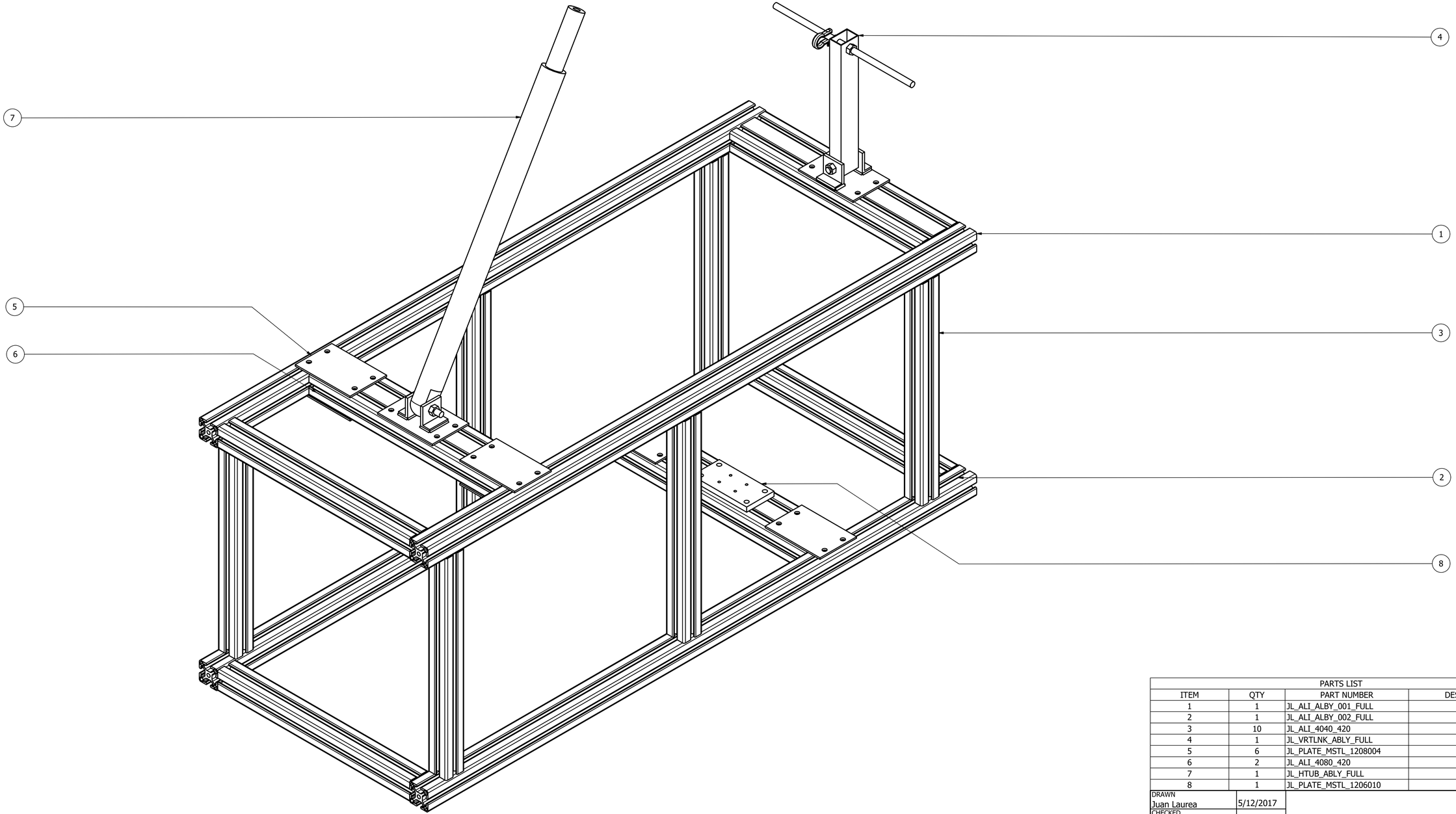

PARTS LIST			
ITEM	QTY	PART NUMBER	DESCRIPTION
1	1	JL_ALI_ALBY_001_FULL	
2	1	JL_ALI_ALBY_002_FULL	
3	10	JL_ALI_4040_420	
4	1	JL_VRTLNK_ABLY_FULL	
5	6	JL_PLATE_MSTL_1208004	
6	2	JL_ALI_4080_420	
7	1	JL_HTUB_ABLY_FULL	
8	1	JL_PLATE_MSTL_1206010	

DRAWN	Juan Laurea	5/12/2017
CHECKED		
QA		
MFG		
APPROVED		

TITLE: LOADING RIG ASSEMBLY

SIZE		DWG NO	REV
D		JL_LOAD_RIG_ABLY_FULL	

SCALE 1/3 SHEET 1 OF 1

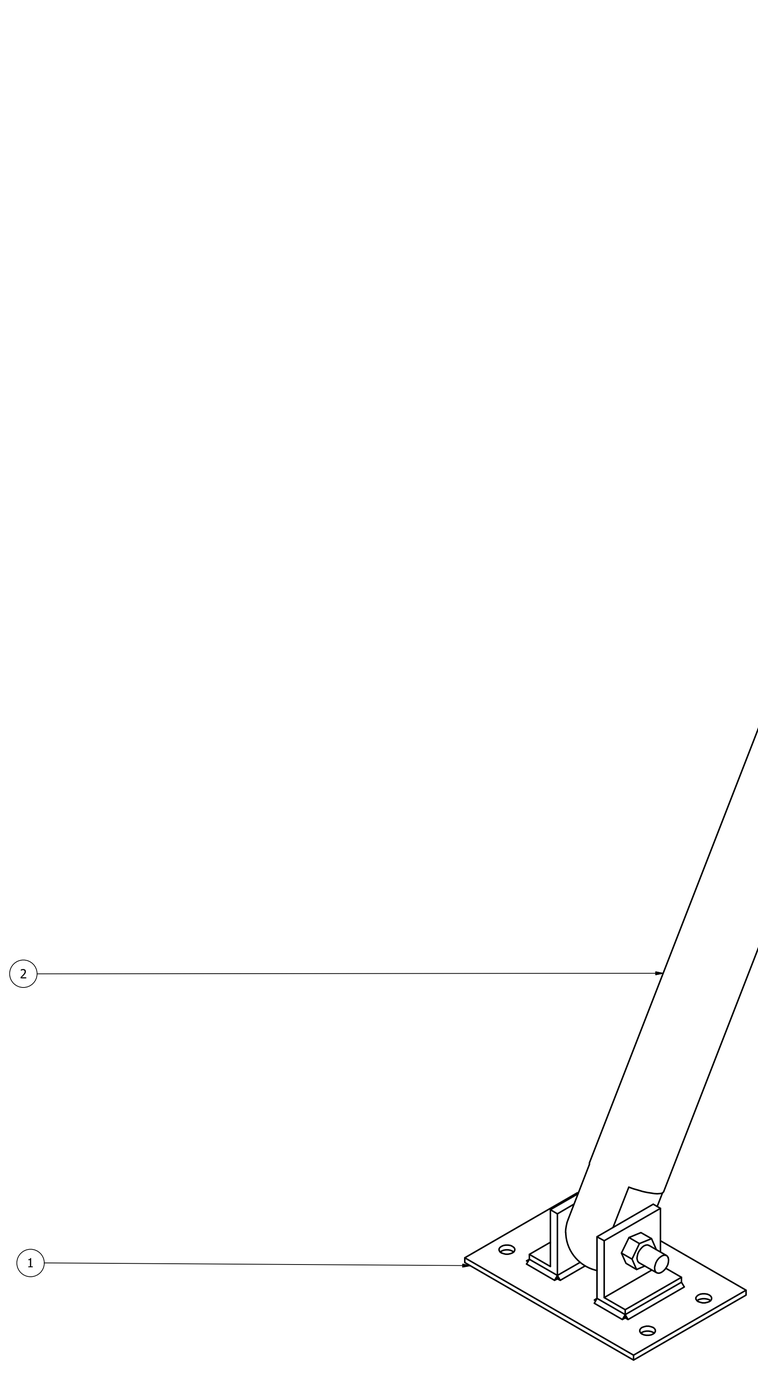

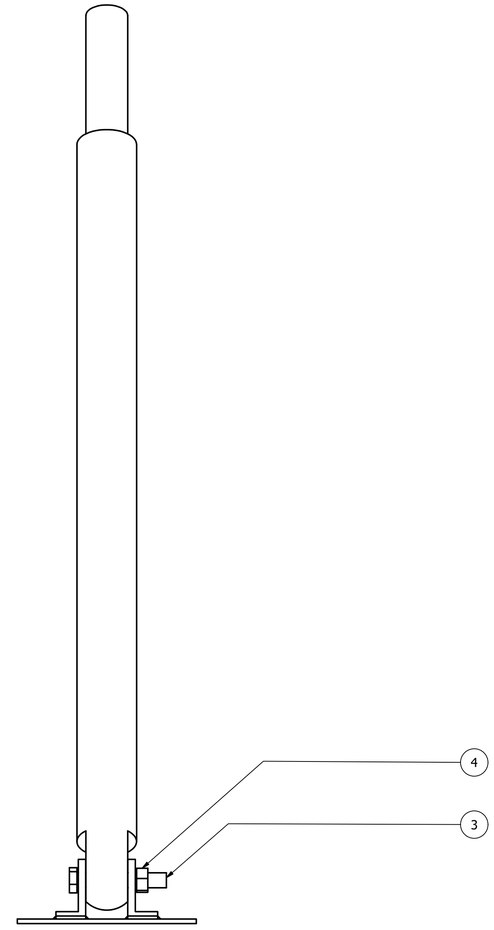

PARTS LIST			
ITEM	QTY	PART NUMBER	DESCRIPTION
1	1	JL_HTUB_BPLAT	
2	1	JL_ALI_HTUBE	
3	1	Bunnings IN 2448945 10mm Bolt	
4	1	Bunnings IN 2448945 10mm Nut	

DRAWN	Juan Laurea	5/12/2017
CHECKED		
QA		
MFG		
APPROVED		

TITLE

SIZE	DWG NO	REV
D	JL_HTUB_ABLY_FULL	

SCALE 1 /1.5 SHEET 1 OF 1

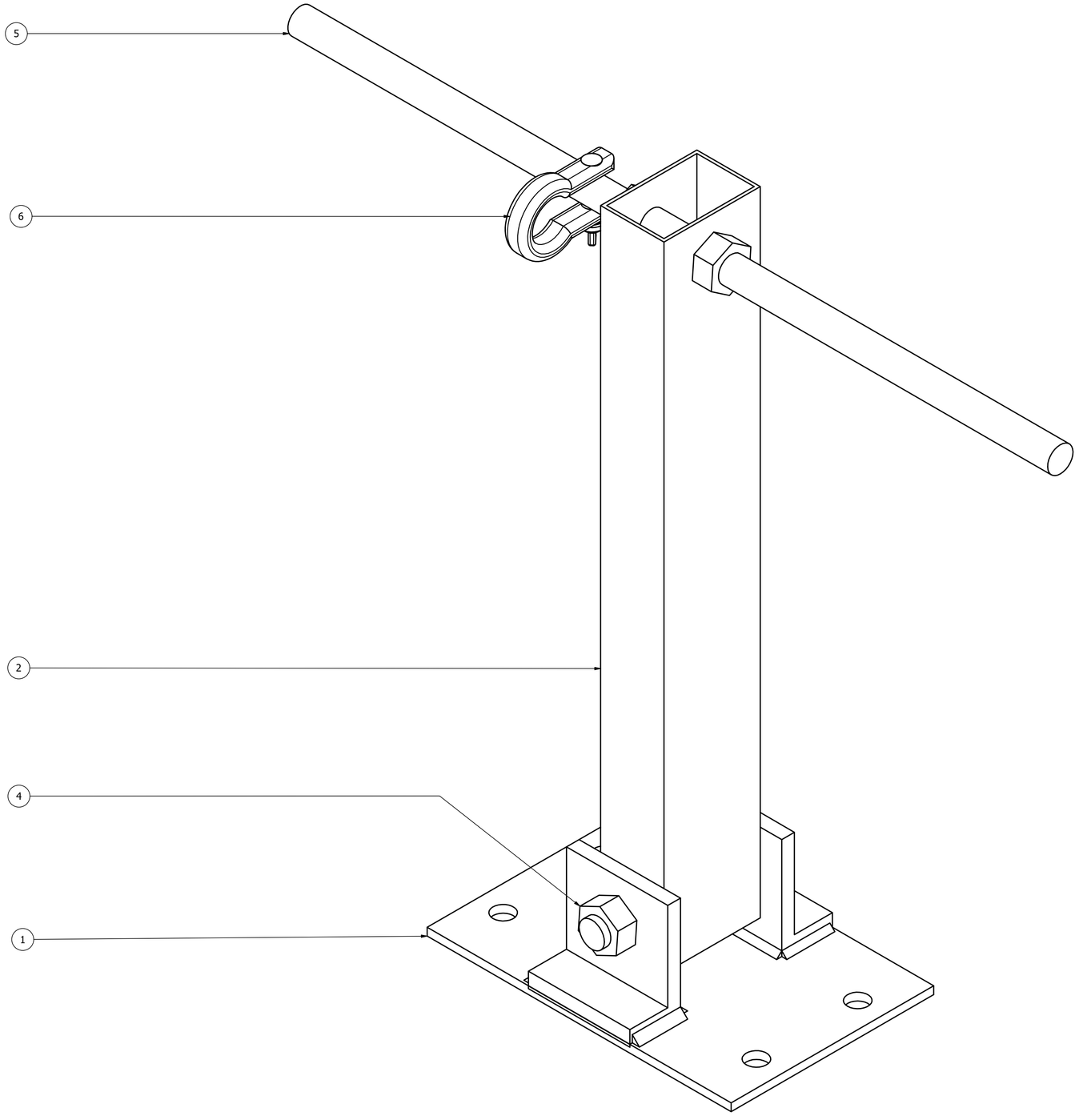

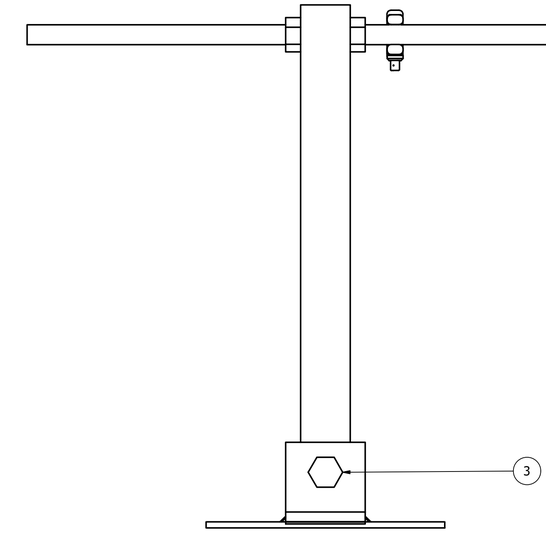

PARTS LIST			
ITEM	QTY	PART NUMBER	DESCRIPTION
1	1	JL_VRTLNK_WLD	
2	1	JL_VLINK_BUN_0910120	
3	1	Bunnings IN 2448945 10mm Bolt	
4	3	Bunnings IN 2448945 10mm Nut	
5	1	JL_BUN_2410267_VLK_ROD	
6	1	Bunnings 4220584 Gorrilla D Shackle	

DRAWN	Juan Laurea	5/12/2017
CHECKED		
QA		
MFG		
APPROVED		

TITLE

VERTICAL LINK FULL ASSEMBLY

SIZE		DWG NO	REV
D		JL_VRTLNK_ABLY_FULL	

SCALE 1.5 SHEET 1 OF 1

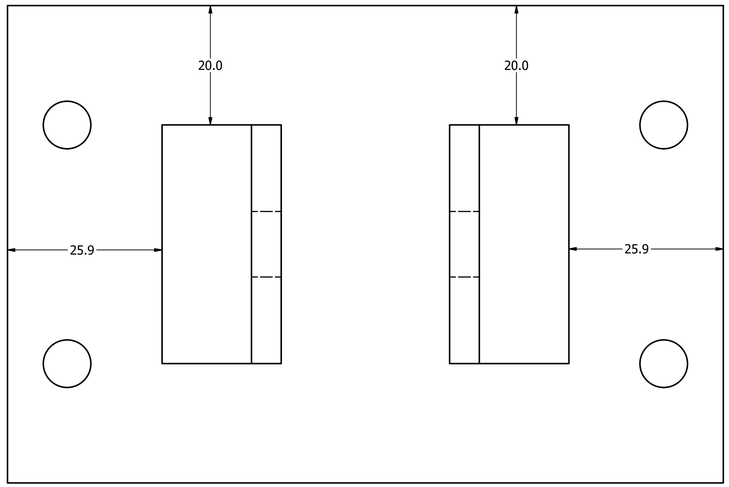

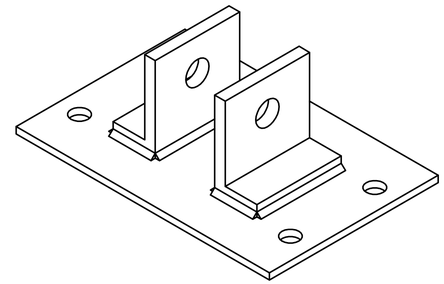

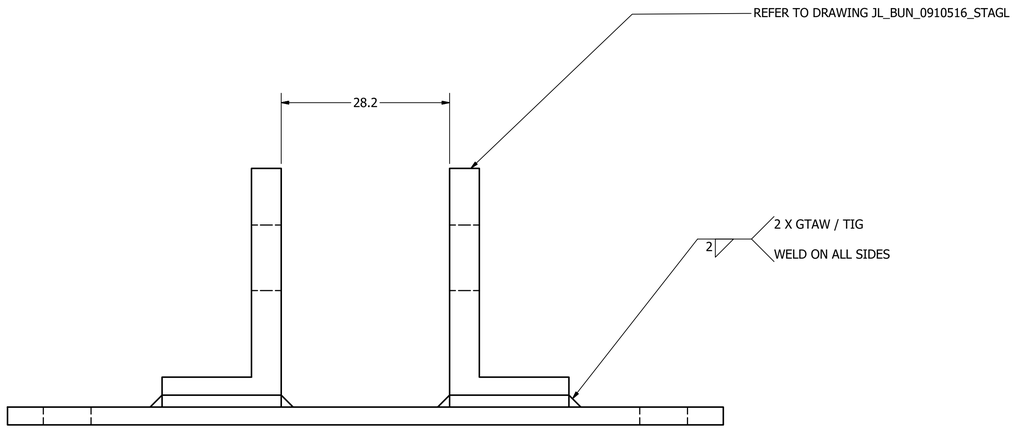

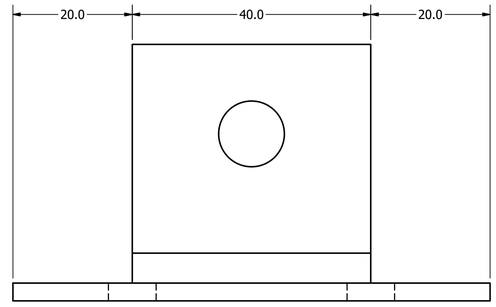

NOTE: PARTS ARE REQUIRED BEFORE THIS WELD
- 1 X JL_PLATE_MSTL_1208004
- 2 X JL_BUN_0910516_STAGL

DRAWN Juan Laurea	29/11/2017	
CHECKED		TITLE
QA		HEADTUBE BASE PLATE
MFG		
APPROVED		SIZE D / DWG NO JL_HTUB_BPLAT / REV
		SCALE 2 : 1 / SHEET 1 OF 1

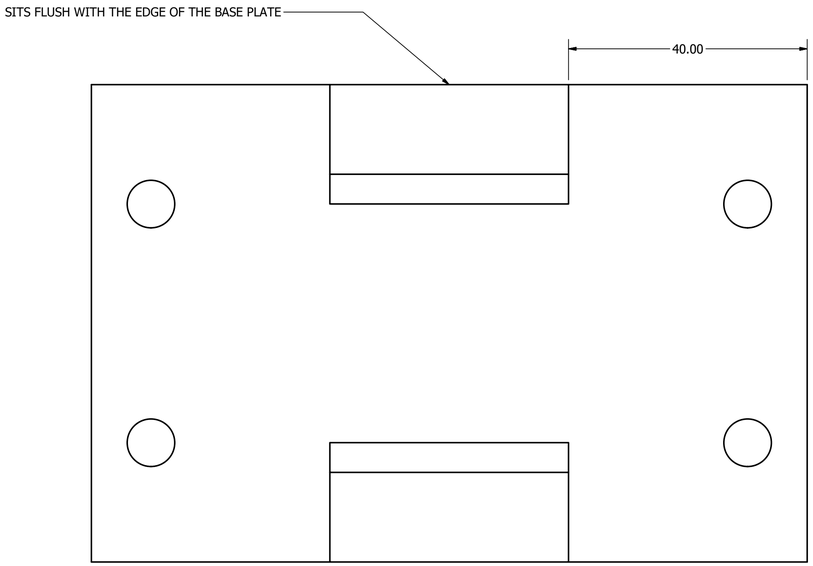

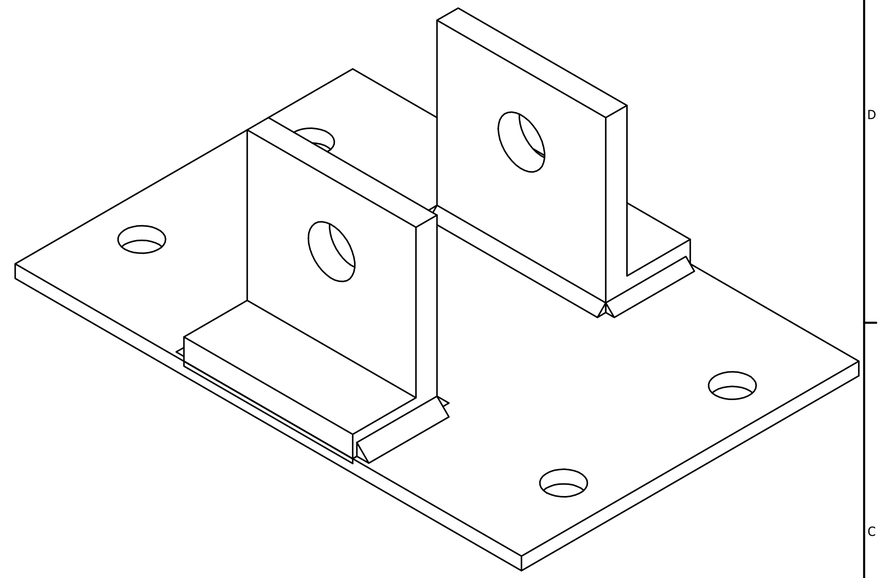

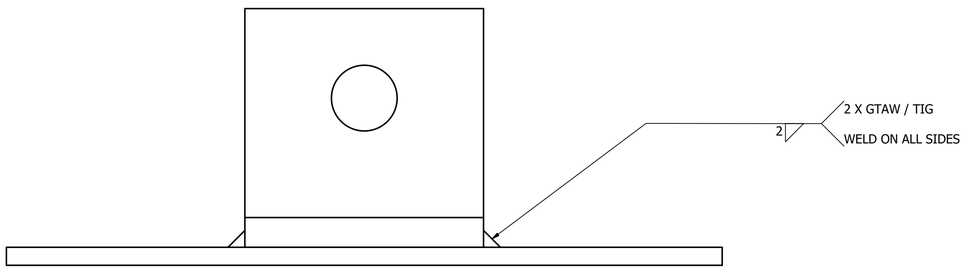

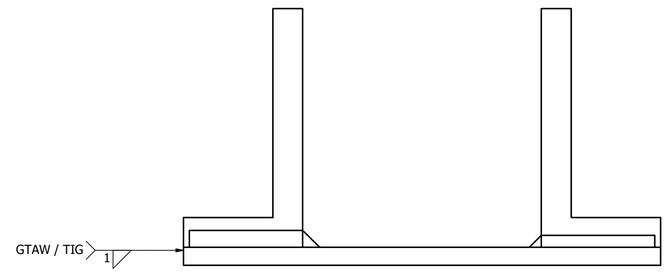

NOTE: PARTS ARE REQUIRED BEFORE THIS WELD
- 1 X JL_PLATE_MSTL_1208004
- 2 X JL_BUN_0910516_STAGL

DRAWN Juan Laurea	5/12/2017	
CHECKED		TITLE: VERTICAL LINK BOTTOM PLATE WELD
QA		
MFG		
APPROVED		
		SIZE D | DWG NO JL_VRTLNK_WLD | REV
		SCALE 2 : 1 | SHEET 1 OF 1

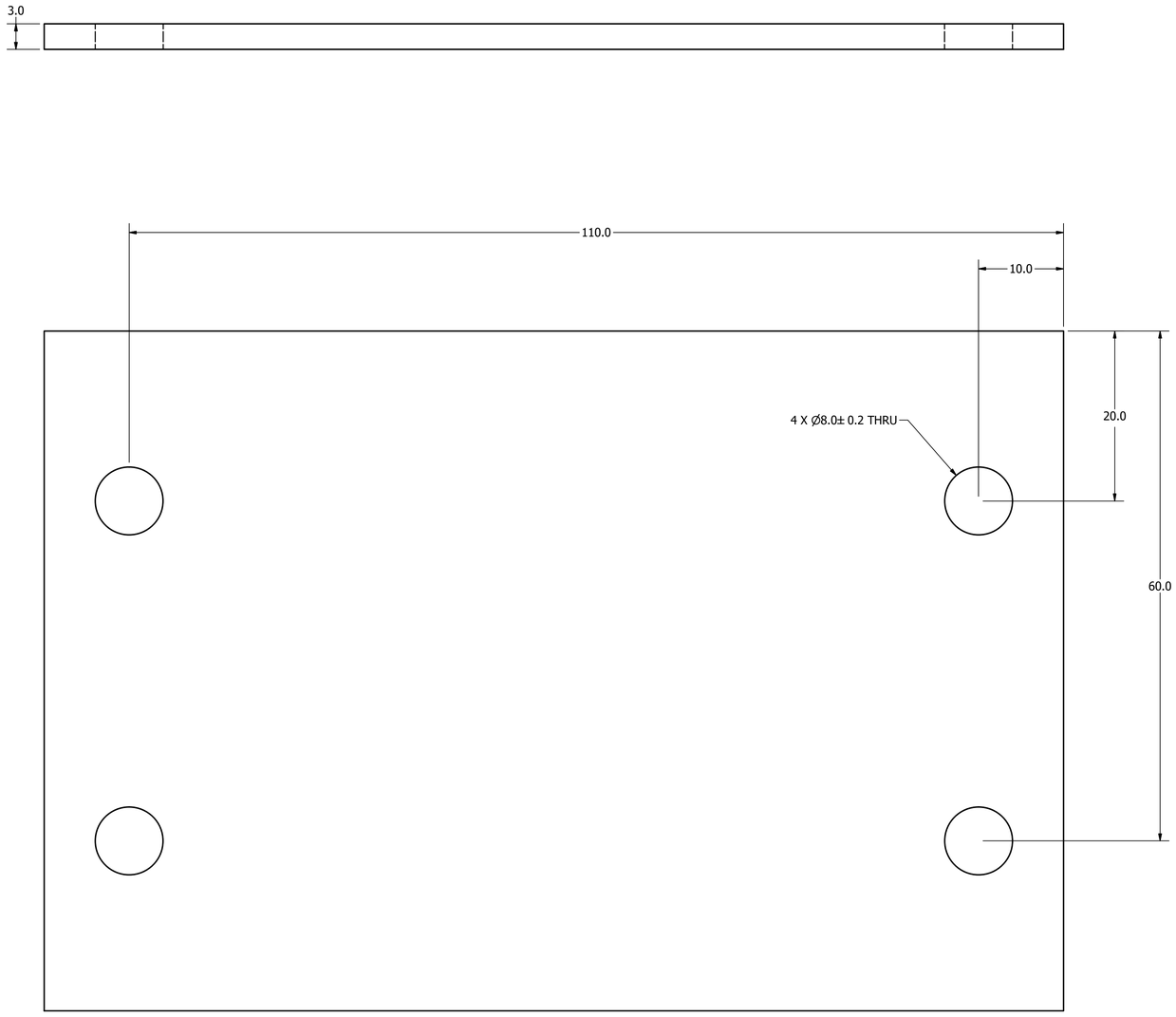

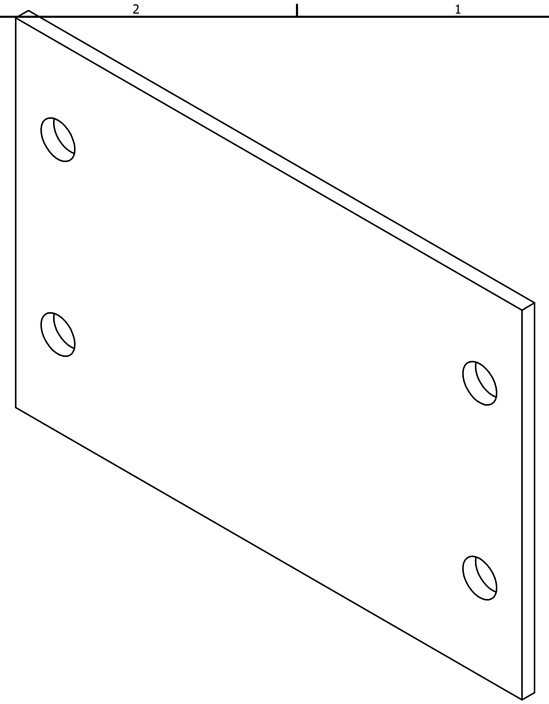

- 10 x 3MM MILD STEEL PLATES ARE REQUIRED

NOTE: REMOVE ALL SHARP EDGES

DRAWN Juan Laurea	27/11/2017	
CHECKED		TITLE 120X80X3MM MILD STEEL PLATE
QA		
MFG		
APPROVED		SIZE D / DWG NO JL_PLATE_MSTL_1208004 / REV
		SCALE 3 : 1 / SHEET 1 OF 1

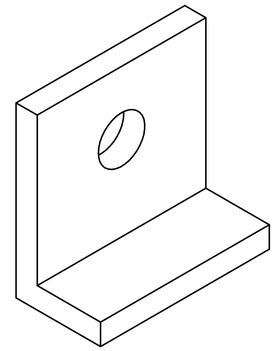

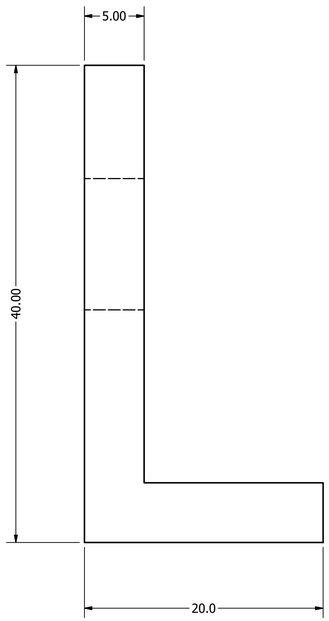

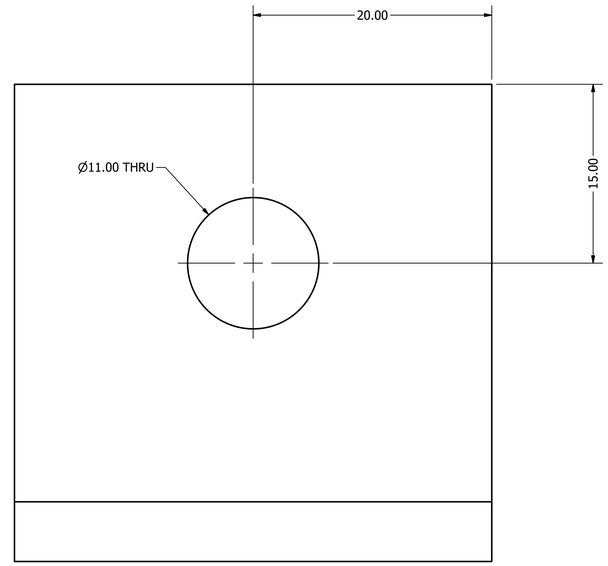

-BLACK MILD STEEL
-4 OFF

NOTE: THIS PART IS FROM BUNNINGS WAREHOUSE I/N 0910516
THESE DIMENSIONS ARE FOR MODIFYING THIS ITEM

DRAWN Juan Laurea	29/11/2017	
CHECKED		TITLE: BUNNINGS 0910516 40X40X5MM STEEL ANGLE
QA		
MFG		
APPROVED		
		SIZE D · DWG NO JL_BUN_0910516_STAGL · REV
		SCALE 4 : 1 · SHEET 1 OF 1

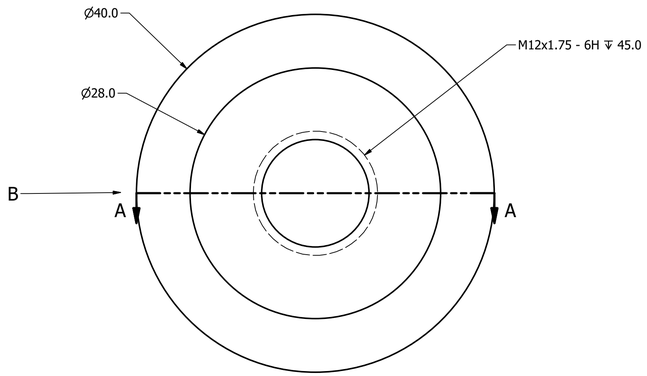

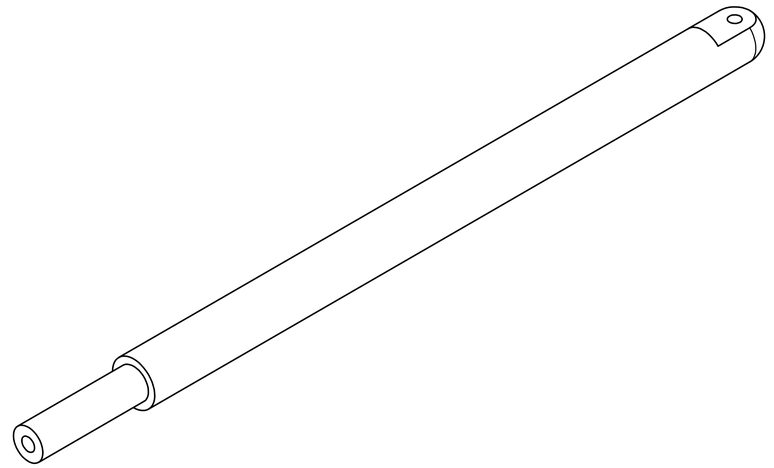

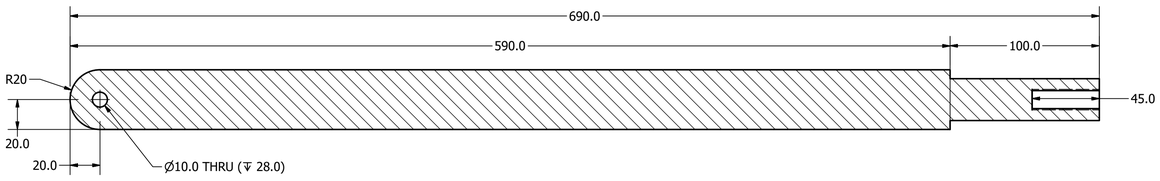

SECTION A-A
SCALE 1 / 2

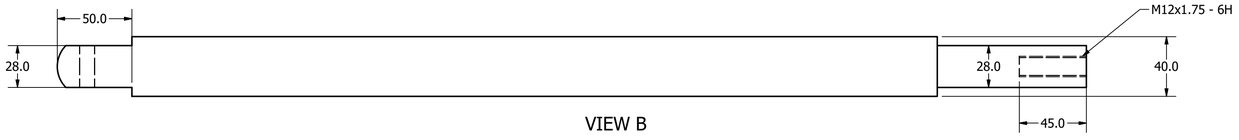

VIEW B

-ALUMINIUM ROD
-1 OFF

DRAWN Juan Laurea	28/11/2017	
CHECKED		TITLE: ALUMINIUM HEADTUBE MOUNT
QA		
MFG		
APPROVED		
		SIZE D · DWG NO JL_ALI_HTUBE · REV
		SCALE 3 : 1 · SHEET 1 OF 1

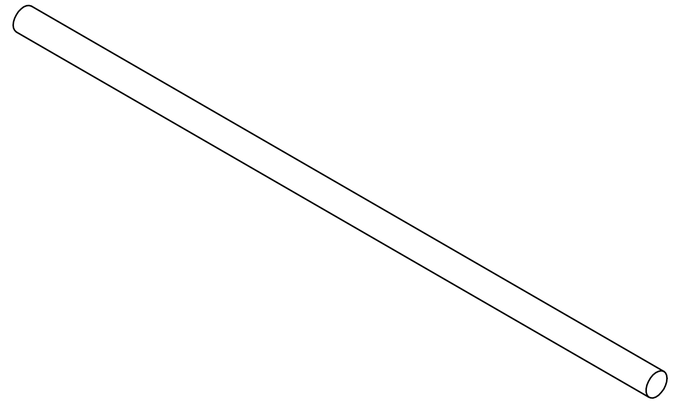

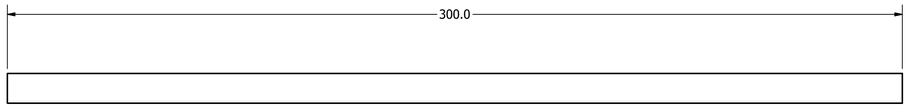

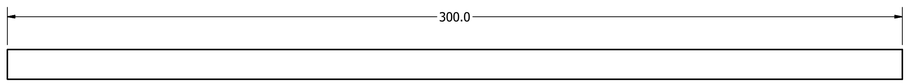

2 OFF X M10 GALVANISED STEEL ROD

DRAWN Juan Laurea	29/11/2017	
CHECKED		TITLE: BUNNINGS 2410267 M10 VERTICAL LINK ROD
QA		
MFG		
APPROVED		
		SIZE D | DWG NO JL_BUN_2410267_VLK_ROD | REV
		SCALE 1 : 1 | SHEET 1 OF 1

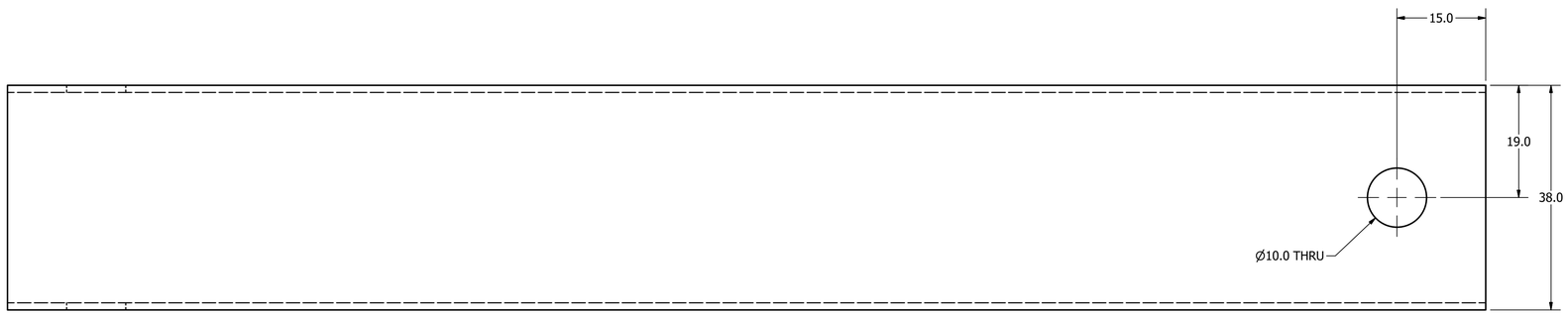

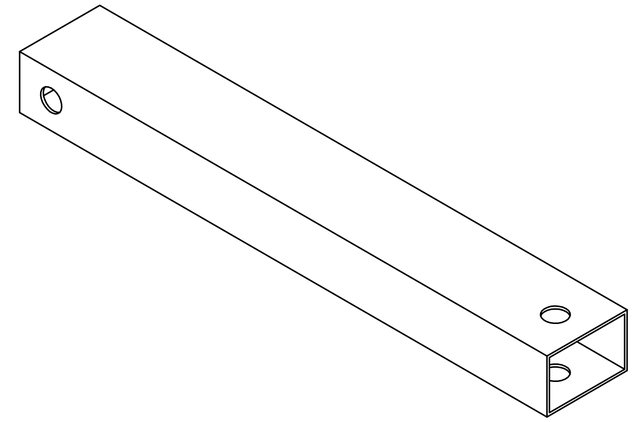

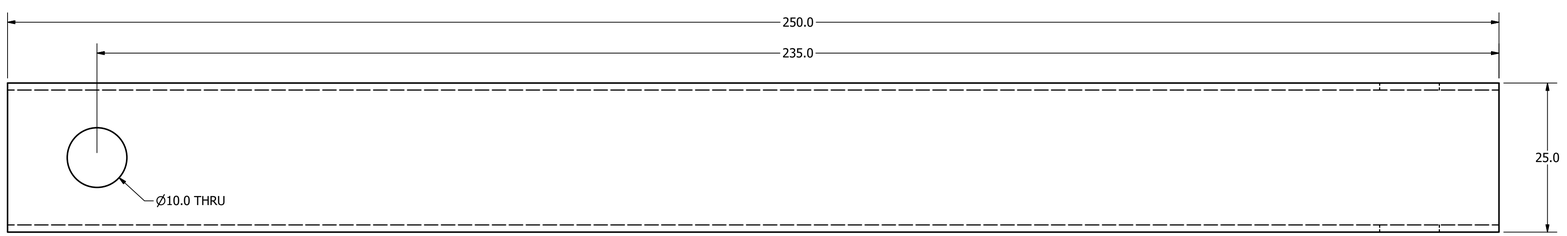

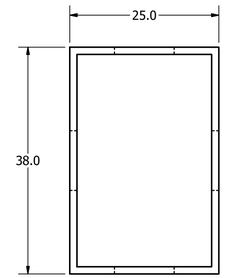

NOTE: FENCING TUBE FROM BUNNINGS - I/N:0910120
1 OFF - GALVINISED STEEL FENCING TUBE

DRAWN Juan Laurea	28/11/2017	
CHECKED		TITLE
QA		
MFG		BUNNINGS 0910120 VERTICAL LINK
APPROVED		
		SIZE D / DWG NO JL_VLINK_BUN_0910120 / REV
		SCALE 2 : 1 / SHEET 1 OF 1

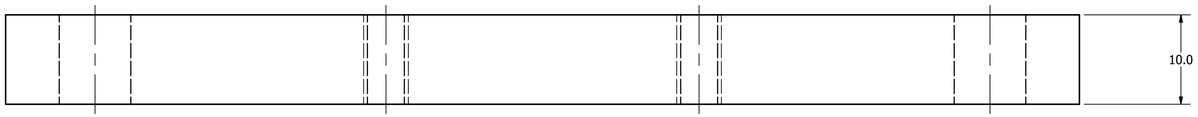

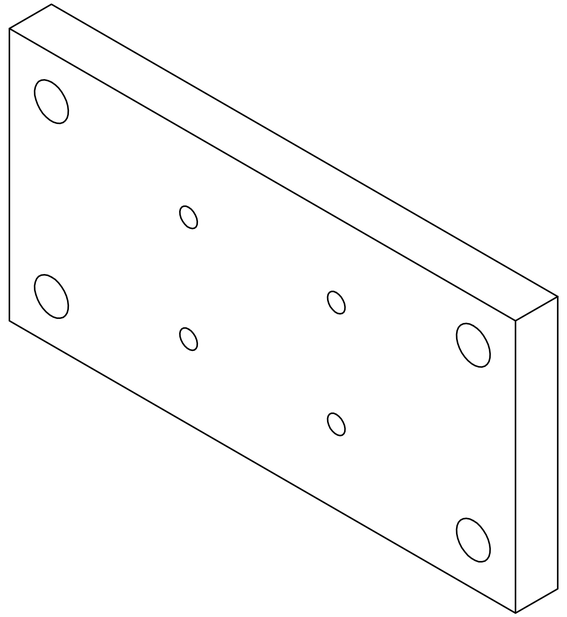

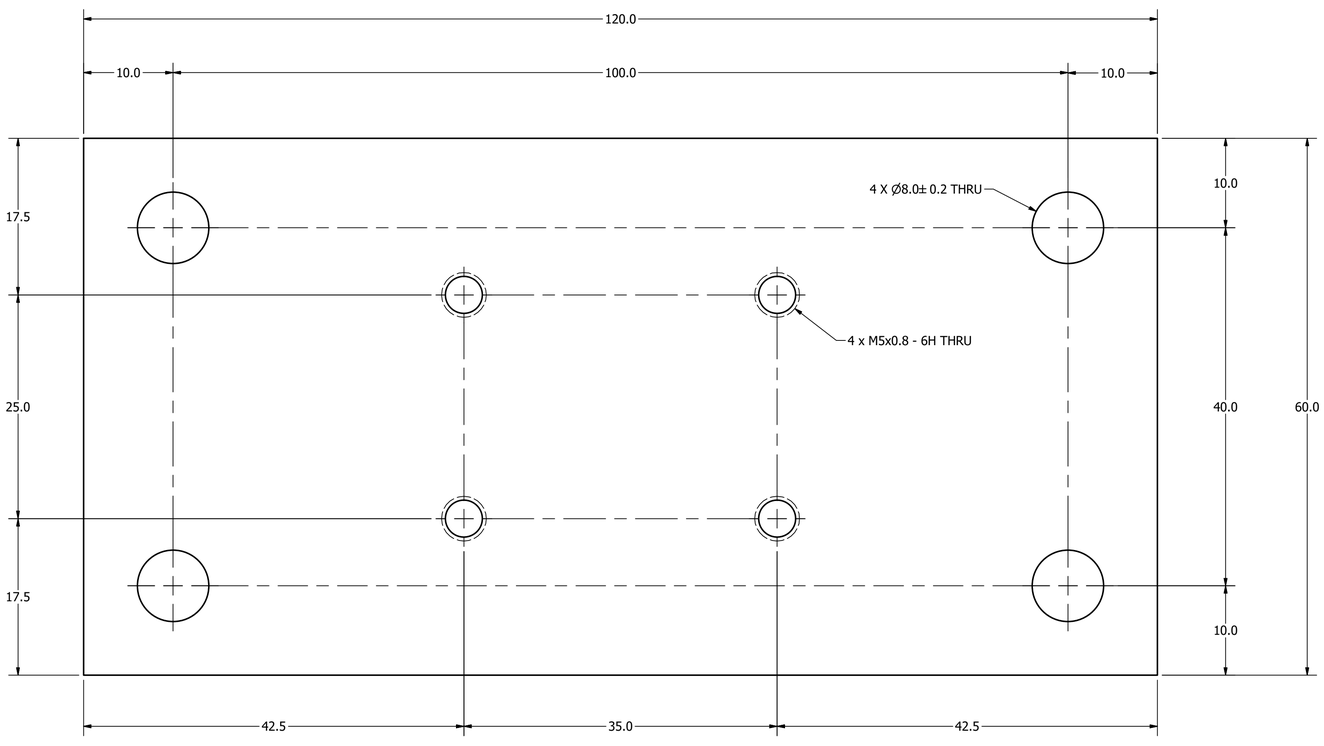

- 1 x 10MM MILD STEEL PLATE IS REQUIRED

NOTE: REMOVE SHARP EDGES

DRAWN Juan Laurea	28/11/2017		
CHECKED		TITLE 120x60x10MM MILD STEEL PLATE	
QA			
MFG			
APPROVED		SIZE D	DWG NO JL_PLATE_MSTL_1206010 REV
		SCALE 3 : 1	SHEET 1 OF 1

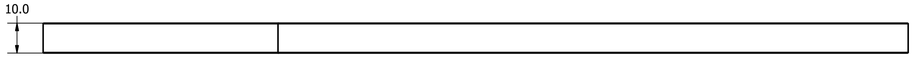

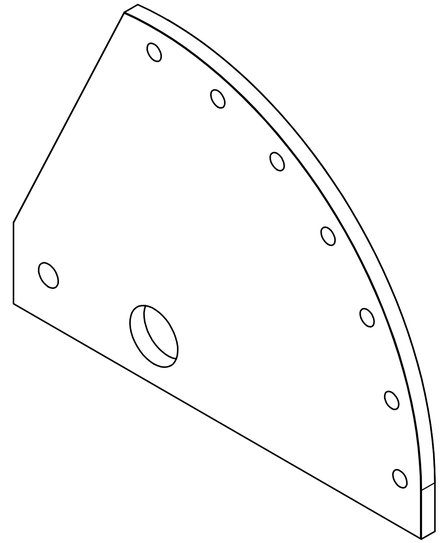

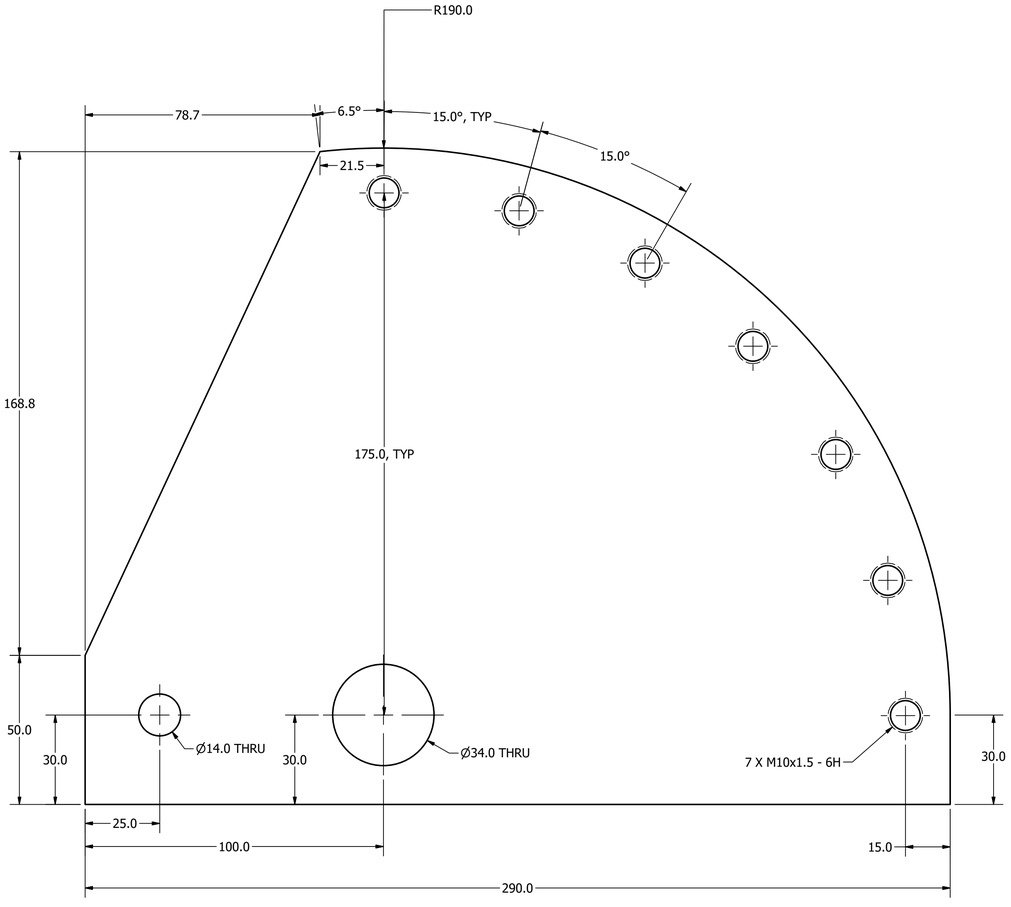

-MILD STEEL
-1 OFF
-REMOVE SHARP EDGES

DRAWN Juan Laurea	2/12/2017			
CHECKED		TITLE		
QA		MILD STEEL LOADING PLATE		
MFG				
APPROVED		SIZE D	DWG NO JL_MSTL_LPLATE	REV
		SCALE 1 : 1	SHEET 1 OF 1	

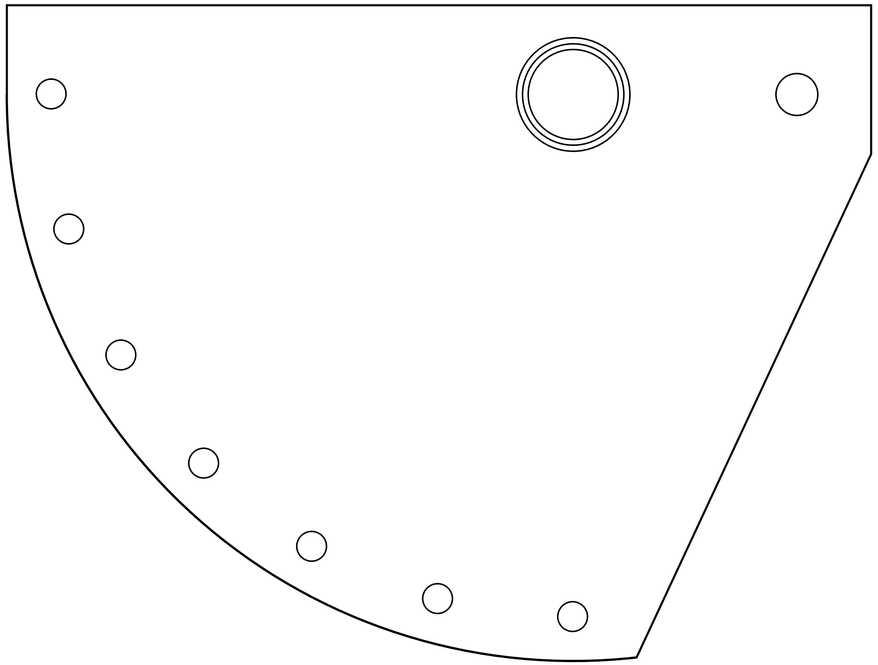

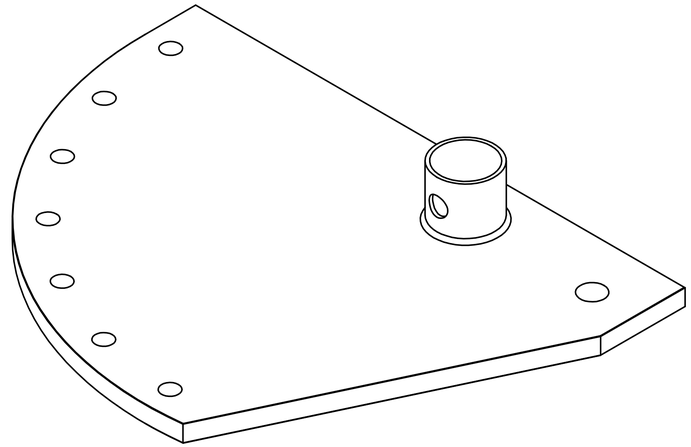

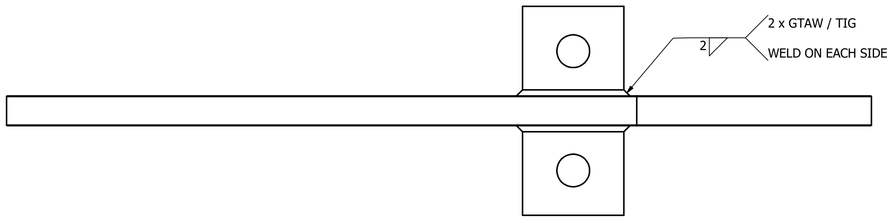

PARTS LIST			
ITEM	QTY	PART NUMBER	DESCRIPTION
1	1	JL_MS_RDNTUB	
2	1	JL_MSTL_LPLATE	10MM MILD STEEL PLATE

DRAWN	Juan Laurea	12/02/2018
CHECKED		
QA		
MFG		
APPROVED		

TITLE

MILD STEEL LOADING PLATE WELD

SIZE	DWG NO	REV
D	JL_MSTL_LPLATE_REVB	

SCALE 1 SHEET 1 OF 1

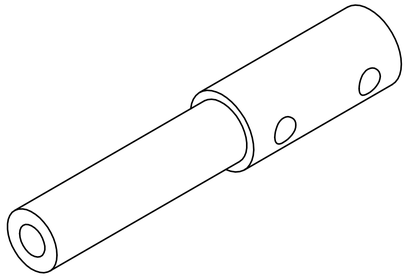

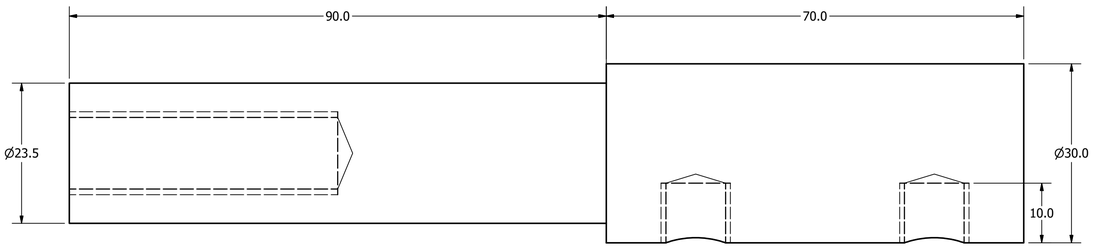

TOP

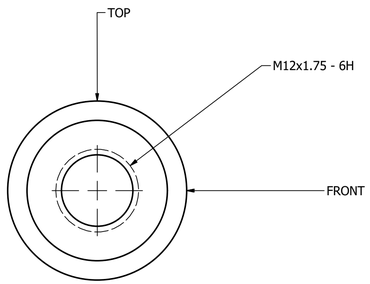

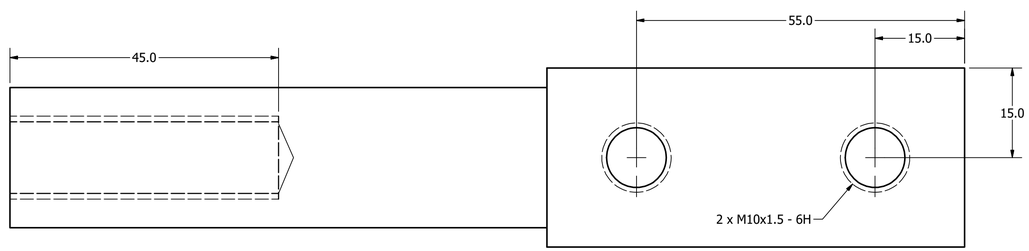

FRONT

STEEL SUPPLIED FROM SURMAN METALS
-STAINLESS STEEL
-1 OFF

DRAWN Juan Laurea	18/12/2017	
CHECKED		TITLE: 18122017 BOTTOM BRACKET ATTACHMENT
QA		
MFG		
APPROVED		
		SIZE D | DWG NO JL_BATTACHMENT | REV
		SCALE 2 | SHEET 1 OF 1

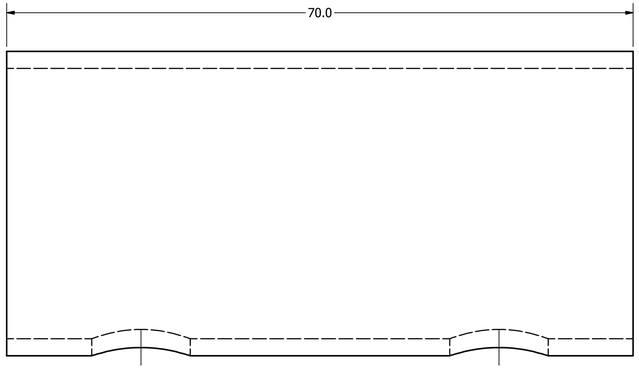

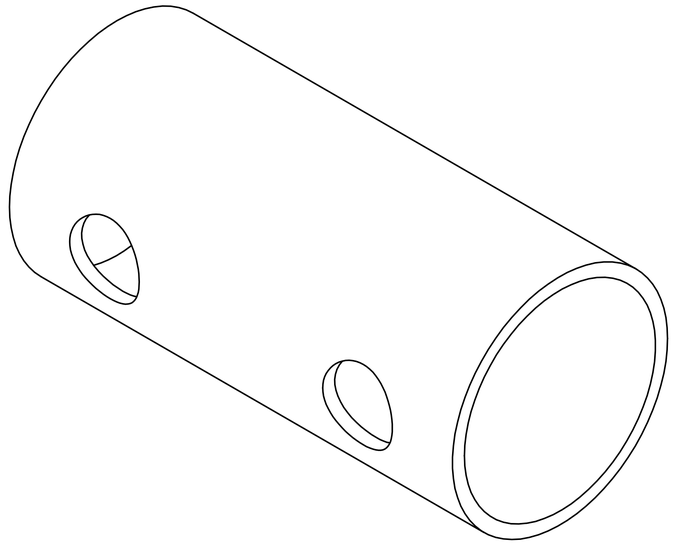

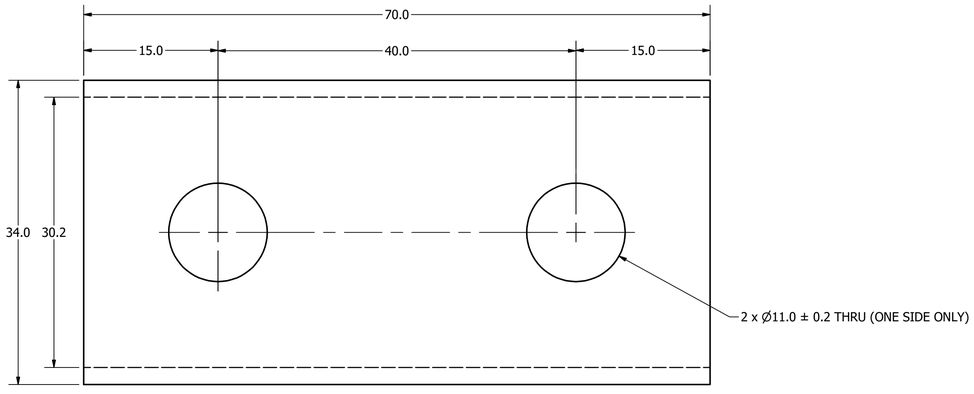

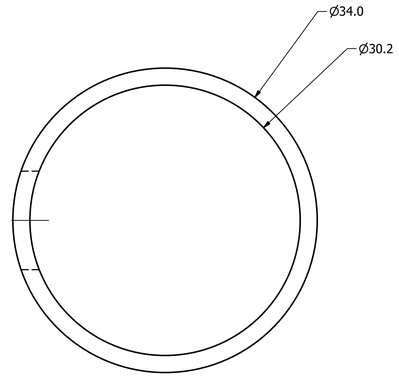

1 OFF Ø34MM ROUND BAR, 70MM LONG

DRAWN Juan Laurea	12/02/2018	
CHECKED		TITLE
QA		70MM LONG ROUND TUBE
MFG		
APPROVED		SIZE D / DWG NO JL_MS_RNDTUB / REV
		SCALE 3 : 1 / SHEET 1 OF 1

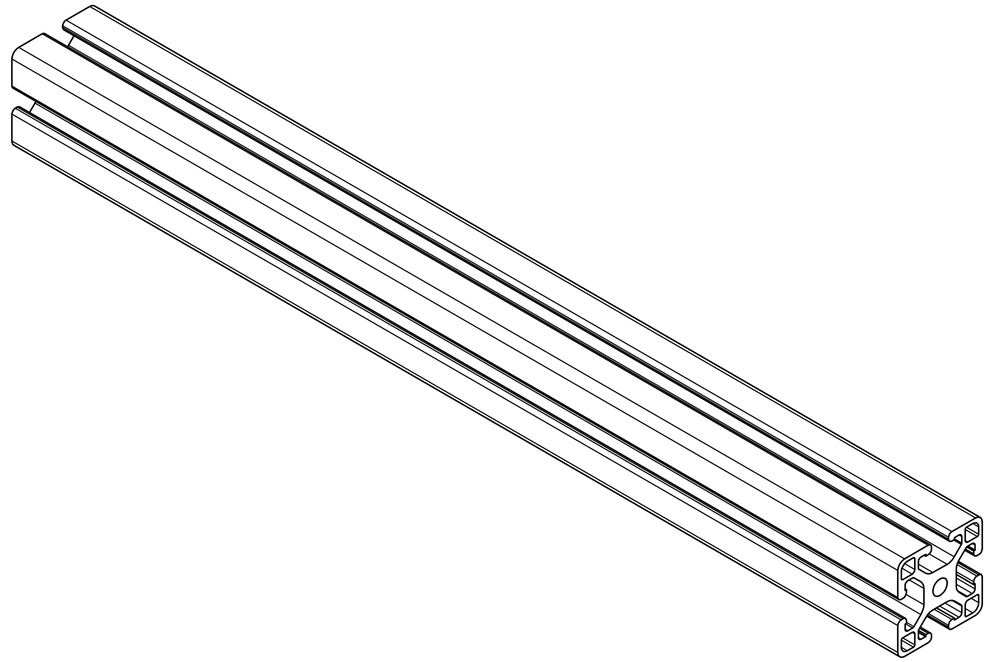

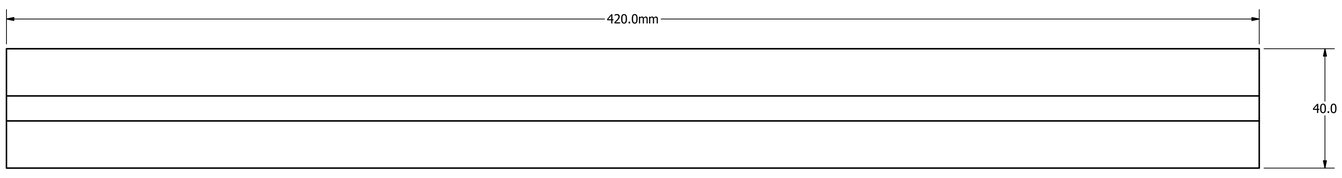

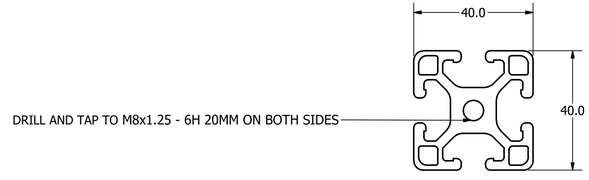

NOTE: THIS WILL BE PROCURED BY CYCLING AUSTRALIA AND SOURCED FROM PROFILIUM

9 OFF - 420x40x40MM ALUMINIUM EXTRUSION

DRAWN Juan Laurea	27/11/2017	
CHECKED		TITLE: PROFILE 4040 420MM ALUMINIUM EXTRUSION
QA		
MFG		
APPROVED		
		SIZE D / DWG NO JL_ALI_4040_420 / REV
		SCALE 1 : 1 / SHEET 1 OF 1

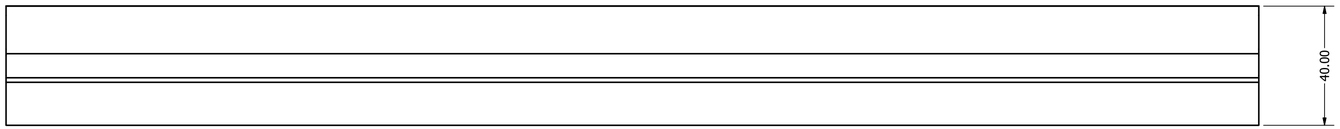

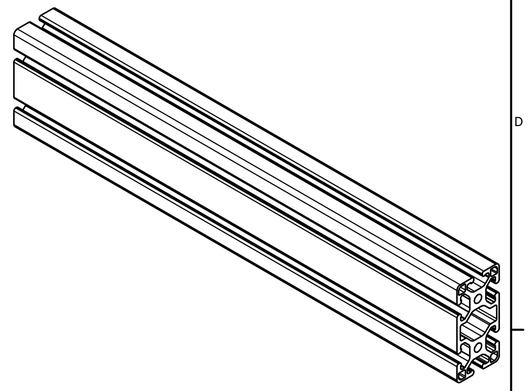

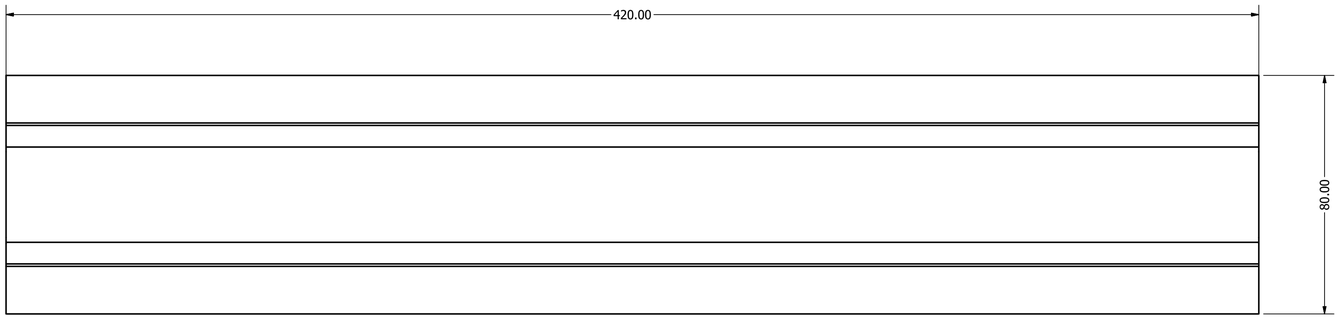

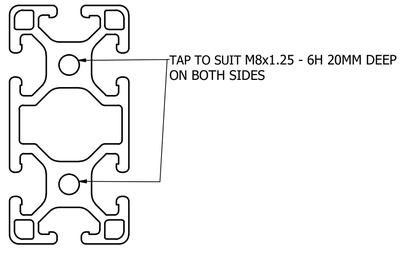

NOTE: THIS WILL BE PROCURED BY CYCLING AUSTRALIA AND SOURCED FROM PROFILIUM

1 OFF - 420x80x40MM ALUMINIUM EXTRUSION

DRAWN	Juan Laurea	28/11/2017		
CHECKED			TITLE	
QA			PROFILE 8040 420MM EXTRUSION	
MFG				
APPROVED			SIZE D	DWG NO JL_ALI_4080_420 REV
			SCALE 1 : 1	SHEET 1 OF 1

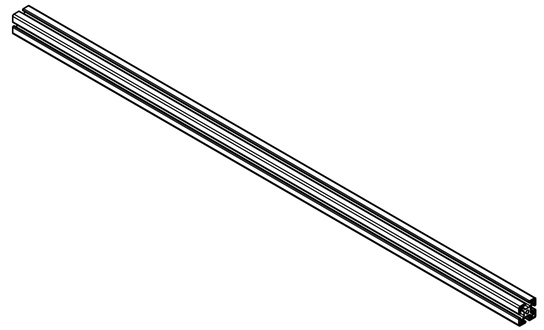

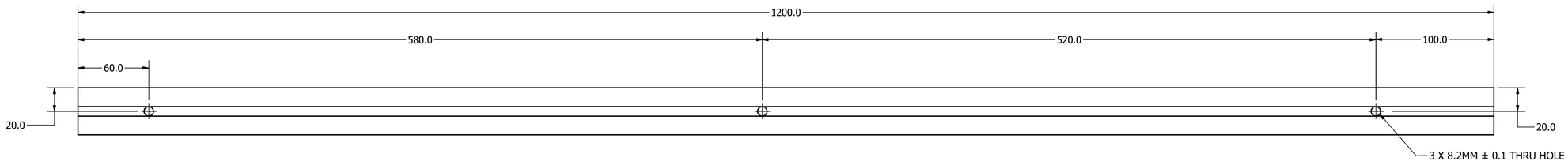

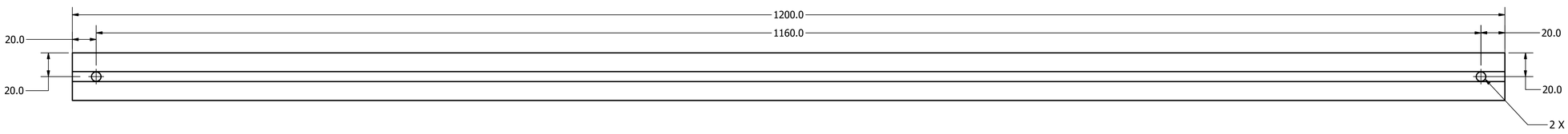

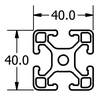

NOTE: THIS WILL BE PROCURED BY CYCLING AUSTRALIA AND SOURCED FROM PROFILIUM

2 OFF - 1200x40x40 ALUMINIUM EXTRUSION

DRAWN Juan Laurea	3/12/2017		
CHECKED		TITLE	
QA		PROFILE 4040 1200MM EXTRUSION BOTTOM SECTION	
MFG			
APPROVED		SIZE D	DWG NO JL_ALI_4040_1200_02 REV
		SCALE 1 / 2	SHEET 1 OF 1

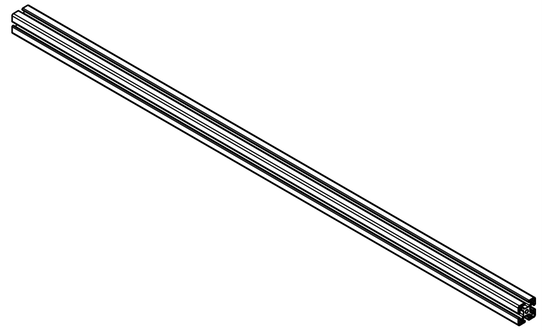

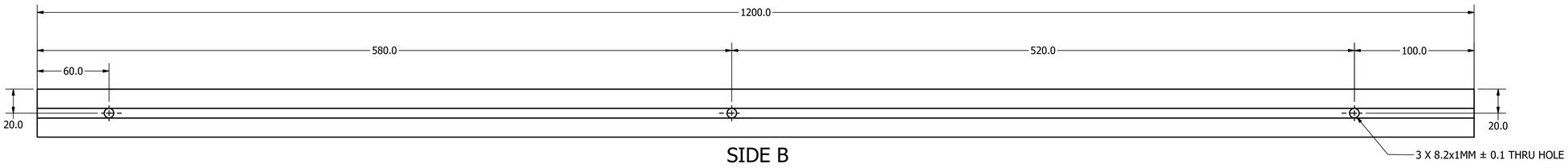

SIDE B

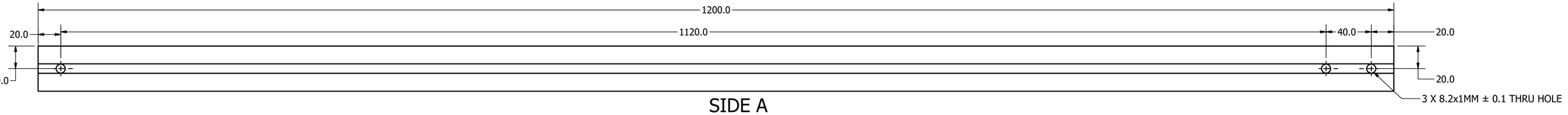

SIDE A

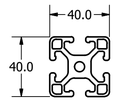

NOTE: THIS WILL BE PROCURED BY CYCLING AUSTRALIA AND SOURCED FROM PROFILIUM

2 OFF - 1200X40X40MM ALUMINIUM EXTRUSION

DRAWN Juan Laurea	2/12/2017		
CHECKED		TITLE	
QA		PROFILE 4040 1200MM EXTRUSION TOP SECTION	
MFG			
APPROVED		SIZE D	DWG NO JL_ALI_4040_1200_01 REV
		SCALE 1 / 2	SHEET 1 OF 1

13 Appendix E – Load, V[mm] and W[mm] Data

Below show raw data for Load[N], U[mm], V[mm], and W[mm].

Refer to Figure 36.

For The Pilot Tests:

- P0 – Bottom Bracket Marker Point
- P1 to P5 – Down Tube Marker Points
- P6 to P9 – Seat Tube Marker Points

For the Comparison Tests:

- C0 – Bottom Bracket Marker Points
- C1 to C5 – Down Tube Marker Points
- C6 to C10 – Seat Tube Marker Points
- C11 to C13 – Chain Stay Marker Points

CA01 LHS at 90 Deg

	C1		C2		C3		C4		C5		C6		C7		C8		C9		C10		C11		C12		C13		C0	
Load [N]	V [mm]	W [mm]	V [mm]	W [mm]	V [mm]	W [mm]	V [mm]	W [mm]	V [mm]	W [mm]	V [mm]	W [mm]	V [mm]	W [mm]	V [mm]	W [mm]	V [mm]	W [mm]	V [mm]	W [mm]	V [mm]	W [mm]	V [mm]	W [mm]	V [mm]	W [mm]	V [mm]	W [mm]
0	0	0	0	0	0	0	0	0	0	0	0	0	0	0	0	0	0	0	0	0	0	0	0	0	0	0	0	0
306	0.17758	1.88385	0.150401	1.64827	0.119008	1.36413	0.099932	1.07249	0.082749	0.862891	0.178167	1.7248	0.180222	1.27619	0.177353	0.754423	0.178825	0.346652	0.183985	-0.04098	0.397457	2.52203	0.427783	2.28597	0.476204	1.90516	0.197837	2.16454
600	0.330474	3.10712	0.275915	2.69042	0.222827	2.20185	0.190426	1.75048	0.156338	1.35943	0.335562	2.79544	0.342035	1.97012	0.337723	1.04721	0.342498	0.337973	0.34897	-0.3895	0.738434	4.22437	0.791996	3.76786	0.88195	3.09224	0.37137	3.57062
903	0.506312	4.18849	0.421599	3.60484	0.339828	2.90487	0.285185	2.29547	0.23048	1.75928	0.516908	3.68612	0.520069	2.52158	0.508683	1.2124	0.511604	0.173523	0.515782	-0.86159	1.11242	5.72328	1.18096	5.02855	1.30715	4.05992	0.571571	4.79218
1205	0.65046	5.25127	0.539325	4.51477	0.432861	3.61654	0.36125	2.84391	0.290493	2.15694	0.667137	4.68447	0.66963	3.25779	0.649624	1.62147	0.649634	0.329852	0.653767	-0.96411	1.43082	7.28026	1.51607	6.45618	1.66583	5.24158	0.739923	6.03883
1502	0.788569	6.24157	0.650538	5.35087	0.520423	4.27943	0.429677	3.36801	0.344155	2.5411	0.810888	5.5631	0.809338	3.85925	0.783638	1.90331	0.784145	0.383986	0.788991	-1.17397	1.73515	8.69216	1.83327	7.71227	2.00661	6.22939	0.899729	7.18266
1205	0.646445	5.15886	0.536054	4.4296	0.430204	3.56037	0.36029	2.80272	0.29008	2.11249	0.661759	4.56289	0.66243	3.10248	0.643673	1.44269	0.646015	0.1084	0.650624	-1.19475	1.42969	7.16433	1.51285	6.31236	1.66469	5.02176	0.734815	5.93296
900	0.500283	3.92953	0.416587	3.39634	0.337623	2.73081	0.287669	2.16159	0.234648	1.62345	0.510216	3.37591	0.51432	2.20888	0.501845	0.869285	0.505172	-0.17767	0.512544	-1.24705	1.10302	5.38611	1.17389	4.68547	1.29647	3.6234	0.56529	4.51534
602	0.343243	2.79216	0.287597	2.41256	0.233474	1.95275	0.198519	1.53166	0.163278	1.17968	0.349596	2.3371	0.35429	1.4509	0.349063	0.471902	0.355917	-0.32815	0.361479	-1.11862	0.773592	3.77101	0.825287	3.1814	0.917748	2.37691	0.387186	3.17994
300	0.182033	1.28668	0.154465	1.11735	0.126358	0.91262	0.109706	0.695565	0.090168	0.547719	0.187369	1.06403	0.19223	0.611528	0.19375	0.120928	0.200176	-0.30058	0.205406	-0.68168	0.393369	1.73958	0.423386	1.42187	0.469701	0.980632	0.204075	1.48605
0	0.015017	-0.50803	0.013942	-0.43064	0.012999	-0.35536	0.012861	-0.32043	0.010065	-0.23817	0.020028	-0.52258	0.020202	-0.5315	0.024118	-0.51419	0.02742	-0.5025	0.027766	-0.46779	0.010438	-0.65778	0.012363	-0.70372	0.006083	-0.78135	0.01858	-0.5524

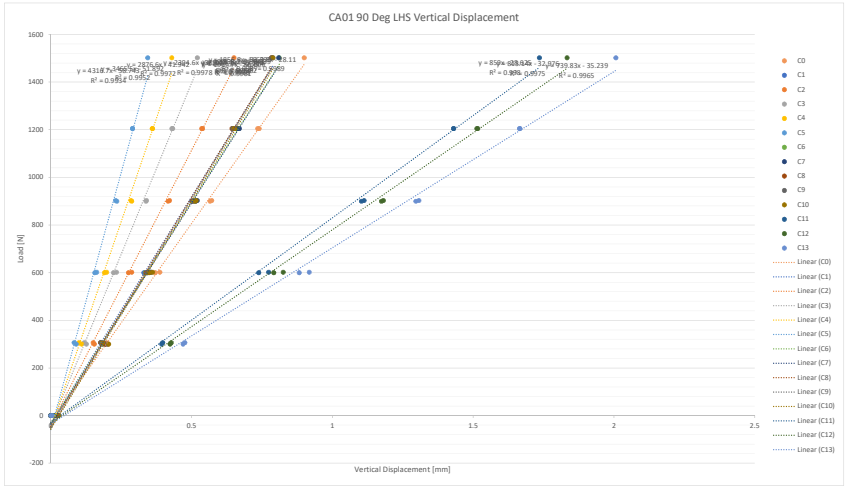

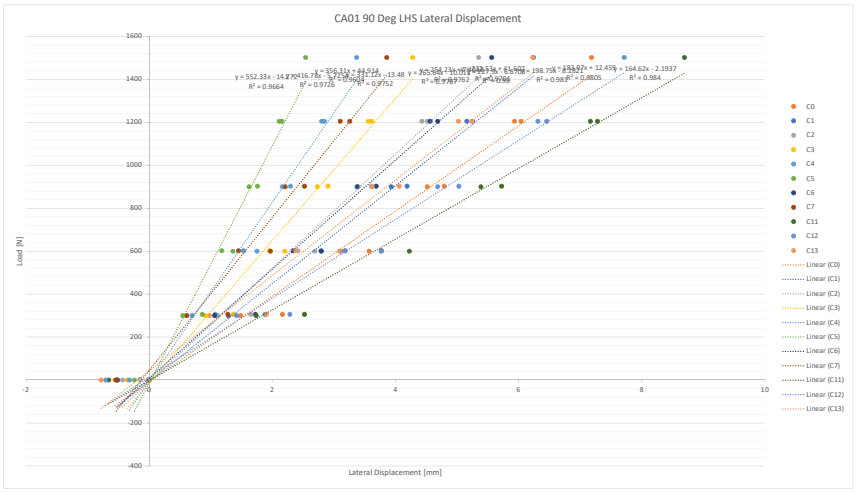

CA01 LHS at 105 Deg

	C0		C1		C2		C3		C4		C5		C6		C7		C8		C9		C10		C11		C12		C13	
Load [N]	V [mm]	W [mm]	V [mm]	W [mm]	V [mm]	W [mm]	V [mm]	W [mm]	V [mm]	W [mm]	V [mm]	W [mm]	V [mm]	W [mm]	V [mm]	W [mm]	V [mm]	W [mm]	V [mm]	W [mm]	V [mm]	W [mm]	V [mm]	W [mm]	V [mm]	W [mm]	V [mm]	W [mm]
0	0	0	0	0	0	0	0	0	0	0	0	0	0	0	0	0	0	0	0	0	0	0	0	0	0	0	0	0
306	0.207347	1.79649	0.186874	1.58429	0.157001	1.35037	0.13114	1.09281	0.112269	0.872328	0.094327	0.641757	0.188944	1.34053	0.19273	0.894223	0.188256	0.419869	0.192364	-0.00508	0.196569	-0.41441	0.407103	2.06745	0.436081	1.79346	0.488477	1.41522
595	0.36234	3.6326	0.323894	3.22746	0.26796	2.7628	0.219145	2.24498	0.185051	1.80573	0.154144	1.38363	0.32422	2.85381	0.325966	2.02383	0.315094	1.15515	0.318859	0.39694	0.321725	-0.32554	0.730801	4.22497	0.775696	3.7579	0.86649	3.12443
900	0.55155	4.64578	0.490405	4.08252	0.405346	3.48359	0.331477	2.82185	0.279676	2.23508	0.229077	1.68887	0.497138	3.55519	0.496531	2.43673	0.481912	1.19901	0.482197	0.163028	0.486245	-0.8616	1.07464	5.46917	1.13662	4.81542	1.25914	3.87823
1195	0.708628	6.06088	0.625464	5.30977	0.512327	4.52827	0.416264	3.66608	0.347423	2.90241	0.282775	2.21387	0.632885	4.67932	0.629369	3.27085	0.604919	1.71847	0.603737	0.419608	0.603904	-0.87809	1.3811	7.14372	1.45851	6.35512	1.60965	5.23675
1503	0.890182	6.82683	0.782118	5.9272	0.64322	5.05212	0.520748	4.04671	0.434869	3.15436	0.353102	2.35924	0.800059	5.20958	0.794562	3.5168	0.763987	1.66405	0.759823	0.10383	0.759459	-1.42537	1.70573	8.16217	1.79635	7.21518	1.97034	5.82932
1200	0.732365	5.9856	0.647599	5.24913	0.532811	4.47594	0.434515	3.59612	0.362216	2.83715	0.296349	2.17395	0.65664	4.5875	0.652171	3.12914	0.628641	1.54457	0.627475	0.191248	0.62627	-1.14454	1.41943	7.08492	1.49936	6.24791	1.65191	5.0719
900	0.55424	4.63753	0.492816	4.05797	0.410209	3.49473	0.337225	2.80478	0.284471	2.21728	0.234419	1.67345	0.497202	3.4826	0.497667	2.3093	0.480927	0.990562	0.480949	-0.12752	0.483195	-1.20224	1.0898	5.42072	1.15535	4.71778	1.27659	3.67893
600	0.400761	2.77949	0.360735	2.45611	0.302166	2.09697	0.250549	1.66034	0.212891	1.28904	0.179217	0.957939	0.362379	1.96538	0.365315	1.13691	0.35584	0.237622	0.357782	-0.55728	0.362062	-1.30971	0.770759	3.26504	0.815847	2.70468	0.906148	1.93988
302	0.214972	1.37014	0.194881	1.23875	0.164061	1.02984	0.136699	0.808751	0.117198	0.623622	0.098301	0.465988	0.195154	0.912487	0.196021	0.447759	0.191188	-0.07476	0.192915	-0.52631	0.196959	-0.93929	0.41562	1.60598	0.440413	1.25637	0.492673	0.787695
0	0.042618	-0.76526	0.03913	-0.67075	0.03779	-0.59358	0.033091	-0.51586	0.028396	-0.43091	0.02591	-0.3587	0.044152	-0.7621	0.045512	-0.72593	0.04378	-0.70928	0.042906	-0.68986	0.042085	-0.66443	0.03172	-0.88608	0.029988	-0.97428	0.027515	-1.04746

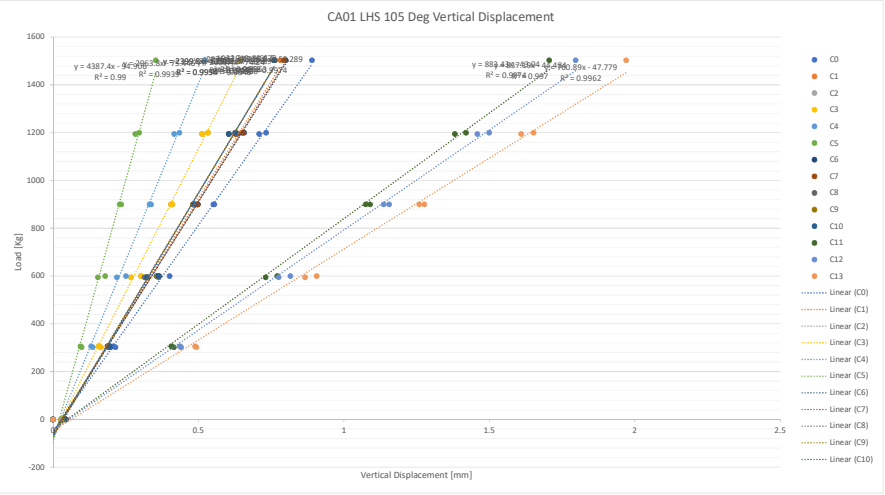

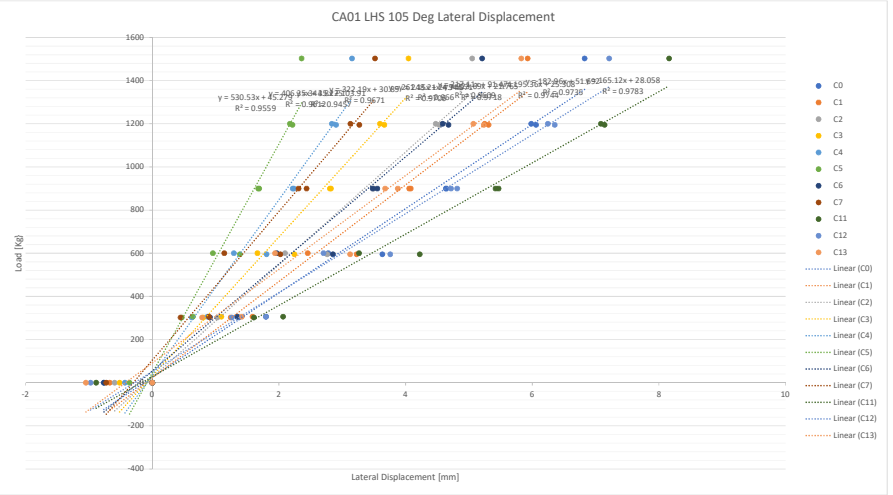

CA01 LHS at 120 Deg

	C0		C1		C2		C3		C4		C5		C6		C7		C8		C9		C10		C11		C12		C13	
Load [N]	V [mm]	W [mm]	V [mm]	W [mm]	V [mm]	W [mm]	V [mm]	W [mm]	V [mm]	W [mm]	V [mm]	W [mm]	V [mm]	W [mm]	V [mm]	W [mm]	V [mm]	W [mm]	V [mm]	W [mm]	V [mm]	W [mm]	V [mm]	W [mm]	V [mm]	W [mm]	V [mm]	W [mm]
0	0	0	0	0	0	0	0	0	0	0	0	0	0	0	0	0	0	0	0	0	0	0	0	0	0	0	0	0
303	0.186893	2.69911	0.166859	2.40645	0.143503	2.15816	0.113297	1.76763	0.096661	1.45846	0.082427	1.202	0.156894	2.17044	0.155822	1.67143	0.150376	1.10984	0.150205	0.65588	0.152305	0.233831	0.414927	3.07673	0.441294	2.79399	0.497044	2.4436
603	0.368777	4.12314	0.325435	3.61174	0.273829	3.189	0.220827	2.59899	0.189406	2.12311	0.161584	1.67921	0.310535	3.13527	0.3046	2.22118	0.290095	1.12509	0.287384	0.278617	0.286203	-0.52237	0.789447	4.73779	0.833703	4.15233	0.928757	3.40198
900	0.524032	5.34087	0.46427	4.69245	0.3897	4.11814	0.311407	3.31706	0.266426	2.64836	0.224133	2.07397	0.438918	3.96381	0.424178	2.69064	0.396007	1.18193	0.386768	-0.02493	0.379269	-1.1529	1.11575	6.16772	1.17104	5.30767	1.29334	4.23763
1200	0.679296	7.06808	0.598981	6.20774	0.499721	5.47504	0.396205	4.43757	0.334737	3.57993	0.280956	2.78698	0.564534	5.37419	0.541127	3.72912	0.498769	1.83993	0.481199	0.328778	0.468509	-1.09858	1.43981	8.20143	1.50338	7.15671	1.65291	5.8401
1505	0.824138	8.24359	0.721966	7.21401	0.597832	6.29902	0.471877	5.08839	0.395938	4.06265	0.327901	3.14937	0.684378	6.22983	0.65446	4.28652	0.598077	2.07628	0.573983	0.272966	0.55619	-1.41715	1.73898	9.63241	1.81665	8.44043	1.99185	6.89299
1205	0.634777	7.38563	0.55662	6.49684	0.461524	5.70841	0.361483	4.6388	0.303295	3.73957	0.25147	2.93266	0.514549	5.6293	0.491159	3.936	0.447365	1.96933	0.426444	0.413564	0.41255	-1.082	1.41323	8.56933	1.47557	7.51562	1.62733	6.1542
900	0.481736	6.02124	0.425266	5.30744	0.352953	4.66746	0.279645	3.78549	0.236831	3.0783	0.200536	2.39238	0.387009	4.61034	0.369793	3.25393	0.336195	1.68887	0.322917	0.43908	0.313612	-0.75233	1.09204	6.9437	1.14147	6.09092	1.26384	5.00924
600	0.368032	4.10334	0.326781	3.62481	0.279117	3.20044	0.225208	2.59431	0.192929	2.11385	0.164321	1.66138	0.30527	3.07547	0.298007	2.07947	0.277061	0.957628	0.271506	0.042607	0.267491	-0.80839	0.803475	4.69817	0.84268	4.02756	0.937762	3.1946
306	0.196936	2.31738	0.17709	2.0519	0.150918	1.81605	0.124236	1.48295	0.108773	1.20803	0.092956	0.957541	0.163198	1.75399	0.158721	1.21257	0.149689	0.588148	0.143923	0.083367	0.140919	-0.38646	0.432941	2.6323	0.455494	2.28866	0.508141	1.82739
0	-0.01332	0.38344	-0.01141	0.352735	-0.00812	0.343785	-0.00708	0.289013	-0.00586	0.273405	-0.00403	0.251135	-0.01515	0.377903	-0.01624	0.394362	-0.01516	0.384815	-0.01739	0.402609	-0.01865	0.447537	-0.01281	0.406416	-0.01529	0.475845	-0.01919	0.501334

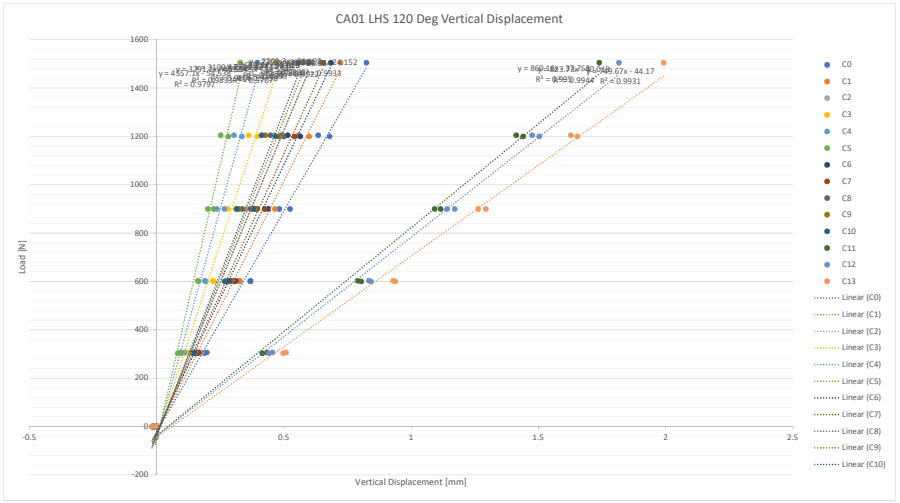

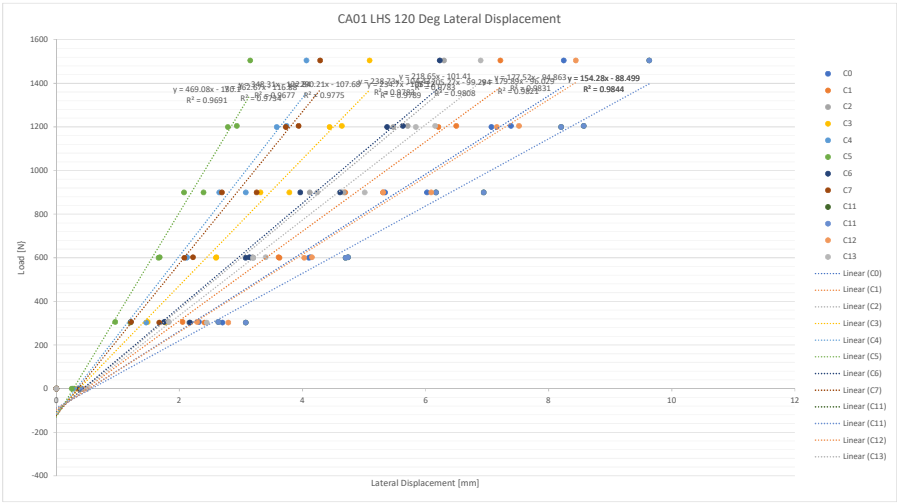

CA01 LHS at 135 Deg

	C0		C1		C2		C3		C4		C5		C6		C7		C8		C9		C10		C11		C12		C13	
Load [N]	V [mm]	W [mm]	V [mm]	W [mm]	V [mm]	W [mm]	V [mm]	W [mm]	V [mm]	W [mm]	V [mm]	W [mm]	V [mm]	W [mm]	V [mm]	W [mm]	V [mm]	W [mm]	V [mm]	W [mm]	V [mm]	W [mm]	V [mm]	W [mm]	V [mm]	W [mm]	V [mm]	W [mm]
0	0	0	0	0	0	0	0	0	0	0	0	0	0	0	0	0	0	0	0	0	0	0	0	0	0	0	0	0
305	0.172618	2.40587	0.154682	2.13709	0.128442	1.86349	0.109754	1.52885	0.090314	1.22952	0.075115	0.968749	0.140291	1.83417	0.137163	1.27871	0.131157	0.72434	0.132149	0.195677	0.135017	-0.25798	0.397147	2.70024	0.425452	2.42006	0.482361	2.04567
603	0.330861	4.03957	0.290555	3.54417	0.240245	3.14212	0.19986	2.58841	0.164811	2.0607	0.135687	1.61468	0.267104	3.01748	0.258512	2.00227	0.240394	0.993125	0.232816	0.084458	0.23934	-0.75873	0.743152	4.55683	0.792694	4.04176	0.890504	3.32921
907	0.486643	5.28845	0.427381	4.64498	0.35451	4.07032	0.291913	3.31361	0.237485	2.60124	0.196515	2.00271	0.39306	3.86606	0.374244	2.45192	0.346176	1.05502	0.331312	-0.22879	0.336612	-1.41782	1.06657	5.9969	1.1332	5.27231	1.26312	4.23806
1200	0.584204	6.66615	0.507862	5.83844	0.415211	5.11235	0.337416	4.15806	0.273707	3.27199	0.223123	2.51192	0.460958	4.94843	0.431943	3.22546	0.390051	1.49605	0.364627	-0.06673	0.362843	-1.47592	1.30179	7.59259	1.37394	6.70223	1.52284	5.42953
1505	0.717345	8.02839	0.621004	7.02594	0.508762	6.14381	0.40917	5.02004	0.331931	3.93235	0.26863	3.05179	0.566281	6.00558	0.527164	3.95737	0.471922	1.9254	0.437835	0.058247	0.433442	-1.59758	1.58006	9.21147	1.66685	8.21359	1.8389	6.7681
1205	0.588664	6.52802	0.511238	5.70908	0.420548	5.01019	0.3402	4.08287	0.275046	3.19346	0.224229	2.46408	0.46102	4.76415	0.431222	2.98328	0.3877	1.21096	0.364042	-0.40742	0.360635	-1.88495	1.31805	7.45531	1.39263	6.50857	1.54385	5.22496
900	0.450089	5.30392	0.393066	4.65646	0.322841	4.10217	0.264619	3.35817	0.217185	2.63894	0.18272	2.04655	0.351026	3.8457	0.332288	2.37751	0.300956	0.905944	0.284485	-0.43643	0.287323	-1.64844	1.03621	5.99171	1.09957	5.19649	1.22775	4.11744
608	0.311385	4.09452	0.275255	3.61254	0.225625	3.19347	0.18407	2.61355	0.151596	2.06274	0.12538	1.63971	0.243507	2.99949	0.231675	1.92065	0.208383	0.846759	0.200228	-0.14763	0.202143	-1.07284	0.741239	4.61831	0.788069	4.00454	0.88854	3.23063
302	0.145476	1.86805	0.130955	1.64371	0.108602	1.46061	0.090815	1.17008	0.075046	0.912032	0.064426	0.704314	0.114523	1.29845	0.111567	0.73256	0.102342	0.185582	0.102326	-0.30936	0.10413	-0.7858	0.360994	2.08894	0.384793	1.74508	0.436305	1.31939
0	-0.02212	-0.04188	-0.01989	-0.03396	-0.0176	-0.02468	-0.01171	-0.01307	-0.01061	-0.00166	-0.00976	0.016385	-0.01966	-0.0538	-0.01682	-0.03137	-0.01852	-0.02705	-0.01662	-0.00114	-0.01696	-0.00351	-0.02171	-0.04757	-0.02691	-0.07598	-0.02833	-0.08258

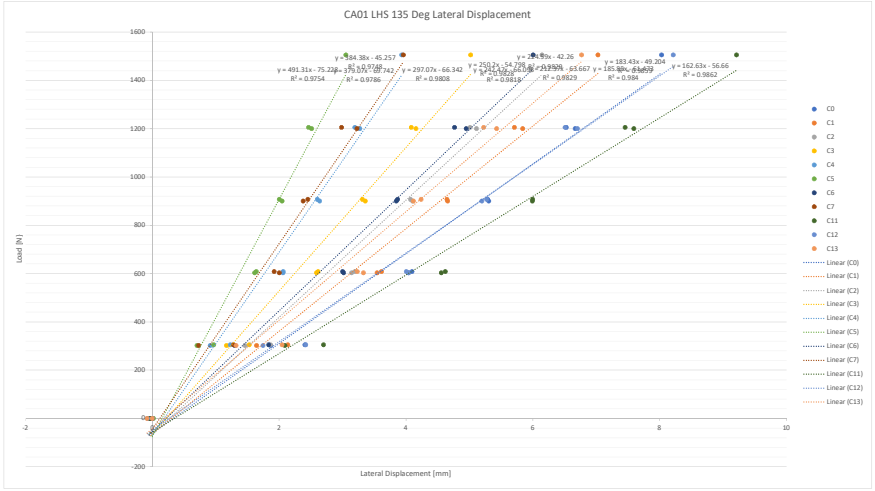

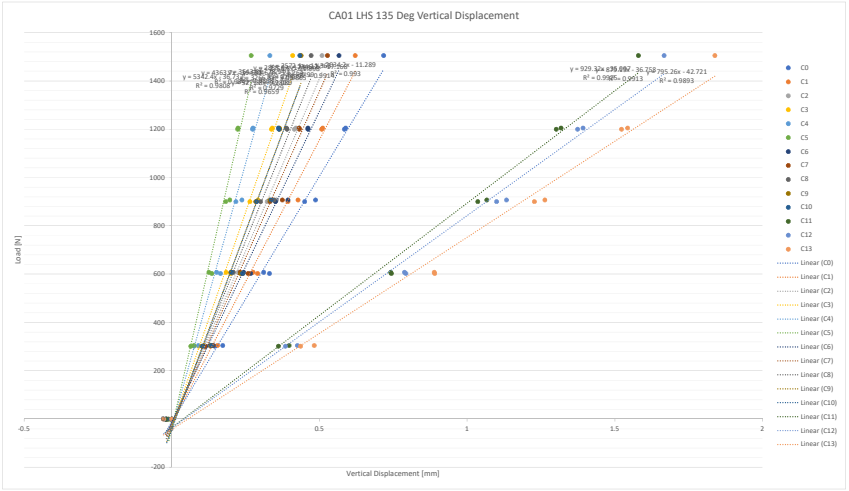

CA01 LHS at 150 Deg

	C0		C1		C2		C3		C4		C5		C7		C8		C9		C12		C13		C14		C10		C11	
Load [N]	V [mm]	W [mm]	V [mm]	W [mm]	V [mm]	W [mm]	V [mm]	W [mm]	V [mm]	W [mm]	V [mm]	W [mm]	V [mm]	W [mm]	V [mm]	W [mm]	V [mm]	W [mm]	V [mm]	W [mm]	V [mm]	W [mm]	V [mm]	W [mm]	V [mm]	W [mm]	V [mm]	W [mm]
0	0	0	0	0	0	0	0	0	0	0	0	0	0	0	0	0	0	0	0	0	0	0	0	0	0	0	0	0
307	0.181131	2.34026	0.163443	2.04771	0.134827	1.78138	0.117477	1.47276	0.100612	1.1949	0.087359	0.912322	0.147564	1.74919	0.144824	1.18332	0.138703	0.56009	0.428884	2.73263	0.457501	2.35825	0.5157	1.92329	0.131418	0.057727	0.13081	-0.38611
607	0.355739	4.32957	0.318326	3.85133	0.269475	3.37467	0.223893	2.77731	0.189425	2.27207	0.164409	1.75463	0.289325	3.29976	0.276475	2.25344	0.258778	1.18735	0.811531	5.01884	0.858604	4.36936	0.956608	3.59453	0.250284	0.242301	0.248095	-0.57127
903	0.497286	5.6979	0.443654	5.04089	0.373864	4.44077	0.308406	3.64258	0.259257	2.99119	0.222787	2.30583	0.404949	4.31734	0.382854	2.9623	0.353277	1.53055	1.11573	6.66364	1.17355	5.86055	1.29697	4.80646	0.336411	0.307205	0.326821	-0.77635
1205	0.627421	6.54082	0.55791	5.75467	0.470408	5.06133	0.384595	4.0995	0.318985	3.32274	0.271949	2.49384	0.509274	4.84935	0.482397	3.1689	0.440923	1.42063	1.39791	7.71363	1.46298	6.69262	1.61267	5.382	0.413296	-0.10609	0.397912	-1.43021
1506	0.754843	7.58686	0.667136	6.67262	0.55877	5.83394	0.451129	4.72621	0.371512	3.80619	0.315862	2.83642	0.609357	5.57924	0.571326	3.60665	0.512476	1.52597	1.6749	8.96961	1.74997	7.76815	1.9239	6.23406	0.477766	-0.26662	0.457334	-1.84866
1200	0.633989	6.81594	0.563675	5.98577	0.474818	5.24014	0.388405	4.27384	0.320798	3.46932	0.276293	2.62534	0.511348	5.06874	0.480241	3.34436	0.435935	1.54482	1.41758	7.98525	1.48377	6.92866	1.63491	5.63618	0.40941	-0.0348	0.393438	-1.40165
900	0.44804	5.77802	0.399115	5.14012	0.33207	4.5052	0.269523	3.69708	0.226616	2.96686	0.195601	2.29809	0.349624	4.32394	0.329359	2.91352	0.296481	1.44899	1.07453	6.76951	1.12889	5.89395	1.25315	4.82485	0.276351	0.173874	0.263116	-0.94581
603	0.326921	4.24082	0.29322	3.77272	0.247125	3.31342	0.206135	2.71019	0.177497	2.17186	0.153638	1.70483	0.261881	3.20919	0.249816	2.19025	0.236629	1.12349	0.76854	4.9407	0.80929	4.31981	0.902074	3.54039	0.228448	0.193022	0.226389	-0.60154
302	0.169488	2.46424	0.150654	2.15261	0.128971	1.91132	0.108498	1.57581	0.092152	1.28917	0.079459	1.01997	0.135046	1.89785	0.129627	1.33697	0.120977	0.790629	0.411037	2.86828	0.435368	2.50858	0.490954	2.09684	0.116263	0.270039	0.113126	-0.15096
0	0.026296	-0.14047	0.02251	-0.12402	0.020581	-0.11876	0.021913	-0.1107	0.020495	-0.10181	0.019568	-0.09163	0.026062	-0.13361	0.021622	-0.11052	0.018867	-0.0821	0.021763	-0.14395	0.021345	-0.18698	0.015156	-0.22801	0.016275	-0.05833	0.014509	-0.04473

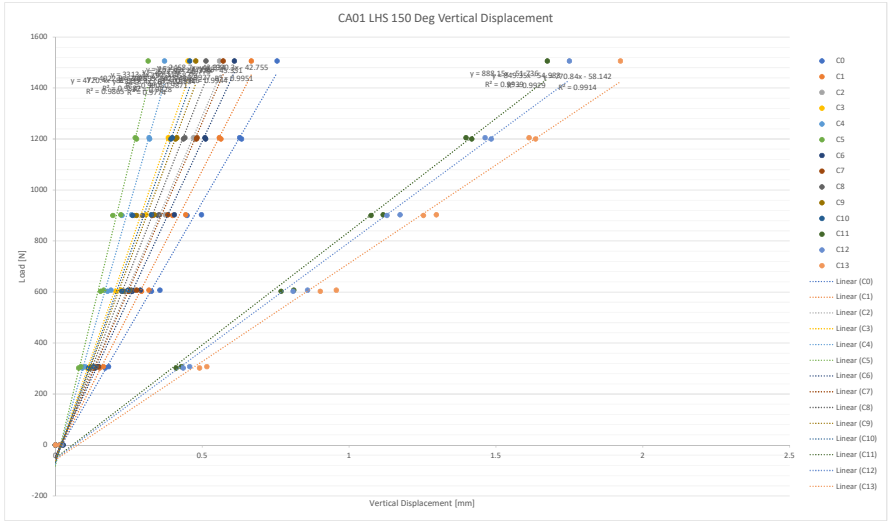

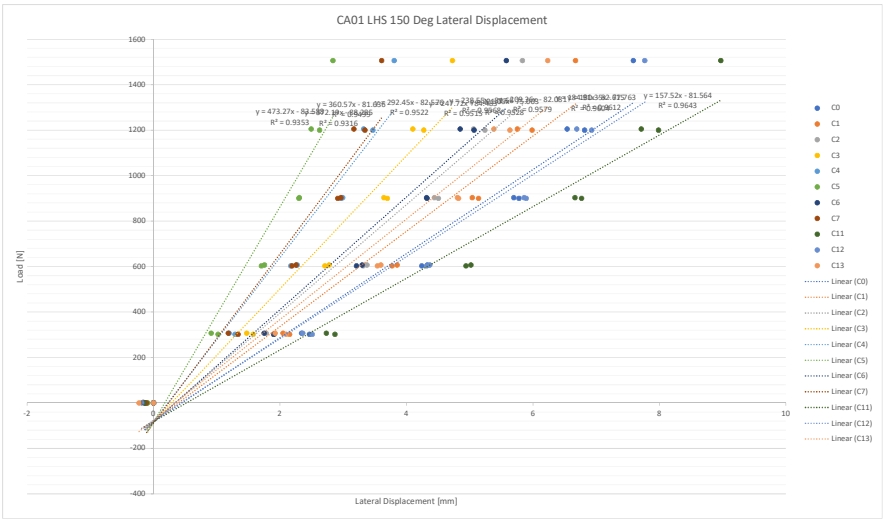

CA01 LHS at 165 Deg

	C0		C1		C2		C3		C4		C5		C6		C7		C8		C9		C10		C11		C12		C13	
Load [N]	V [mm]	W [mm]	V [mm]	W [mm]	V [mm]	W [mm]	V [mm]	W [mm]	V [mm]	W [mm]	V [mm]	W [mm]	V [mm]	W [mm]	V [mm]	W [mm]	V [mm]	W [mm]	V [mm]	W [mm]	V [mm]	W [mm]	V [mm]	W [mm]	V [mm]	W [mm]	V [mm]	W [mm]
0	0	0	0	0	0	0	0	0	0	0	0	0	0	0	0	0	0	0	0	0	0	0	0	0	0	0	0	0
305	0.168211	2.20216	0.150409	1.93585	0.124327	1.68512	0.101604	1.36978	0.089004	1.12131	0.073363	0.864273	0.139514	1.6223	0.139528	1.09712	0.134258	0.485231	0.133953	-0.01373	0.133572	-0.45518	0.407875	2.4982	0.441791	2.14681	0.501307	1.8281
605	0.311055	3.94072	0.274037	3.50907	0.218936	3.03474	0.17737	2.50323	0.153235	2.03365	0.122794	1.58951	0.250218	2.89863	0.241946	1.97387	0.226476	0.935652	0.222628	0.043515	0.220235	-0.71123	0.733197	4.42347	0.787824	3.80724	0.885646	3.21861
900	0.444349	5.46035	0.392186	4.83412	0.314372	4.16774	0.254321	3.44121	0.217922	2.78156	0.174936	2.1669	0.35126	4.06316	0.335134	2.8009	0.30813	1.37587	0.297764	0.189799	0.291154	-0.86569	1.02864	6.22267	1.0937	5.39753	1.22426	4.66876
1205	0.556827	6.49716	0.487859	5.75283	0.388118	4.91499	0.310749	4.02065	0.265839	3.23868	0.212385	2.49273	0.438711	4.8052	0.416486	3.23022	0.377475	1.5083	0.363348	0.039693	0.352209	-1.22579	1.27999	7.42086	1.35554	6.40234	1.51411	5.49304
1501	0.698335	7.86751	0.610508	6.95692	0.486395	5.9562	0.387701	4.87115	0.330092	3.92026	0.26225	3.03086	0.551038	5.89036	0.516249	4.02245	0.465581	1.95509	0.441675	0.210818	0.425719	-1.27818	1.5697	9.0495	1.6601	7.86985	1.84299	6.79867
1205	0.573422	6.66369	0.504097	5.88026	0.402002	5.03562	0.322323	4.10805	0.276179	3.31463	0.22271	2.5386	0.450163	4.89351	0.422978	3.2512	0.381607	1.44123	0.364882	-0.09135	0.352757	-1.39172	1.31511	7.63032	1.39204	6.58476	1.55528	5.63373
905	0.433478	5.52802	0.380677	4.89061	0.300039	4.22433	0.239457	3.45342	0.207982	2.79104	0.166518	2.14078	0.33451	4.05778	0.315232	2.70404	0.285689	1.22136	0.275132	-0.07258	0.264727	-1.15429	1.04191	6.2902	1.10981	5.42042	1.25019	4.62034
603	0.273853	4.46812	0.242914	3.95658	0.188648	3.41593	0.150564	2.82506	0.130291	2.30437	0.104765	1.80613	0.206755	3.35727	0.197177	2.40192	0.178254	1.30813	0.172136	0.362848	0.165797	-0.43046	0.709867	5.03269	0.75686	4.41162	0.858457	3.8726
305	0.168849	2.65859	0.150065	2.37397	0.121606	2.06279	0.098537	1.70705	0.085266	1.41136	0.06916	1.1411	0.13298	1.99372	0.129006	1.43163	0.121739	0.800563	0.118837	0.244799	0.118051	-0.24283	0.419559	2.95561	0.451378	2.56787	0.514143	2.27152
0	0.012838	-0.07502	0.011948	-0.07038	0.015005	-0.05655	0.014183	-0.06328	0.012026	-0.03232	0.011905	-0.01087	0.016001	-0.10976	0.016792	-0.13523	0.020293	-0.17303	0.021492	-0.20481	0.02049	-0.23755	0.023502	-0.10525	0.028503	-0.1407	0.030563	-0.14834

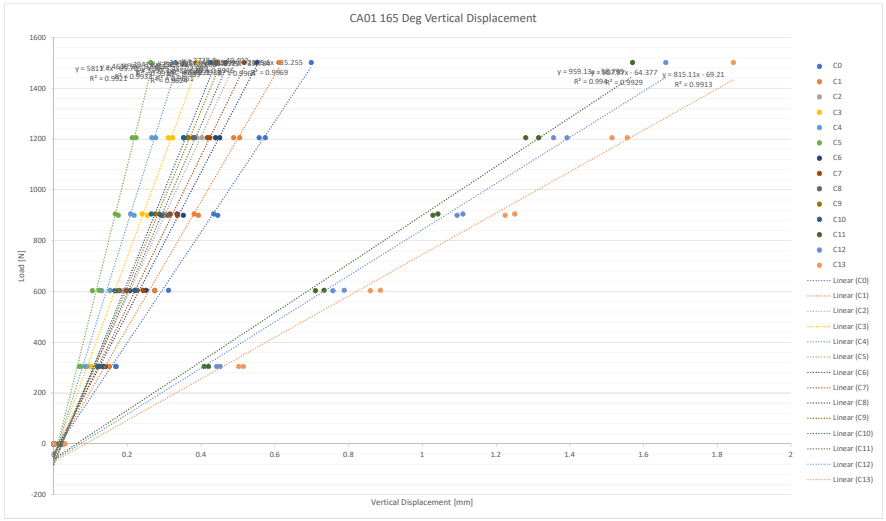

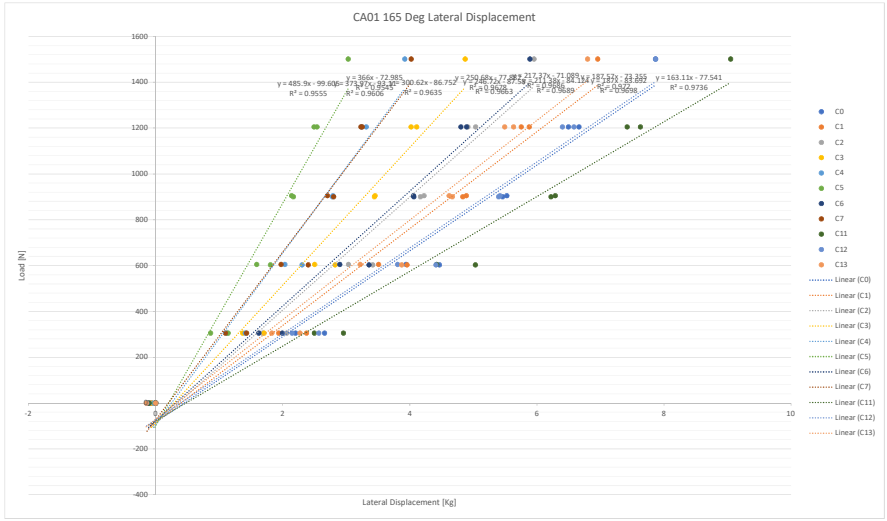

CA01 LHS at 180 Deg

	C0		C1		C2		C3		C4		C5		C6		C7		C8		C9		C10		C11		C12		C13	
Load [N]	V [mm]	W [mm]	V [mm]	W [mm]	V [mm]	W [mm]	V [mm]	W [mm]	V [mm]	W [mm]	V [mm]	W [mm]	V [mm]	W [mm]	V [mm]	W [mm]	V [mm]	W [mm]	V [mm]	W [mm]	V [mm]	W [mm]	V [mm]	W [mm]	V [mm]	W [mm]	V [mm]	W [mm]
0	0	0	0	0	0	0	0	0	0	0	0	0	0	0	0	0	0	0	0	0	0	0	0	0	0	0	0	0
307	0.148284	1.82002	0.133524	1.62062	0.112255	1.41734	0.095349	1.1382	0.083148	0.89591	0.07331	0.682181	0.119666	1.28911	0.118155	0.740788	0.115092	0.197297	0.11391	-0.2476	0.114536	-0.69901	0.374498	2.11442	0.40334	1.79796	0.459803	1.42568
605	0.270176	3.97995	0.241169	3.54139	0.20045	3.09821	0.164695	2.56475	0.141083	2.06159	0.123417	1.62931	0.206881	2.99491	0.198932	2.0064	0.184713	1.01854	0.18057	0.212468	0.177545	-0.61103	0.692518	4.62576	0.740827	4.07505	0.83544	3.43711
900	0.376645	5.14486	0.333903	4.56564	0.278177	3.99571	0.224203	3.27686	0.191746	2.63606	0.16549	2.04485	0.285322	3.82224	0.269959	2.4702	0.247753	1.1639	0.239667	0.068002	0.231664	-1.05528	0.954213	6.01271	1.01503	5.25541	1.1445	4.42765
1200	0.486251	6.38763	0.431172	5.65461	0.358166	4.93971	0.285233	4.02248	0.242234	3.21571	0.204636	2.50973	0.366125	4.71528	0.345284	3.00378	0.313374	1.33737	0.296838	-0.02869	0.285058	-1.44425	1.22443	7.50639	1.29584	6.53113	1.45898	5.52767
1503	0.611143	7.62254	0.539599	6.72792	0.450269	5.88388	0.357967	4.81416	0.302716	3.8691	0.256456	3.00349	0.464656	5.65915	0.430605	3.6922	0.383674	1.78014	0.361052	0.180816	0.344802	-1.45428	1.48917	8.9631	1.57284	7.88296	1.75791	6.75457
1200	0.495052	6.74135	0.437236	5.94866	0.363339	5.22166	0.288943	4.25671	0.247053	3.41981	0.209098	2.66612	0.370298	5.02566	0.344817	3.25202	0.311269	1.56377	0.291735	0.157615	0.278106	-1.2993	1.24889	7.89311	1.32147	6.91821	1.49095	5.91052
900	0.375977	5.31602	0.335291	4.70023	0.277991	4.12148	0.223168	3.37457	0.193083	2.69563	0.168502	2.09631	0.280853	3.93729	0.26554	2.55679	0.239855	1.16922	0.229137	0.048709	0.221234	-1.13215	0.967475	6.19927	1.02827	5.43682	1.16144	4.5924
600	0.260799	4.17533	0.23103	3.72029	0.190519	3.26905	0.153683	2.68751	0.133368	2.19189	0.114248	1.75542	0.191778	3.13003	0.183564	2.09118	0.1693	1.06326	0.165216	0.199271	0.16001	-0.6799	0.693548	4.81654	0.741925	4.25017	0.842625	3.55948
301	0.11815	2.59509	0.107265	2.31651	0.090588	2.04029	0.07281	1.69522	0.0633	1.37487	0.055709	1.11266	0.084512	2.0166	0.082112	1.42506	0.075291	0.857624	0.074409	0.409916	0.075087	-0.09144	0.35849	3.0201	0.387588	2.73704	0.448044	2.39823
0	0.011268	0.091863	0.01091	0.101053	0.009756	0.084874	0.00819	0.063433	0.006762	0.022139	0.007501	0.035348	0.013013	0.058424	0.013017	0.016838	0.014691	-0.06211	0.012601	-0.0496	0.014437	-0.10904	0.024478	0.108063	0.034139	0.121061	0.038473	0.03685

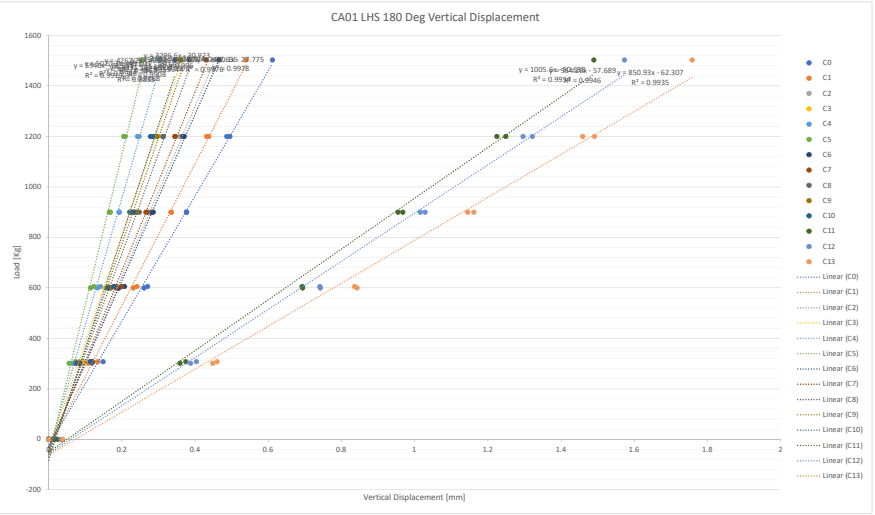

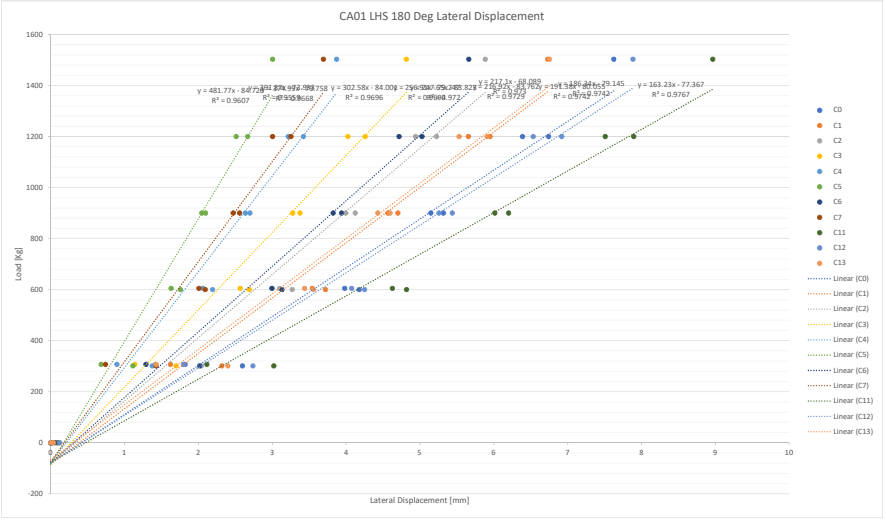

CA01 RHS at 90 Deg

	C0		C1		C2		C3		C4		C5		C6		C7		C8		C9		C10		C11		C12		C13	
Load [N]	V [mm]	W [mm]	V [mm]	W [mm]	V [mm]	W [mm]	V [mm]	W [mm]	V [mm]	W [mm]	V [mm]	W [mm]	V [mm]	W [mm]	V [mm]	W [mm]	V [mm]	W [mm]	V [mm]	W [mm]	V [mm]	W [mm]	V [mm]	W [mm]	V [mm]	W [mm]	V [mm]	W [mm]
0	0	0	0	0	0	0	0	0	0	0	0	0	0	0	0	0	0	0	0	0	0	0	0	0	0	0	0	0
307	0.405635	1.63841	0.370421	1.42235	0.31018	1.2111	0.258912	0.934436	0.218969	0.718529	0.181089	0.528741	0.404265	1.16549	0.406376	0.695789	0.412855	0.189954	0.426743	-0.33294	0.447259	-0.84495	0.65802	1.97788	0.716135	1.66092	0.793252	1.2041
607	0.483314	3.36099	0.442205	2.95828	0.361329	2.5265	0.29389	2.01272	0.244927	1.59617	0.20018	1.21112	0.467761	2.5963	0.466425	1.75917	0.465474	0.906434	0.466946	0.098116	0.477253	-0.67039	0.89463	4.04748	0.961949	3.55182	1.06231	2.82553
903	0.618915	5.16773	0.569455	4.56192	0.459118	3.90823	0.365437	3.11909	0.301243	2.47324	0.247857	1.89414	0.584756	3.97224	0.573034	2.73361	0.560969	1.44809	0.553622	0.244707	0.557731	-0.92402	1.2307	6.21573	1.31201	5.45821	1.44489	4.42257
1200	0.806217	6.45496	0.73859	5.71322	0.595932	4.88484	0.476029	3.87406	0.390625	3.03527	0.32187	2.26401	0.753889	4.91602	0.725717	3.31342	0.702669	1.67342	0.691094	0.126226	0.688325	-1.34263	1.6009	7.79975	1.70037	6.84227	1.8626	5.52176
1502	0.915579	7.4587	0.841108	6.58565	0.672527	5.59247	0.531461	4.3847	0.436873	3.41829	0.357775	2.55332	0.848886	5.66791	0.810683	3.76846	0.77572	1.79402	0.751103	-0.05967	0.743124	-1.82238	1.86802	9.11925	1.9747	7.9914	2.15582	6.42492
1203	0.81331	6.38124	0.748817	5.62518	0.602752	4.78617	0.479986	3.7761	0.395367	2.95689	0.326534	2.21257	0.761305	4.81603	0.732969	3.1839	0.706674	1.47887	0.690719	-0.13097	0.689898	-1.66678	1.62271	7.73656	1.72023	6.73828	1.88049	5.34691
900	0.590771	4.95347	0.547596	4.37557	0.440265	3.73726	0.352205	2.9608	0.291431	2.31737	0.24438	1.72977	0.553376	3.72334	0.535136	2.45563	0.518736	1.13318	0.508771	-0.12406	0.510657	-1.32802	1.20274	5.9681	1.27668	5.15929	1.40063	4.06773
603	0.38514	3.3026	0.356108	2.91969	0.286002	2.49942	0.231166	1.97415	0.192816	1.55132	0.162813	1.14009	0.361728	2.45061	0.35278	1.5609	0.346013	0.65377	0.341266	-0.21139	0.345117	-1.04408	0.793668	3.95181	0.845075	3.37549	0.93132	2.56252
303	0.228435	2.02332	0.213227	1.78081	0.173784	1.53678	0.141576	1.25707	0.116709	1.02499	0.095496	0.771654	0.220395	1.57512	0.21757	1.0869	0.217386	0.587306	0.217549	0.098451	0.223208	-0.37106	0.452108	2.39703	0.486632	2.10883	0.539325	1.66525
0	0.056002	0.258075	0.049528	0.200429	0.044146	0.18046	0.039366	0.171033	0.032834	0.138036	0.029588	0.112303	0.05669	0.208336	0.061144	0.198685	0.063184	0.176838	0.067193	0.133703	0.073038	0.092991	0.077307	0.295492	0.085804	0.288779	0.094853	0.281837

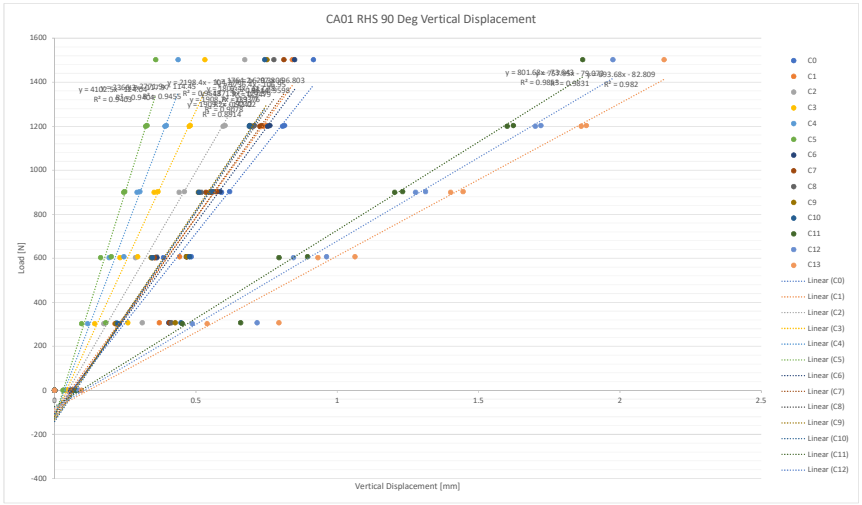

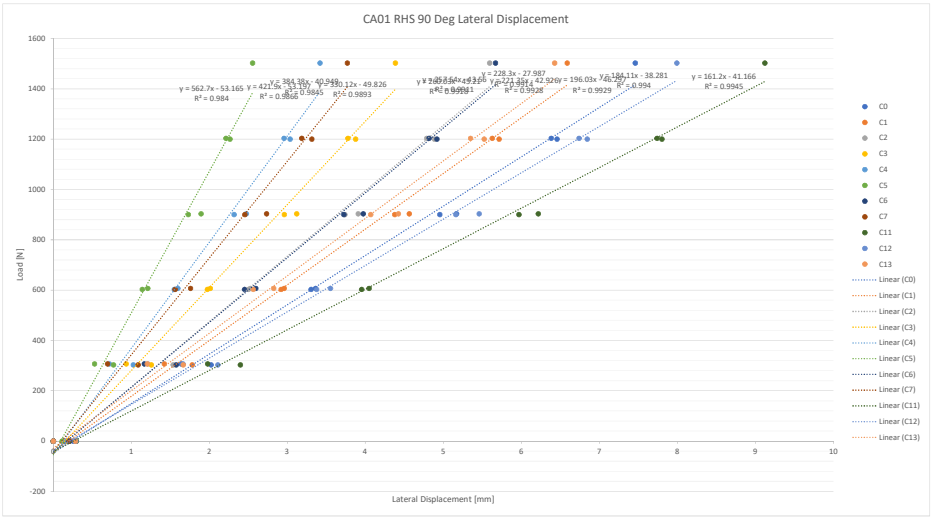

CA01 RHS at 105 Deg

	C0		C1		C2		C3		C4		C5		C7		C8		C9		C10		C11		C12		C13		C14	
Load [N]	V [mm]	W [mm]	V [mm]	W [mm]	V [mm]	W [mm]	V [mm]	W [mm]	V [mm]	W [mm]	V [mm]	W [mm]	V [mm]	W [mm]	V [mm]	W [mm]	V [mm]	W [mm]	V [mm]	W [mm]	V [mm]	W [mm]	V [mm]	W [mm]	V [mm]	W [mm]	V [mm]	W [mm]
0	0	0	0	0	0	0	0	0	0	0	0	0	0	0	0	0	0	0	0	0	0	0	0	0	0	0	0	0
300	0.240843	1.79329	0.225534	1.60414	0.18326	1.38425	0.149703	1.11326	0.122821	0.879918	0.101427	0.641305	0.232774	1.33922	0.2359	0.858946	0.230504	0.384376	0.225012	-0.06609	0.233378	-0.52459	0.464681	2.13754	0.499838	1.79723	0.560044	1.39001
605	0.38099	3.40649	0.355373	3.09231	0.287294	2.67844	0.231427	2.23321	0.180287	1.80311	0.140579	1.37735	0.348475	2.56828	0.33838	1.69029	0.32085	0.787709	0.314788	-0.07715	0.31404	-0.89288	0.797418	4.03046	0.843676	3.35829	0.935628	2.62594
905	0.52884	5.05867	0.495611	4.49305	0.396048	3.83567	0.318043	3.07178	0.26135	2.42603	0.213827	1.85309	0.487204	3.84447	0.473148	2.53509	0.44838	1.20755	0.431522	-0.04463	0.42798	-1.23437	1.14489	6.07745	1.20978	5.19673	1.34248	4.11233
1203	0.714626	6.22199	0.661196	5.54393	0.526437	4.69731	0.420662	3.73544	0.341838	2.92196	0.278446	2.18871	0.652993	4.69732	0.627158	3.03442	0.587183	1.34245	0.562682	-0.23022	0.553283	-1.73386	1.51143	7.57274	1.59124	6.45245	1.75416	5.09282
1505	0.872886	8.0819	0.806721	7.19352	0.640231	6.10272	0.506289	4.86353	0.408323	3.83415	0.32944	2.92982	0.799027	6.28715	0.763319	4.31297	0.708938	2.30329	0.673926	0.412952	0.658081	-1.38037	1.85314	9.89664	1.94807	8.64905	2.13842	7.05333
1195	0.681478	6.90556	0.634807	6.15907	0.505324	5.19428	0.403002	4.1664	0.32603	3.31381	0.266374	2.52119	0.624522	5.42284	0.598947	3.80448	0.55225	2.15387	0.521852	0.589914	0.514345	-0.90896	1.4789	8.41821	1.55646	7.3807	1.71809	6.05787
905	0.510502	5.14831	0.476133	4.59555	0.376827	3.92011	0.301205	3.1429	0.246076	2.48051	0.20112	1.88384	0.465776	3.90737	0.448922	2.56319	0.420265	1.20127	0.40294	-0.08235	0.398421	-1.30339	1.1321	6.21743	1.19352	5.29478	1.32254	4.15289
602	0.302473	3.96022	0.285756	3.57566	0.223639	3.08239	0.177928	2.50556	0.144813	2.01102	0.120803	1.55131	0.271353	3.10667	0.26203	2.16097	0.242612	1.20662	0.23148	0.309834	0.230963	-0.54809	0.725746	4.74589	0.764118	4.1225	0.854835	3.3186
305	0.176938	1.8418	0.168692	1.65376	0.135746	1.39376	0.1129	1.11115	0.092636	0.881984	0.076389	0.662842	0.164824	1.34855	0.164532	0.812366	0.156613	0.275264	0.152041	-0.24118	0.154368	-0.72483	0.403362	2.18321	0.428137	1.78669	0.482684	1.31895
0	0.022168	0.033394	0.021154	0.044585	0.018786	0.025763	0.019835	0.028591	0.015783	0.036606	0.015034	0.013049	0.019458	0.008122	0.023196	-0.01969	0.019566	-0.03023	0.017727	-0.04256	0.017371	-0.06395	0.028269	0.027398	0.028339	0.007458	0.029832	0.003305

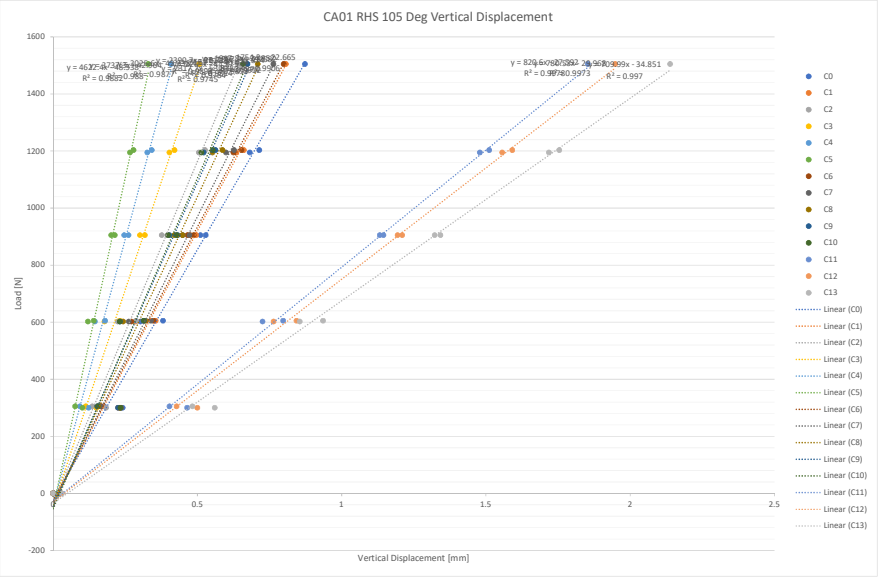

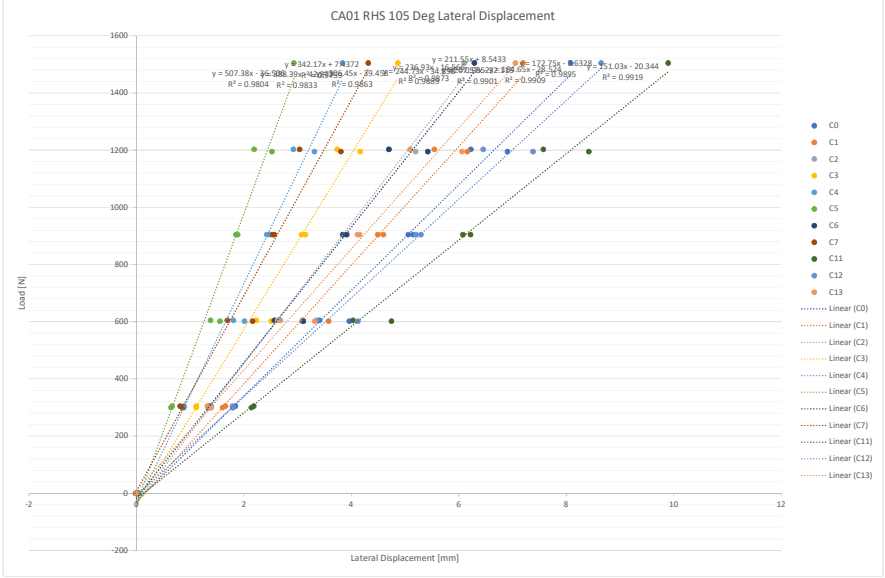

CA01 RHS at 120 Deg

	C0		C1		C2		C4		C3		C5		C6		C7		C8		C9		C10		C11		C12		C13	
Load [N]	V [mm]	W [mm]	V [mm]	W [mm]	V [mm]	W [mm]	V [mm]	W [mm]	V [mm]	W [mm]	V [mm]	W [mm]	V [mm]	W [mm]	V [mm]	W [mm]	V [mm]	W [mm]	V [mm]	W [mm]	V [mm]	W [mm]	V [mm]	W [mm]	V [mm]	W [mm]	V [mm]	W [mm]
0	0	0	0	0	0	0	0	0	0	0	0	0	0	0	0	0	0	0	0	0	0	0	0	0	0	0	0	0
300	0.223443	1.92785	0.207289	1.74471	0.166683	1.51609	0.111215	1.01473	0.134723	1.18219	0.092731	0.760778	0.215033	1.50216	0.214303	1.02876	0.208627	0.557912	0.209266	0.106397	0.214925	-0.33315	0.439587	2.31539	0.474523	2.04927	0.535455	1.65377
600	0.364234	3.11114	0.343342	2.78283	0.273507	2.38052	0.182636	1.52953	0.219461	1.85347	0.149089	1.13285	0.339028	2.27245	0.329242	1.34018	0.313757	0.422891	0.305894	-0.43885	0.305886	-1.25153	0.780741	3.77943	0.832083	3.20107	0.929364	2.41073
907	0.466595	5.20748	0.439135	4.65723	0.34268	3.99674	0.221706	2.57139	0.264842	3.14205	0.181456	1.93443	0.422542	4.00989	0.402625	2.70247	0.373736	1.38248	0.35692	0.153971	0.350958	-1.00491	1.07794	6.34441	1.14175	5.54157	1.27282	4.49667
1206	0.636298	6.49119	0.600526	5.77664	0.477505	4.89606	0.314989	3.08839	0.372964	3.8286	0.258272	2.30004	0.580983	4.99107	0.550893	3.34722	0.512696	1.64062	0.48493	0.122356	0.471188	-1.30989	1.42683	7.96846	1.50535	7.00453	1.66253	5.71877
1505	0.786855	8.06369	0.732351	7.18376	0.570974	6.12714	0.358483	3.88225	0.437665	4.80914	0.288532	2.88872	0.710992	6.25813	0.669161	4.26031	0.614777	2.24221	0.578723	0.384066	0.560038	-1.35831	1.75551	9.91243	1.84955	8.77167	2.04107	7.16792
1203	0.632406	6.86288	0.593279	6.13955	0.463488	5.22466	0.299477	3.33962	0.357653	4.1299	0.242847	2.51431	0.569778	5.31261	0.536432	3.61133	0.492258	1.88413	0.46488	0.286657	0.451755	-1.21913	1.4419	8.38976	1.51869	7.37338	1.68101	6.02949
901	0.453694	5.28178	0.420178	4.7375	0.315801	4.07591	0.184296	2.64514	0.22931	3.21354	0.145793	1.99432	0.395898	4.06537	0.36019	2.71796	0.320231	1.34017	0.299782	0.051227	0.294732	-1.16638	1.08206	6.41885	1.14063	5.60517	1.26916	4.50361
600	0.330047	3.12542	0.315514	2.811	0.251094	2.42105	0.166959	1.56476	0.196087	1.89597	0.140559	1.16881	0.2987	2.23756	0.285898	1.2397	0.26769	0.235769	0.257081	-0.66425	0.254272	-1.55176	0.753566	3.79605	0.794697	3.11634	0.88848	2.22358
305	0.137638	2.01626	0.134514	1.79732	0.105072	1.55363	0.069042	1.0003	0.081876	1.19371	0.06153	0.726075	0.125418	1.53689	0.122982	0.974879	0.117161	0.457275	0.114665	-0.04525	0.114853	-0.50747	0.35057	2.38383	0.372987	2.06515	0.420664	1.59684
0	-0.0143	-0.18187	-0.01088	-0.18858	-0.01029	-0.1603	-0.00737	-0.12944	-0.00765	-0.18472	-0.00401	-0.12303	-0.01184	-0.18885	-0.01044	-0.21389	-0.00884	-0.24125	-0.00884	-0.24972	-0.00279	-0.28187	-0.01025	-0.14874	-0.00546	-0.08025	0.00176	-0.03873

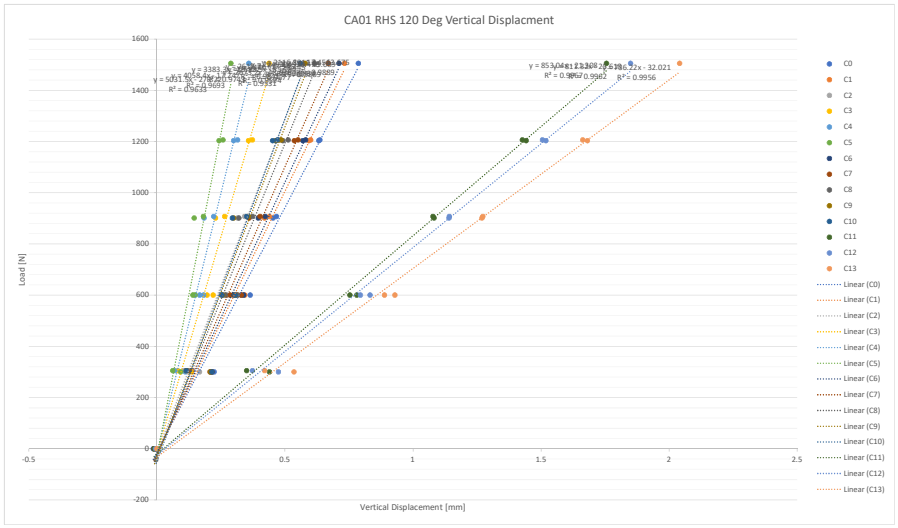

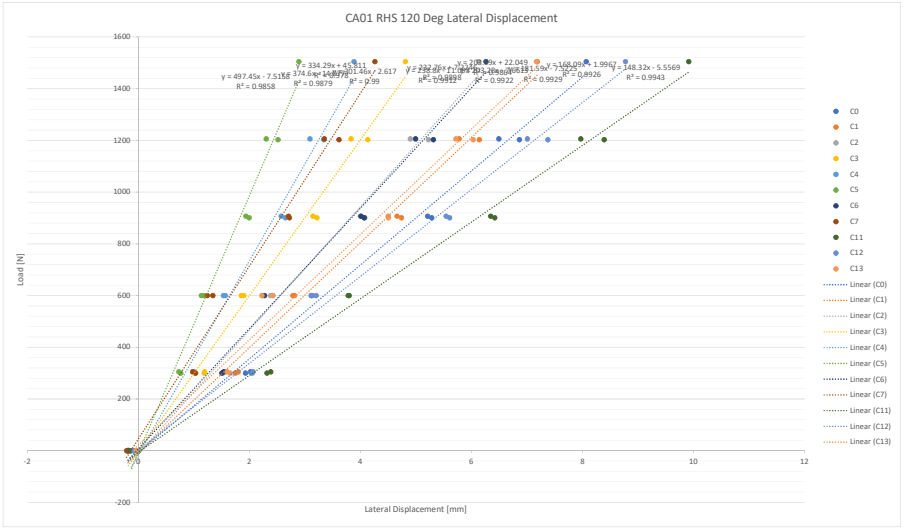

CA01 RHS at 135 Deg

	C0		C1		C2		C3		C4		C5		C6		C7		C8		C9		C10		C11		C12		C13	
Load [N]	V [mm]	W [mm]	V [mm]	W [mm]	V [mm]	W [mm]	V [mm]	W [mm]	V [mm]	W [mm]	V [mm]	W [mm]	V [mm]	W [mm]	V [mm]	W [mm]	V [mm]	W [mm]	V [mm]	W [mm]	V [mm]	W [mm]	V [mm]	W [mm]	V [mm]	W [mm]	V [mm]	W [mm]
0	0	0	0	0	0	0	0	0	0	0	0	0	0	0	0	0	0	0	0	0	0	0	0	0	0	0	0	0
300	0.294363	2.10804	0.274196	1.88753	0.227221	1.65218	0.192807	1.34431	0.159819	1.09387	0.131973	0.871516	0.288352	1.64514	0.292863	1.15655	0.296457	0.658702	0.299597	0.209867	0.30628	-0.2204	0.540176	2.53042	0.585316	2.23211	0.658082	1.87188
603	0.416906	3.90586	0.389036	3.50745	0.317979	3.03225	0.261735	2.45991	0.216419	1.99342	0.181126	1.56173	0.389462	3.05352	0.385394	2.13135	0.376281	1.17644	0.372927	0.347599	0.373056	-0.4685	0.861101	4.72369	0.922349	4.1743	1.03532	3.5115
900	0.529033	5.12083	0.496303	4.57023	0.39963	3.93843	0.328713	3.16702	0.269617	2.53592	0.223476	1.96291	0.486317	3.94031	0.469435	2.67704	0.447696	1.35211	0.433237	0.194686	0.427361	-0.93238	1.1437	6.22518	1.2144	5.45884	1.35452	4.51935
1200	0.661141	6.57227	0.621225	5.87178	0.495802	5.03309	0.4033	4.07014	0.327318	3.24808	0.268922	2.51193	0.600886	5.07928	0.575011	3.48893	0.536005	1.78931	0.513452	0.293484	0.503835	-1.16018	1.4547	8.0414	1.53931	7.09629	1.71463	5.92263
1501	0.81227	7.64357	0.757778	6.84385	0.603359	5.83536	0.489789	4.69525	0.395667	3.70793	0.324599	2.85277	0.737012	5.89321	0.701285	3.97174	0.651749	1.98793	0.618756	0.208246	0.60533	-1.51197	1.76357	9.41175	1.86226	8.29408	2.06579	6.90868
1205	0.692422	6.65921	0.649579	5.93046	0.520344	5.09245	0.424531	4.12368	0.345061	3.27883	0.286722	2.52219	0.627963	5.12311	0.594855	3.47965	0.557221	1.73503	0.538256	0.18737	0.52651	-1.30778	1.49962	8.14657	1.58577	7.19343	1.76504	5.92602
906	0.533433	5.62477	0.503331	5.02843	0.402379	4.34427	0.330621	3.52262	0.26897	2.83417	0.222826	2.21083	0.487186	4.38101	0.465665	3.03804	0.438963	1.65503	0.425736	0.408654	0.417582	-0.81092	1.17634	6.81413	1.24711	6.00498	1.39231	5.02577
605	0.383411	3.8293	0.362542	3.42875	0.295517	2.95476	0.246055	2.38787	0.201063	1.93281	0.168868	1.50633	0.353683	2.92918	0.346739	1.97561	0.333049	1.00454	0.325511	0.10672	0.323853	-0.76619	0.832485	4.63003	0.884315	4.03793	0.992249	3.29254
303	0.242952	2.48842	0.22978	2.22929	0.187843	1.95338	0.160044	1.60294	0.131004	1.31182	0.110542	1.0507	0.231202	1.98755	0.230029	1.45677	0.229275	0.909917	0.228579	0.407634	0.230645	-0.07329	0.497625	2.96464	0.534133	2.65347	0.601941	2.28951
0	0.119616	0.457238	0.111476	0.414829	0.097978	0.385607	0.086401	0.314535	0.070092	0.291153	0.058114	0.257927	0.126542	0.415494	0.131943	0.367148	0.137701	0.315537	0.1424	0.303035	0.148153	0.236739	0.159678	0.537954	0.177631	0.530196	0.19777	0.555869

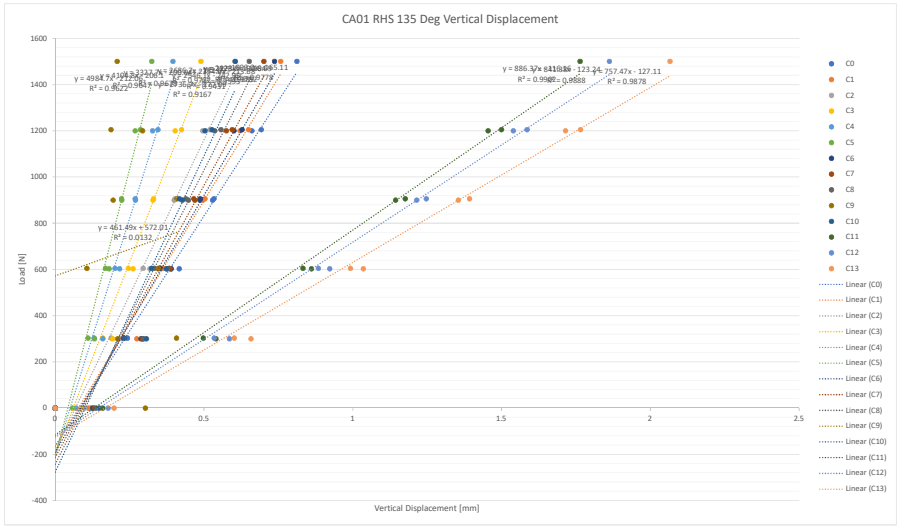

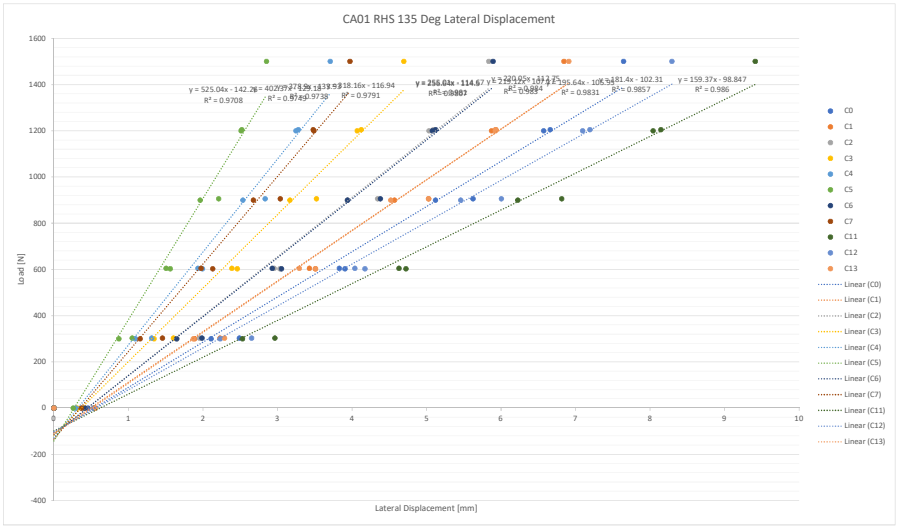

CA01 RHS at 150 Deg

	C0		C1		C2		C3		C4		C5		C6		C7		C8		C9		C10		C11		C12		C13	
Load [N]	V [mm]	W [mm]	V [mm]	W [mm]	V [mm]	W [mm]	V [mm]	W [mm]	V [mm]	W [mm]	V [mm]	W [mm]	V [mm]	W [mm]	V [mm]	W [mm]	V [mm]	W [mm]	V [mm]	W [mm]	V [mm]	W [mm]	V [mm]	W [mm]	V [mm]	W [mm]	V [mm]	W [mm]
0	0	0	0	0	0	0	0	0	0	0	0	0	0	0	0	0	0	0	0	0	0	0	0	0	0	0	0	0
300	0.257964	1.49327	0.242899	1.31798	0.204993	1.16906	0.172904	0.956036	0.143031	0.736374	0.12292	0.541049	0.244805	0.968863	0.242956	0.455362	0.234118	-0.05958	0.232312	-0.55149	0.238353	-1.04459	0.493644	1.78116	0.527725	1.41825	0.588506	0.990212
601	0.290063	3.46245	0.277245	3.10128	0.219198	2.66846	0.17645	2.16437	0.144602	1.67245	0.122103	1.27227	0.25727	2.60282	0.245038	1.68861	0.222732	0.811134	0.215262	-0.05601	0.21566	-0.86707	0.704536	4.14088	0.749666	3.60529	0.841375	2.94074
907	0.424769	4.9221	0.403966	4.41065	0.320046	3.8347	0.258226	3.09654	0.209929	2.39369	0.178028	1.82699	0.372442	3.6989	0.349596	2.42871	0.313204	1.16484	0.295523	-0.03577	0.290213	-1.20358	1.03002	5.98497	1.09197	5.26033	1.22161	4.32714
1200	0.580452	6.39281	0.550816	5.70538	0.441587	4.91545	0.35489	3.97987	0.288971	3.11888	0.244578	2.3792	0.512034	4.85742	0.480091	3.25983	0.431943	1.62047	0.403812	0.150874	0.394175	-1.31258	1.35602	7.7594	1.43677	6.89264	1.60268	5.78801
1500	0.670769	7.67375	0.632217	6.86371	0.497522	5.93006	0.396883	4.75578	0.317196	3.72119	0.262939	2.86101	0.581999	5.91894	0.53872	4.00856	0.479811	2.10513	0.444908	0.353511	0.423842	-1.33115	1.6015	9.40752	1.68835	8.38546	1.87801	7.11374
1200	0.501414	6.66548	0.477406	6.02098	0.374165	5.1904	0.298811	4.22215	0.23841	3.2977	0.197196	2.54127	0.428086	5.13242	0.397511	3.51575	0.349541	1.91573	0.319661	0.420914	0.303276	-1.04008	1.27421	8.09525	1.34369	7.20205	1.50164	6.10218
900	0.404545	5.42497	0.387923	4.8637	0.306321	4.22849	0.244649	3.42665	0.197787	2.70676	0.166352	2.11199	0.348476	4.19759	0.323661	2.83516	0.288775	1.52427	0.269289	0.295167	0.261645	-0.88832	1.01998	6.54913	1.0792	5.82275	1.21193	4.9012
602	0.284752	4.0732	0.270438	3.64903	0.2132	3.1482	0.170722	2.56202	0.136774	2.01827	0.116296	1.54634	0.243858	3.11674	0.227967	2.13826	0.207309	1.14332	0.194643	0.246155	0.192749	-0.63338	0.731272	4.86964	0.774523	4.29747	0.873726	3.61857
307	0.18448	2.32331	0.176492	2.04909	0.140273	1.82671	0.115733	1.51322	0.094726	1.17737	0.080316	0.911266	0.166685	1.76412	0.162956	1.18747	0.154803	0.622097	0.151716	0.079203	0.15652	-0.4569	0.441202	2.77058	0.472535	2.43024	0.538704	2.03361
0	0.052728	-0.05934	0.050074	-0.06434	0.045298	-0.03303	0.039449	-0.04054	0.034229	-0.07416	0.029854	-0.09377	0.054117	-0.09243	0.057488	-0.15265	0.055835	-0.1824	0.058227	-0.24359	0.060082	-0.28808	0.071262	-0.08682	0.077825	-0.11339	0.088958	-0.12837

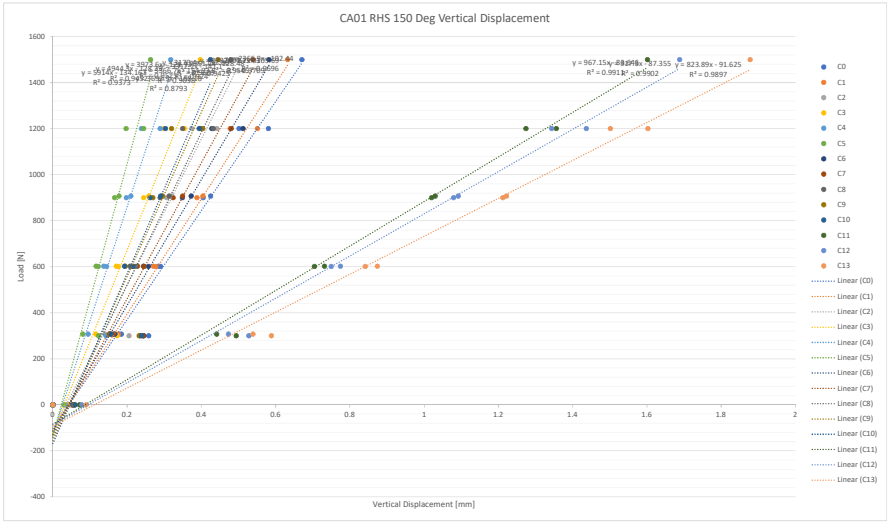

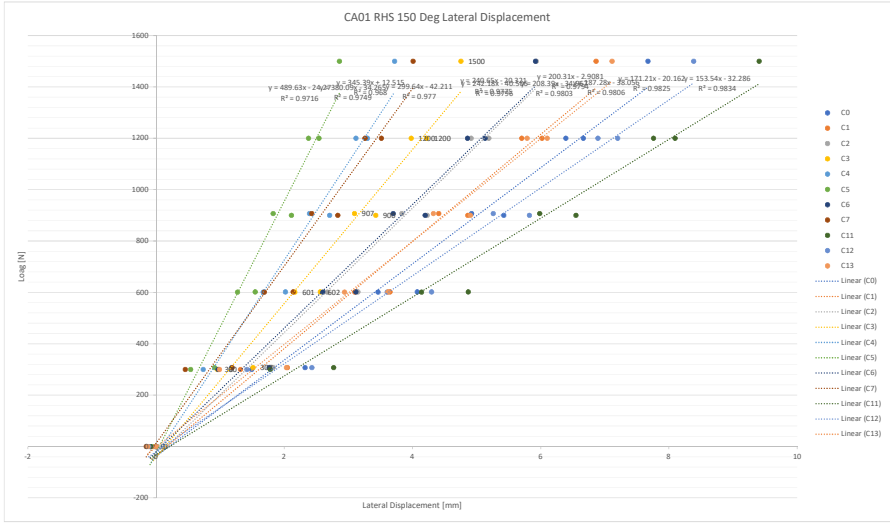

CA01 RHS at 165 Deg

	C0		C1		C2		C3		C4		C5		C6		C7		C8		C9		C10		C11		C12		C13	
Load [N]	V [mm]	W [mm]	V [mm]	W [mm]	V [mm]	W [mm]	V [mm]	W [mm]	V [mm]	W [mm]	V [mm]	W [mm]	V [mm]	W [mm]	V [mm]	W [mm]	V [mm]	W [mm]	V [mm]	W [mm]	V [mm]	W [mm]	V [mm]	W [mm]	V [mm]	W [mm]	V [mm]	W [mm]
0	0	0	0	0	0	0	0	0	0	0	0	0	0	0	0	0	0	0	0	0	0	0	0	0	0	0	0	0
303	0.208091	1.93362	0.194731	1.78542	0.161088	1.51537	0.130344	1.22857	0.108941	1.00772	0.092482	0.754305	0.193545	1.48816	0.189884	1.00814	0.186581	0.528964	0.184356	0.10079	0.188167	-0.2617	0.435908	2.35125	0.47213	2.08061	0.534677	1.73577
605	0.317457	3.52752	0.301027	3.21724	0.240897	2.75142	0.195239	2.22275	0.161643	1.79474	0.134268	1.35259	0.285229	2.65823	0.271722	1.77877	0.260038	0.887364	0.251065	0.07628	0.248148	-0.66383	0.744547	4.3042	0.800924	3.7782	0.901985	3.15396
900	0.430168	4.72468	0.406577	4.28049	0.3226	3.65665	0.257546	2.93424	0.214815	2.34982	0.178924	1.7647	0.374743	3.53337	0.347382	2.29648	0.322597	1.06906	0.304708	-0.05257	0.30332	-1.12519	1.02981	5.81239	1.1002	5.11444	1.23574	4.24858
1193	0.566503	6.38584	0.538331	5.79505	0.427152	4.93011	0.341327	3.96896	0.281568	3.17437	0.229246	2.38892	0.494499	4.84339	0.455478	3.2078	0.41953	1.60757	0.390926	0.146428	0.378678	-1.21854	1.34926	7.8184	1.43732	6.92059	1.61143	5.85226
1501	0.682005	7.69392	0.645077	6.96475	0.51073	5.95768	0.404696	4.78956	0.331639	3.8356	0.267077	2.9135	0.591553	5.90432	0.541129	4.00493	0.491887	2.13179	0.454862	0.388861	0.434991	-1.21264	1.62027	9.47268	1.72269	8.47907	1.92742	7.25384
1207	0.582573	6.73323	0.553199	6.08963	0.43952	5.20659	0.351714	4.18412	0.288947	3.38234	0.236936	2.56733	0.506998	5.16024	0.465693	3.50769	0.425436	1.86521	0.398017	0.399239	0.381091	-0.98013	1.3803	8.21582	1.47097	7.35384	1.64904	6.25928
905	0.440413	5.40855	0.420232	4.89758	0.334751	4.1846	0.267672	3.39465	0.222299	2.71962	0.181196	2.07544	0.380596	4.15904	0.352321	2.81407	0.324576	1.50312	0.30178	0.29396	0.29251	-0.83573	1.07187	6.61661	1.14304	5.89089	1.28633	5.02128
605	0.324126	4.07299	0.31078	3.69072	0.24839	3.19111	0.2015	2.59677	0.168573	2.08425	0.140547	1.59255	0.285143	3.16355	0.268075	2.22636	0.253833	1.27563	0.237205	0.431471	0.233073	-0.36691	0.772476	4.92834	0.828088	4.43601	0.932297	3.8122
305	0.227748	2.54541	0.216632	2.31072	0.178315	1.97945	0.145216	1.6201	0.12109	1.32974	0.100982	1.02011	0.211104	2.01083	0.20487	1.47783	0.200235	0.939932	0.196462	0.455214	0.197936	-0.00866	0.488402	3.05307	0.529443	2.79499	0.599169	2.4473
0	0.150195	0.403172	0.137451	0.389587	0.122837	0.331848	0.106053	0.284184	0.091025	0.239147	0.075802	0.177668	0.151377	0.364106	0.157038	0.319445	0.163311	0.257504	0.163874	0.197619	0.164933	0.166126	0.192854	0.488913	0.214406	0.502612	0.236517	0.480844

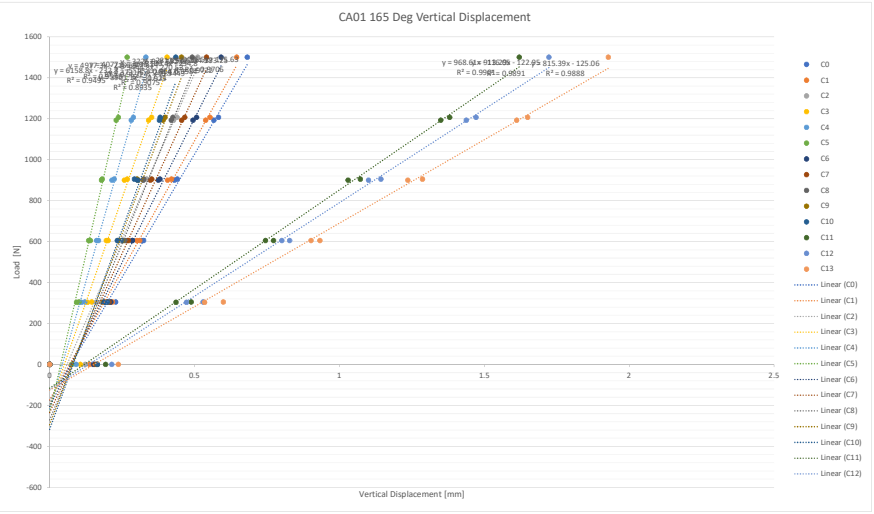

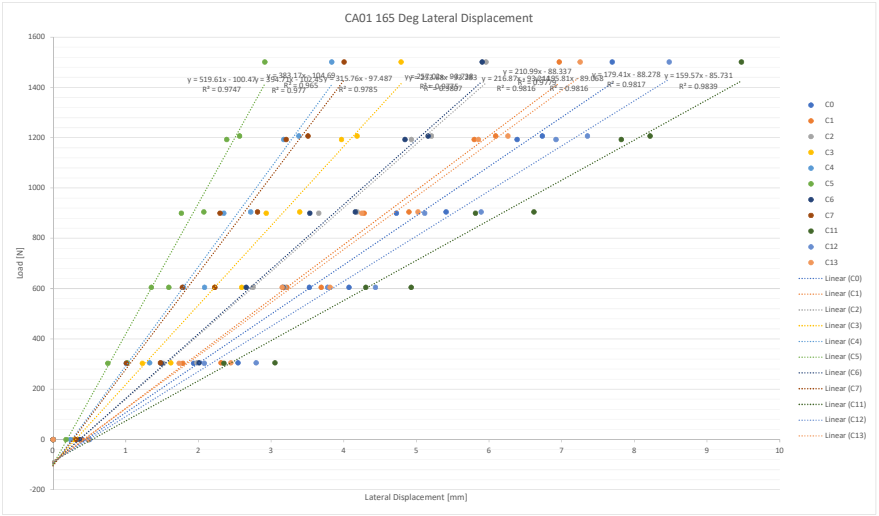

CA01 RHS at 180 Deg

	C0		C1		C2		C3		C4		C5		C6		C7		C8		C9		C10		C11		C12		C13	
Load [N]	V [mm]	W [mm]	V [mm]	W [mm]	V [mm]	W [mm]	V [mm]	W [mm]	V [mm]	W [mm]	V [mm]	W [mm]	V [mm]	W [mm]	V [mm]	W [mm]	V [mm]	W [mm]	V [mm]	W [mm]	V [mm]	W [mm]	V [mm]	W [mm]	V [mm]	W [mm]	V [mm]	W [mm]
0	0	0	0	0	0	0	0	0	0	0	0	0	0	0	0	0	0	0	0	0	0	0	0	0	0	0	0	0
305	0.122991	1.91011	0.118931	1.75404	0.094373	1.50823	0.07218	1.23711	0.062979	0.990567	0.053711	0.763941	0.097545	1.5009	0.084862	1.06031	0.073284	0.607391	0.068241	0.180869	0.064343	-0.20279	0.334984	2.32378	0.355173	2.098	0.399005	1.82947
603	0.28137	3.79864	0.265276	3.43342	0.214053	2.96709	0.167848	2.41792	0.143168	1.94761	0.124368	1.49381	0.239491	2.92332	0.224394	2.01495	0.204332	1.09637	0.195138	0.268424	0.188891	-0.49269	0.717843	4.51552	0.769783	4.0678	0.87592	3.52754
900	0.38814	4.86553	0.371857	4.38612	0.297842	3.80492	0.234636	3.07512	0.202393	2.43738	0.172331	1.89642	0.337352	3.69843	0.313098	2.48739	0.283652	1.26724	0.270891	0.191267	0.261358	-0.82179	0.975458	5.89833	1.04056	5.27578	1.18048	4.61364
1200	0.504149	6.00973	0.481248	5.39623	0.38646	4.67514	0.300753	3.7491	0.252852	2.97799	0.213486	2.29728	0.433856	4.57212	0.39916	3.04383	0.362042	1.51466	0.342541	0.176653	0.327718	-1.10931	1.25371	7.35691	1.33662	6.59331	1.50855	5.73665
1501	0.622858	7.00582	0.594022	6.27519	0.477458	5.40434	0.372592	4.31515	0.313426	3.42397	0.268124	2.60512	0.537153	5.28032	0.488034	3.46468	0.440411	1.62139	0.414601	0.003315	0.394702	-1.53919	1.53054	8.64012	1.62725	7.7829	1.83611	6.79616
1200	0.518459	6.70333	0.49772	6.04247	0.401843	5.22676	0.314901	4.26365	0.268997	3.42785	0.227511	2.66446	0.446351	5.20401	0.408582	3.6496	0.369259	2.08355	0.34723	0.686532	0.33431	-0.66598	1.28994	8.18595	1.37332	7.50023	1.55283	6.75013
900	0.400321	5.33619	0.383915	4.80762	0.309809	4.16567	0.241748	3.37247	0.205367	2.67857	0.175668	2.06894	0.344892	4.12681	0.320702	2.88002	0.290771	1.58983	0.277689	0.48332	0.265859	-0.60081	1.01392	6.47337	1.08318	5.86952	1.22932	5.18072
603	0.317144	4.41339	0.305497	3.99238	0.250062	3.47856	0.200284	2.84433	0.1724	2.27912	0.150953	1.7751	0.275648	3.53379	0.254398	2.59832	0.22847	1.64569	0.21823	0.77793	0.207024	-0.00791	0.761986	5.27851	0.812346	4.85374	0.918867	4.371
305	0.114651	2.39119	0.114184	2.14122	0.088375	1.85721	0.067953	1.53257	0.060168	1.23136	0.053598	0.955288	0.094794	1.90378	0.086024	1.39911	0.077806	0.876227	0.074792	0.421815	0.06996	0.002548	0.347909	2.8833	0.372376	2.65702	0.427868	2.38932
0	0.037073	0.613743	0.036546	0.561628	0.030422	0.487453	0.024519	0.436637	0.019424	0.342853	0.0163	0.275224	0.039694	0.603145	0.043199	0.574145	0.041671	0.52918	0.045199	0.506117	0.042599	0.500977	0.062695	0.722542	0.071459	0.779075	0.082162	0.815963

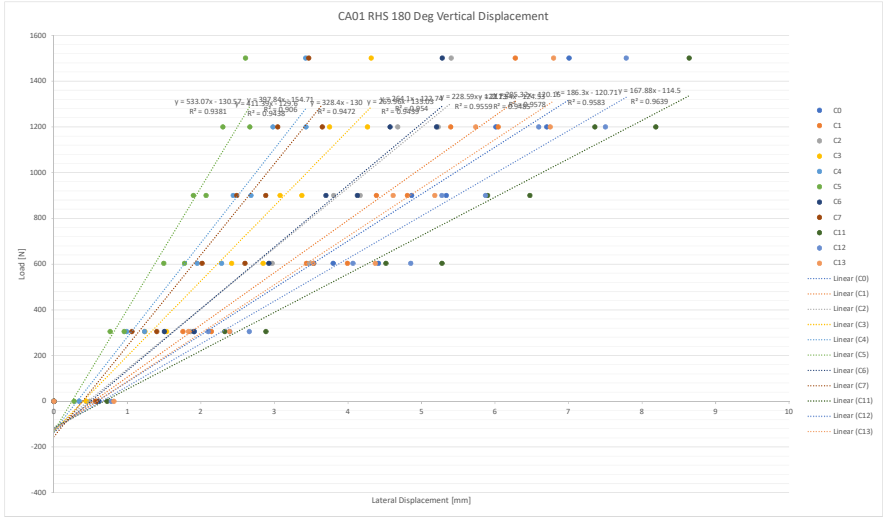

CA02 RHS at 90 Deg

	C0		C1		C2		C3		C4		C5		C6		C7		C8		C9		C10		C11		C12		C13	
Load [N]	V [mm]	W [mm]	V [mm]	W [mm]	V [mm]	W [mm]	V [mm]	W [mm]	V [mm]	W [mm]	V [mm]	W [mm]	V [mm]	W [mm]	V [mm]	W [mm]	V [mm]	W [mm]	V [mm]	W [mm]	V [mm]	W [mm]	V [mm]	W [mm]	V [mm]	W [mm]	V [mm]	W [mm]
0	0	0	0	0	0	0	0	0	0	0	0	0	0	0	0	0	0	0	0	0	0	0	0	0	0	0	0	0
307	0.161079	2.03347	0.141973	1.80975	0.111505	1.52328	0.091583	1.27012	0.076841	1.01803	0.060804	0.788608	0.155119	1.59142	0.164061	1.06832	0.162246	0.601116	0.164286	0.137341	0.170046	-0.27406	0.38702	2.50646	0.416818	2.18731	0.471375	1.79313
901	0.43387	4.98406	0.377345	4.4065	0.291822	3.6625	0.237779	2.93355	0.194456	2.33836	0.157217	1.76939	0.408994	3.86945	0.415176	2.55917	0.402367	1.38116	0.396106	0.2133	0.397554	-0.8397	1.0383	6.2961	1.10277	5.51752	1.21771	4.46448
1202	0.558845	6.46299	0.482432	5.70888	0.371714	4.73294	0.299368	3.80055	0.244327	3.05675	0.196544	2.31131	0.525449	5.13045	0.528282	3.52384	0.504936	2.06854	0.494487	0.643621	0.492121	-0.66384	1.32695	8.22942	1.39998	7.26576	1.53601	6.00225
1507	0.657952	7.78742	0.565784	6.85454	0.429065	5.66859	0.344208	4.54785	0.278974	3.63435	0.222292	2.75523	0.611201	6.17994	0.606057	4.26382	0.572087	2.52714	0.553308	0.828023	0.543799	-0.72727	1.58849	9.93478	1.6643	8.84677	1.81116	7.29465
1205	0.557865	6.56409	0.484363	5.80521	0.37009	4.79583	0.300537	3.83792	0.246429	3.05998	0.197987	2.33217	0.521887	5.17902	0.520707	3.48856	0.495418	1.96344	0.483938	0.473698	0.478404	-0.89327	1.34675	8.36542	1.41417	7.37375	1.54945	6.03807
906	0.401729	5.36121	0.348798	4.75607	0.266589	3.9659	0.214932	3.18528	0.178878	2.56307	0.144539	1.95932	0.372665	4.23425	0.374535	2.86737	0.356604	1.63876	0.350594	0.418592	0.348722	-0.69099	1.01723	6.77173	1.07276	5.97011	1.18438	4.89776
600	0.248255	3.57319	0.216779	3.17229	0.164488	2.65466	0.133246	2.11578	0.110813	1.71839	0.089715	1.29387	0.231659	2.78544	0.235389	1.83737	0.22755	0.985549	0.224199	0.139268	0.225131	-0.61961	0.662039	4.47773	0.700553	3.89069	0.781065	3.12849
302	0.128207	1.84808	0.11322	1.64802	0.087399	1.37495	0.070865	1.09789	0.060125	0.884732	0.050035	0.675105	0.12209	1.43546	0.128432	0.932817	0.126065	0.483294	0.127312	0.046294	0.130129	-0.35544	0.339234	2.29672	0.36345	2.00154	0.408198	1.57763
0	-0.02352	0.137966	-0.01904	0.114917	-0.01754	0.090309	-0.01454	0.077853	-0.00899	0.055715	-0.0077	0.023163	-0.02362	0.118414	-0.02226	0.060865	-0.02378	0.029048	-0.0224	0.000808	-0.02156	-0.02155	-0.01313	0.162553	-0.01287	0.156906	-0.01143	0.129405

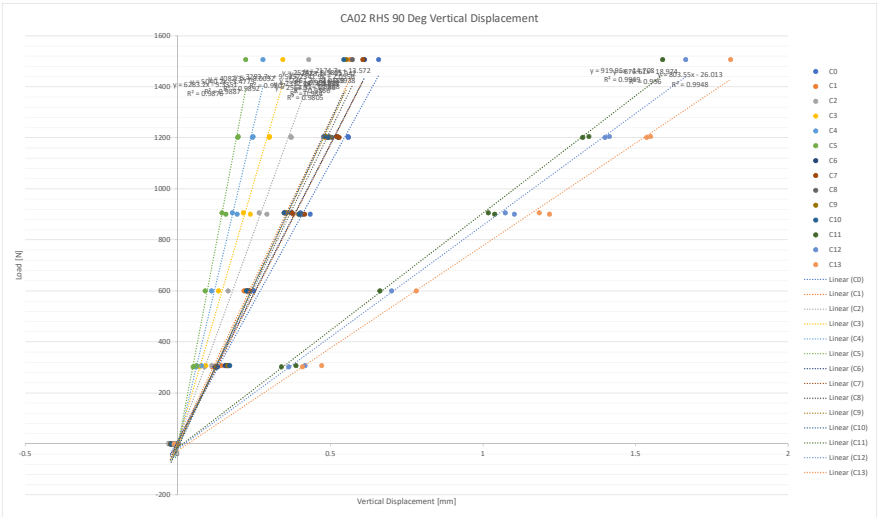

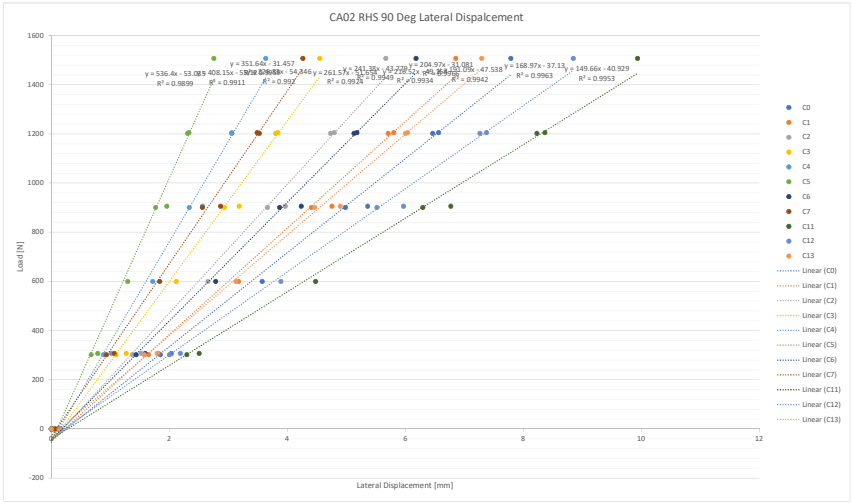

CA02 RHS at 105 Deg

	C0		C1		C2		C3		C4		C5		C6		C7		C8		C9		C10		C11		C12		C13	
Load [N]	V [mm]	W [mm]	V [mm]	W [mm]	V [mm]	W [mm]	V [mm]	W [mm]	V [mm]	W [mm]	V [mm]	W [mm]	V [mm]	W [mm]	V [mm]	W [mm]	V [mm]	W [mm]	V [mm]	W [mm]	V [mm]	W [mm]	V [mm]	W [mm]	V [mm]	W [mm]	V [mm]	W [mm]
0	0	0	0	0	0	0	0	0	0	0	0	0	0	0	0	0	0	0	0	0	0	0	0	0	0	0	0	0
306	0.134253	2.26112	0.116977	2.00776	0.088427	1.69036	0.075054	1.38601	0.061107	1.14326	0.049979	0.906862	0.127902	1.84166	0.137752	1.35022	0.134437	0.846923	0.132187	0.36834	0.137198	-0.06684	0.369023	2.81863	0.399034	2.5698	0.446477	2.1424
604	0.281079	3.94308	0.245594	3.53256	0.184416	2.98428	0.152316	2.42144	0.126159	1.95456	0.104208	1.54027	0.262689	3.14426	0.272628	2.19214	0.263343	1.32348	0.258201	0.460474	0.260339	-0.33895	0.711471	4.84199	0.762403	4.29227	0.84985	3.5224
903	0.424096	5.18624	0.369116	4.57198	0.277161	3.79466	0.229905	3.05238	0.189485	2.45366	0.153494	1.89109	0.398428	4.07953	0.406053	2.75501	0.391434	1.5397	0.383347	0.349823	0.38303	-0.76306	1.03683	6.53354	1.10439	5.79651	1.22434	4.76819
1200	0.536519	6.8203	0.461443	6.00653	0.344047	4.98173	0.281799	4.03385	0.231745	3.23343	0.186618	2.49606	0.49939	5.48301	0.506302	3.8644	0.481733	2.38695	0.468813	0.94436	0.466984	-0.41369	1.31496	8.65866	1.38885	7.79492	1.52992	6.56293
1503	0.690169	7.77983	0.594109	6.81051	0.446604	5.5891	0.36835	4.49011	0.304038	3.54861	0.246133	2.70777	0.647322	6.23677	0.647033	4.3389	0.61564	2.59333	0.594573	0.901326	0.588818	-0.68707	1.63609	10.0452	1.72369	9.08918	1.884	7.64423
1207	0.551007	6.55322	0.47836	5.77432	0.361162	4.76775	0.296635	3.83066	0.245078	3.05362	0.200163	2.33688	0.518434	5.18496	0.524529	3.52658	0.501747	1.98057	0.484916	0.518919	0.485212	-0.87999	1.34236	8.40077	1.41716	7.48494	1.55782	6.17012
902	0.387616	5.73042	0.33587	5.06968	0.246778	4.22674	0.203328	3.43166	0.167735	2.77518	0.135387	2.17208	0.359851	4.6072	0.365464	3.27214	0.3494	2.03657	0.338833	0.820751	0.338484	-0.348	1.00892	7.19469	1.0684	6.49727	1.18366	5.45917
602	0.243917	3.98141	0.211744	3.5394	0.156142	2.9661	0.127681	2.40283	0.107634	1.9611	0.087838	1.53787	0.224389	3.21635	0.231375	2.27038	0.221374	1.43128	0.215209	0.55896	0.215617	-0.24245	0.666676	4.9788	0.707336	4.48322	0.787368	3.74469
301	0.146993	2.19977	0.129041	1.95733	0.097781	1.66586	0.083589	1.36431	0.070521	1.14246	0.05991	0.912974	0.138977	1.78727	0.146473	1.2559	0.144808	0.766405	0.145181	0.291683	0.148375	-0.17965	0.372552	2.71335	0.400003	2.4362	0.446203	1.9993
0	-0.00041	0.30524	0.002043	0.295865	-0.0015	0.230971	0.001903	0.157279	0.003186	0.15715	0.001028	0.135411	-0.00416	0.28246	-0.00229	0.282408	-0.00305	0.247955	-0.00599	0.186162	-0.00837	0.129345	0.012356	0.398422	0.009696	0.379599	0.010133	0.325285

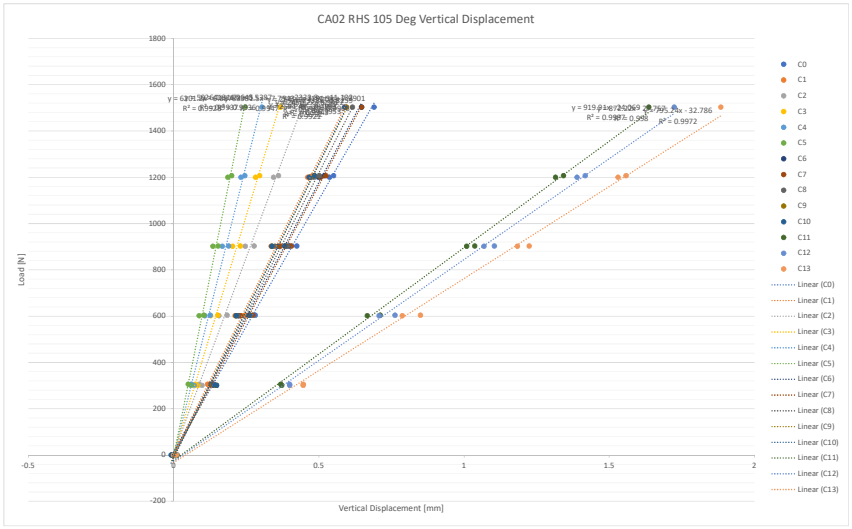

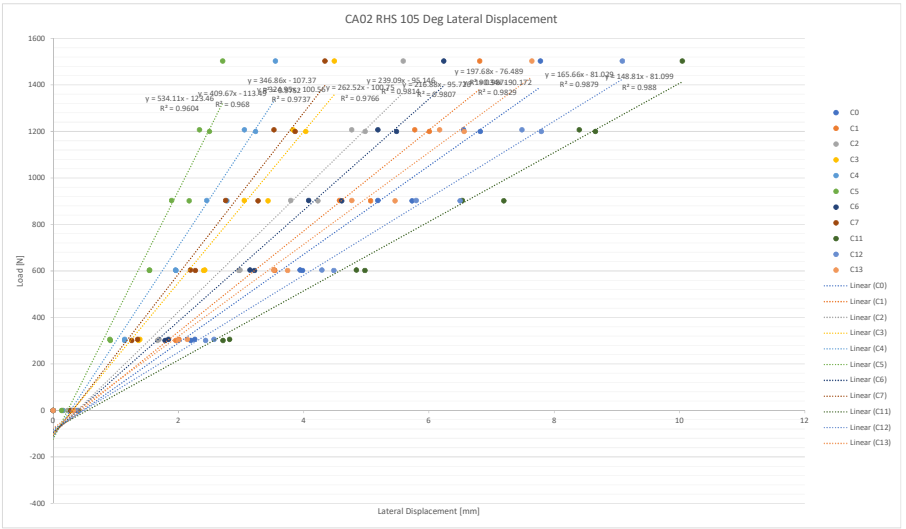

CA02 RHS at 120 Deg

	C0		C1		C2		C3		C4		C5		C6		C7		C8		C9		C10		C11		C12		C13	
Load [N]	V [mm]	W [mm]	V [mm]	W [mm]	V [mm]	W [mm]	V [mm]	W [mm]	V [mm]	W [mm]	V [mm]	W [mm]	V [mm]	W [mm]	V [mm]	W [mm]	V [mm]	W [mm]	V [mm]	W [mm]	V [mm]	W [mm]	V [mm]	W [mm]	V [mm]	W [mm]	V [mm]	W [mm]
0	0	0	0	0	0	0	0	0	0	0	0	0	0	0	0	0	0	0	0	0	0	0	0	0	0	0	0	0
303	0.168444	1.82317	0.149718	1.64091	0.117365	1.36693	0.099285	1.10957	0.084805	0.924549	0.070071	0.698079	0.16223	1.34857	0.166931	0.821423	0.164245	0.298359	0.163761	-0.10979	0.167792	-0.56864	0.402205	2.2557	0.435831	1.9822	0.485279	1.52925
603	0.331234	3.21901	0.294367	2.86372	0.22733	2.36417	0.192084	1.88095	0.161955	1.52525	0.13325	1.12613	0.316079	2.3693	0.323904	1.36629	0.316923	0.477966	0.313567	-0.38734	0.316757	-1.22988	0.779578	4.10074	0.832461	3.47677	0.92591	2.65335
900	0.444976	4.63698	0.394406	4.12133	0.303095	3.43918	0.255859	2.77432	0.215848	2.2546	0.17467	1.76555	0.423213	3.47356	0.428361	2.09659	0.414332	0.874905	0.408043	-0.2964	0.409769	-1.43353	1.07307	5.88283	1.14027	5.07701	1.26406	4.00028
1205	0.561847	6.0405	0.493004	5.34822	0.370105	4.39767	0.306197	3.50646	0.255346	2.79172	0.206162	2.11822	0.530301	4.67002	0.533449	3.01251	0.515249	1.52626	0.502155	0.116399	0.499777	-1.26668	1.3406	7.75638	1.42103	6.87829	1.56563	5.58095
1500	0.676587	7.53568	0.590315	6.65665	0.440703	5.49112	0.363499	4.41832	0.30053	3.50999	0.242381	2.66742	0.636037	5.907	0.636115	3.89737	0.605449	2.15527	0.586174	0.477482	0.578398	-1.13797	1.62237	9.67503	1.71095	8.67629	1.88109	7.18151
1205	0.566058	6.62031	0.498281	5.89267	0.373991	4.8753	0.308994	3.90933	0.256841	3.14531	0.208838	2.41053	0.531065	5.21808	0.532798	3.49373	0.50734	1.97309	0.493618	0.495642	0.487891	-0.93281	1.37168	8.42643	1.45148	7.56889	1.60221	6.31054
906	0.449605	4.71688	0.399335	4.20158	0.302667	3.48223	0.253282	2.772	0.213218	2.19044	0.178164	1.6365	0.426206	3.55305	0.433668	2.15354	0.420243	0.871235	0.413773	-0.32425	0.417215	-1.50232	1.0855	6.05092	1.15347	5.28078	1.27814	4.19004
607	0.287605	3.52806	0.254817	3.15344	0.190087	2.628	0.159289	2.10758	0.133898	1.68874	0.110562	1.29801	0.271769	2.68569	0.280066	1.69838	0.272611	0.796154	0.268585	-0.05799	0.271052	-0.89292	0.727004	4.48469	0.777233	3.91179	0.866702	3.11986
307	0.171503	1.82638	0.15575	1.66204	0.121188	1.37377	0.102922	1.09209	0.088334	0.915444	0.073295	0.713853	0.16977	1.35483	0.177795	0.807416	0.176923	0.285933	0.176751	-0.18612	0.182962	-0.64848	0.408806	2.32376	0.439158	2.00257	0.49024	1.5391
0	-0.00542	-0.35182	-0.00245	-0.3472	-0.00272	-0.33367	-0.00054	-0.28815	0.000724	-0.2231	0.001464	-0.18695	-0.00346	-0.32603	-0.00447	-0.33781	-0.0073	-0.37411	-0.01032	-0.37773	-0.00937	-0.40206	-0.01434	-0.40679	-0.01946	-0.43585	-0.02545	-0.5039

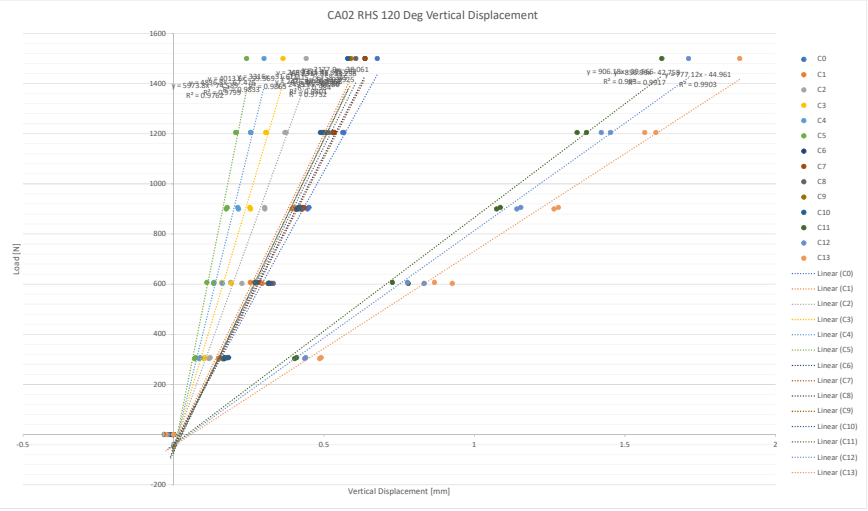

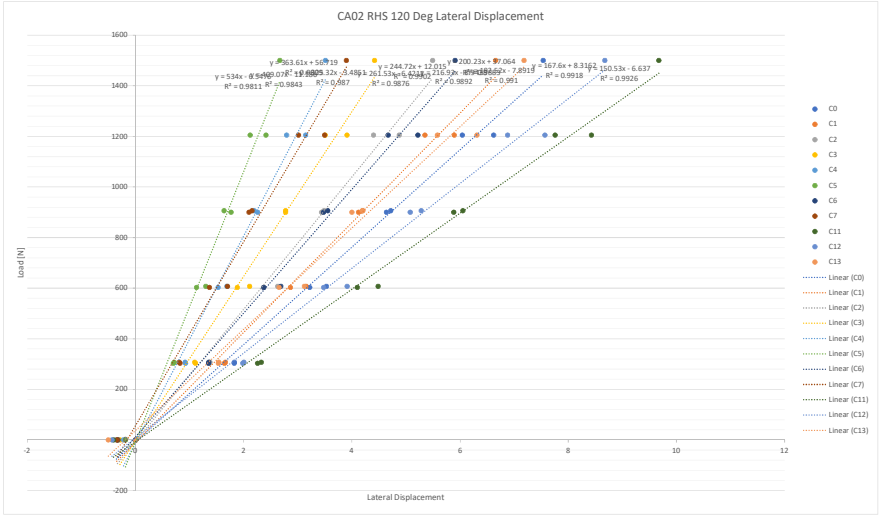

CA02 RHS at 135 Deg

	C0		C1		C2		C3		C4		C5		C6		C7		C8		C9		C10		C11		C12		C13	
Load [N]	V [mm]	W [mm]	V [mm]	W [mm]	V [mm]	W [mm]	V [mm]	W [mm]	V [mm]	W [mm]	V [mm]	W [mm]	V [mm]	W [mm]	V [mm]	W [mm]	V [mm]	W [mm]	V [mm]	W [mm]	V [mm]	W [mm]	V [mm]	W [mm]	V [mm]	W [mm]	V [mm]	W [mm]
0	0	0	0	0	0	0	0	0	0	0	0	0	0	0	0	0	0	0	0	0	0	0	0	0	0	0	0	0
300	0.144222	1.73371	0.126544	1.52073	0.100612	1.28019	0.082687	1.03017	0.067588	0.830066	0.054208	0.609401	0.139133	1.27513	0.145068	0.744813	0.146271	0.269128	0.145602	-0.20922	0.146695	-0.64862	0.369008	2.15428	0.397062	1.81793	0.449239	1.3725
601	0.286866	3.62901	0.254618	3.22257	0.200812	2.72905	0.162459	2.18197	0.133297	1.75919	0.106872	1.32587	0.273182	2.78076	0.280774	1.80965	0.274309	0.935647	0.272868	0.069716	0.276949	-0.72399	0.723536	4.52702	0.777422	3.95624	0.872746	3.16964
855	0.398755	5.17385	0.349876	4.57604	0.276302	3.87653	0.224839	3.11674	0.185142	2.51568	0.146979	1.91687	0.375455	4.03275	0.378357	2.73441	0.362434	1.53917	0.353907	0.37095	0.355018	-0.70531	1.01183	6.53941	1.07491	5.77638	1.20434	4.7987
1195	0.519518	6.37048	0.452568	5.62853	0.354964	4.73238	0.289064	3.78276	0.235006	3.02212	0.186548	2.29702	0.489183	4.97846	0.486009	3.37119	0.463944	1.93178	0.450927	0.504657	0.444533	-0.81737	1.2938	8.12764	1.3763	7.26368	1.52964	6.05445
1506	0.626028	7.93583	0.542125	6.97343	0.420408	5.87921	0.34215	4.73439	0.275694	3.79386	0.219461	2.88801	0.583657	6.28533	0.578122	4.40295	0.545588	2.67501	0.527051	0.977082	0.518693	-0.62412	1.56286	10.1203	1.65684	9.17702	1.84095	7.82163
1201	0.485854	6.40455	0.423711	5.64647	0.328871	4.75401	0.265927	3.80748	0.214602	3.04707	0.17121	2.28409	0.454996	4.97012	0.453384	3.35783	0.428411	1.85453	0.415057	0.382613	0.411097	-0.98344	1.27151	8.18743	1.3524	7.30323	1.51065	6.09646
900	0.380298	5.14255	0.33167	4.53747	0.259809	3.81628	0.210456	3.06723	0.172222	2.45886	0.138012	1.85692	0.355801	3.99027	0.355482	2.68956	0.339133	1.4702	0.32954	0.279634	0.329183	-0.82181	0.9929	6.51879	1.05603	5.80834	1.1835	4.80418
605	0.27812	3.66685	0.246087	3.24108	0.194614	2.74285	0.158104	2.18683	0.13076	1.77575	0.106767	1.34494	0.26626	2.86532	0.268032	1.92734	0.262158	1.06878	0.26186	0.203647	0.261818	-0.581	0.706257	4.61938	0.753681	4.09193	0.849325	3.38488
304	0.147517	1.70274	0.132839	1.49208	0.104851	1.24275	0.085371	0.959009	0.070385	0.792621	0.056171	0.55317	0.144849	1.2676	0.151562	0.735345	0.14974	0.270507	0.151384	-0.19724	0.155105	-0.61822	0.368151	2.12475	0.393605	1.81243	0.442894	1.38795
0	0.010384	0.413772	0.010317	0.348164	0.006287	0.293915	0.003269	0.220405	-7.84E-06	0.236811	-0.00218	0.175342	0.010083	0.379507	0.013417	0.342681	0.015583	0.340297	0.016628	0.303347	0.016264	0.281131	0.019193	0.455364	0.015893	0.448796	0.020149	0.438782

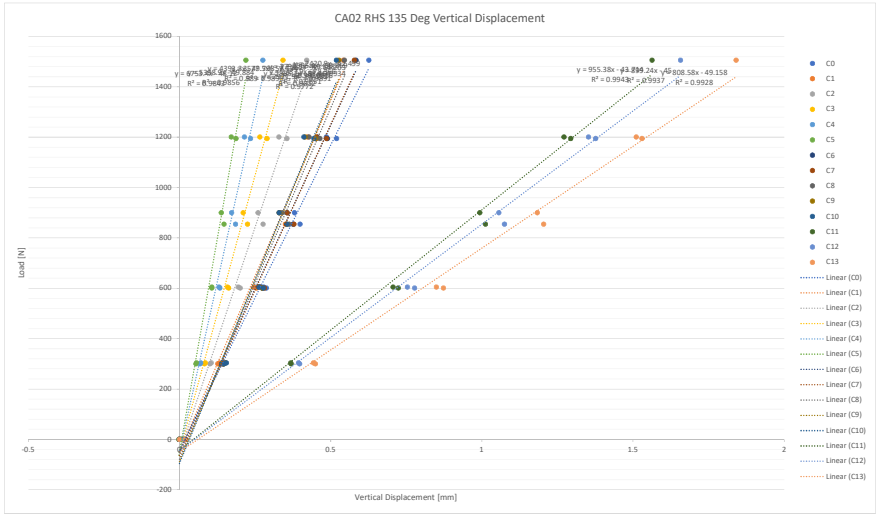

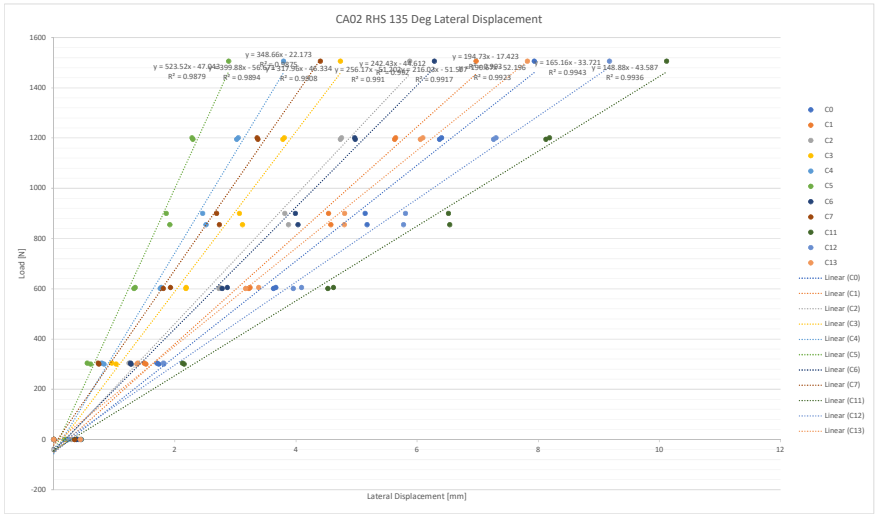

CA02 RHS at 150 Deg

	C0		C1		C2		C3		C4		C5		C6		C7		C8		C9		C10		C11		C12		C13	
Load [N]	V [mm]	W [mm]	V [mm]	W [mm]	V [mm]	W [mm]	V [mm]	W [mm]	V [mm]	W [mm]	V [mm]	W [mm]	V [mm]	W [mm]	V [mm]	W [mm]	V [mm]	W [mm]	V [mm]	W [mm]	V [mm]	W [mm]	V [mm]	W [mm]	V [mm]	W [mm]	V [mm]	W [mm]
0	0	0	0	0	0	0	0	0	0	0	0	0	0	0	0	0	0	0	0	0	0	0	0	0	0	0	0	0
300	0.150353	2.2686	0.132259	2.04021	0.101191	1.73463	0.082831	1.45652	0.066395	1.17279	0.055301	0.9371	0.142264	1.80529	0.148442	1.30454	0.147233	0.827917	0.147367	0.38275	0.148686	-0.05468	0.393687	2.81276	0.431777	2.54828	0.492586	2.23833
600	0.279392	3.80035	0.247125	3.41156	0.191582	2.86928	0.161101	2.33213	0.134323	1.89427	0.112086	1.46902	0.260416	2.94932	0.267023	2.00029	0.258355	1.11848	0.251971	0.284389	0.254748	-0.51167	0.729631	4.8096	0.785536	4.28043	0.884489	3.68928
905	0.360716	5.25966	0.314593	4.6666	0.239167	3.93163	0.200261	3.18154	0.167694	2.59146	0.142081	1.97623	0.326166	4.08957	0.331144	2.76748	0.315195	1.54704	0.304235	0.386485	0.30181	-0.71328	0.995972	6.71232	1.06581	6.02821	1.20047	5.22453
1202	0.459449	6.82557	0.39988	6.05924	0.299741	5.1079	0.244612	4.13793	0.200378	3.32087	0.163947	2.58657	0.410381	5.36717	0.406177	3.7087	0.375904	2.22602	0.354515	0.775368	0.346589	-0.61763	1.25732	8.64263	1.34592	7.84647	1.51081	6.89332
1503	0.563942	8.09485	0.490903	7.16688	0.368975	6.04072	0.302726	4.89253	0.245865	3.95351	0.203019	3.03642	0.504582	6.36358	0.493478	4.36661	0.4539	2.57892	0.424123	0.876302	0.413387	-0.75788	1.52739	10.3069	1.63019	9.36588	1.82744	8.24268
1202	0.455342	6.74559	0.399763	5.9603	0.302975	5.0057	0.250664	4.02711	0.210638	3.23285	0.176001	2.49825	0.406283	5.27494	0.398243	3.59527	0.368315	2.06976	0.346726	0.598027	0.338015	-0.78933	1.25619	8.58989	1.33875	7.75588	1.50493	6.81942
904	0.35039	5.57584	0.308722	4.95835	0.232641	4.18746	0.191672	3.38814	0.1578	2.73954	0.131134	2.14553	0.314167	4.39633	0.314791	3.04317	0.294059	1.83074	0.280313	0.639982	0.276095	-0.485	0.988831	7.03895	1.06091	6.37192	1.19631	5.5857
602	0.260729	4.06073	0.229935	3.61728	0.176003	3.05201	0.145733	2.4769	0.122094	2.01756	0.101783	1.55963	0.239778	3.1881	0.244112	2.22018	0.232732	1.34731	0.225015	0.480539	0.225954	-0.33667	0.717879	5.10469	0.774498	4.61372	0.874085	4.01635
305	0.168785	2.49528	0.150862	2.23519	0.118243	1.91054	0.097665	1.53805	0.079092	1.2851	0.066822	0.99899	0.16219	2.05871	0.165926	1.50709	0.163192	1.04086	0.162456	0.595304	0.162774	0.1431	0.422478	3.13192	0.457423	2.89992	0.520486	2.63701
0	0.037658	0.115176	0.032604	0.101889	0.026589	0.082697	0.021426	0.062756	0.01621	0.073169	0.013717	0.058585	0.04057	0.103741	0.044581	0.120612	0.04277	0.129051	0.044381	0.094354	0.046837	0.102898	0.043556	0.152803	0.055929	0.205094	0.062152	0.22043

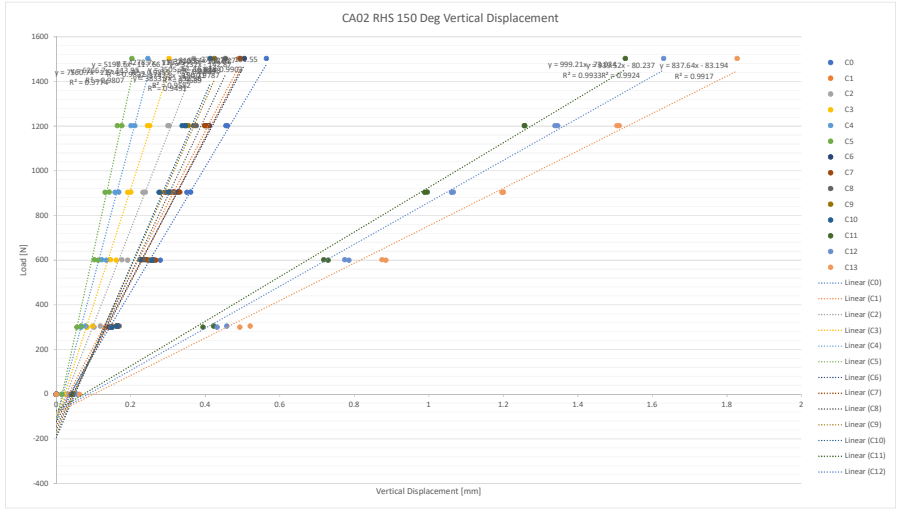

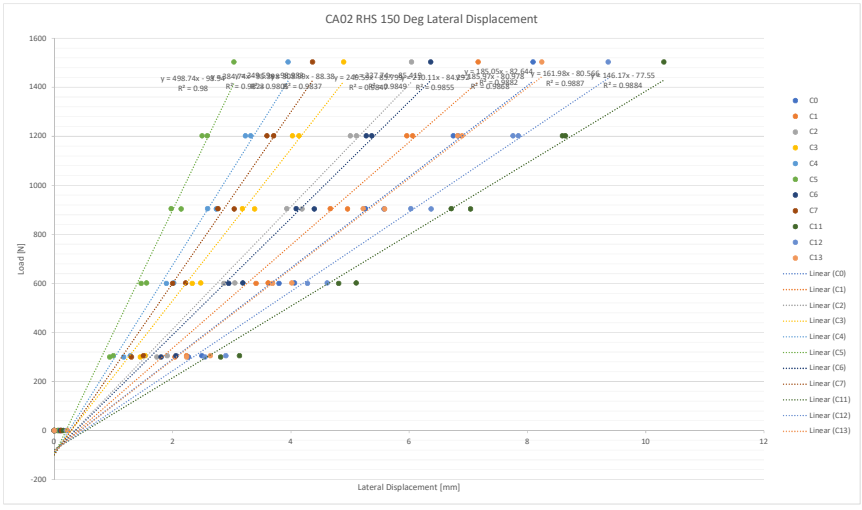

CA02 RHS at 165 Deg

	C0		C1		C2		C3		C4		C5		C6		C7		C8		C9		C10		C11		C12		C13	
Load [N]	V [mm]	W [mm]	V [mm]	W [mm]	V [mm]	W [mm]	V [mm]	W [mm]	V [mm]	W [mm]	V [mm]	W [mm]	V [mm]	W [mm]	V [mm]	W [mm]	V [mm]	W [mm]	V [mm]	W [mm]	V [mm]	W [mm]	V [mm]	W [mm]	V [mm]	W [mm]	V [mm]	W [mm]
0	0	0	0	0	0	0	0	0	0	0	0	0	0	0	0	0	0	0	0	0	0	0	0	0	0	0	0	0
301	0.156063	1.95989	0.13853	1.74228	0.112926	1.49902	0.095038	1.23345	0.082537	0.997068	0.066844	0.743771	0.144154	1.46194	0.150884	0.918966	0.147453	0.445451	0.145618	-0.02207	0.14686	-0.47403	0.406049	2.46271	0.440434	2.14365	0.499378	1.7965
605	0.27862	3.66942	0.253401	3.28112	0.207911	2.83137	0.179135	2.33595	0.162257	1.8767	0.13806	1.41538	0.250549	2.79327	0.253212	1.82361	0.238501	0.985218	0.228786	0.172704	0.223565	-0.62792	0.730097	4.54865	0.787436	4.05475	0.887337	3.46302
901	0.341977	5.42808	0.305472	4.85932	0.237119	4.14641	0.196604	3.42685	0.171495	2.76403	0.140228	2.11848	0.292877	4.17528	0.289883	2.77252	0.263132	1.55922	0.246234	0.377776	0.238294	-0.7654	0.987768	6.77929	1.05341	6.06259	1.19048	5.2779
1200	0.406354	6.46384	0.361578	5.75776	0.279066	4.87541	0.22878	3.99103	0.198391	3.20226	0.161429	2.44799	0.342586	4.89627	0.332135	3.15875	0.299266	1.62581	0.274381	0.137379	0.261884	-1.28361	1.21525	8.15752	1.2944	7.25538	1.46222	6.28306
1504	0.477448	8.10226	0.427714	7.2173	0.324751	6.13454	0.263248	4.98924	0.227444	4.04013	0.184641	3.09534	0.398326	6.29892	0.37994	4.23325	0.332658	2.44546	0.29902	0.724722	0.277367	-0.95262	1.44236	10.219	1.53458	9.29742	1.73609	8.25968
1200	0.387843	6.7371	0.345643	5.99449	0.264285	5.08632	0.216456	4.12678	0.189783	3.33276	0.156107	2.54491	0.321117	5.17583	0.307941	3.39905	0.269551	1.86053	0.242913	0.370061	0.22518	-1.06833	1.20263	8.5113	1.27868	7.63868	1.44854	6.70877
910	0.293345	5.38363	0.265249	4.81023	0.204403	4.08722	0.167009	3.31878	0.146761	2.69715	0.120086	2.06164	0.243273	4.10368	0.237394	2.68496	0.209034	1.43211	0.190096	0.23489	0.180114	-0.93856	0.939476	6.78972	1.00319	6.05379	1.13814	5.28229
605	0.223201	3.92364	0.20188	3.49703	0.161431	3.00355	0.132642	2.42247	0.120222	1.98063	0.099834	1.50918	0.193789	3.01483	0.196518	1.98549	0.1788	1.11203	0.168315	0.245543	0.164187	-0.59237	0.688011	4.93445	0.734836	4.39133	0.839054	3.85357
306	0.148719	1.96719	0.132988	1.75244	0.108808	1.4946	0.093616	1.1988	0.083279	0.963134	0.068556	0.722954	0.135029	1.46341	0.141165	0.915563	0.135363	0.446683	0.132926	-0.02882	0.132244	-0.47738	0.39832	2.4953	0.427941	2.19247	0.486769	1.8861
0	0.062011	-0.08614	0.053992	-0.09938	0.048011	-0.07182	0.041877	-0.0812	0.039599	-0.0738	0.030757	-0.07681	0.062766	-0.10764	0.066913	-0.14226	0.069178	-0.14061	0.069731	-0.1546	0.072741	-0.16307	0.076639	-0.07684	0.079962	-0.12075	0.087431	-0.1346

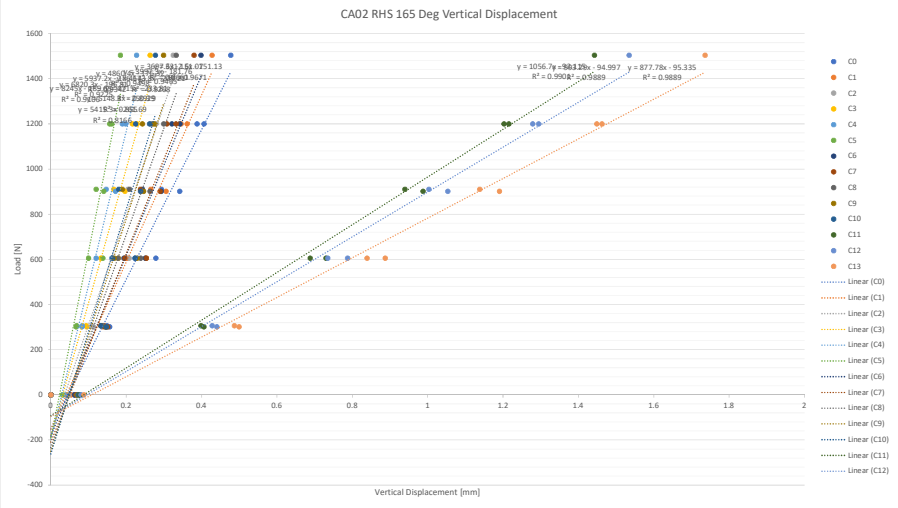

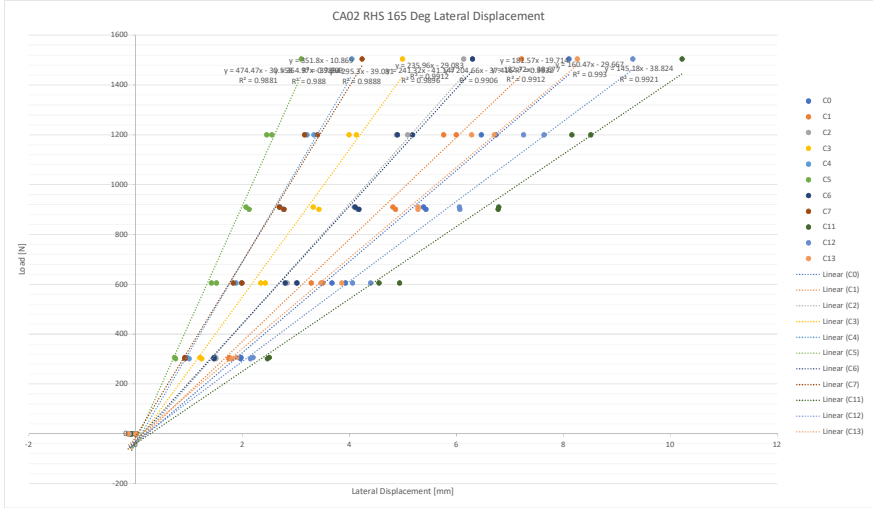

CA02 RHS at 180 Deg

	C0		C1		C2		C3		C4		C5		C6		C7		C8		C9		C10		C11		C12		C13	
Load [N]	V [mm]	W [mm]	V [mm]	W [mm]	V [mm]	W [mm]	V [mm]	W [mm]	V [mm]	W [mm]	V [mm]	W [mm]	V [mm]	W [mm]	V [mm]	W [mm]	V [mm]	W [mm]	V [mm]	W [mm]	V [mm]	W [mm]	V [mm]	W [mm]	V [mm]	W [mm]	V [mm]	W [mm]
0	0	0	0	0	0	0	0	0	0	0	0	0	0	0	0	0	0	0	0	0	0	0	0	0	0	0	0	0
300	0.152668	2.02319	0.137798	1.81647	0.109672	1.56135	0.093568	1.28599	0.08257	1.05982	0.070473	0.819564	0.1441	1.55928	0.150901	1.06992	0.147993	0.597562	0.151406	0.183681	0.157013	-0.22567	0.396484	2.5016	0.435903	2.24533	0.500845	1.982
600	0.246083	3.56914	0.221641	3.18732	0.172815	2.74763	0.146971	2.25435	0.127661	1.84653	0.108653	1.41541	0.220582	2.71835	0.224931	1.79546	0.213658	0.950142	0.209982	0.169641	0.210986	-0.58038	0.693658	4.49613	0.750054	4.00034	0.855049	3.46973
900	0.298529	5.13435	0.268009	4.58147	0.204374	3.90725	0.168117	3.2127	0.148539	2.6019	0.125062	2.01706	0.255681	3.94602	0.254839	2.68285	0.232705	1.51346	0.219268	0.43035	0.216754	-0.61199	0.916206	6.4494	0.986115	5.82654	1.12704	5.15594
1200	0.378347	6.9255	0.336714	6.16165	0.251054	5.22976	0.205826	4.30582	0.177091	3.50124	0.147637	2.70974	0.320802	5.44705	0.314282	3.83031	0.282159	2.31604	0.261719	0.936536	0.254558	-0.37575	1.17164	8.69445	1.2631	8.00186	1.44136	7.18035
1505	0.485301	7.84975	0.432928	6.97895	0.327297	5.91285	0.270626	4.86434	0.232761	3.919	0.196822	3.02919	0.40949	6.09088	0.398751	4.19312	0.35427	2.41757	0.328189	0.773638	0.315821	-0.78267	1.43394	9.96998	1.53701	9.09984	1.75146	8.21125
1205	0.390804	6.90815	0.347821	6.1238	0.263668	5.22446	0.219726	4.30028	0.189744	3.47543	0.159697	2.6988	0.328886	5.40947	0.32033	3.79655	0.287592	2.27595	0.266346	0.886488	0.259054	-0.43539	1.18816	8.68743	1.27606	7.95902	1.4575	7.18932
901	0.286063	5.49191	0.258879	4.88808	0.193704	4.17291	0.160464	3.43251	0.143174	2.78163	0.122826	2.14926	0.241439	4.29466	0.238761	3.00661	0.215411	1.80899	0.201721	0.701098	0.196392	-0.35931	0.916942	6.91957	0.985694	6.32048	1.13081	5.66716
605	0.198219	4.07868	0.182391	3.63737	0.138485	3.13305	0.114762	2.58174	0.101729	2.12416	0.090852	1.65687	0.170059	3.24225	0.172918	2.35232	0.161186	1.51003	0.153847	0.73002	0.152177	-0.00819	0.640942	5.09479	0.69276	4.71618	0.796635	4.28924
304	0.122935	2.16513	0.113664	1.92719	0.090172	1.66643	0.075276	1.36091	0.070043	1.12305	0.062016	0.867201	0.110679	1.71001	0.115642	1.23353	0.110618	0.784099	0.109422	0.380296	0.113154	-0.03128	0.36257	2.69786	0.394092	2.49772	0.45166	2.25296
0	0.018995	-0.07543	0.022934	-0.05165	0.022955	-0.0298	0.018333	-0.07543	0.019221	-0.05062	0.021925	-0.04845	0.02264	-0.03592	0.023913	-0.00772	0.026146	0.037434	0.028053	0.094748	0.0285	0.12871	0.014009	-0.06368	0.014591	-0.02414	0.013019	0.017956

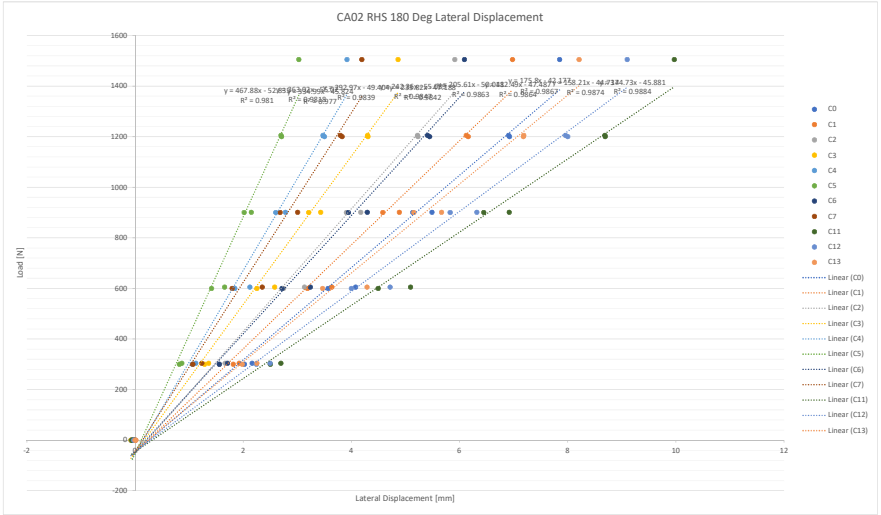

AR01 RHS at 90 Deg

	C0		C1		C2		C3		C4		C5		C6		C7		C8		C9		C10		C11		C12		C13	
Load [N]	V [mm]	W [mm]	V [mm]	W [mm]	V [mm]	W [mm]	V [mm]	W [mm]	V [mm]	W [mm]	V [mm]	W [mm]	V [mm]	W [mm]	V [mm]	W [mm]	V [mm]	W [mm]	V [mm]	W [mm]	V [mm]	W [mm]	V [mm]	W [mm]	V [mm]	W [mm]	V [mm]	W [mm]
0	0	0	0	0	0	0	0	0	0	0	0	0	0	0	0	0	0	0	0	0	0	0	0	0	0	0	0	0
300	0.216363	2.14836	0.149128	1.88668	0.086551	1.5017	0.067191	1.25472	0.055133	1.00242	0.044	0.831782	0.181731	1.87211	0.182109	1.53734	0.183439	1.17867	0.188332	0.866973	0.19512	0.538401	0.321818	2.63722	0.380149	2.41535	0.441068	2.11279
603	0.51446	2.92196	0.360879	2.61875	0.232652	2.05529	0.183464	1.65382	0.154414	1.31799	0.124045	1.01751	0.449	2.38489	0.448473	1.70422	0.456696	1.05899	0.463852	0.416107	0.474746	-0.16909	0.73129	3.6147	0.849892	3.03172	0.972629	2.28561
900	0.750197	4.4391	0.527805	3.90652	0.338091	3.09802	0.265706	2.49613	0.223482	1.96757	0.178121	1.51753	0.650627	3.689	0.646232	2.72641	0.654291	1.78476	0.660095	0.893232	0.677778	0.070903	1.06695	5.51444	1.23225	4.65514	1.40276	3.62363
1205	0.915127	5.55145	0.63272	4.77972	0.394836	3.75062	0.304898	3.0206	0.256497	2.40754	0.201858	1.82861	0.788872	4.57422	0.784416	3.42435	0.795074	2.25002	0.803657	1.15729	0.8213	0.138579	1.31187	6.9519	1.51196	5.85958	1.71312	4.54735
1500	1.13034	6.61657	0.778411	5.65122	0.484768	4.3435	0.375932	3.48848	0.31502	2.73182	0.248267	2.06736	0.975386	5.46964	0.969615	4.08312	0.979162	2.72228	0.987895	1.4072	1.01006	0.225467	1.60409	8.29946	1.84677	7.03516	2.08378	5.47883
1201	0.95851	5.41348	0.672062	4.61788	0.432614	3.57086	0.344407	2.87873	0.291079	2.27905	0.23153	1.72732	0.8345	4.47033	0.831868	3.28824	0.843986	2.10419	0.850545	0.975035	0.86865	-0.01896	1.34956	6.79194	1.5578	5.77745	1.76198	4.44891
906	0.726293	3.70713	0.50995	3.13522	0.327727	2.36334	0.25878	1.88926	0.221908	1.46629	0.176664	1.09716	0.63984	2.9937	0.640097	2.0961	0.647601	1.20108	0.659157	0.359706	0.674294	-0.39606	1.01957	4.64005	1.17664	3.77329	1.3329	2.70298
600	0.493736	2.27397	0.352574	2.02543	0.228692	1.51023	0.179982	1.1906	0.151965	0.912282	0.122258	0.685082	0.441691	1.78044	0.443304	1.16893	0.451125	0.57134	0.455426	0.022452	0.468066	-0.48002	0.689131	2.88811	0.801124	2.23992	0.907413	1.45253
302	0.323521	0.553792	0.242715	0.538164	0.175025	0.299144	0.143853	0.221633	0.125098	0.129938	0.100212	0.090941	0.301704	0.288467	0.299873	-0.07522	0.303978	-0.44299	0.305615	-0.74021	0.315905	-1.06377	0.428603	0.670713	0.492325	0.267168	0.547319	-0.25811
0	0.019645	-0.0441	0.019952	-0.04577	0.01205	-0.08839	0.009525	-0.11985	0.00922	-0.09253	0.004146	-0.08331	0.027725	-0.01526	0.028268	-0.04259	0.023971	-0.06982	0.020487	-0.07182	0.020366	-0.08632	0.020362	-0.06386	0.017195	-0.09107	0.011761	-0.19631

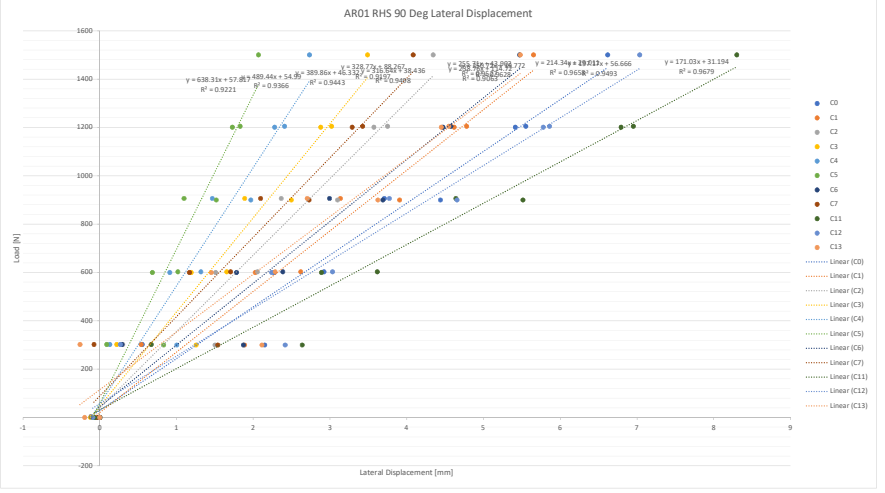

AR01 RHS at 105 Deg

	C0		C1		C2		C3		C4		C5		C6		C7		C8		C9		C10		C11		C12		C13	
Load [N]	V [mm]	W [mm]	V [mm]	W [mm]	V [mm]	W [mm]	V [mm]	W [mm]	V [mm]	W [mm]	V [mm]	W [mm]	V [mm]	W [mm]	V [mm]	W [mm]	V [mm]	W [mm]	V [mm]	W [mm]	V [mm]	W [mm]	V [mm]	W [mm]	V [mm]	W [mm]	V [mm]	W [mm]
0	0	0	0	0	0	0	0	0	0	0	0	0	0	0	0	0	0	0	0	0	0	0	0	0	0	0	0	0
306	0.219915	2.0812	0.146155	1.78533	0.084391	1.43455	0.063449	1.23226	0.052902	0.974744	0.041423	0.802683	0.177046	1.85714	0.177441	1.57092	0.1808	1.24714	0.180955	0.915356	0.189441	0.620395	0.335705	2.51146	0.38967	2.35585	0.451723	2.05706
600	0.433125	3.02557	0.289053	2.56299	0.177311	2.0623	0.13828	1.69818	0.116935	1.32966	0.092693	1.00913	0.353652	2.54383	0.352436	1.99135	0.357898	1.41168	0.360155	0.824959	0.370239	0.305997	0.644194	3.73374	0.739284	3.31437	0.849154	2.69154
900	0.662484	4.55916	0.448146	3.87936	0.276272	3.12002	0.21502	2.59893	0.177092	2.07035	0.142621	1.63621	0.548625	3.84781	0.539759	3.01794	0.550301	2.15127	0.554538	1.26788	0.57293	0.510785	0.975192	5.56324	1.11358	4.96007	1.27286	4.06795
1206	0.874301	6.17589	0.586966	5.2264	0.359418	4.19133	0.281449	3.42652	0.232128	2.72309	0.185431	2.12662	0.726536	5.22837	0.720891	4.14984	0.731489	3.03161	0.735986	1.92712	0.756036	0.966194	1.28832	7.59402	1.46899	6.80557	1.67571	5.66788
1500	1.04441	6.47232	0.699497	5.45384	0.426057	4.29694	0.332674	3.4708	0.27652	2.70386	0.222023	2.0657	0.869212	5.30611	0.863172	4.00617	0.874714	2.65929	0.880448	1.3526	0.903991	0.194888	1.54407	7.9961	1.75242	6.9151	1.98765	5.42803
1205	0.927118	5.43293	0.632467	4.57838	0.399431	3.6312	0.316351	2.96901	0.265169	2.29482	0.213549	1.75963	0.780478	4.44639	0.775928	3.3323	0.786666	2.18779	0.789408	1.03267	0.809954	0.023233	1.3511	6.68885	1.5331	5.76413	1.74529	4.54134
900	0.678492	4.46261	0.463195	3.76631	0.291557	3.00183	0.23126	2.45279	0.195454	1.91026	0.159664	1.47784	0.571658	3.78533	0.568724	2.9421	0.579129	2.06769	0.583419	1.21777	0.597295	0.472982	0.992708	5.49312	1.13347	4.85328	1.2936	3.94077
604	0.47272	3.39814	0.318327	2.87688	0.198137	2.3435	0.156241	1.97307	0.131684	1.56881	0.102486	1.26885	0.396132	2.89879	0.396926	2.32008	0.407822	1.69545	0.411772	1.09211	0.426679	0.544919	0.692614	4.08864	0.796821	3.67339	0.916902	3.04643
303	0.187309	1.33945	0.125669	1.08503	0.074458	0.856774	0.058431	0.710665	0.050596	0.527679	0.040401	0.393089	0.153247	1.16843	0.154004	0.95207	0.156856	0.67222	0.152795	0.401694	0.158743	0.177554	0.278754	1.63397	0.322287	1.41256	0.365743	1.07466
0	-0.02895	-0.1022	-0.02165	-0.15881	-0.01915	-0.16446	-0.0151	-0.13716	-0.01177	-0.12268	-0.00947	-0.09913	-0.02929	-0.02825	-0.03505	0.016442	-0.03617	0.058871	-0.04234	0.065456	-0.04275	0.080464	-0.03522	-0.11596	-0.03668	-0.03855	-0.04573	-0.01985

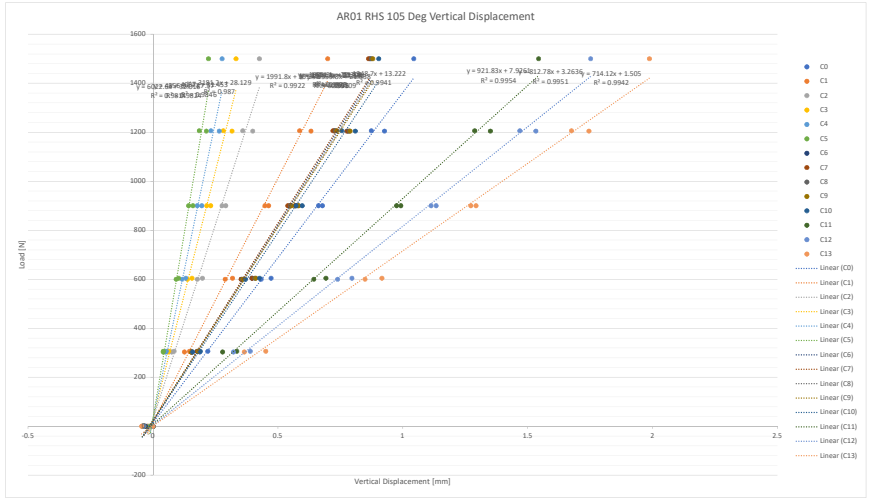

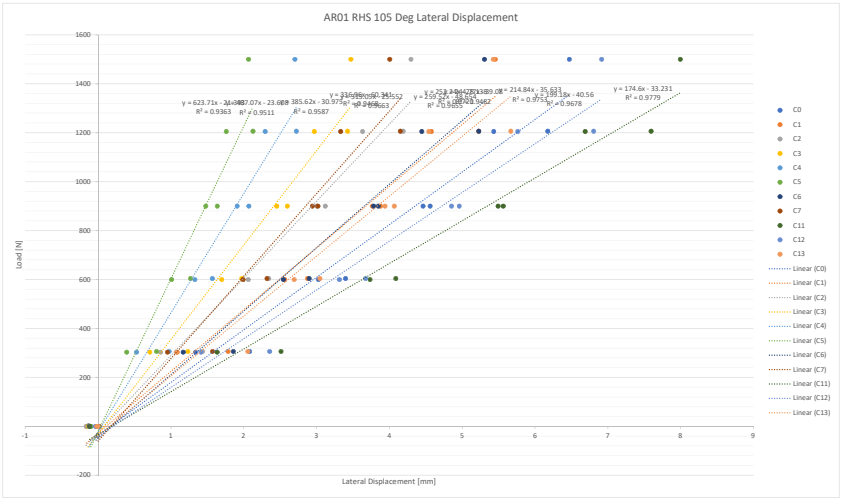

AR01 RHS at 120 Deg

	C0		C1		C2		C3		C4		C5		C6		C7		C8		C9		C10		C11		C12		C13	
Load [N]	V [mm]	W [mm]	V [mm]	W [mm]	V [mm]	W [mm]	V [mm]	W [mm]	V [mm]	W [mm]	V [mm]	W [mm]	V [mm]	W [mm]	V [mm]	W [mm]	V [mm]	W [mm]	V [mm]	W [mm]	V [mm]	W [mm]	V [mm]	W [mm]	V [mm]	W [mm]	V [mm]	W [mm]
0	0	0	0	0	0	0	0	0	0	0	0	0	0	0	0	0	0	0	0	0	0	0	0	0	0	0	0	0
300	0.235122	2.25455	0.159525	1.99655	0.096724	1.69287	0.075248	1.41251	0.066092	1.14837	0.051061	0.932194	0.186796	1.94961	0.187333	1.60001	0.19387	1.25746	0.198928	0.951704	0.200654	0.678427	0.349524	2.76079	0.402338	2.54997	0.462561	2.22299
601	0.394506	2.6382	0.265976	2.313	0.160817	1.89052	0.127697	1.54807	0.112252	1.21311	0.086864	0.892811	0.319441	2.1245	0.321508	1.54406	0.326132	0.971013	0.333224	0.471784	0.338788	-0.02251	0.598643	3.35213	0.684045	2.89077	0.792712	2.37445
900	0.664104	4.64701	0.452123	4.00318	0.275017	3.19021	0.214195	2.56129	0.179524	2.00752	0.142436	1.53592	0.549932	3.85905	0.547997	2.96208	0.553104	2.06964	0.559643	1.2594	0.569924	0.491679	0.972835	5.74658	1.10276	5.01951	1.25629	4.18257
1200	0.79378	6.17721	0.531815	5.36527	0.318495	4.39846	0.247781	3.61988	0.207698	2.91791	0.161508	2.2609	0.650642	5.21023	0.649763	4.09694	0.662157	3.01607	0.673473	1.96876	0.685156	1.04676	1.17036	7.59637	1.3345	6.78573	1.52971	5.7363
1500	1.02229	6.72334	0.694701	5.77318	0.425567	4.61928	0.332125	3.73676	0.279824	2.93913	0.220486	2.19559	0.847159	5.51484	0.837373	4.17831	0.8443	2.83493	0.845415	1.64721	0.854803	0.552881	1.50604	8.35468	1.70151	7.28083	1.93209	6.01603
1201	0.826724	5.85621	0.561349	5.00606	0.344529	4.00798	0.271586	3.27514	0.228286	2.60682	0.182151	2.00153	0.686576	4.89105	0.684004	3.79071	0.6936	2.70084	0.700803	1.71458	0.715663	0.78357	1.22599	7.29746	1.38763	6.42928	1.58497	5.38637
905	0.64377	4.85672	0.436091	4.1873	0.267045	3.41273	0.210938	2.83219	0.181572	2.23209	0.141754	1.75064	0.533147	4.09325	0.533536	3.18834	0.544554	2.31072	0.550244	1.53203	0.562339	0.78036	0.96167	6.02028	1.09621	5.3731	1.25188	4.49518
606	0.469837	3.40801	0.322946	2.97548	0.206957	2.43643	0.163917	2.00444	0.139967	1.61554	0.109514	1.26001	0.391673	2.89086	0.393318	2.23666	0.400503	1.61679	0.406378	1.05159	0.412979	0.538208	0.688404	4.16876	0.78314	3.70361	0.89086	3.05553
300	0.248078	1.95894	0.1705	1.72475	0.108823	1.47185	0.085391	1.22266	0.073403	1.02354	0.056741	0.795284	0.209884	1.69066	0.211883	1.30771	0.21915	0.963714	0.224201	0.679465	0.228718	0.384507	0.371141	2.42681	0.421853	2.1658	0.481755	1.81523
0	-0.06965	1.13851	-0.06157	0.964887	-0.05713	0.878818	-0.05029	0.790229	-0.04434	0.670059	-0.04198	0.576972	-0.07444	1.16597	-0.07987	1.13668	-0.08265	1.12928	-0.08296	1.15735	-0.08612	1.13875	-0.07963	1.35756	-0.09204	1.38476	-0.09427	0

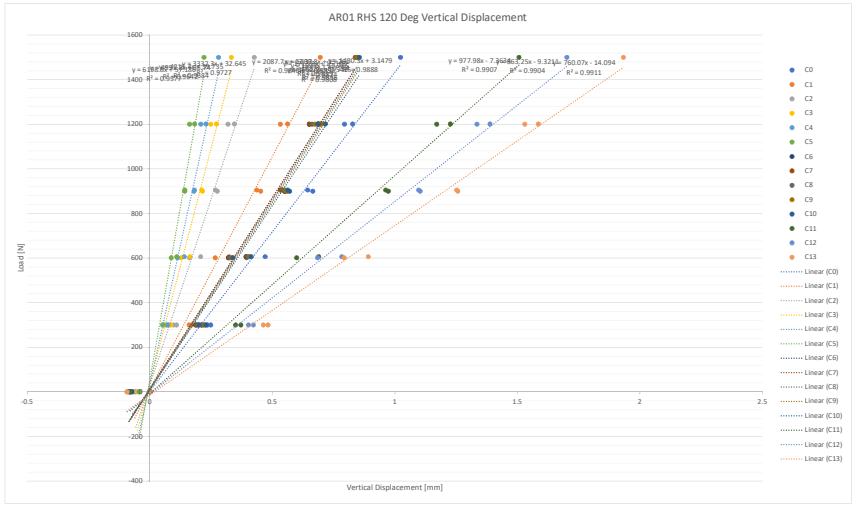

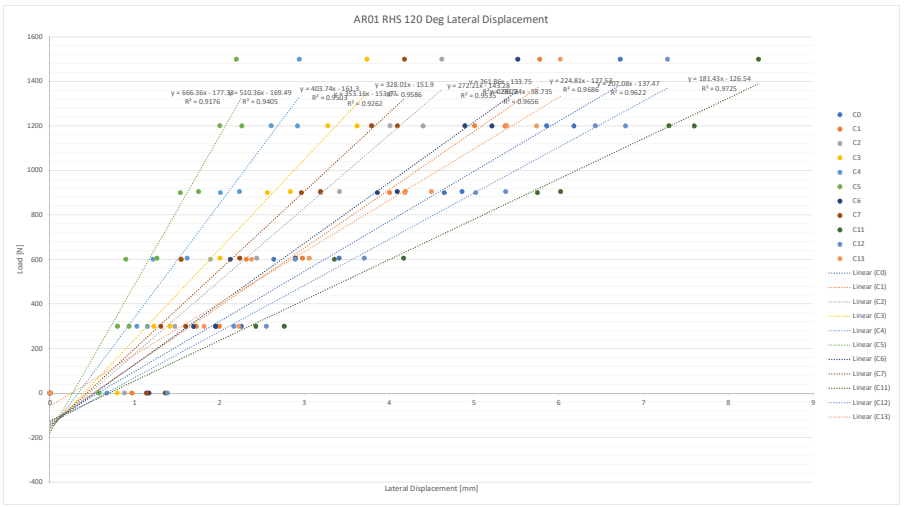

AR01 RHS at 135 Deg

	C0		C1		C2		C3		C4		C5		C6		C7		C8		C9		C10		C11		C12		C13	
Load [N]	V [mm]	W [mm]	V [mm]	W [mm]	V [mm]	W [mm]	V [mm]	W [mm]	V [mm]	W [mm]	V [mm]	W [mm]	V [mm]	W [mm]	V [mm]	W [mm]	V [mm]	W [mm]	V [mm]	W [mm]	V [mm]	W [mm]	V [mm]	W [mm]	V [mm]	W [mm]	V [mm]	W [mm]
0	0	0	0	0	0	0	0	0	0	0	0	0	0	0	0	0	0	0	0	0	0	0	0	0	0	0	0	0
301	0.234476	0.703558	0.165396	0.653037	0.10782	0.48214	0.093646	0.36248	0.080179	0.180388	0.06554	0.086161	0.195831	0.394451	0.192834	0.071472	0.1942	-0.26487	0.201578	-0.55964	0.208173	-0.8984	0.337656	0.95289	0.386335	0.649573	0.448195	0.339245
600	0.501224	2.04629	0.359507	1.80479	0.242423	1.3857	0.202393	1.13425	0.174658	0.821146	0.145278	0.554812	0.428505	1.49419	0.425574	0.868869	0.427738	0.282122	0.43916	-0.30224	0.447427	-0.82879	0.712406	2.68733	0.816084	2.29791	0.931709	1.68047
900	0.69698	3.26356	0.4851	2.89119	0.316394	2.2697	0.261871	1.80792	0.221956	1.3757	0.178935	1.00652	0.583448	2.42643	0.584003	1.51582	0.589337	0.659881	0.607508	-0.19397	0.619046	-0.95342	1.00316	4.14004	1.15012	3.52497	1.31732	2.76531
1195	0.833954	4.58566	0.575539	4.06024	0.357876	3.17581	0.296916	2.58204	0.24743	1.9806	0.19732	1.48572	0.691424	3.58642	0.68709	2.49623	0.697497	1.40395	0.711421	0.396375	0.727441	-0.55927	1.22039	5.82556	1.39559	5.08745	1.60168	4.14881
1503	1.03574	5.91186	0.710956	5.14365	0.44056	4.06579	0.362074	3.29656	0.301571	2.55099	0.240766	1.90681	0.858059	4.68194	0.84879	3.35953	0.856228	2.07987	0.872082	0.811103	0.889655	-0.30574	1.5215	7.49812	1.72984	6.58937	1.97972	5.47301
1197	0.840986	5.09103	0.578254	4.42399	0.357445	3.51894	0.295951	2.88246	0.245799	2.23882	0.196481	1.69829	0.691431	4.05088	0.684606	2.95489	0.691217	1.84619	0.705773	0.818039	0.720103	-0.13727	1.23894	6.44993	1.41118	5.70248	1.61936	4.76122
905	0.684769	2.78496	0.482291	2.48368	0.315692	1.9221	0.264399	1.51472	0.223987	1.07906	0.179877	0.717132	0.578713	1.94999	0.57683	1.10102	0.585316	0.229478	0.598815	-0.56726	0.613415	-1.36496	0.993111	3.60936	1.13231	2.94423	1.29296	2.0838
605	0.46537	2.24965	0.32375	1.99064	0.211186	1.58232	0.17658	1.25999	0.150573	0.92792	0.120753	0.687001	0.390985	1.69773	0.388871	1.04528	0.396324	0.411811	0.405521	-0.12452	0.415445	-0.67967	0.678981	2.85649	0.773969	2.38926	0.886954	1.76916
300	0.251149	0.159336	0.183092	0.196607	0.127836	0.085665	0.112318	0.027225	0.099461	-0.07901	0.083204	-0.11933	0.216835	-0.14411	0.218833	-0.46868	0.224731	-0.7947	0.233823	-1.0758	0.241247	-1.39956	0.357374	0.372654	0.409264	0.029111	0.460507	-0.40771
0	-0.04259	-0.52342	-0.02858	-0.43286	-0.02281	-0.35417	-0.01709	-0.32556	-0.01402	-0.30665	-0.01059	-0.27278	-0.04056	-0.50738	-0.0417	-0.50439	-0.0473	-0.51374	-0.04662	-0.48711	-0.0504	-0.5233	-0.05992	-0.5998	-0.06824	-0.63951	-0.08015	-0.69494

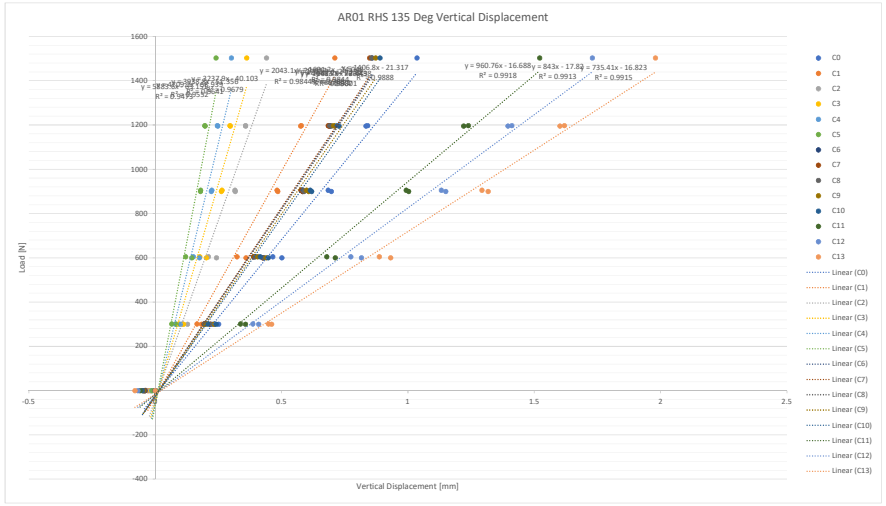

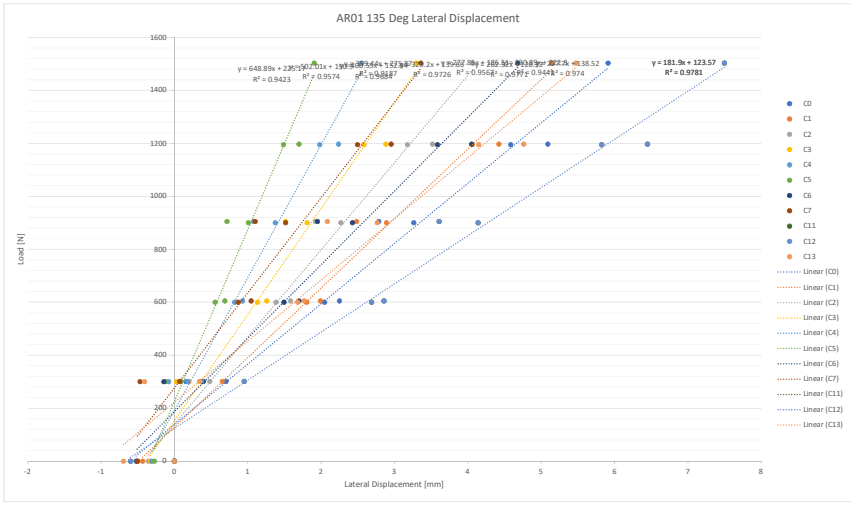

AR01 RHS at 150 Deg

	C0		C1		C2		C3		C4		C5		C6		C7		C8		C9		C10		C11		C12		C13	
Load [N]	V [mm]	W [mm]	V [mm]	W [mm]	V [mm]	W [mm]	V [mm]	W [mm]	V [mm]	W [mm]	V [mm]	W [mm]	V [mm]	W [mm]	V [mm]	W [mm]	V [mm]	W [mm]	V [mm]	W [mm]	V [mm]	W [mm]	V [mm]	W [mm]	V [mm]	W [mm]	V [mm]	W [mm]
0	0	0	0	0	0	0	0	0	0	0	0	0	0	0	0	0	0	0	0	0	0	0	0	0	0	0	0	0
300	0.258172	1.69279	0.186996	1.50587	0.128521	1.26959	0.106106	1.04358	0.09359	0.854649	0.078979	0.668391	0.209594	1.37443	0.205767	1.0686	0.206008	0.789371	0.206535	0.500139	0.212971	0.251719	0.365295	2.08767	0.419895	1.88531	0.474	1.60952
600	0.473246	3.4002	0.323546	3.01934	0.208798	2.53497	0.166682	2.08258	0.142181	1.69198	0.115529	1.34816	0.377438	2.71232	0.380331	2.06258	0.387687	1.39563	0.399861	0.784376	0.415005	0.215442	0.700903	4.16425	0.804564	3.75105	0.921713	3.22464
900	0.667551	3.83022	0.458783	3.40283	0.298884	2.79968	0.240126	2.28093	0.202934	1.7956	0.167346	1.33494	0.542395	2.9426	0.542395	2.09382	0.546179	1.25704	0.543343	0.492743	0.553129	-0.21928	0.974276	4.83973	1.11383	4.22068	1.27499	3.4826
1200	0.803403	5.59298	0.542493	4.88811	0.34393	4.04089	0.272163	3.3141	0.22732	2.66255	0.188443	2.03048	0.639871	4.51585	0.635838	3.48801	0.643163	2.45331	0.651942	1.45908	0.66795	0.603272	1.19437	7.01489	1.36258	6.39698	1.55837	5.59601
1500	1.02357	6.52377	0.692564	5.62124	0.441599	4.60299	0.352035	3.75501	0.294068	3.02033	0.238621	2.37483	0.823616	5.19857	0.818573	3.91657	0.826275	2.6396	0.837456	1.43708	0.85839	0.35549	1.51663	8.22691	1.72653	7.4162	1.97348	6.4144
1198	0.873716	5.68565	0.594897	4.98181	0.384689	4.12385	0.307383	3.368	0.25703	2.74038	0.208458	2.16581	0.70458	4.62108	0.705706	3.5581	0.711106	2.49246	0.719639	1.51198	0.73638	0.61227	1.28301	7.15552	1.46384	6.52094	1.66999	5.69742
907	0.664083	3.95561	0.457092	3.48425	0.297685	2.86244	0.238165	2.32114	0.201968	1.87744	0.165538	1.40736	0.538926	3.10879	0.537088	2.28606	0.539786	1.47914	0.547662	0.706059	0.560136	-0.00163	0.972389	4.96168	1.10674	4.41874	1.2584	3.67538
607	0.451643	2.59295	0.314323	2.29862	0.204791	1.89085	0.166081	1.53436	0.139929	1.21126	0.114641	0.907575	0.37175	2.00898	0.3706	1.42695	0.372842	0.832331	0.381539	0.30218	0.392907	-0.17608	0.660396	3.26278	0.751743	2.82448	0.858403	2.29143
305	0.241331	1.35315	0.166344	1.2002	0.108501	1.00426	0.087611	0.835505	0.075485	0.675513	0.063413	0.499037	0.195126	1.0236	0.195874	0.713517	0.197876	0.416996	0.201349	0.105595	0.212892	-0.17543	0.349169	1.69968	0.399166	1.42863	0.455197	1.1275
0	0.018931	0.124823	0.013627	0.147791	0.009383	0.134877	0.008078	0.124022	0.008185	0.096176	0.007112	0.06581	0.012032	0.051809	0.011939	0.061124	0.010192	0.044569	0.00776	0.045188	0.006955	0.040404	0.027094	0.082709	0.029532	0.060258	0.029064	0.029619

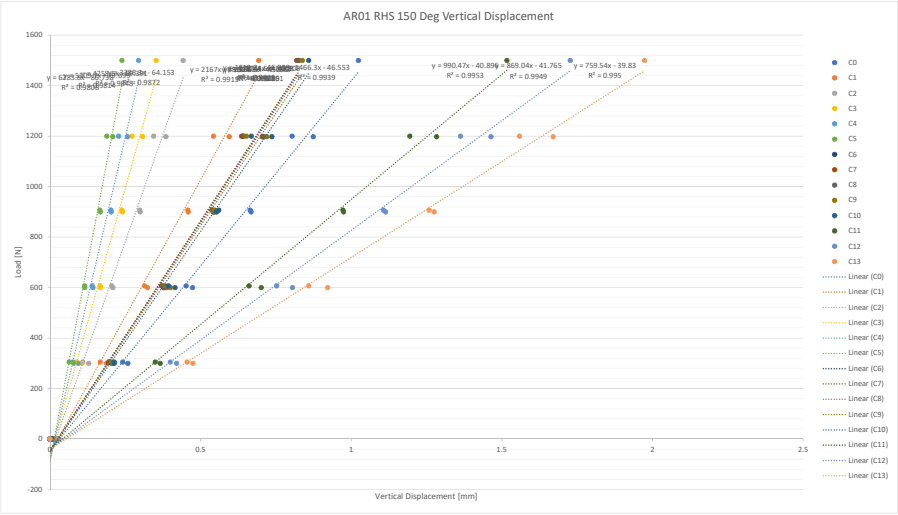

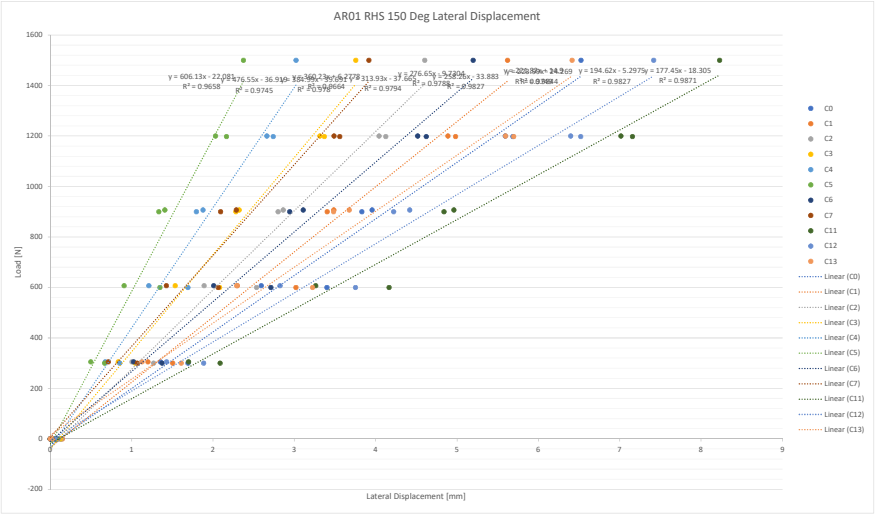

AR01 RHS at 165 Deg

	C0		C1		C2		C3		C4		C5		C6		C7		C8		C9		C10		C11		C12		C13	
Load [N]	V [mm]	W [mm]	V [mm]	W [mm]	V [mm]	W [mm]	V [mm]	W [mm]	V [mm]	W [mm]	V [mm]	W [mm]	V [mm]	W [mm]	V [mm]	W [mm]	V [mm]	W [mm]	V [mm]	W [mm]	V [mm]	W [mm]	V [mm]	W [mm]	V [mm]	W [mm]	V [mm]	W [mm]
0	0	0	0	0	0	0	0	0	0	0	0	0	0	0	0	0	0	0	0	0	0	0	0	0	0	0	0	0
302	0.24931	2.37118	0.166244	2.06757	0.102254	1.75187	0.081803	1.47494	0.069873	1.20104	0.053136	0.995478	0.19449	1.97052	0.192944	1.57902	0.202689	1.26565	0.208958	0.94217	0.216645	0.64555	0.375468	2.92894	0.437624	2.7833	0.511941	2.5886
600	0.426127	3.22621	0.285724	2.82985	0.173901	2.37129	0.141336	1.95371	0.1175	1.55685	0.09382	1.2117	0.331936	2.54196	0.331557	1.93014	0.34383	1.37531	0.350546	0.802211	0.360712	0.306312	0.641098	4.07314	0.742012	3.74219	0.858472	3.37265
902	0.635167	4.5896	0.429501	4.05804	0.261848	3.33246	0.212242	2.77708	0.178293	2.22365	0.141576	1.70553	0.496882	3.61188	0.492238	2.76824	0.505985	1.96031	0.512463	1.13773	0.52842	0.404499	0.952617	5.82682	1.09614	5.37711	1.2678	4.87253
1202	0.810625	6.26052	0.54522	5.45051	0.333966	4.55425	0.268257	3.82479	0.22373	3.04103	0.178288	2.43192	0.625574	5.07439	0.616042	4.02123	0.625113	3.02268	0.63057	2.00782	0.639883	1.12872	1.21917	7.93034	1.39679	7.43501	1.61252	6.85485
1503	0.946167	6.74711	0.636299	5.89364	0.38504	4.84907	0.30947	4.01042	0.258235	3.22767	0.208502	2.53892	0.728157	5.34373	0.715562	4.11477	0.728928	2.9162	0.735968	1.69067	0.750795	0.642038	1.44273	8.63717	1.6473	8.01798	1.90208	7.30389
1200	0.810004	6.16934	0.545046	5.3839	0.334405	4.42077	0.268563	3.6825	0.226497	2.97137	0.181763	2.34213	0.630782	4.99096	0.623778	3.92723	0.638311	2.94048	0.64719	1.9182	0.662483	1.01054	1.22169	7.8394	1.39836	7.36526	1.61746	6.73066
900	0.646891	4.01907	0.4449	3.57422	0.282627	2.93376	0.231696	2.42087	0.196795	1.92646	0.159084	1.4846	0.514628	3.07841	0.515223	2.23129	0.530375	1.43283	0.542197	0.597719	0.557324	-0.10046	0.959387	5.10704	1.10492	4.65325	1.27401	4.10288
303	0.193124	1.82503	0.129132	1.67779	0.07332	1.42119	0.057235	1.16336	0.048302	0.937705	0.034009	0.735623	0.144576	1.47185	0.146569	1.16465	0.157294	0.918794	0.162947	0.643395	0.167134	0.397899	0.308009	2.40667	0.364107	2.28049	0.431187	2.12935
0	0.003935	-0.08075	0.004131	-0.05572	0.004049	-0.07271	0.004393	-0.06565	0.004795	-0.08802	0.000129	-0.08343	0.00456	-0.08643	0.006342	-0.11556	0.00821	-0.07993	0.010899	-0.0664	0.009029	-0.05702	0.000518	-0.09141	0.00707	-0.08751	0.007579	-0.0442

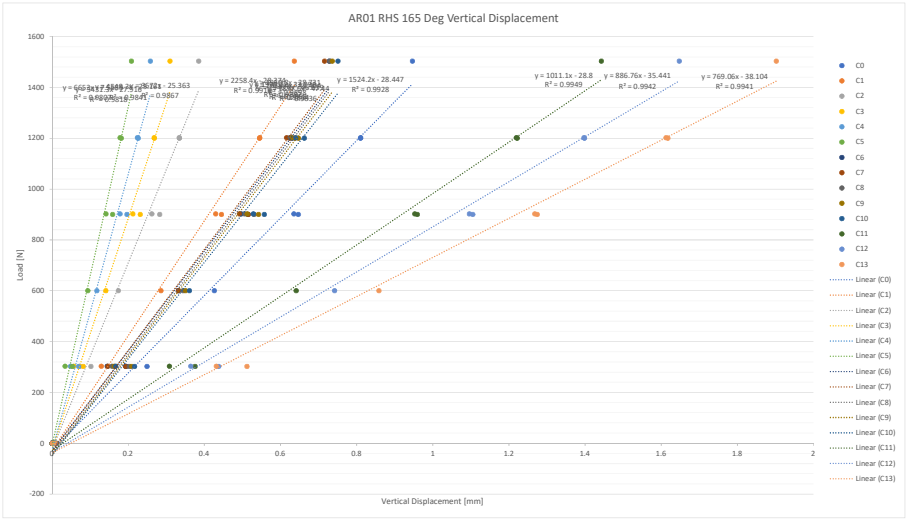

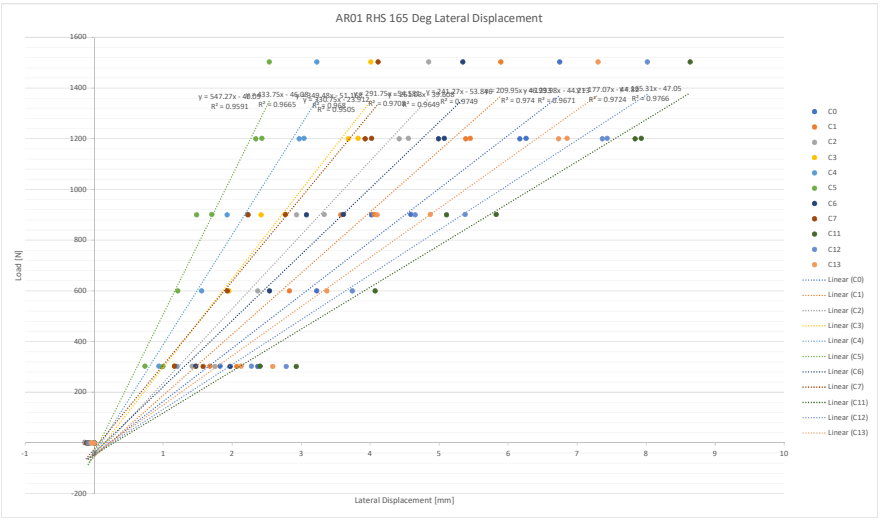

AR01 RHS at 180 Deg

	C0		C1		C2		C3		C4		C5		C6		C7		C8		C9		C10		C11		C12		C13	
Load [N]	V [mm]	W [mm]	V [mm]	W [mm]	V [mm]	W [mm]	V [mm]	W [mm]	V [mm]	W [mm]	V [mm]	W [mm]	V [mm]	W [mm]	V [mm]	W [mm]	V [mm]	W [mm]	V [mm]	W [mm]	V [mm]	W [mm]	V [mm]	W [mm]	V [mm]	W [mm]	V [mm]	W [mm]
0	0	0	0	0	0	0	0	0	0	0	0	0	0	0	0	0	0	0	0	0	0	0	0	0	0	0	0	0
306	0.17697	1.54584	0.10675	1.34609	0.05501	1.10871	0.04365	0.93716	0.03871	0.74872	0.03075	0.55178	0.11798	1.16657	0.11186	0.82365	0.11187	0.5423	0.11892	0.29501	0.12917	0.07332	0.27274	1.89847	0.31573	1.71562	0.37154	1.51668
603	0.41481	3.01471	0.27214	2.64501	0.16423	2.19977	0.1323	1.8394	0.11293	1.46818	0.09218	1.09441	0.30909	2.30113	0.3085	1.70448	0.31508	1.15196	0.3283	0.6242	0.34529	0.14936	0.62803	3.8528	0.72326	3.56872	0.84837	3.29617
900	0.5829	4.81258	0.37665	4.24038	0.21777	3.53458	0.17172	2.96785	0.14315	2.43503	0.11051	1.87928	0.43276	3.84989	0.43116	2.9855	0.44026	2.15036	0.45313	1.43151	0.46936	0.75584	0.88499	6.04552	1.02227	5.71287	1.19622	5.34212
1200	0.75604	4.98293	0.49849	4.35252	0.29839	3.56311	0.24199	2.9522	0.20698	2.35063	0.16447	1.77509	0.56729	3.74261	0.55888	2.72502	0.56849	1.74691	0.57962	0.79856	0.60232	-0.01889	1.14722	6.39952	1.30989	5.97959	1.52365	5.47864
1502	0.93203	6.45809	0.61697	5.64551	0.36965	4.59185	0.29881	3.83555	0.25786	3.08194	0.20363	2.33112	0.69739	4.98943	0.69142	3.72823	0.70035	2.54776	0.71059	1.39324	0.73427	0.34284	1.41793	8.33039	1.62457	7.87365	1.89093	7.3529
1206	0.72378	5.28739	0.47577	4.59655	0.27974	3.76861	0.22697	3.12943	0.19824	2.49576	0.15697	1.88006	0.53409	4.081	0.52766	3.06627	0.5356	2.12627	0.54781	1.22743	0.56675	0.39575	1.10196	6.81427	1.26378	6.44314	1.47354	6.0384
906	0.60604	5.01784	0.39116	4.34342	0.22691	3.59099	0.17843	2.99419	0.15495	2.45337	0.12158	1.88466	0.44977	4.00932	0.44423	3.12876	0.45232	2.32682	0.46737	1.5815	0.49073	0.8752	0.92688	6.38929	1.06892	6.09342	1.2488	5.77502
603	0.40971	3.07892	0.26636	2.64177	0.16078	2.20374	0.13165	1.80812	0.11298	1.45187	0.0901	1.0788	0.30641	2.39434	0.30484	1.7991	0.30969	1.2846	0.32021	0.78041	0.33468	0.28486	0.61416	3.91371	0.70627	3.67005	0.82465	3.43175
303	0.21016	1.91901	0.13023	1.68307	0.07379	1.41566	0.05845	1.17045	0.05121	0.96156	0.03856	0.70265	0.14964	1.51151	0.151	1.16827	0.15798	0.88396	0.16892	0.565	0.18228	0.32749	0.32563	2.43336	0.3758	2.29629	0.44633	2.15256
0	-0.02534	0.24913	-0.03406	0.18326	-0.03019	0.1538	-0.02587	0.12865	-0.02386	0.12782	-0.02121	0.07853	-0.03137	0.22496	-0.03085	0.201	-0.02894	0.18897	-0.02178	0.19185	-0.01669	0.21662	-0.02197	0.3492	-0.01732	0.3448	-0.01046	0.38417

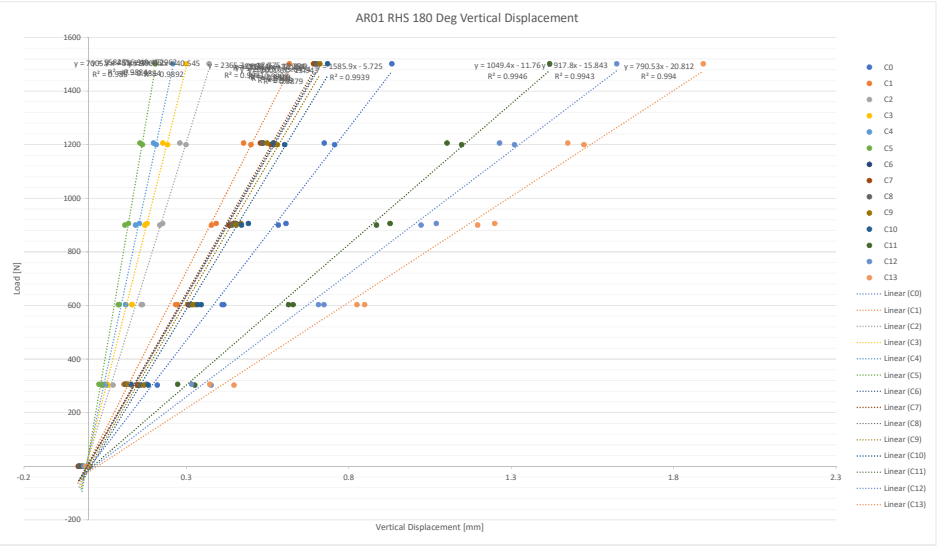

14 Appendix F – Pilot Test Results

Test 1

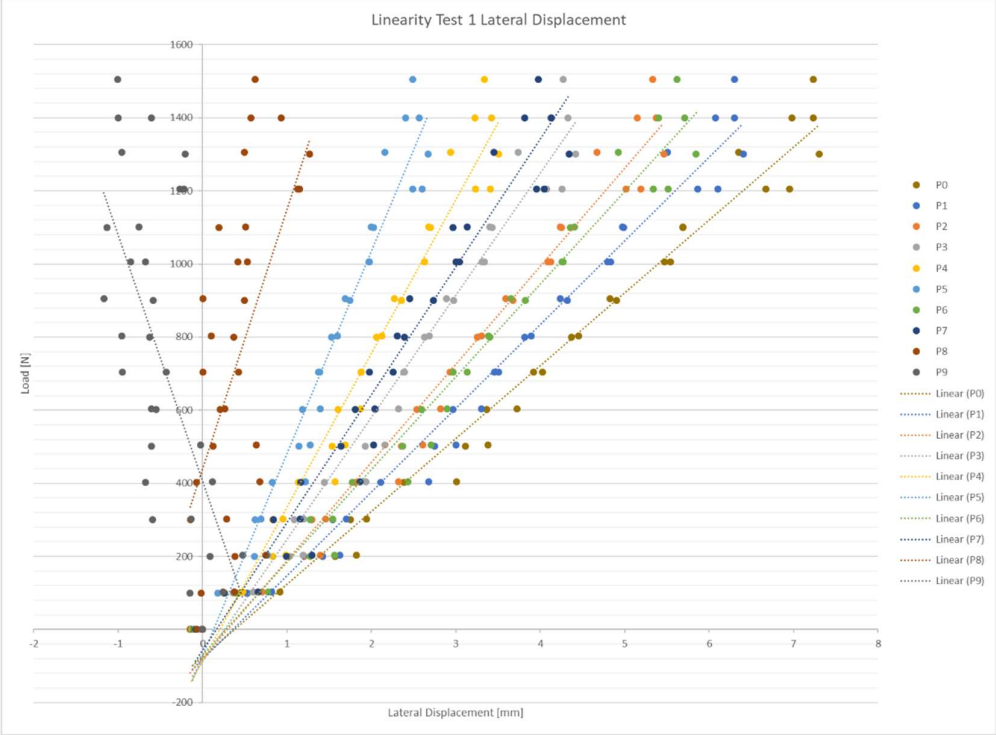

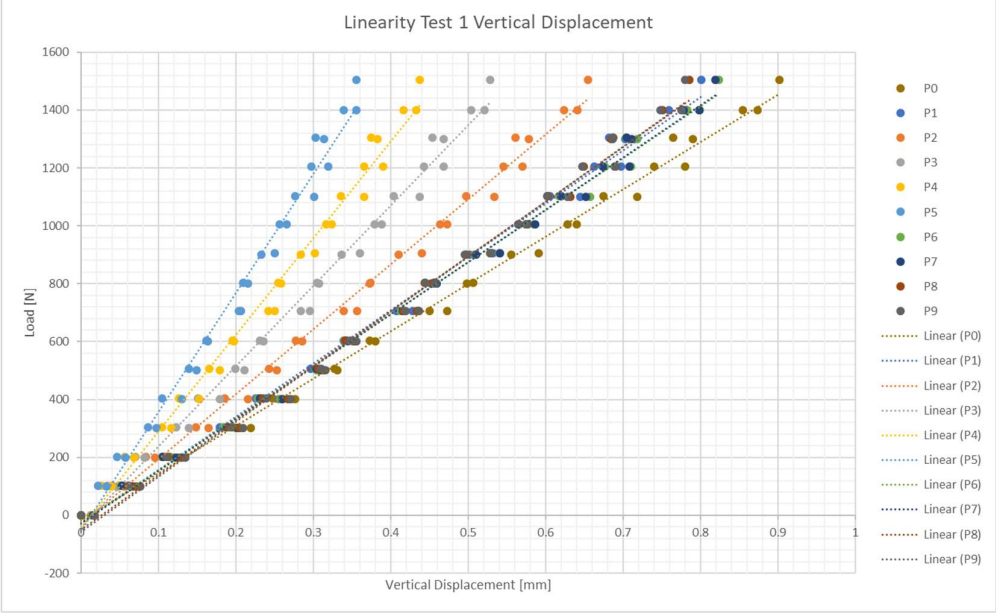

Data Point	Vertical Displacement R^2	Lateral Displacement R^2
0	0.9957	0.98
1	0.9948	0.9775
2	0.9938	0.9749
3	0.9916	0.9694
4	0.9889	0.963
5	0.9857	0.9549
6	0.9958	0.9722
7	0.9955	0.9508
8	0.9937	0.3385
9	0.993	0.416

Test 2

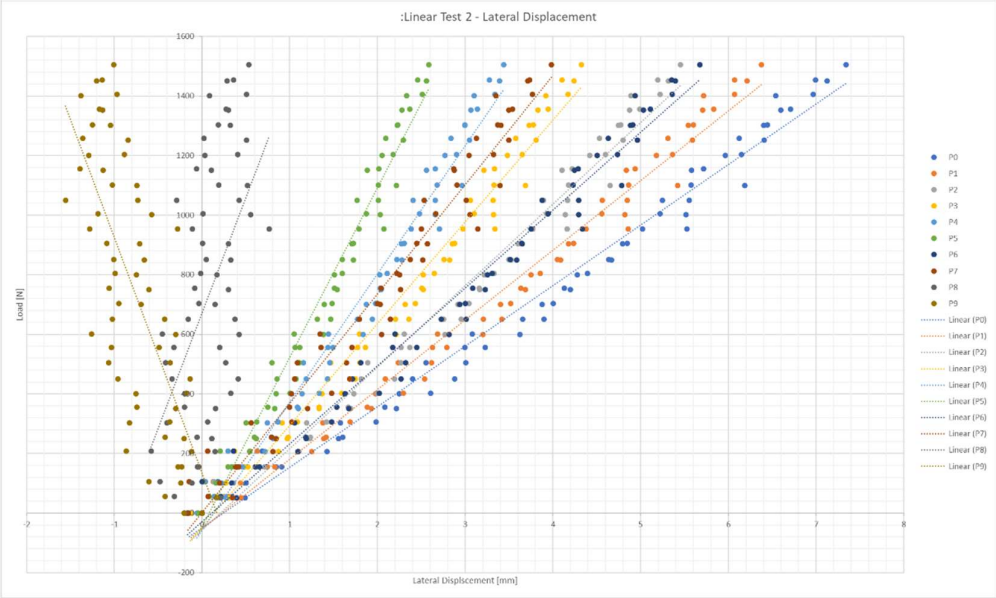

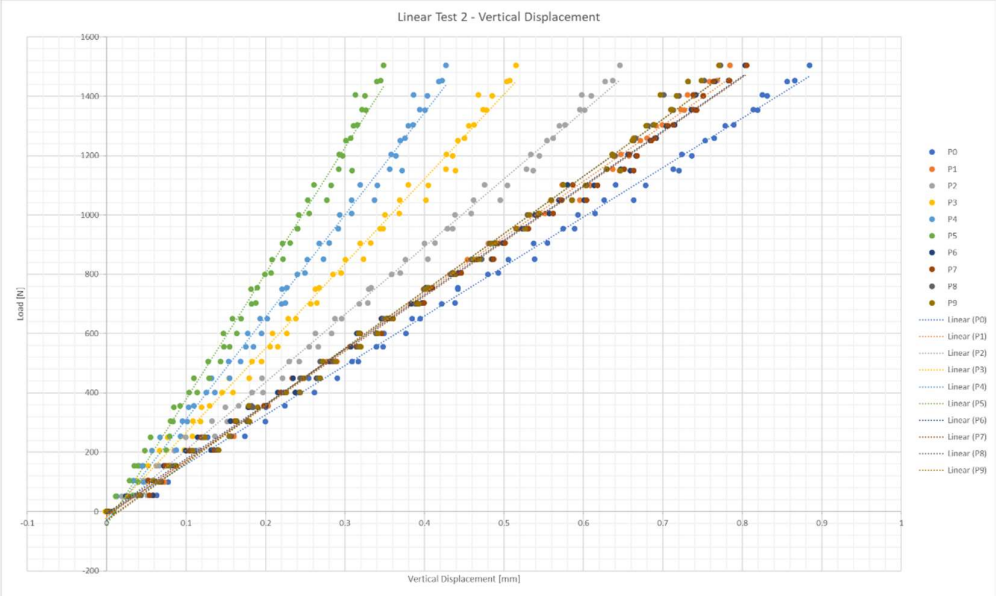

Data Point	Vertical Displacement R^2	Lateral Displacement R^2
0	0.9974	0.9839
1	0.9969	0.9823
2	0.9962	0.9805
3	0.9945	0.9774
4	0.9929	0.9733
5	0.9908	0.9694
6	0.9971	0.9782
7	0.9971	0.9613
8	0.9962	0.2669
9	0.9958	0.5381

Test 3

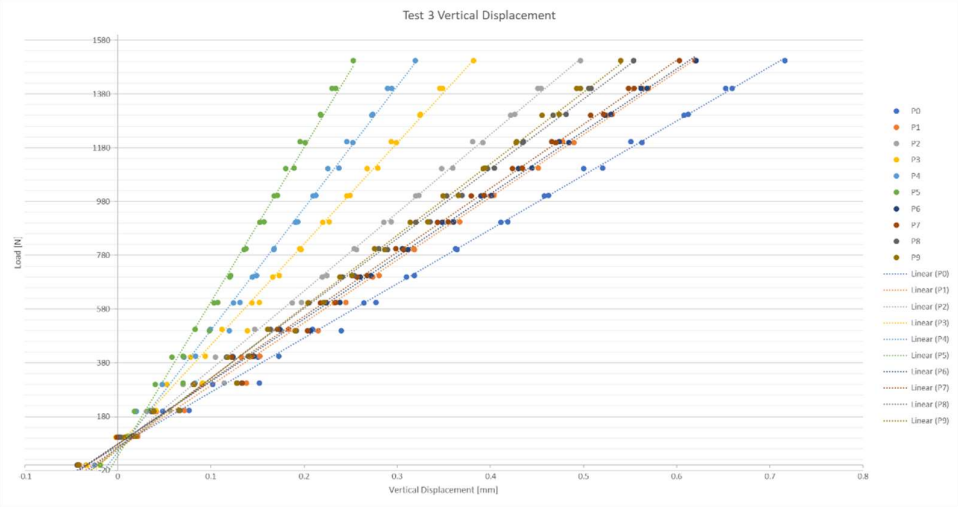

Data Point	Vertical Displacement R^2	Lateral Displacement R^2
0	0.9974	0.9887
1	0.9963	0.9874
2	0.9954	0.9864
3	0.9934	0.9844
4	0.9924	0.983
5	0.99	0.982
6	0.9964	0.9879
7	0.9961	0.9847
8	0.9953	0.88
9	0.9948	0.0628

Test 4

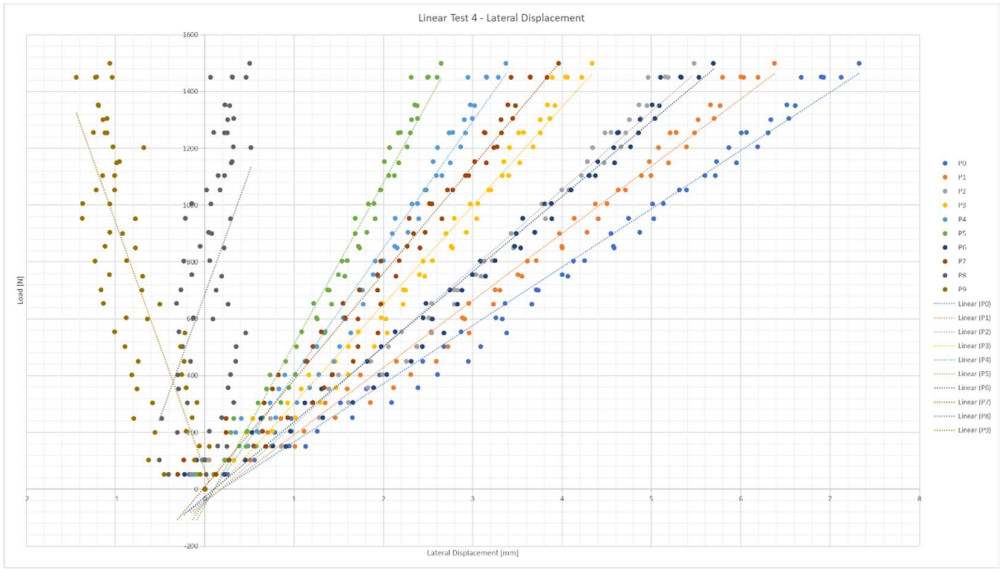
Linear Test 4 - Lateral Displacement
Load [N]
Lateral Displacement [mm]

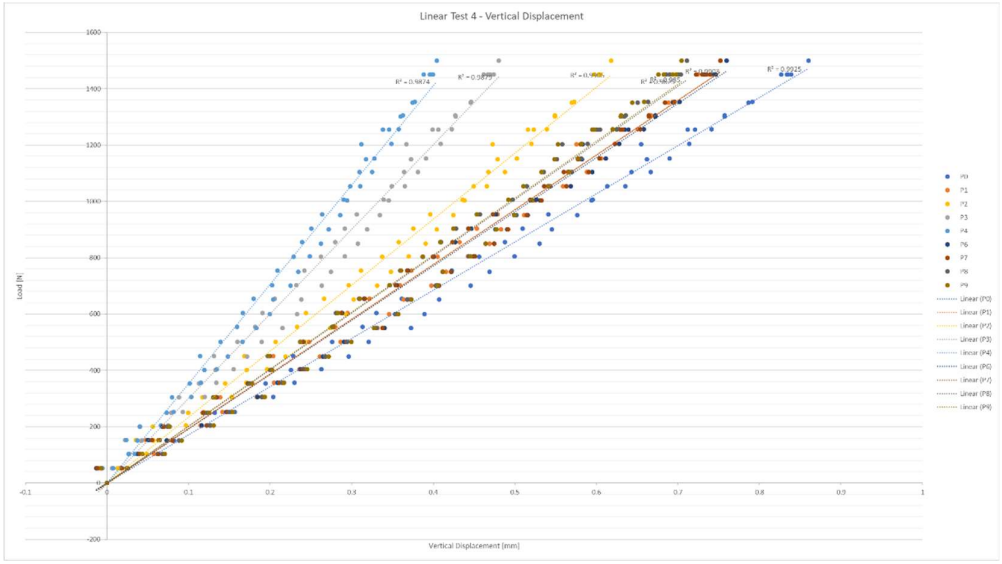
Linear Test 4 - Vertical Displacement
Load [N]
Vertical Displacement [mm]

Data Point	Vertical Displacement R^2	Lateral Displacement R^2
0	0.9755	0.9638
1	0.9751	0.9626
2	0.9733	0.9611
3	0.9707	0.9565
4	0.9706	0.9507
5	0.97	0.9484
6	0.9732	0.9586
7	0.9716	0.941
8	0.9678	0.2239
9	0.9654	0.6543

15 Appendix G – Displacement Maps

Below show the displacement maps for all tests.

CA01 LHS at 90^{O}

Load [N]	Lateral Displacement	W [mm]	Vertical Displacement	V [mm]
0	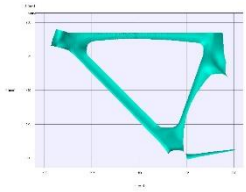	9 7.99375 6.9875 5.98125 4.975 3.96875 2.9625 1.95625 0.95 -0.0562496 -1.0625 -2.06875 -3.075 -4.08125 -5.0875 -6.09375 -7.1	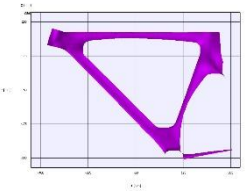	2 1.875 1.75 1.625 1.5 1.375 1.25 1.125 1 0.875 0.75 0.625 0.5 0.375 0.25 0.125 0
300	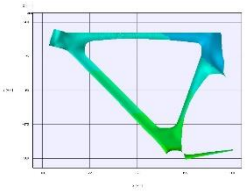		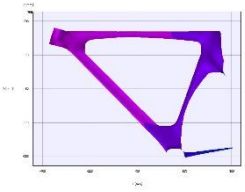	
600	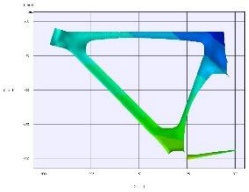		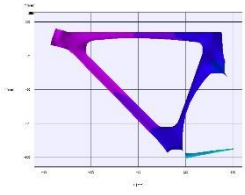	
900	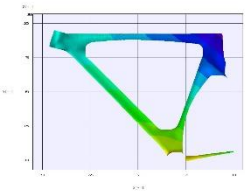		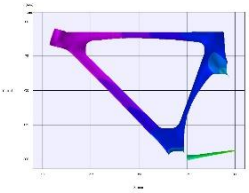	
1200	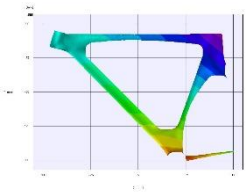		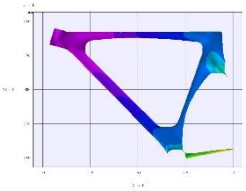	
1500	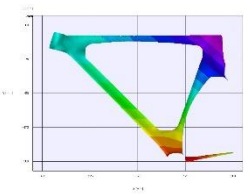		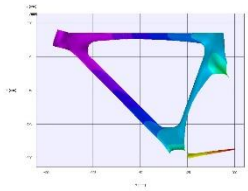	

CA01 LHS at 105^{O}

Load [N]	Lateral Displacement	W [mm]	Vertical Displacement	V [mm]
0	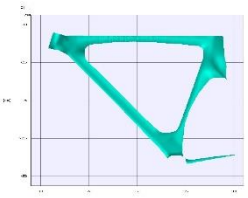	9 7.99375 6.9875 5.98125 4.975 3.96875 2.9625 1.95625 0.95 -0.0562496 -1.0625 -2.06875 -3.075 -4.08125 -5.0875 -6.09375 -7.1	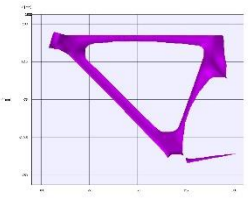	2 1.875 1.75 1.625 1.5 1.375 1.25 1.125 1 0.875 0.75 0.625 0.5 0.375 0.25 0.125 0
300	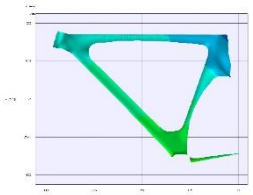		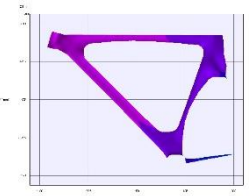	
600	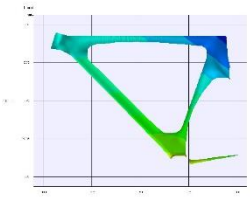		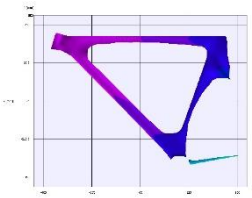	
900	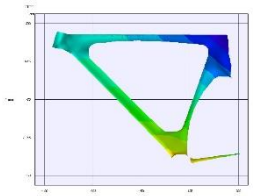		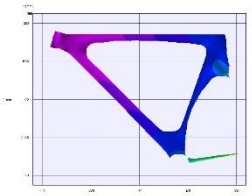	
1200	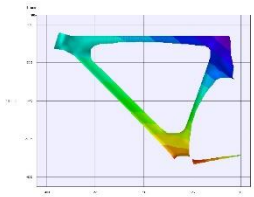		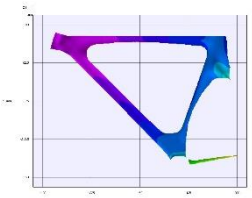	
1500	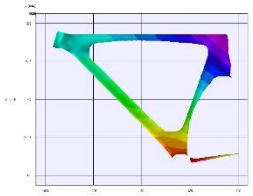		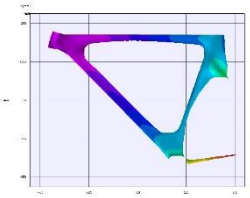	

CA01 LHS at 120^{O}

Load [N]	Lateral Displacement	W [mm]	Vertical Displacement	V [mm]
0	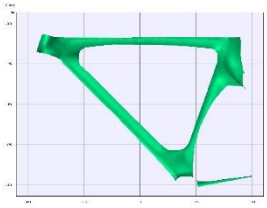	9 7.99375 6.9875 5.98125 4.975 3.96875 2.9625 1.95625 0.95 -0.0562496 -1.0625 -2.06875 -3.075 -4.08125 -5.0875 -6.09375 -7.1		2 1.875 1.75 1.625 1.5 1.375 1.25 1.125 1 0.875 0.75 0.625 0.5 0.375 0.25 0.125 0
300	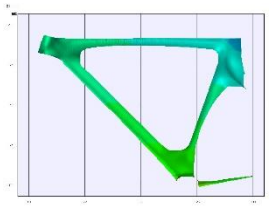		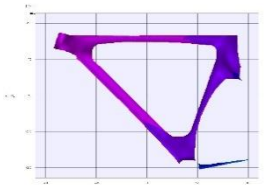	
600	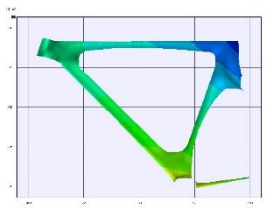		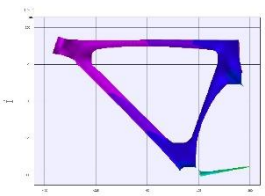	
900	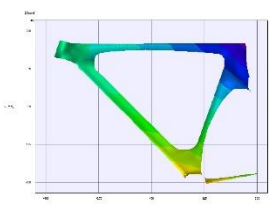		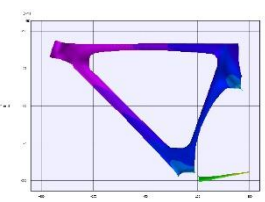	
1200	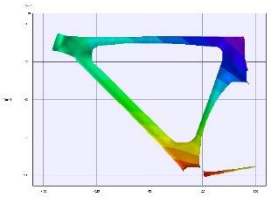		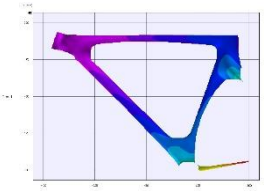	
1500	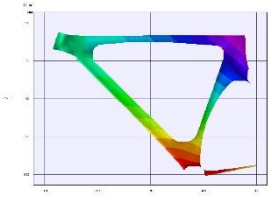		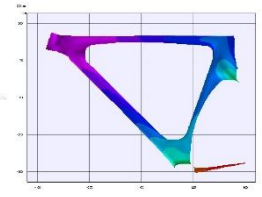	

CA01 LHS at 135^{O}

Load [N]	Lateral Displacement	W [mm]	Vertical Displacement	V [mm]
0	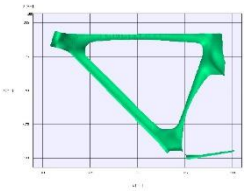	9 7.99375 6.9875 5.98125 4.975 3.96875 2.9625 1.95625 0.95 -0.0562496 -1.0625 -2.06875 -3.075 -4.08125 -5.0875 -6.09375 -7.1	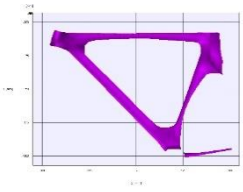	2 1.875 1.75 1.625 1.5 1.375 1.25 1.125 1 0.875 0.75 0.625 0.5 0.375 0.25 0.125 0
300	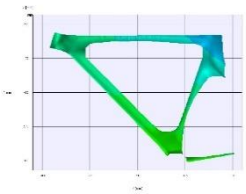		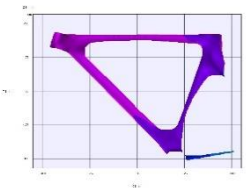	
600	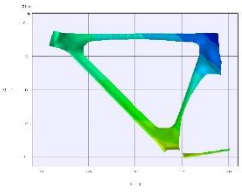		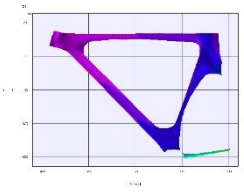	
900	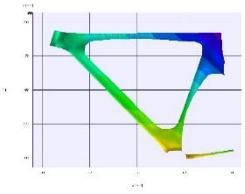		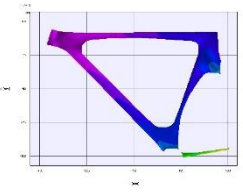	
1200	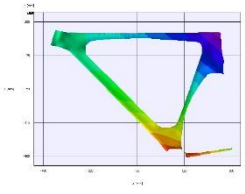		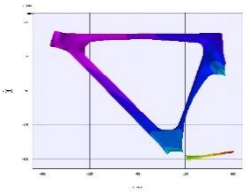	
1500	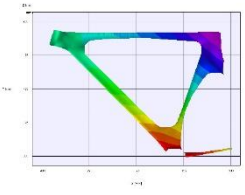		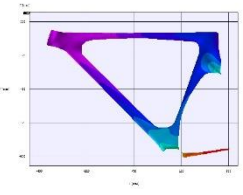	

CA01 LHS at 150^{O}

Load [N]	Lateral Displacement	W [mm]	Vertical Displacement	V [mm]
0	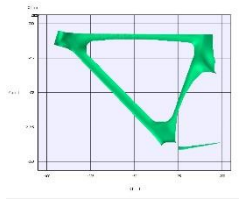	9 7.99375 6.9875 5.98125 4.975 3.96875 2.9625 1.95625 0.95 -0.0562496 -1.0625 -2.06875 -3.075 -4.08125 -5.0875 -6.09375 -7.1	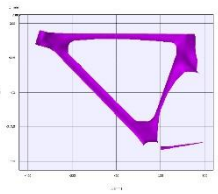	2 1.875 1.75 1.625 1.5 1.375 1.25 1.125 1 0.875 0.75 0.625 0.5 0.375 0.25 0.125 0
300	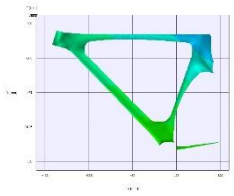		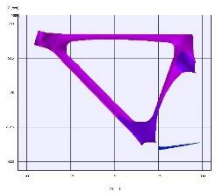	
600	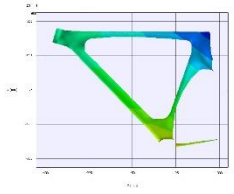		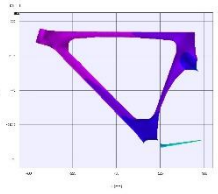	
900	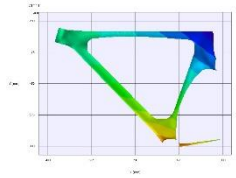		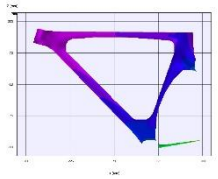	
1200	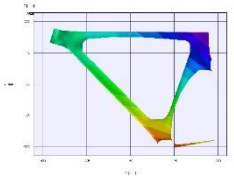		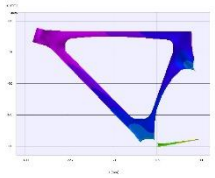	
1500	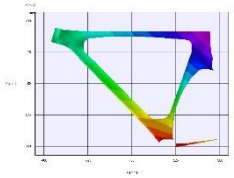		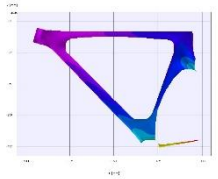	

CA01 LHS at 165^{O}

Load [N]	Lateral Displacement	W [mm]	Vertical Displacement	V [mm]
0	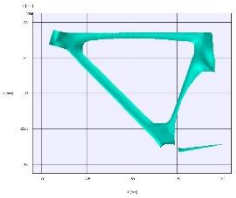	9 7.99375 6.9875 5.98125 4.975 3.96875 2.9625 1.95625 0.95 -0.0562496 -1.0625 -2.06875 -3.075 -4.08125 -5.0875 -6.09375 -7.1	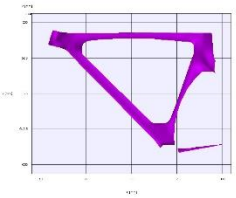	2 1.875 1.75 1.625 1.5 1.375 1.25 1.125 1 0.875 0.75 0.625 0.5 0.375 0.25 0.125 0
300	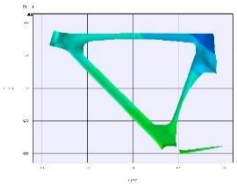		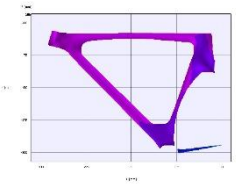	
600	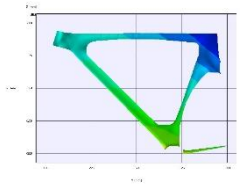		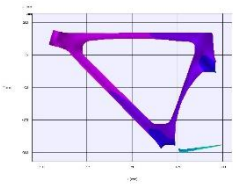	
900	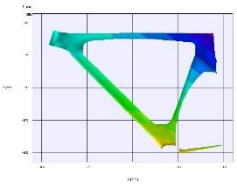		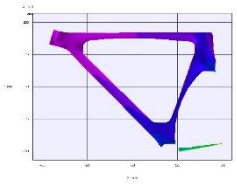	
1200	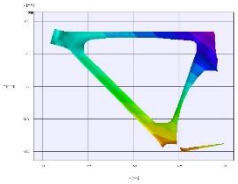		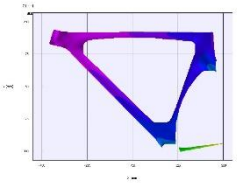	
1500	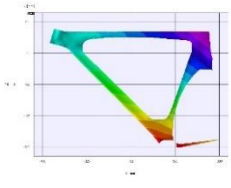		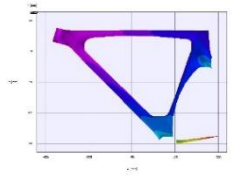	

CA01 LHS at 180^{O}

Load [N]	Lateral Displacement	W [mm]	Vertical Displacement	V [mm]
0	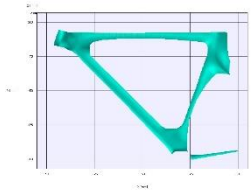	9 7.99375 6.9875 5.98125 4.975 3.96875 2.9625 1.95625 0.95 -0.0562496 -1.0625 -2.06875 -3.075 -4.08125 -5.0875 -6.09375 -7.1	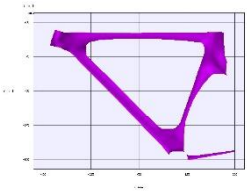	2 1.875 1.75 1.625 1.5 1.375 1.25 1.125 1 0.875 0.75 0.625 0.5 0.375 0.25 0.125 0
300	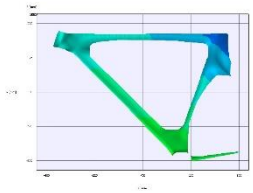		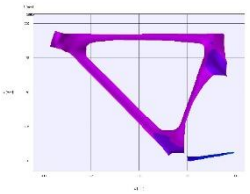	
600	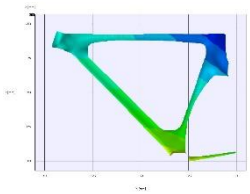		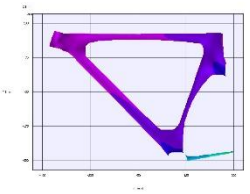	
900	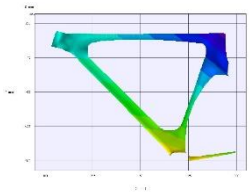		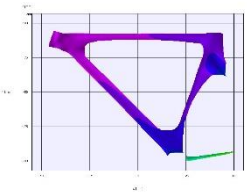	
1200	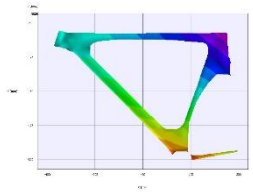		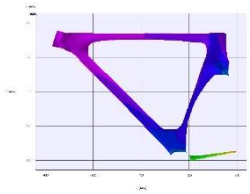	
1500	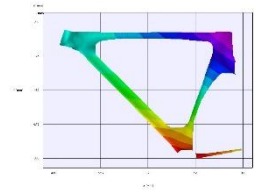		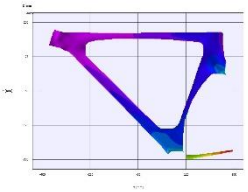	

CA01 RHS at 90^{O}

Load [N]	Lateral Displacement	W [mm]	Vertical Displacement	V [mm]
0	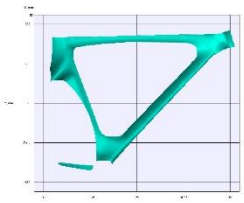	9.76 8.71875 7.6775 6.63625 5.595 4.55375 3.5125 2.47125 1.43 0.38875 -0.6525 -1.69375 -2.735 -3.77625 -4.8175 -5.85875 -6.9	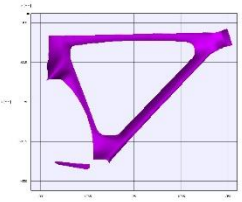	2 1.875 1.75 1.625 1.5 1.375 1.25 1.125 1 0.875 0.75 0.625 0.5 0.375 0.25 0.125 0
300	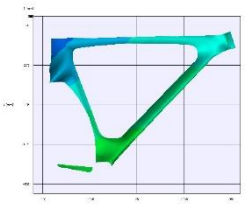		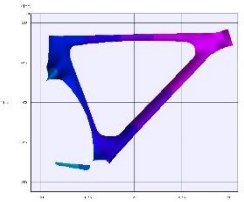	
600	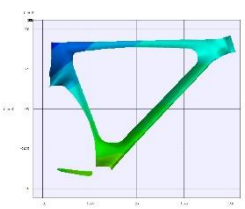		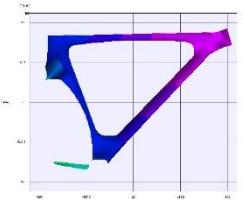	
900	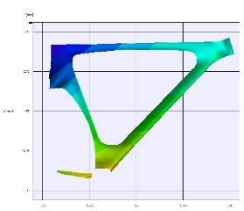		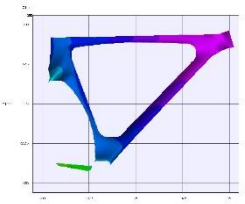	
1200	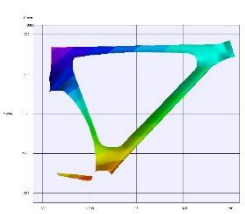		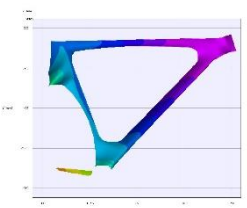	
1500	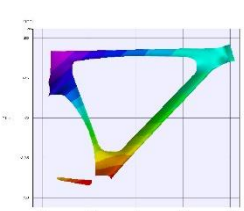		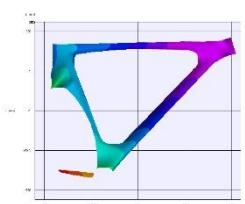	

CA01 RHS at 105^{O}

Load [N]	Lateral Displacement	W [mm]	Vertical Displacement	V [mm]
0	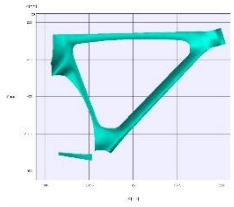	9.76 8.71875 7.6775 6.63625 5.595 4.55375 3.5125 2.47125 1.43 0.38875 -0.6525 -1.69375 -2.735 -3.77625 -4.8175 -5.85875 -6.9	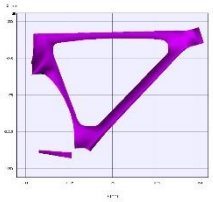	2 1.875 1.75 1.625 1.5 1.375 1.25 1.125 1 0.875 0.75 0.625 0.5 0.375 0.25 0.125 0
300	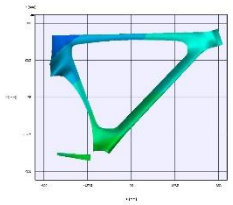		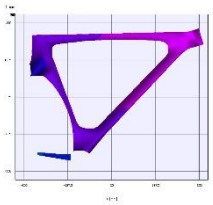	
600	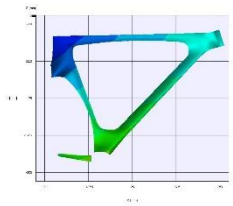		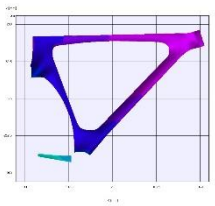	
900	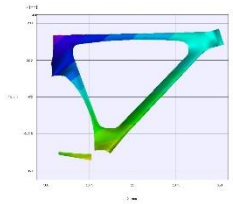		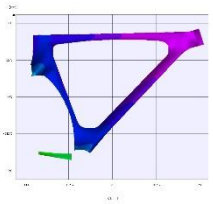	
1200	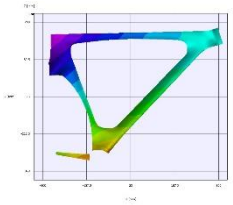		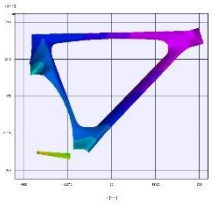	
1500	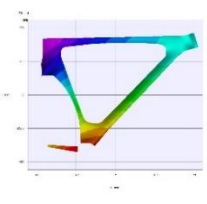		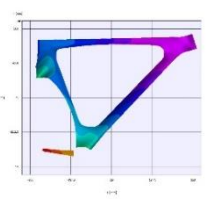	

CA01 RHS at 120^{O}

Load [N]	Lateral Displacement	W [mm]	Vertical Displacement	V [mm]
0	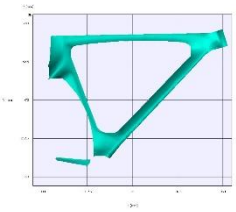	9.76 8.71875 7.6775 6.63625 5.595 4.55375 3.5125 2.47125 1.43 0.38875 -0.6525 -1.69375 -2.735 -3.77625 -4.8175 -5.85875 -6.9	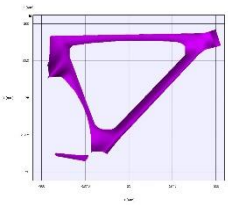	2 1.875 1.75 1.625 1.5 1.375 1.25 1.125 1 0.875 0.75 0.625 0.5 0.375 0.25 0.125 0
300	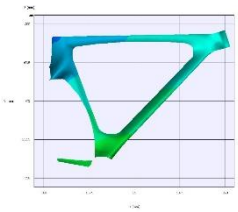		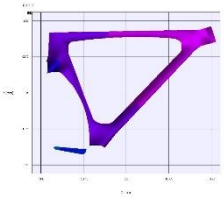	
600	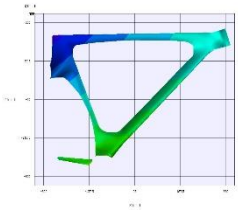		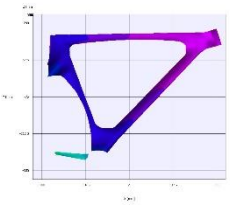	
900	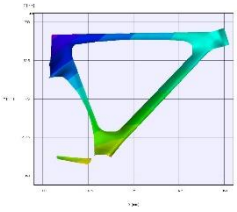		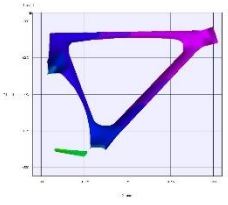	
1200	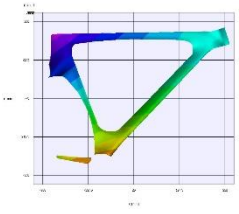		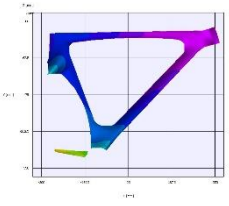	
1500	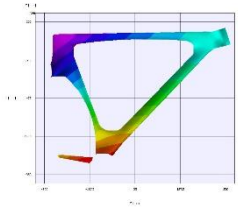		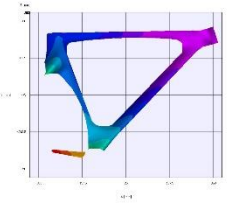	

CA01 RHS at 135^{O}

Load [N]	Lateral Displacement	W [mm]	Vertical Displacement	V [mm]
0	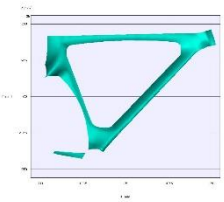	9.76 8.71875 7.6775 6.63625 5.595 4.55375 3.5125 2.47125 1.43 0.38875 -0.6525 -1.69375 -2.735 -3.77625 -4.8175 -5.85875 -6.9	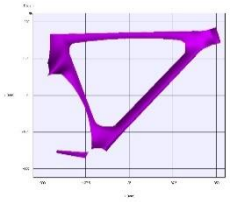	2 1.875 1.75 1.625 1.5 1.375 1.25 1.125 1 0.875 0.75 0.625 0.5 0.375 0.25 0.125 0
300	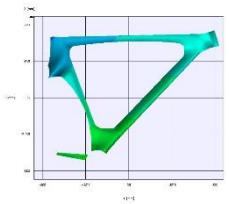		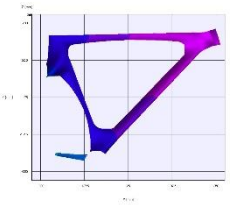	
600	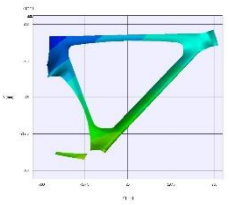		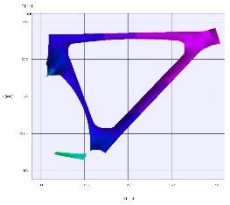	
900	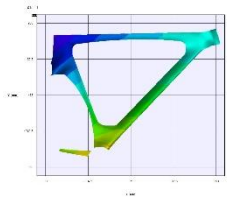		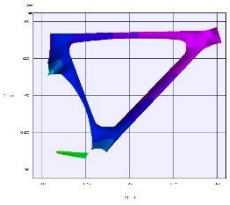	
1200	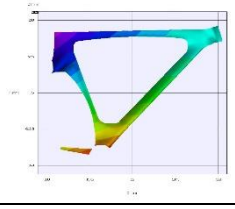		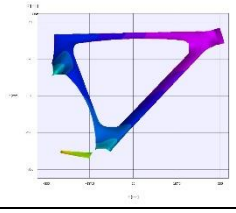	
1500	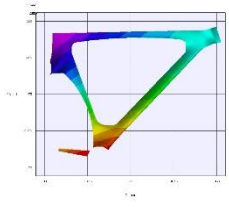		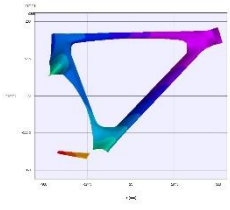	

CA01 RHS at 150^{O}

Load [N]	Lateral Displacement	W [mm]	Vertical Displacement	V [mm]
0	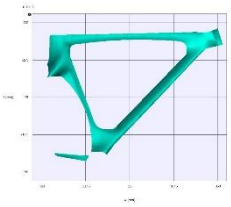	9.76 8.71875 7.6775 6.63625 5.595 4.55375 3.5125 2.47125 1.43 0.38875 -0.6525 -1.69375 -2.735 -3.77625 -4.8175 -5.85875 -6.9	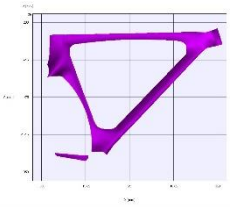	2 1.875 1.75 1.625 1.5 1.375 1.25 1.125 1 0.875 0.75 0.625 0.5 0.375 0.25 0.125 0
300	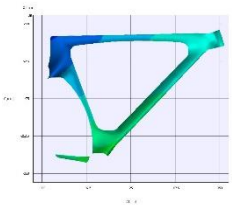		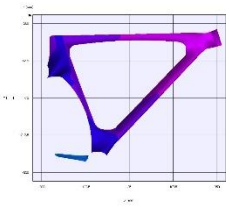	
600	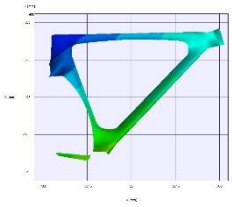		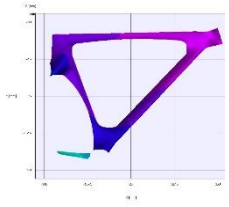	
900	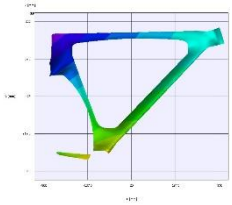		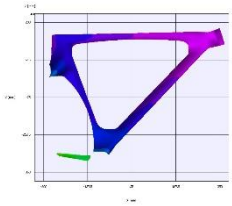	
1200	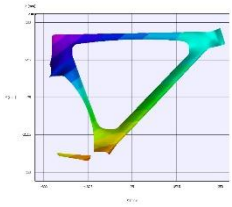		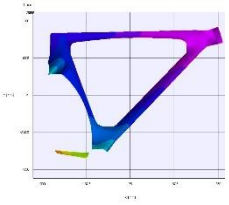	
1500	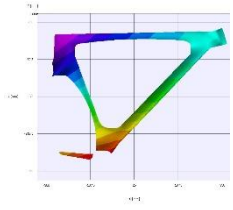		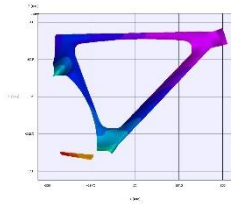	

CA01 RHS at 165^{O}

Load [N]	Lateral Displacement	W [mm]	Vertical Displacement	V [mm]
0	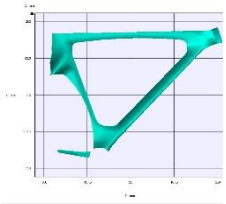	9.76 8.71875 7.6775 6.63625 5.595 4.55375 3.5125 2.47125 1.43 0.38875 -0.6525 -1.69375 -2.735 -3.77625 -4.8175 -5.85875 -6.9	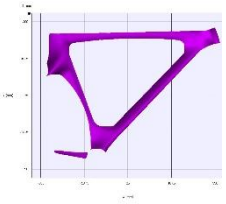	2 1.875 1.75 1.625 1.5 1.375 1.25 1.125 1 0.875 0.75 0.625 0.5 0.375 0.25 0.125 0
300	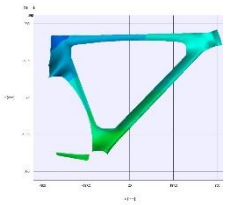		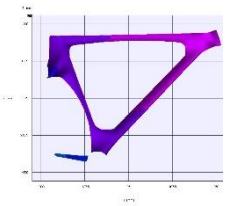	
600	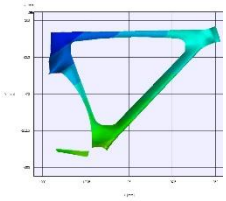		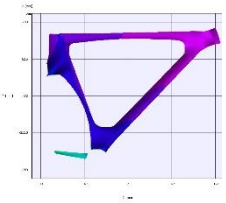	
900	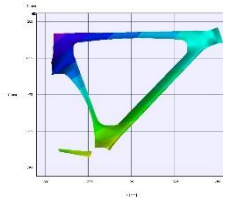		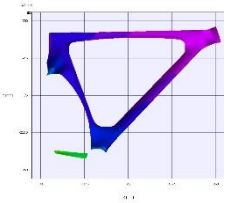	
1200	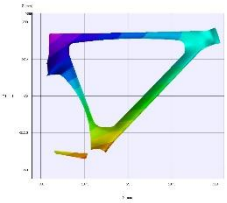		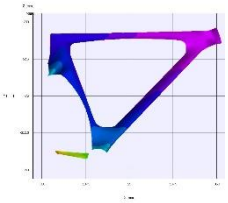	
1500	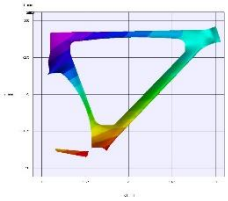		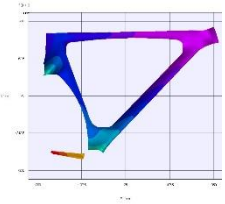	

CA01 RHS at 180^{O}

Load [N]	Lateral Displacement	W [mm]	Vertical Displacement	V [mm]
0	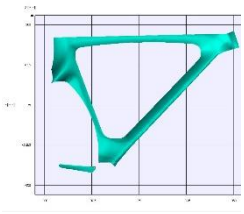	9.76 8.71875 7.6775 6.63625 5.595 4.55375 3.5125 2.47125 1.43 0.38875 -0.6525 -1.69375 -2.735 -3.77625 -4.8175 -5.85875 -6.9	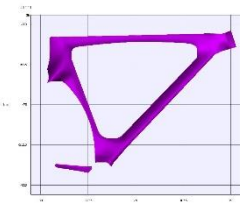	2 1.875 1.75 1.625 1.5 1.375 1.25 1.125 1 0.875 0.75 0.625 0.5 0.375 0.25 0.125 0
300	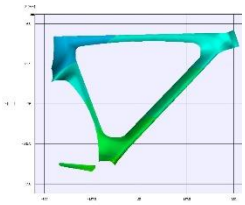		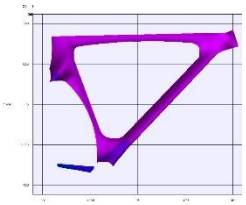	
600	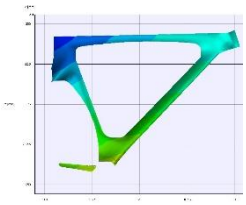		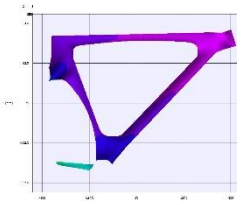	
900	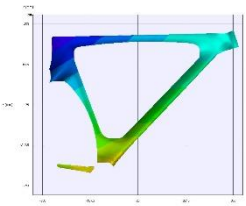		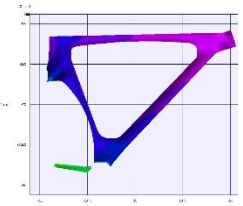	
1200	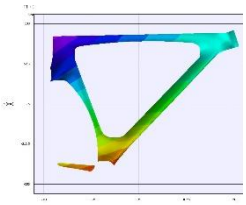		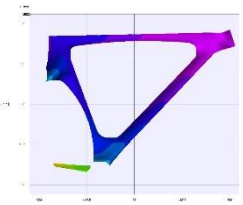	
1500	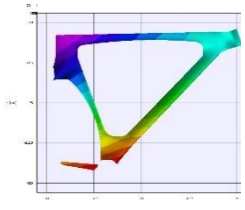		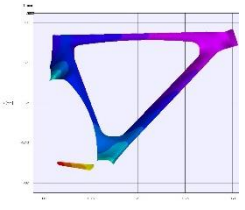	

CA02 RHS at 90^{O}

Load [N]	Lateral Displacement	W [mm]	Vertical Displacement	V [mm]
0	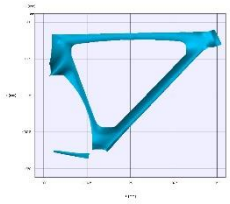	10.4 9.38125 8.3625 7.34375 6.325 5.30625 4.2875 3.26875 2.25 1.23125 0.2125 -0.80625 -1.825 -2.84375 -3.8625 -4.88125 -5.9	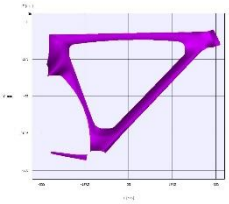	2 1.875 1.75 1.625 1.5 1.375 1.25 1.125 1 0.875 0.75 0.625 0.5 0.375 0.25 0.125 0
300	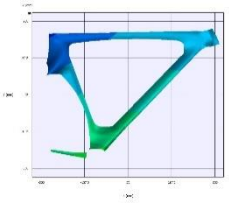		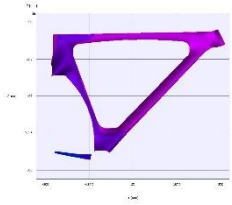	
600	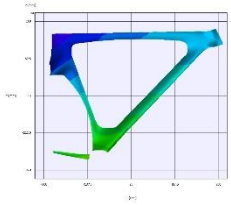		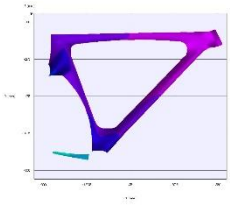	
900	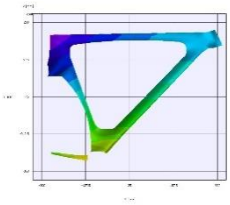		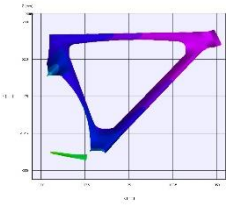	
1200	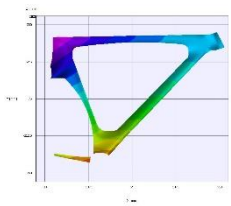		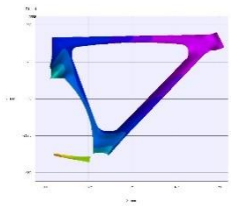	
1500	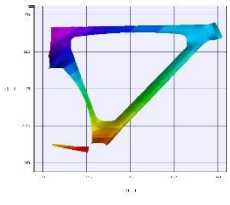		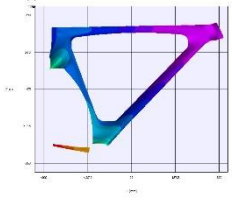	

CA02 RHS at 105^{O}

Load [N]	Lateral Displacement	W [mm]	Vertical Displacement	V [mm]
0	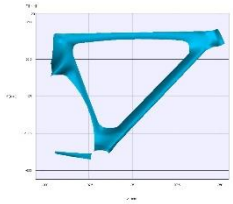	10.4 9.38125 8.3625 7.34375 6.325 5.30625 4.2875 3.26875 2.25 1.23125 0.2125 -0.80625 -1.825 -2.84375 -3.8625 -4.88125 -5.9	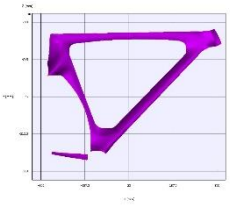	2 1.875 1.75 1.625 1.5 1.375 1.25 1.125 1 0.875 0.75 0.625 0.5 0.375 0.25 0.125 0
300	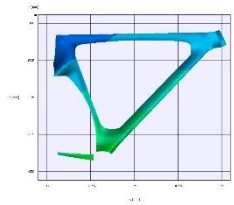		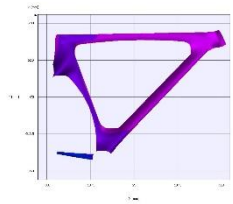	
600	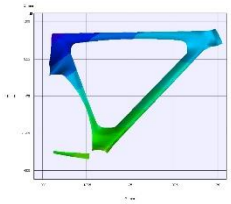		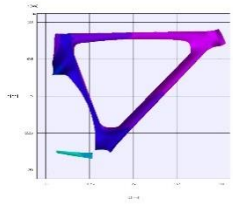	
900	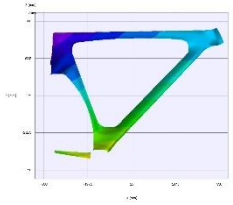		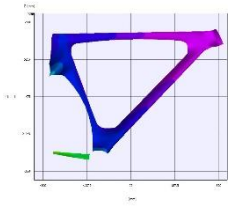	
1200	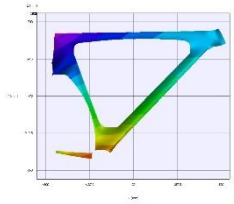		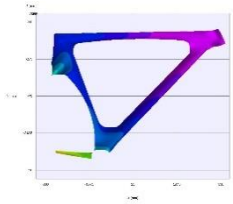	
1500	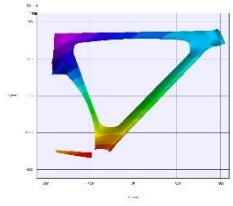		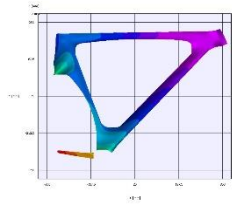	

CA02 RHS at 120^{O}

Load [N]	Lateral Displacement	W [mm]	Vertical Displacement	V [mm]
0	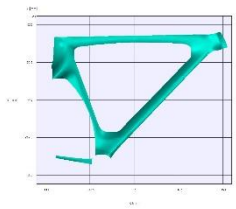	10.4 9.38125 8.3625 7.34375 6.325 5.30625 4.2875 3.26875 2.25 1.23125 0.2125 -0.80625 -1.825 -2.84375 -3.8625 -4.88125 -5.9	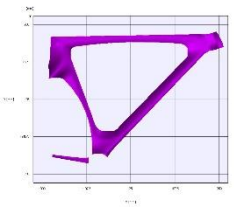	2 1.875 1.75 1.625 1.5 1.375 1.25 1.125 1 0.875 0.75 0.625 0.5 0.375 0.25 0.125 0
300	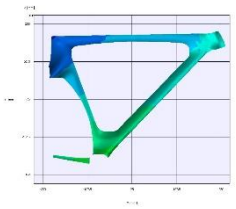		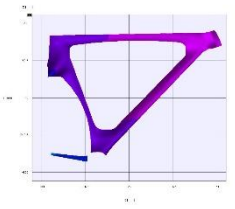	
600	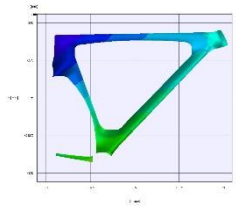		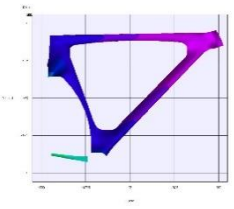	
900	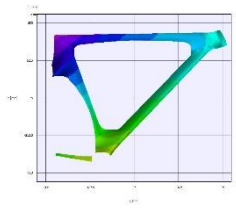		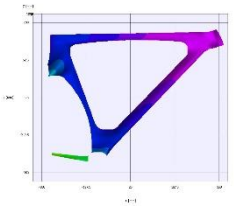	
1200	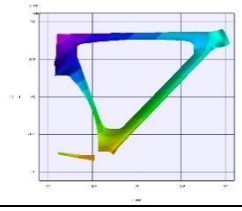		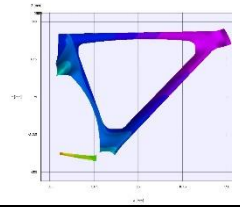	
1500	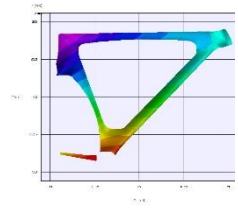		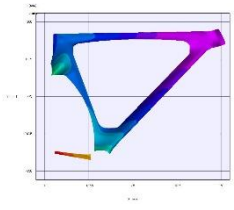	

CA02 RHS at 135^{O}

Load [N]	Lateral Displacement	W [mm]	Vertical Displacement	V [mm]
0	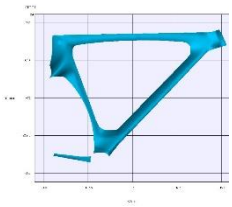	10.4 9.38125 8.3625 7.34375 6.325 5.30625 4.2875 3.26875 2.25 1.23125 0.2125 -0.80625 -1.825 -2.84375 -3.8625 -4.88125 -5.9	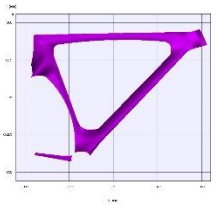	2 1.875 1.75 1.625 1.5 1.375 1.25 1.125 1 0.875 0.75 0.625 0.5 0.375 0.25 0.125 0
300	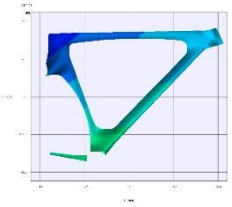		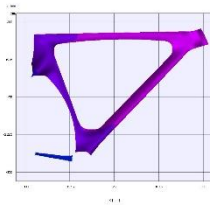	
600	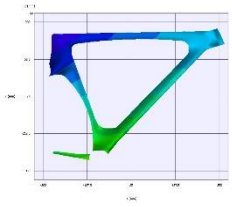		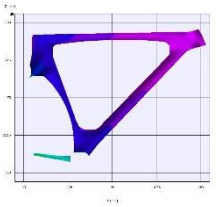	
900	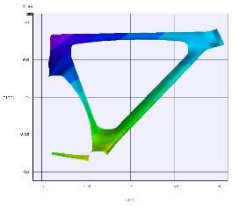		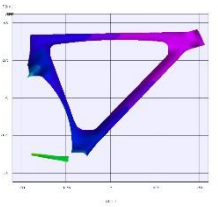	
1200	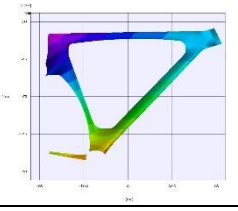		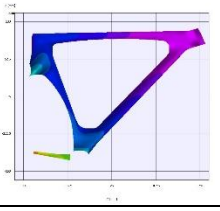	
1500	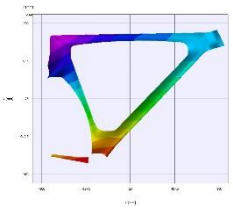		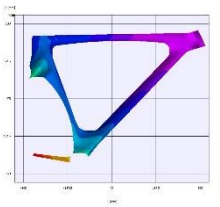	

CA02 RHS at 150^{o}

Load [N]	Lateral Displacement	W [mm]	Vertical Displacement	V [mm]
0	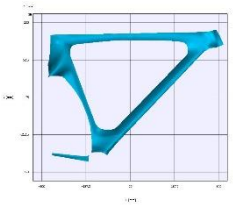	10.4 9.38125 8.3625 7.34375 6.325 5.30625 4.2875 3.26875 2.25 1.23125 0.2125 -0.80625 -1.825 -2.84375 -3.8625 -4.88125 -5.9	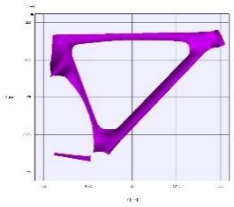	2 1.875 1.75 1.625 1.5 1.375 1.25 1.125 1 0.875 0.75 0.625 0.5 0.375 0.25 0.125 0
300	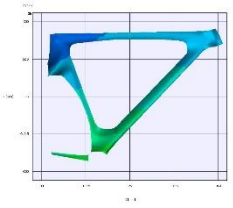		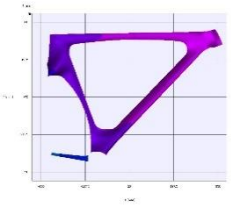	
600	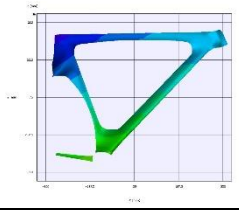		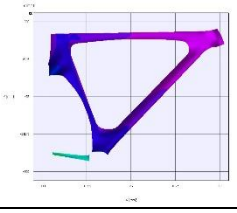	
900	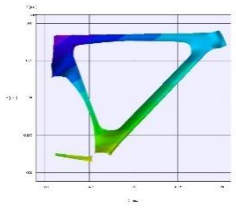		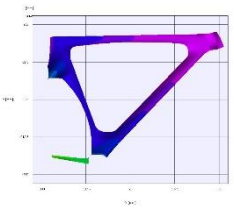	
1200	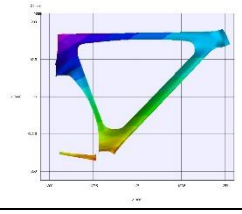		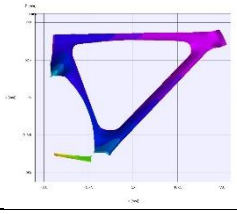	
1500	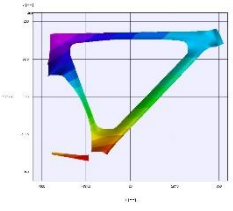		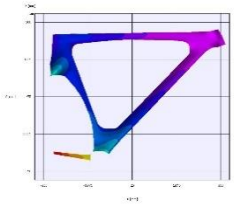	

CA02 RHS at 165^{O}

Load [N]	Lateral Displacement	W [mm]	Vertical Displacement	V [mm]
0	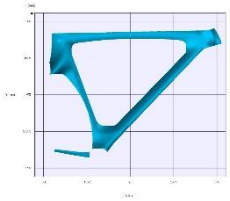	10.4 9.38125 8.3625 7.34375 6.325 5.30625 4.2875 3.26875 2.25 1.23125 0.2125 -0.80625 -1.825 -2.84375 -3.8625 -4.88125 -5.9	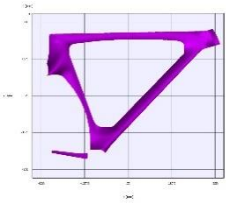	2 1.875 1.75 1.625 1.5 1.375 1.25 1.125 1 0.875 0.75 0.625 0.5 0.375 0.25 0.125 0
300	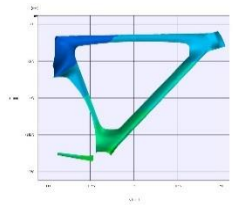		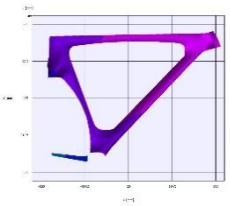	
600	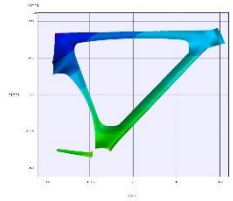		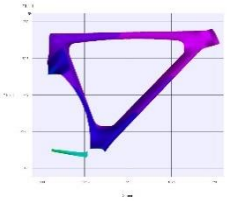	
900	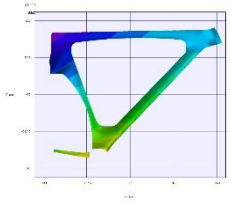		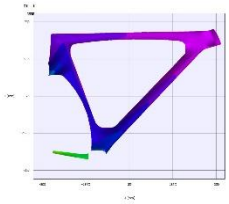	
1200	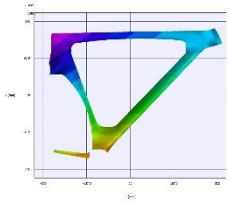		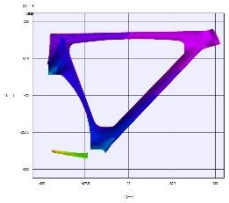	
1500	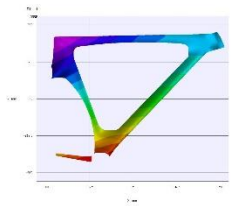		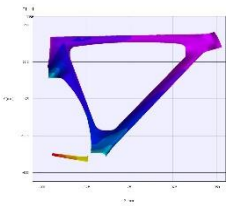	

CA02 RHS at 180^{O}

Load [N]	Lateral Displacement	W [mm]	Vertical Displacement	V [mm]
0	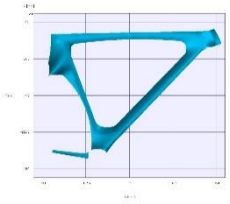	10.4 9.38125 8.3625 7.34375 6.325 5.30625 4.2875 3.26875 2.25 1.23125 0.2125 -0.80625 -1.825 -2.84375 -3.8625 -4.88125 -5.9	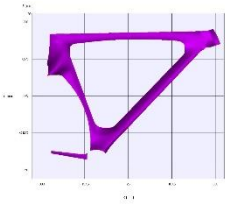	2 1.875 1.75 1.625 1.5 1.375 1.25 1.125 1 0.875 0.75 0.625 0.5 0.375 0.25 0.125 0
300	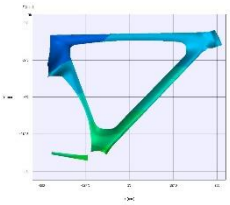		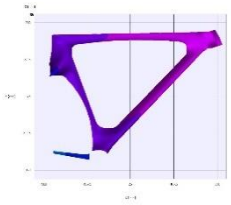	
600	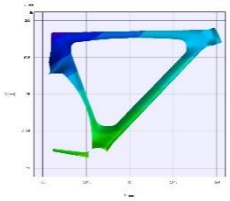		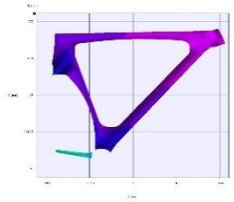	
900	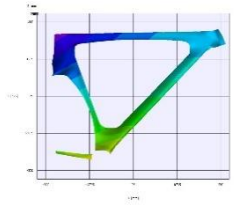		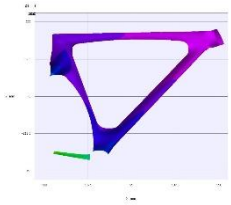	
1200	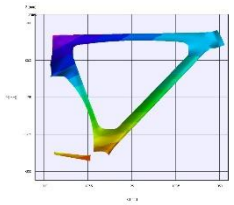		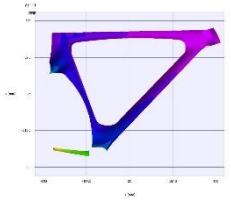	
1500	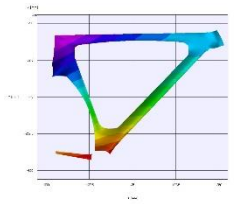		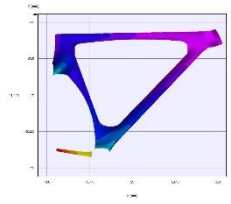	

AR01 RHS at 90^{O}

Load [N]	Lateral Displacement	W [mm]	Vertical Displacement	V [mm]
0	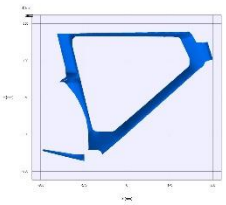	8.6 7.84063 7.08125 6.32188 5.5625 4.80313 4.04375 3.28438 2.525 1.76563 1.00625 0.246875 -0.5125 -1.27187 -2.03125 -2.79062 -3.55	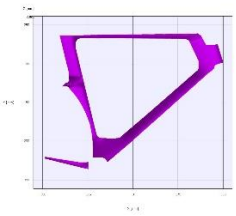	2 1.875 1.75 1.625 1.5 1.375 1.25 1.125 1 0.875 0.75 0.625 0.5 0.375 0.25 0.125 0
300	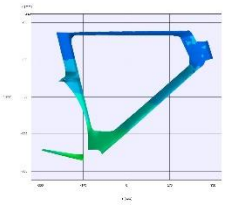		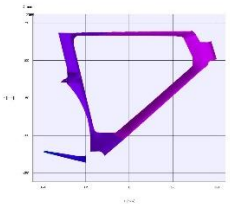	
600	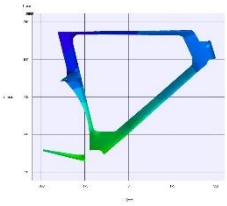		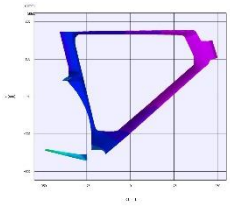	
900	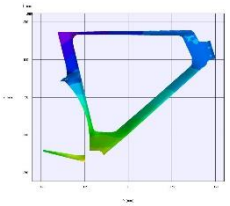		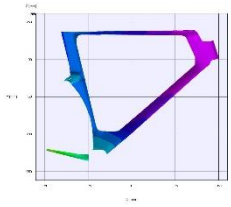	
1200	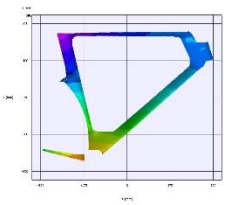		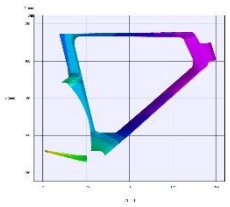	
1500	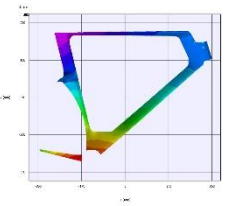		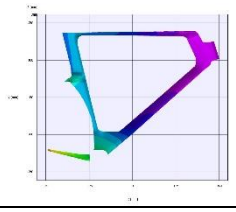	

AR01 RHS at 105^{O}

Load [N]	Lateral Displacement	W [mm]	Vertical Displacement	V [mm]
0	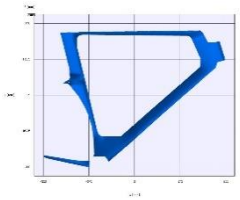	8.6 7.84063 7.08125 6.32188 5.5625 4.80313 4.04375 3.28438 2.525 1.76563 1.00625 0.246875 -0.5125 -1.27187 -2.03125 -2.79062 -3.55	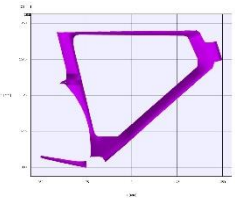	2 1.875 1.75 1.625 1.5 1.375 1.25 1.125 1 0.875 0.75 0.625 0.5 0.375 0.25 0.125 0
300	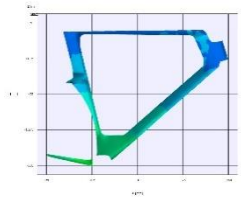		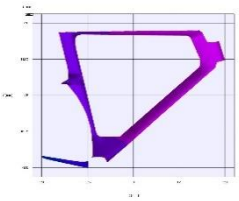	
600	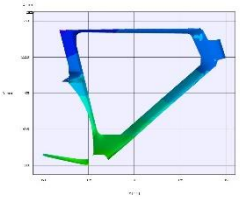		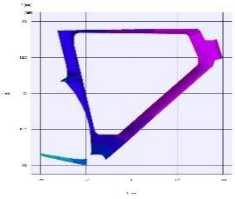	
900	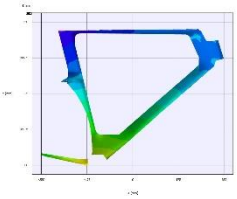		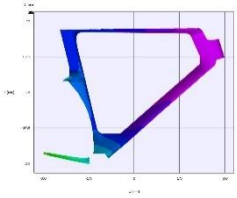	
1200	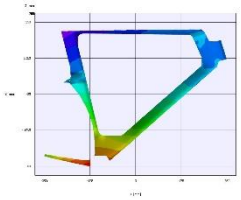		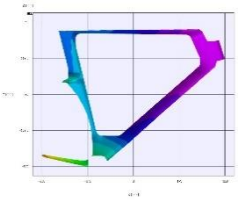	
1500	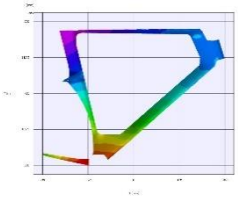		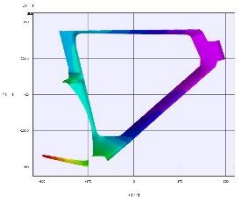	

AR01 RHS at 120^{O}

Load [N]	Lateral Displacement	W [mm]	Vertical Displacement	V [mm]
0	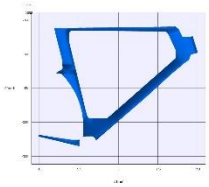	8.6 7.84063 7.08125 6.32188 5.5625 4.80313 4.04375 3.28438 2.525 1.76563 1.00625 0.246875 -0.5125 -1.27187 -2.03125 -2.79062 -3.55	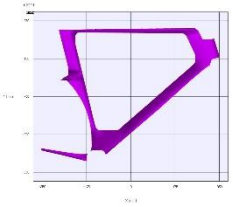	2 1.875 1.75 1.625 1.5 1.375 1.25 1.125 1 0.875 0.75 0.625 0.5 0.375 0.25 0.125 0
300	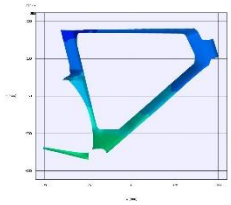		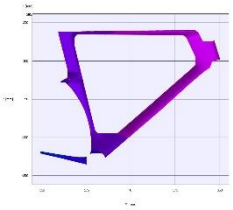	
600	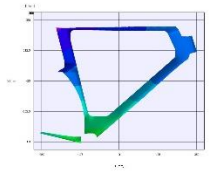		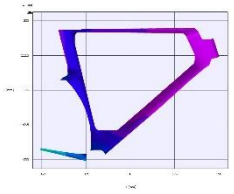	
900	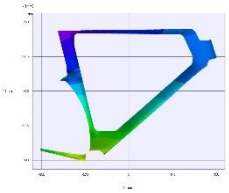		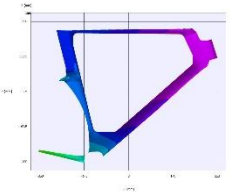	
1200	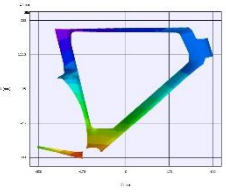		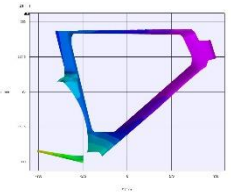	
1500	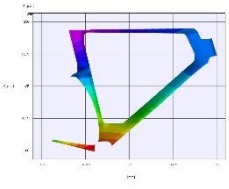		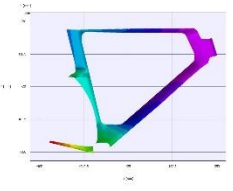	

AR01 RHS at 135^{O}

Load [N]	Lateral Displacement	W [mm]	Vertical Displacement	V [mm]
0	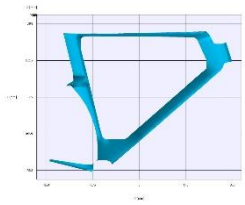	8.6 7.84063 7.08125 6.32188 5.5625 4.80313 4.04375 3.28438 2.525 1.76563 1.00625 0.246875 -0.5125 -1.27187 -2.03125 -2.79062 -3.55	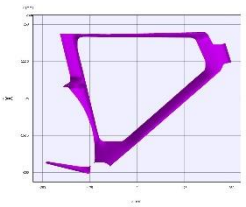	2 1.875 1.75 1.625 1.5 1.375 1.25 1.125 1 0.875 0.75 0.625 0.5 0.375 0.25 0.125 0
300	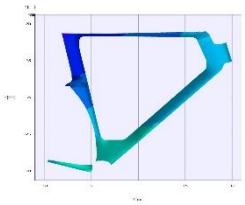		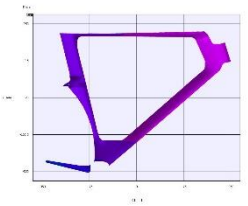	
600	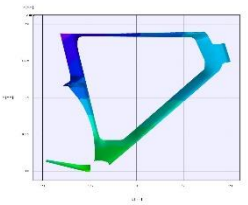		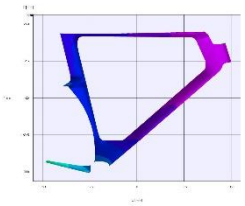	
900	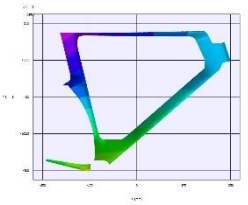		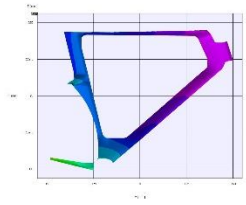	
1200	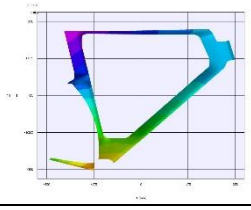		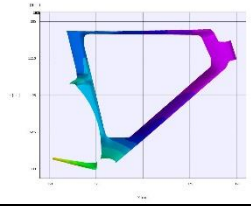	
1500	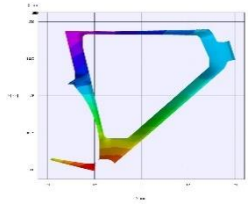		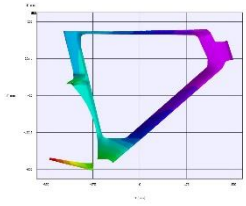	

AR01 RHS at 150^{O}

Load [N]	Lateral Displacement	W [mm]	Vertical Displacement	V [mm]
0	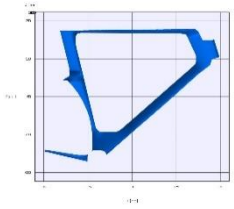	8.6 7.84063 7.08125 6.32188 5.5625 4.80313 4.04375 3.28438 2.525 1.76563 1.00625 0.246875 -0.5125 -1.27187 -2.03125 -2.79062 -3.55	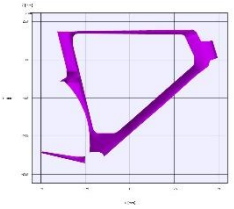	2 1.875 1.75 1.625 1.5 1.375 1.25 1.125 1 0.875 0.75 0.625 0.5 0.375 0.25 0.125 0
300	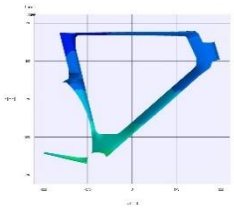		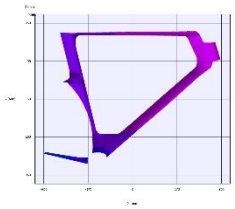	
600	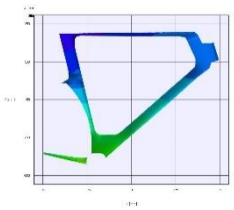		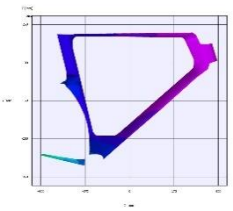	
900	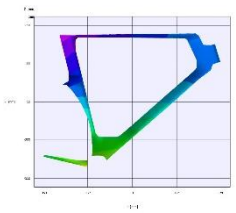		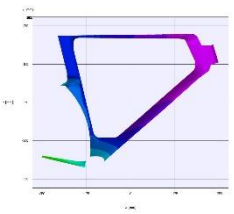	
1200	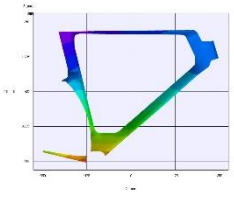		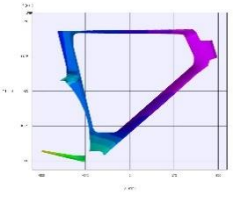	
1500	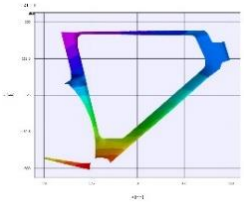		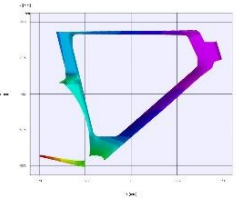	

AR01 RHS at 165^{O}

Load [N]	Lateral Displacement	W [mm]	Vertical Displacement	V [mm]
0	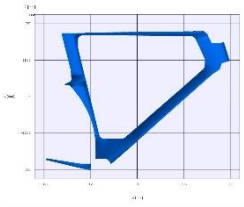	8.6 7.84063 7.08125 6.32188 5.5625 4.80313 4.04375 3.28438 2.525 1.76563 1.00625 0.246875 -0.5125 -1.27187 -2.03125 -2.79062 -3.55	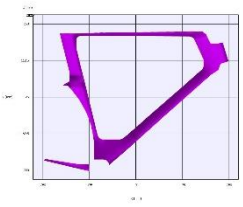	2 1.875 1.75 1.625 1.5 1.375 1.25 1.125 1 0.875 0.75 0.625 0.5 0.375 0.25 0.125 0
300	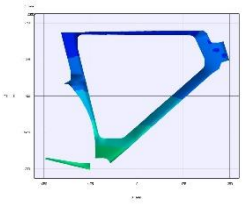		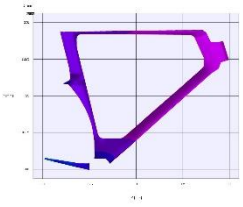	
600	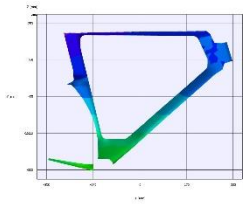		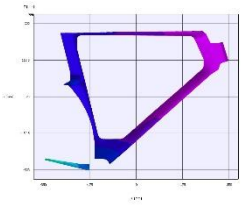	
900	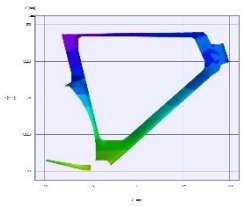		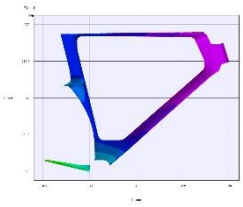	
1200	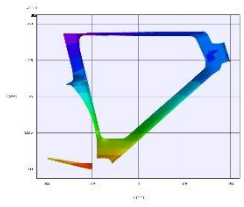		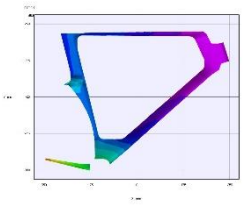	
1500	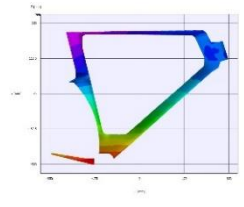		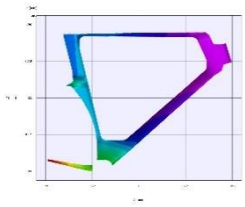	

AR01 RHS at 180^{O}

Load [N]	Lateral Displacement	W [mm]	Vertical Displacement	V [mm]
0	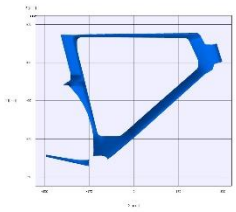	8.6 7.84063 7.08125 6.32188 5.5625 4.80313 4.04375 3.28438 2.525 1.76563 1.00625 0.246875 -0.5125 -1.27187 -2.03125 -2.79062 -3.55	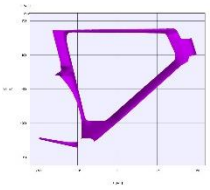	2 1.875 1.75 1.625 1.5 1.375 1.25 1.125 1 0.875 0.75 0.625 0.5 0.375 0.25 0.125 0
300	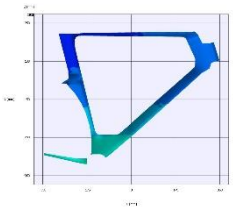		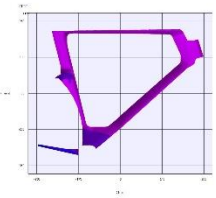	
600	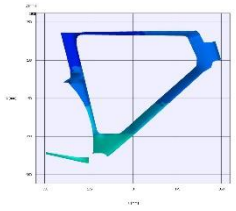		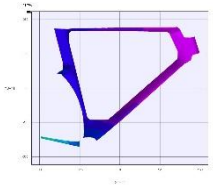	
900	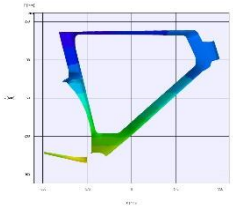		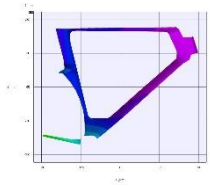	
1200	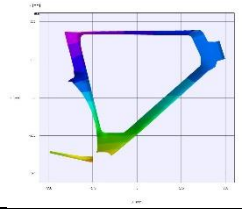		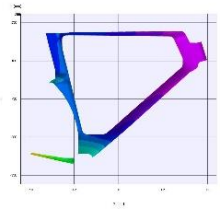	
1500	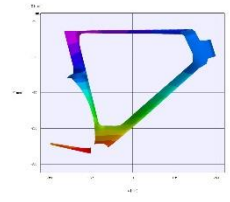		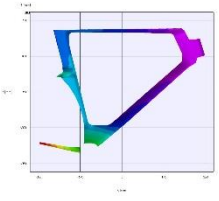	

16 Appendix H – Crank Angle Test Case Data

Below show the crank angle test case data.

AR01 Displacement Differences																									
		C0		C1		C2		C3		C4		C5		C6		C7		C11		C12		C13			
90	Load [Kg]	V [mm]	W [mm]	V [mm]	W [mm]	V [mm]	W [mm]	V [mm]	W [mm]	V [mm]	W [mm]	V [mm]	W [mm]	V [mm]	W [mm]	V [mm]	W [mm]	V [mm]	W [mm]	V [mm]	W [mm]	V [mm]	W [mm]	V [mm]	W [mm]
	150	1.13034	6.61657	0.778411	5.65122	0.484768	4.3435	0.375932	3.48848	0.31502	2.73182	0.248267	2.06736	0.975386	5.46964	0.969615	4.08312	1.60409	8.29946	1.84677	7.03516	2.08378	5.47883		
		C0		C1		C2		C3		C4		C5		C6		C7		C11		C12		C13			
105	Load [Kg]	V [mm]	W [mm]	V [mm]	W [mm]	V [mm]	W [mm]	V [mm]	W [mm]	V [mm]	W [mm]	V [mm]	W [mm]	V [mm]	W [mm]	V [mm]	W [mm]	V [mm]	W [mm]	V [mm]	W [mm]	V [mm]	W [mm]	V [mm]	W [mm]
	150	1.04441	6.47232	0.699497	5.45384	0.426057	4.29694	0.332674	3.4708	0.27652	2.70386	0.222023	2.0657	0.869212	5.30611	0.863172	4.00617	1.54407	7.9961	1.75242	6.9151	1.98765	5.42803		
		C0		C1		C2		C3		C4		C5		C6		C7		C11		C12		C13			
120	Load [Kg]	V [mm]	W [mm]	V [mm]	W [mm]	V [mm]	W [mm]	V [mm]	W [mm]	V [mm]	W [mm]	V [mm]	W [mm]	V [mm]	W [mm]	V [mm]	W [mm]	V [mm]	W [mm]	V [mm]	W [mm]	V [mm]	W [mm]	V [mm]	W [mm]
	150	1.02229	6.72334	0.694701	5.77318	0.425567	4.61928	0.332125	3.73676	0.279824	2.93913	0.220486	2.19559	0.847159	5.51484	0.837373	4.17831	1.50604	8.35468	1.70151	7.28083	1.93209	6.01603		
		C0		C1		C2		C3		C4		C5		C6		C7		C11		C12		C13			
135	Load [Kg]	V [mm]	W [mm]	V [mm]	W [mm]	V [mm]	W [mm]	V [mm]	W [mm]	V [mm]	W [mm]	V [mm]	W [mm]	V [mm]	W [mm]	V [mm]	W [mm]	V [mm]	W [mm]	V [mm]	W [mm]	V [mm]	W [mm]	V [mm]	W [mm]
	150.3	1.03574	5.91186	0.710956	5.14365	0.44056	4.06579	0.362074	3.29656	0.301571	2.55099	0.240766	1.90681	0.858059	4.68194	0.84879	3.35953	1.5215	7.49812	1.72984	6.58937	1.97972	5.47301		
		C0		C1		C2		C3		C4		C5		C6		C7		C11		C12		C13			
150	Load [Kg]	V [mm]	W [mm]	V [mm]	W [mm]	V [mm]	W [mm]	V [mm]	W [mm]	V [mm]	W [mm]	V [mm]	W [mm]	V [mm]	W [mm]	V [mm]	W [mm]	V [mm]	W [mm]	V [mm]	W [mm]	V [mm]	W [mm]	V [mm]	W [mm]
	150	1.02357	6.52377	0.692564	5.62124	0.441599	4.60299	0.352035	3.75501	0.294068	3.02033	0.238621	2.37483	0.823616	5.19857	0.818573	3.91657	1.51663	8.22691	1.72653	7.4162	1.97348	6.4144		
		C0		C1		C2		C3		C4		C5		C6		C7		C11		C12		C13			
165	Load [Kg]	V [mm]	W [mm]	V [mm]	W [mm]	V [mm]	W [mm]	V [mm]	W [mm]	V [mm]	W [mm]	V [mm]	W [mm]	V [mm]	W [mm]	V [mm]	W [mm]	V [mm]	W [mm]	V [mm]	W [mm]	V [mm]	W [mm]	V [mm]	W [mm]
	150.3	0.946167	6.74711	0.636299	5.89364	0.38504	4.84907	0.30947	4.01042	0.258235	3.22767	0.208502	2.53892	0.728157	5.34373	0.715562	4.11477	1.44273	8.63717	1.6473	8.01798	1.90208	7.30389		
		C0		C1		C2		C3		C4		C5		C6		C7		C11		C12		C13			
180	Load [Kg]	V [mm]	W [mm]	V [mm]	W [mm]	V [mm]	W [mm]	V [mm]	W [mm]	V [mm]	W [mm]	V [mm]	W [mm]	V [mm]	W [mm]	V [mm]	W [mm]	V [mm]	W [mm]	V [mm]	W [mm]	V [mm]	W [mm]	V [mm]	W [mm]
	150.2	0.932034	6.45809	0.616974	5.64551	0.36965	4.59185	0.298812	3.83555	0.257861	3.08194	0.203625	2.33112	0.69739	4.98943	0.691422	3.72823	1.41793	8.33039	1.62457	7.87365	1.89093	7.3529		
	Compare.	C0		C1		C2		C3		C4		C5		C6		C7		C11		C12		C13			
		V [mm]	W [mm]	V [mm]	W [mm]	V [mm]	W [mm]	V [mm]	W [mm]	V [mm]	W [mm]	V [mm]	W [mm]	V [mm]	W [mm]	V [mm]	W [mm]	V [mm]	W [mm]	V [mm]	W [mm]	V [mm]	W [mm]	V [mm]	W [mm]
	90-105	0.09	0.14	0.08	0.20	0.06	0.05	0.04	0.02	0.04	0.03	0.03	0.00	0.11	0.16	0.11	0.08	0.06	0.30	0.09	0.12	0.10	0.05		
	90-120	0.11	-0.11	0.08	-0.12	0.06	-0.28	0.04	-0.25	0.04	-0.21	0.03	-0.13	0.13	-0.05	0.13	-0.10	0.10	-0.06	0.15	-0.25	0.15	-0.54		
	90-135	0.09	0.70	0.07	0.51	0.04	0.28	0.01	0.19	0.01	0.18	0.01	0.16	0.12	0.79	0.12	0.72	0.08	0.80	0.12	0.45	0.10	0.01		
	90-150	0.11	0.09	0.09	0.03	0.04	-0.26	0.02	-0.27	0.02	-0.29	0.01	-0.31	0.15	0.27	0.15	0.17	0.09	0.07	0.12	-0.38	0.11	-0.94		
	90-165	0.18	-0.13	0.14	-0.24	0.10	-0.51	0.07	-0.52	0.06	-0.50	0.04	-0.47	0.25	0.13	0.25	-0.03	0.16	-0.34	0.20	-0.98	0.18	-1.83		
	90-180	0.20	0.16	0.16	0.01	0.12	-0.25	0.08	-0.35	0.06	-0.35	0.04	-0.26	0.28	0.48	0.28	0.35	0.19	-0.03	0.22	-0.84	0.19	-1.87		

CA01 LHS Degree Difference																							
Interval		C0		C1		C2		C3		C4		C5		C6		C7		C11		C12		C13	
90	Load [Kg]																						
	150.2	0.899729	7.18266	0.788569	6.24157	0.650538	5.35087	0.520423	4.27943	0.429677	3.36801	0.344155	2.5411	0.810888	5.5631	0.809338	3.85925	1.73515	8.69216	1.83327	7.71227	2.00661	6.22939
		C0		C1		C2		C3		C4		C5		C6		C7		C11		C12		C13	
105	Load [Kg]	V [mm]	W [mm]	V [mm]	W [mm]	V [mm]	W [mm]	V [mm]	W [mm]	V [mm]	W [mm]	V [mm]	W [mm]	V [mm]	W [mm]	V [mm]	W [mm]	V [mm]	W [mm]	V [mm]	W [mm]	V [mm]	W [mm]
	150.3	0.890182	6.82683	0.782118	5.9272	0.64322	5.05212	0.520748	4.04671	0.434869	3.15436	0.353102	2.35924	0.800059	5.20958	0.794562	3.5168	1.70573	8.16217	1.79635	7.21518	1.97034	5.82932
		C0		C1		C2		C3		C4		C5		C6		C7		C11		C12		C13	
120	Index [1]	V [mm]	W [mm]	V [mm]	W [mm]	V [mm]	W [mm]	V [mm]	W [mm]	V [mm]	W [mm]	V [mm]	W [mm]	V [mm]	W [mm]	V [mm]	W [mm]	V [mm]	W [mm]	V [mm]	W [mm]	V [mm]	W [mm]
	150.5	0.824138	8.24359	0.721966	7.21401	0.597832	6.29902	0.471877	5.08839	0.395938	4.06265	0.327901	3.14937	0.684378	6.22983	0.65446	4.28652	1.73898	9.63241	1.81665	8.44043	1.99185	6.89299
		C0		C1		C2		C3		C4		C5		C6		C7		C11		C12		C13	
135	Index [1]	V [mm]	W [mm]	V [mm]	W [mm]	V [mm]	W [mm]	V [mm]	W [mm]	V [mm]	W [mm]	V [mm]	W [mm]	V [mm]	W [mm]	V [mm]	W [mm]	V [mm]	W [mm]	V [mm]	W [mm]	V [mm]	W [mm]
	150.5	0.717345	8.02839	0.621004	7.02594	0.508762	6.14381	0.40917	5.02004	0.331931	3.93235	0.26863	3.05179	0.566281	6.00558	0.527164	3.95737	1.58006	9.21147	1.66685	8.21359	1.8389	6.7681
		C0		C1		C2		C3		C4		C5		C6		C7		C11		C12		C13	
150	Load [Kg]	V [mm]	W [mm]	V [mm]	W [mm]	V [mm]	W [mm]	V [mm]	W [mm]	V [mm]	W [mm]	V [mm]	W [mm]	V [mm]	W [mm]	V [mm]	W [mm]	V [mm]	W [mm]	V [mm]	W [mm]	V [mm]	W [mm]
	150.6	0.754843	7.58686	0.667136	6.67262	0.55877	5.83394	0.451129	4.72621	0.371512	3.80619	0.315862	2.83642	0.609357	5.57924	0.571326	3.60665	1.6749	8.96961	1.74997	7.76815	1.9239	6.23406
		C0		C1		C2		C3		C4		C5		C6		C7		C11		C12		C13	
165	Load [Kg]	V [mm]	W [mm]	V [mm]	W [mm]	V [mm]	W [mm]	V [mm]	W [mm]	V [mm]	W [mm]	V [mm]	W [mm]	V [mm]	W [mm]	V [mm]	W [mm]	V [mm]	W [mm]	V [mm]	W [mm]	V [mm]	W [mm]
	150.1	0.698335	7.86751	0.610508	6.95692	0.486395	5.9562	0.387701	4.87115	0.330092	3.92026	0.26225	3.03086	0.551038	5.89036	0.516249	4.02245	1.5697	9.0495	1.6601	7.86985	1.84299	6.79867
		C0		C1		C2		C3		C4		C5		C6		C7		C11		C12		C13	
180	Load [Kg]	V [mm]	W [mm]	V [mm]	W [mm]	V [mm]	W [mm]	V [mm]	W [mm]	V [mm]	W [mm]	V [mm]	W [mm]	V [mm]	W [mm]	V [mm]	W [mm]	V [mm]	W [mm]	V [mm]	W [mm]	V [mm]	W [mm]
	150.3	0.611143	7.62254	0.539599	6.72792	0.450269	5.88388	0.357967	4.81416	0.302716	3.8691	0.256456	3.00349	0.464656	5.65915	0.430605	3.6922	1.48917	8.9631	1.57284	7.88296	1.75791	6.75457
	Compare	C0		C1		C2		C3		C4		C5		C6		C7		C11		C12		C13	
		V [mm]	W [mm]	V [mm]	W [mm]	V [mm]	W [mm]	V [mm]	W [mm]	V [mm]	W [mm]	V [mm]	W [mm]	V [mm]	W [mm]	V [mm]	W [mm]	V [mm]	W [mm]	V [mm]	W [mm]	V [mm]	W [mm]
	90-105	0.01	0.36	0.01	0.31	0.01	0.30	0.00	0.23	-0.01	0.21	-0.01	0.18	0.01	0.35	0.01	0.34	0.03	0.53	0.04	0.50	0.04	0.40
	90-120	0.08	-1.06	0.07	-0.97	0.05	-0.95	0.05	-0.81	0.03	-0.69	0.02	-0.61	0.13	-0.67	0.15	-0.43	0.00	-0.94	0.02	-0.73	0.01	-0.66
	90-135	0.18	-0.85	0.17	-0.78	0.14	-0.79	0.11	-0.74	0.10	-0.56	0.08	-0.51	0.24	-0.44	0.28	-0.10	0.16	-0.52	0.17	-0.50	0.17	-0.54
	90-150	0.14	-0.40	0.12	-0.43	0.09	-0.48	0.07	-0.45	0.06	-0.44	0.03	-0.30	0.20	-0.02	0.24	0.25	0.06	-0.28	0.08	-0.06	0.08	0.00
	90-165	0.20	-0.68	0.18	-0.72	0.16	-0.61	0.13	-0.59	0.10	-0.55	0.08	-0.49	0.26	-0.33	0.29	-0.16	0.17	-0.36	0.17	-0.16	0.16	-0.57
	90-180	0.29	-0.44	0.25	-0.49	0.20	-0.53	0.16	-0.53	0.13	-0.50	0.09	-0.46	0.35	-0.10	0.38	0.17	0.25	-0.27	0.26	-0.17	0.25	-0.53

CA01 RHS Degree Difference																							
90		C0		C1		C2		C3		C4		C5		C6		C7		C11		C12		C13	
	Load [Kg]	V [mm]	W [mm]	V [mm]	W [mm]	V [mm]	W [mm]	V [mm]	W [mm]	V [mm]	W [mm]	V [mm]	W [mm]	V [mm]	W [mm]	V [mm]	W [mm]	V [mm]	W [mm]	V [mm]	W [mm]	V [mm]	W [mm]
	150.2	0.915579	7.4587	0.841108	6.58565	0.672527	5.59247	0.531461	4.3847	0.436873	3.41829	0.357775	2.55332	0.848886	5.66791	0.810683	3.76846	1.86802	9.11925	1.9747	7.9914	2.15582	6.42492
		C0		C1		C2		C3		C4		C5		C6		C7		C11		C12		C13	
105	Load [Kg]	V [mm]	W [mm]	V [mm]	W [mm]	V [mm]	W [mm]	V [mm]	W [mm]	V [mm]	W [mm]	V [mm]	W [mm]	V [mm]	W [mm]	V [mm]	W [mm]	V [mm]	W [mm]	V [mm]	W [mm]	V [mm]	W [mm]
	150.5	0.872886	8.0819	0.806721	7.19352	0.640231	6.10272	0.506289	4.86353	0.408323	3.83415	0.32944	2.92982	0.247028	6.28715	0.799027	4.31297	1.85314	9.89664	1.94807	8.64905	2.13842	7.05333
		C0		C1		C2		C3		C4		C5		C6		C7		C11		C12		C13	
120	Load [Kg]	V [mm]	W [mm]	V [mm]	W [mm]	V [mm]	W [mm]	V [mm]	W [mm]	V [mm]	W [mm]	V [mm]	W [mm]	V [mm]	W [mm]	V [mm]	W [mm]	V [mm]	W [mm]	V [mm]	W [mm]	V [mm]	W [mm]
	150.5	0.786855	8.06369	0.732351	7.18376	0.570974	6.12714	0.437665	4.80914	0.358483	3.88225	0.288532	2.88872	0.710992	6.25813	0.669161	4.26031	1.75551	9.91243	1.84955	8.77167	2.04107	7.16792
		C0		C1		C2		C3		C4		C5		C6		C7		C11		C12		C13	
135	Load [Kg]	V [mm]	W [mm]	V [mm]	W [mm]	V [mm]	W [mm]	V [mm]	W [mm]	V [mm]	W [mm]	V [mm]	W [mm]	V [mm]	W [mm]	V [mm]	W [mm]	V [mm]	W [mm]	V [mm]	W [mm]	V [mm]	W [mm]
	150.1	0.81227	7.64357	0.757778	6.84385	0.603359	5.83536	0.489789	4.69525	0.395667	3.70793	0.324599	2.85277	0.737012	5.89321	0.701285	3.97174	1.76357	9.41175	1.86226	8.29408	2.06579	6.90868
150		C0		C1		C2		C3		C4		C5		C6		C7		C11		C12		C13	
	Load [Kg]	V [mm]	W [mm]	V [mm]	W [mm]	V [mm]	W [mm]	V [mm]	W [mm]	V [mm]	W [mm]	V [mm]	W [mm]	V [mm]	W [mm]	V [mm]	W [mm]	V [mm]	W [mm]	V [mm]	W [mm]	V [mm]	W [mm]
	150	0.670769	7.67375	0.632217	6.86371	0.497522	5.93006	0.396883	4.75578	0.317196	3.72119	0.262939	2.86101	0.581999	5.91894	0.53872	4.00856	1.6015	9.40752	1.68835	8.38546	1.87801	7.11374
165		C0		C1		C2		C3		C4		C5		C6		C7		C11		C12		C13	
	Load [Kg]	V [mm]	W [mm]	V [mm]	W [mm]	V [mm]	W [mm]	V [mm]	W [mm]	V [mm]	W [mm]	V [mm]	W [mm]	V [mm]	W [mm]	V [mm]	W [mm]	V [mm]	W [mm]	V [mm]	W [mm]	V [mm]	W [mm]
	150.1	0.682005	7.69392	0.645077	6.96475	0.51073	5.95768	0.404696	4.78956	0.331639	3.8356	0.267077	2.9135	0.591553	5.90432	0.541129	4.00493	1.62027	9.47268	1.72269	8.47907	1.92742	7.25384
180		C0		C1		C2		C3		C4		C5		C6		C7		C11		C12		C13	
	Load [Kg]	V [mm]	W [mm]	V [mm]	W [mm]	V [mm]	W [mm]	V [mm]	W [mm]	V [mm]	W [mm]	V [mm]	W [mm]	V [mm]	W [mm]	V [mm]	W [mm]	V [mm]	W [mm]	V [mm]	W [mm]	V [mm]	W [mm]
	150.1	0.622858	7.00582	0.594022	6.27519	0.477458	5.40434	0.372592	4.31515	0.313426	3.42397	0.268124	2.60512	0.537153	5.28032	0.488034	3.46468	1.53054	8.64012	1.62725	7.7829	1.83611	6.79616
	Compare	C0		C1		C2		C3		C4		C5		C6		C7		C11		C12		C13	
		V [mm]	W [mm]	V [mm]	W [mm]	V [mm]	W [mm]	V [mm]	W [mm]	V [mm]	W [mm]	V [mm]	W [mm]	V [mm]	W [mm]	V [mm]	W [mm]	V [mm]	W [mm]	V [mm]	W [mm]	V [mm]	W [mm]
	90-105	0.04	-0.62	0.03	-0.61	0.03	-0.51	0.03	-0.48	0.03	-0.42	0.03	-0.38	0.60	-0.62	0.01	-0.54	0.01	-0.78	0.03	-0.66	0.02	-0.63
	90-120	0.13	-0.60	0.11	-0.60	0.10	-0.53	0.09	-0.42	0.08	-0.46	0.07	-0.34	0.14	-0.59	0.14	-0.49	0.11	-0.79	0.13	-0.78	0.11	-0.74
	90-135	0.10	-0.18	0.08	-0.26	0.07	-0.24	0.04	-0.31	0.04	-0.29	0.03	-0.30	0.11	-0.23	0.11	-0.20	0.10	-0.29	0.11	-0.30	0.09	-0.48
	90-150	0.24	-0.22	0.21	-0.28	0.18	-0.34	0.13	-0.37	0.12	-0.30	0.09	-0.31	0.27	-0.25	0.27	-0.24	0.27	-0.29	0.29	-0.39	0.28	-0.69
	90-165	0.23	-0.24	0.20	-0.38	0.16	-0.37	0.13	-0.40	0.11	-0.42	0.09	-0.36	0.26	-0.24	0.27	-0.24	0.25	-0.35	0.25	-0.49	0.23	-0.83
	90-180	0.29	0.45	0.25	0.31	0.20	0.19	0.16	0.07	0.12	-0.01	0.09	-0.05	0.31	0.39	0.32	0.30	0.34	0.48	0.35	0.21	0.32	-0.37

CA02 RHS Degree Difference																							
		C0		C1		C2		C3		C4		C5		C6		C7		C11		C12		C13	
90	Index [1]	V [mm]	W [mm]	V [mm]	W [mm]	V [mm]	W [mm]	V [mm]	W [mm]	V [mm]	W [mm]	V [mm]	W [mm]	V [mm]	W [mm]	V [mm]	W [mm]	V [mm]	W [mm]	V [mm]	W [mm]	V [mm]	W [mm]
	150.7	0.657952	7.78742	0.565784	6.85454	0.429065	5.66859	0.344208	4.54785	0.278974	3.63435	0.222292	2.75523	0.611201	6.17994	0.606057	4.26382	1.58849	9.93478	1.6643	8.84677	1.81116	7.29465
		C0		C1		C2		C3		C4		C5		C6		C7		C11		C12		C13	
105	Index [1]	V [mm]	W [mm]	V [mm]	W [mm]	V [mm]	W [mm]	V [mm]	W [mm]	V [mm]	W [mm]	V [mm]	W [mm]	V [mm]	W [mm]	V [mm]	W [mm]	V [mm]	W [mm]	V [mm]	W [mm]	V [mm]	W [mm]
	150.3	0.690169	7.77983	0.594109	6.81051	0.446604	5.5891	0.36835	4.49011	0.304038	3.54861	0.246133	2.70777	0.647322	6.23677	0.647033	4.3389	1.63609	10.0452	1.72369	9.08918	1.884	7.64423
		C0		C1		C2		C3		C4		C5		C6		C7		C11		C12		C13	
120	Load [Kg]	V [mm]	W [mm]	V [mm]	W [mm]	V [mm]	W [mm]	V [mm]	W [mm]	V [mm]	W [mm]	V [mm]	W [mm]	V [mm]	W [mm]	V [mm]	W [mm]	V [mm]	W [mm]	V [mm]	W [mm]	V [mm]	W [mm]
	150	0.676587	7.53568	0.590315	6.65665	0.440703	5.49112	0.363499	4.41832	0.30053	3.50999	0.242381	2.66742	0.636037	5.907	0.636115	3.89737	1.62237	9.67503	1.71095	8.67629	1.88109	7.18151
		C0		C1		C2		C3		C4		C5		C6		C7		C11		C12		C13	
135	Load [Kg]	V [mm]	W [mm]	V [mm]	W [mm]	V [mm]	W [mm]	V [mm]	W [mm]	V [mm]	W [mm]	V [mm]	W [mm]	V [mm]	W [mm]	V [mm]	W [mm]	V [mm]	W [mm]	V [mm]	W [mm]	V [mm]	W [mm]
	150.6	0.626028	7.93583	0.542125	6.97343	0.420408	5.87921	0.34215	4.73439	0.275694	3.79386	0.219461	2.88801	0.583657	6.28533	0.578122	4.40295	1.56286	10.1203	1.65684	9.17702	1.84095	7.82163
		C0		C1		C2		C3		C4		C5		C6		C7		C11		C12		C13	
150	Load [Kg]	V [mm]	W [mm]	V [mm]	W [mm]	V [mm]	W [mm]	V [mm]	W [mm]	V [mm]	W [mm]	V [mm]	W [mm]	V [mm]	W [mm]	V [mm]	W [mm]	V [mm]	W [mm]	V [mm]	W [mm]	V [mm]	W [mm]
	150.3	0.563942	8.09485	0.490903	7.16688	0.368975	6.04072	0.302726	4.89253	0.245865	3.95351	0.203019	3.03642	0.504582	6.36358	0.493478	4.36661	1.52739	10.3069	1.63019	9.36588	1.82744	8.24268
		C0		C1		C2		C3		C4		C5		C6		C7		C11		C12		C13	
165	Load [Kg]	V [mm]	W [mm]	V [mm]	W [mm]	V [mm]	W [mm]	V [mm]	W [mm]	V [mm]	W [mm]	V [mm]	W [mm]	V [mm]	W [mm]	V [mm]	W [mm]	V [mm]	W [mm]	V [mm]	W [mm]	V [mm]	W [mm]
	150.4	0.477448	8.10226	0.427714	7.2173	0.324751	6.13454	0.263248	4.98924	0.227444	4.04013	0.184641	3.09534	0.398326	6.29892	0.37994	4.23325	1.44236	10.219	1.53458	9.29742	1.73609	8.25968
		C0		C1		C2		C3		C4		C5		C6		C7		C11		C12		C13	
180	Load [Kg]	V [mm]	W [mm]	V [mm]	W [mm]	V [mm]	W [mm]	V [mm]	W [mm]	V [mm]	W [mm]	V [mm]	W [mm]	V [mm]	W [mm]	V [mm]	W [mm]	V [mm]	W [mm]	V [mm]	W [mm]	V [mm]	W [mm]
	150.5	0.485301	7.84975	0.432928	6.97895	0.327297	5.91285	0.270626	4.86434	0.232761	3.919	0.196822	3.02919	0.40949	6.09088	0.398751	4.19312	1.43394	9.96998	1.53701	9.09984	1.75146	8.21125
	Compare	C0		C1		C2		C3		C4		C5		C6		C7		C11		C12		C13	
		V [mm]	W [mm]	V [mm]	W [mm]	V [mm]	W [mm]	V [mm]	W [mm]	V [mm]	W [mm]	V [mm]	W [mm]	V [mm]	W [mm]	V [mm]	W [mm]	V [mm]	W [mm]	V [mm]	W [mm]	V [mm]	W [mm]
	90-105	0.0	0.0	0.0	0.0	0.0	0.1	0.0	0.1	0.0	0.1	0.0	0.0	0.0	-0.1	0.0	-0.1	0.0	-0.1	-0.1	-0.2	-0.1	-0.3
	90-120	0.0	0.3	0.0	0.2	0.0	0.2	0.0	0.1	0.0	0.1	0.0	0.1	0.0	0.3	0.0	0.4	0.0	0.3	0.0	0.2	-0.1	0.1
	90-135	0.0	-0.1	0.0	-0.1	0.0	-0.2	0.0	-0.2	0.0	-0.2	0.0	-0.1	0.0	-0.1	0.0	-0.1	0.0	-0.2	0.0	-0.3	0.0	-0.5
	90-150	0.1	-0.3	0.1	-0.3	0.1	-0.4	0.0	-0.3	0.0	-0.3	0.0	-0.3	0.1	-0.2	0.1	-0.1	0.1	-0.4	0.0	-0.5	0.0	-0.9
	90-165	0.2	-0.3	0.1	-0.4	0.1	-0.5	0.1	-0.4	0.1	-0.4	0.0	-0.3	0.2	-0.1	0.2	0.0	0.1	-0.3	0.1	-0.5	0.1	-1.0
	90-180	0.2	-0.1	0.1	-0.1	0.1	-0.2	0.1	-0.3	0.0	-0.3	0.0	-0.3	0.2	0.1	0.2	0.1	0.2	0.0	0.1	-0.3	0.1	-0.9

17 Appendix I – Comparison Data

Below show the comparison data.

Interval	C0		C1		C2		C3		C4		C5		C6		C7		C11		C12		C13	
	V [mm]	W [mm]	V [mm]	W [mm]	V [mm]	W [mm]	V [mm]	W [mm]	V [mm]	W [mm]	V [mm]	W [mm]	V [mm]	W [mm]	V [mm]	W [mm]	V [mm]	W [mm]	V [mm]	W [mm]	V [mm]	W [mm]
CA01 LHS 90 Deg	0.89973	7.18266	0.78857	6.24157	0.65054	5.35087	0.52042	4.27943	0.42968	3.36801	0.34416	2.5411	0.81089	5.5631	0.80934	3.85925	1.73515	8.69216	1.83327	7.71227	2.00661	6.22939
CA01 RHS 90 Deg	0.91558	7.4587	0.84111	6.58565	0.67253	5.59247	0.53146	4.3847	0.43687	3.41829	0.35778	2.55332	0.84889	5.66791	0.81068	3.76846	1.86802	9.11925	1.9747	7.9914	2.15582	6.42492
CA01 LHS 105 Deg	0.89018	6.82683	0.78212	5.9272	0.64322	5.05212	0.52075	4.04671	0.43487	3.15436	0.3531	2.35924	0.80006	5.20958	0.79456	3.5168	1.70573	8.16217	1.79635	7.21518	1.97034	5.82932
CA01 RHS 105 Deg	0.87289	8.0819	0.80672	7.19352	0.64023	6.10272	0.50629	4.86353	0.40832	3.83415	0.32944	2.92982	0.24703	6.28715	0.79903	4.31297	1.85314	9.89664	1.94807	8.64905	2.13842	7.05333
CA01 LHS 120 Deg	0.82414	8.24359	0.72197	7.21401	0.59783	6.29902	0.47188	5.08839	0.39594	4.06265	0.3279	3.14937	0.68438	6.22983	0.65446	4.28652	1.73898	9.63241	1.81665	8.44043	1.99185	6.89299
CA01 RHS 120 Deg	0.78686	8.06369	0.73235	7.18376	0.57097	6.12714	0.43767	4.80914	0.35848	3.88225	0.28853	2.88872	0.71099	6.25813	0.66916	4.26031	1.75551	9.91243	1.84955	8.77167	2.04107	7.16792
CA01 LHS 135 Deg	0.71735	8.02839	0.621	7.02594	0.50876	6.14381	0.40917	5.02004	0.33193	3.93235	0.26863	3.05179	0.56628	6.00558	0.52716	3.95737	1.58006	9.21147	1.66685	8.21359	1.8389	6.7681
CA01 RHS 135 Deg	0.81227	7.64357	0.75778	6.84385	0.60336	5.83536	0.48979	4.69525	0.39567	3.70793	0.3246	2.85277	0.73701	5.89321	0.70129	3.97174	1.76357	9.41175	1.86226	8.29408	2.06579	6.90868
CA01 LHS 150 Deg	0.75484	7.58686	0.66714	6.67262	0.55877	5.83394	0.45113	4.72621	0.37151	3.80619	0.31586	2.83642	0.60936	5.57924	0.57133	3.60665	1.6749	8.96961	1.74997	7.76815	1.9239	6.23406
CA01 RHS 150 Deg	0.67077	7.67375	0.63222	6.86371	0.49752	5.93006	0.39688	4.75578	0.3172	3.72119	0.26294	2.86101	0.582	5.91894	0.53872	4.00856	1.6015	9.40752	1.68835	8.38546	1.87801	7.11374
CA01 LHS 165 Deg	0.69834	7.86751	0.61051	6.95692	0.4864	5.9562	0.3877	4.87115	0.33009	3.92026	0.26225	3.03086	0.55104	5.89036	0.51625	4.02245	1.5697	9.0495	1.6601	7.86985	1.84299	6.79867
CA01 RHS 165 Deg	0.68201	7.69392	0.64508	6.96475	0.51073	5.95768	0.4047	4.78956	0.33164	3.8356	0.26708	2.9135	0.59155	5.90432	0.54113	4.00493	1.62027	9.47268	1.72269	8.47907	1.92742	7.25384
CA01 LHS 180 Deg	0.61114	7.62254	0.5396	6.72792	0.45027	5.88388	0.35797	4.81416	0.30272	3.8691	0.25646	3.00349	0.46466	5.65915	0.43061	3.6922	1.48917	8.9631	1.57284	7.88296	1.75791	6.75457
CA01 RHS 180 Deg	0.62286	7.00582	0.59402	6.27519	0.47746	5.40434	0.37259	4.31515	0.31343	3.42397	0.26812	2.60512	0.53715	5.28032	0.48803	3.46468	1.53054	8.64012	1.62725	7.7829	1.83611	6.79616

CA01 LHS - CA01 RHS																						
Angle (Deg)		C0		C1		C2		C3		C4		C5		C6		C7		C11		C12		C13
	V [mm]	W [mm]	V [mm]	W [mm]	V [mm]	W [mm]	V [mm]	W [mm]	V [mm]	W [mm]	V [mm]	W [mm]	V [mm]	W [mm]	V [mm]	W [mm]	V [mm]	W [mm]	V [mm]	W [mm]	V [mm]	W [mm]
90	-0.02	-0.28	-0.05	-0.34	-0.02	-0.24	-0.01	-0.11	-0.01	-0.05	-0.01	-0.01	-0.04	-0.10	0.00	0.09	-0.13	-0.43	-0.14	-0.28	-0.15	-0.20
105	0.02	-1.26	-0.02	-1.27	0.00	-1.05	0.01	-0.82	0.03	-0.68	0.02	-0.57	0.55	-1.08	0.00	-0.80	-0.15	-1.73	-0.15	-1.43	-0.17	-1.22
120	0.04	0.18	-0.01	0.03	0.03	0.17	0.03	0.28	0.04	0.18	0.04	0.26	-0.03	-0.03	-0.01	0.03	-0.02	-0.28	-0.03	-0.33	-0.05	-0.27
135	-0.09	0.38	-0.14	0.18	-0.09	0.31	-0.08	0.32	-0.06	0.22	-0.06	0.20	-0.17	0.11	-0.17	-0.01	-0.18	-0.20	-0.20	-0.08	-0.23	-0.14
150	0.08	-0.09	0.03	-0.19	0.06	-0.10	0.05	-0.03	0.05	0.09	0.05	-0.02	0.03	-0.34	0.03	-0.40	0.07	-0.44	0.06	-0.62	0.05	-0.88
165	0.02	0.17	-0.03	-0.01	-0.02	0.00	-0.02	0.08	0.00	0.08	0.00	0.12	-0.04	-0.01	-0.02	0.02	-0.05	-0.42	-0.06	-0.61	-0.08	-0.46
180	-0.01	0.62	-0.05	0.45	-0.03	0.48	-0.01	0.50	-0.01	0.45	-0.01	0.40	-0.07	0.38	-0.06	0.23	-0.04	0.32	-0.05	0.10	-0.08	-0.04

Interval	C0		C1		C2		C3		C4		C5		C6		C7		C11		C12		C13	
	V [mm]	W [mm]	V [mm]	W [mm]	V [mm]	W [mm]	V [mm]	W [mm]	V [mm]	W [mm]	V [mm]	W [mm]	V [mm]	W [mm]	V [mm]	W [mm]	V [mm]	W [mm]	V [mm]	W [mm]	V [mm]	W [mm]
CA01 RHS 90 Deg	0.91558	7.4587	0.84111	6.58565	0.67253	5.59247	0.53146	4.3847	0.43687	3.41829	0.35778	2.55332	0.84889	5.66791	0.81068	3.76846	1.86802	9.11925	1.9747	7.9914	2.15582	6.42492
CA02 RHS 90 Deg	0.65795	7.78742	0.56578	6.85454	0.42907	5.66859	0.34421	4.54785	0.27897	3.63435	0.22229	2.75523	0.6112	6.17994	0.60606	4.26382	1.58849	9.93478	1.6643	8.84677	1.81116	7.29465
CA01 RHS 105 Deg	0.87289	8.0819	0.80672	7.19352	0.64023	6.10272	0.50629	4.86353	0.40832	3.83415	0.32944	2.92982	0.24703	6.28715	0.79903	4.31297	1.85314	9.89664	1.94807	8.64905	2.13842	7.05333
CA02 RHS 105 Deg	0.69017	7.77983	0.59411	6.81051	0.4466	5.5891	0.36835	4.49011	0.30404	3.54861	0.24613	2.70777	0.64732	6.23677	0.64703	4.3389	1.63609	10.0452	1.72369	9.08918	1.884	7.64423
CA01 RHS 120 Deg	0.78686	8.06369	0.73235	7.18376	0.57097	6.12714	0.43767	4.80914	0.35848	3.88225	0.28853	2.88872	0.71099	6.25813	0.66916	4.26031	1.75551	9.91243	1.84955	8.77167	2.04107	7.16792
CA02 RHS 120 Deg	0.67659	7.53568	0.59032	6.65665	0.4407	5.49112	0.3635	4.41832	0.30053	3.50999	0.24238	2.66742	0.63604	5.907	0.63612	3.89737	1.62237	9.67503	1.71095	8.67629	1.88109	7.18151
CA01 RHS 135 Deg	0.81227	7.64357	0.75778	6.84385	0.60336	5.83536	0.48979	4.69525	0.39567	3.70793	0.3246	2.85277	0.73701	5.89321	0.70129	3.97174	1.76357	9.41175	1.86226	8.29408	2.06579	6.90868
CA02 RHS 135 Deg	0.62603	7.93583	0.54213	6.97343	0.42041	5.87921	0.34215	4.73439	0.27569	3.79386	0.21946	2.88801	0.58366	6.28533	0.57812	4.40295	1.56286	10.1203	1.65684	9.17702	1.84095	7.82163
CA01 RHS 150 Deg	0.67077	7.67375	0.63222	6.86371	0.49752	5.93006	0.39688	4.75578	0.3172	3.72119	0.26294	2.86101	0.582	5.91894	0.53872	4.00856	1.6015	9.40752	1.68835	8.38546	1.87801	7.11374
CA02 RHS 150 Deg	0.56394	8.09485	0.4909	7.16688	0.36898	6.04072	0.30273	4.89253	0.24587	3.95351	0.20302	3.03642	0.50458	6.36358	0.49348	4.36661	1.52739	10.3069	1.63019	9.36588	1.82744	8.24268
CA01 RHS 165 Deg	0.68201	7.69392	0.64508	6.96475	0.51073	5.95768	0.4047	4.78956	0.33164	3.8356	0.26708	2.9135	0.59155	5.90432	0.54113	4.00493	1.62027	9.47268	1.72269	8.47907	1.92742	7.25384
CA02 RHS 165 Deg	0.47745	8.10226	0.42771	7.2173	0.32475	6.13454	0.26325	4.98924	0.22744	4.04013	0.18464	3.09534	0.39833	6.29892	0.37994	4.23325	1.44236	10.219	1.53458	9.29742	1.73609	8.25968
CA01 RHS 180 Deg	0.62286	7.00582	0.59402	6.27519	0.47746	5.40434	0.37259	4.31515	0.31343	3.42397	0.26812	2.60512	0.53715	5.28032	0.48803	3.46468	1.53054	8.64012	1.62725	7.7829	1.83611	6.79616
CA02 RHS 180 Deg	0.4853	7.84975	0.43293	6.97895	0.3273	5.91285	0.27063	4.86434	0.23276	3.919	0.19682	3.02919	0.40949	6.09088	0.39875	4.19312	1.43394	9.96998	1.53701	9.09984	1.75146	8.21125

CA01 RHS - CA02RHS																						
Angle (Deg)	C0		C1		C2		C3		C4		C5		C6		C7		C11		C12		C13	
	V [mm]	W [mm]	V [mm]	W [mm]	V [mm]	W [mm]	V [mm]	W [mm]	V [mm]	W [mm]	V [mm]	W [mm]	V [mm]	W [mm]	V [mm]	W [mm]	V [mm]	W [mm]	V [mm]	W [mm]	V [mm]	W [mm]
90	0.26	-0.33	0.28	-0.27	0.24	-0.08	0.19	-0.16	0.16	-0.22	0.14	-0.20	0.24	-0.51	0.20	-0.50	0.28	-0.82	0.31	-0.86	0.34	-0.87
105	0.18	0.30	0.21	0.38	0.19	0.51	0.14	0.37	0.10	0.29	0.08	0.22	-0.40	0.05	0.15	-0.03	0.22	-0.15	0.22	-0.44	0.25	-0.59
120	0.11	0.53	0.14	0.53	0.13	0.64	0.07	0.39	0.06	0.37	0.05	0.22	0.07	0.35	0.03	0.36	0.13	0.24	0.14	0.10	0.16	-0.01
135	0.19	-0.29	0.22	-0.13	0.18	-0.04	0.15	-0.04	0.12	-0.09	0.11	-0.04	0.15	-0.39	0.12	-0.43	0.20	-0.71	0.21	-0.88	0.22	-0.91
150	0.11	-0.42	0.14	-0.30	0.13	-0.11	0.09	-0.14	0.07	-0.23	0.06	-0.18	0.08	-0.44	0.05	-0.36	0.07	-0.90	0.06	-0.98	0.05	-1.13
165	0.20	-0.41	0.22	-0.25	0.19	-0.18	0.14	-0.20	0.10	-0.20	0.08	-0.18	0.19	-0.39	0.16	-0.23	0.18	-0.75	0.19	-0.82	0.19	-1.01
180	0.14	-0.84	0.16	-0.70	0.15	-0.51	0.10	-0.55	0.08	-0.50	0.07	-0.42	0.13	-0.81	0.09	-0.73	0.10	-1.33	0.09	-1.32	0.08	-1.42

Interval	C0	C1		C2		C3		C4		C5		C6		C7		C11		C12		C13	
	W [mm]	V [mm]	W [mm]	V [mm]	W [mm]	V [mm]	W [mm]	V [mm]	W [mm]	V [mm]	W [mm]	V [mm]	W [mm]	V [mm]	W [mm]	V [mm]	W [mm]	V [mm]	W [mm]	V [mm]	W [mm]
CA01 RHS 90 Deg	7.4587	0.84111	6.58565	0.67253	5.59247	0.53146	4.3847	0.43687	3.41829	0.35778	2.55332	0.84889	5.66791	0.81068	3.76846	1.86802	9.11925	1.9747	7.9914	2.15582	6.42492
AR01 RHS 90 Deg	6.61657	0.77841	5.65122	0.48477	4.3435	0.37593	3.48848	0.31502	2.73182	0.24827	2.06736	0.97539	5.46964	0.96962	4.08312	1.60409	8.29946	1.84677	7.03516	2.08378	5.47883
CA01 RHS 105 Deg	8.0819	0.80672	7.19352	0.64023	6.10272	0.50629	4.86353	0.40832	3.83415	0.32944	2.92982	0.24703	6.28715	0.79903	4.31297	1.85314	9.89664	1.94807	8.64905	2.13842	7.05333
AR01 RHS 105 Deg	6.47232	0.6995	5.45384	0.42606	4.29694	0.33267	3.4708	0.27652	2.70386	0.22202	2.0657	0.86921	5.30611	0.86317	4.00617	1.54407	7.9961	1.75242	6.9151	1.98765	5.42803
CA01 RHS 120 Deg	8.06369	0.73235	7.18376	0.57097	6.12714	0.43767	4.80914	0.35848	3.88225	0.28853	2.88872	0.71099	6.25813	0.66916	4.26031	1.75551	9.91243	1.84955	8.77167	2.04107	7.16792
AR01 RHS 120 Deg	6.72334	0.6947	5.77318	0.42557	4.61928	0.33213	3.73676	0.27982	2.93913	0.22049	2.19559	0.84716	5.51484	0.83737	4.17831	1.50604	8.35468	1.70151	7.28083	1.93209	6.01603
CA01 RHS 135 Deg	7.64357	0.75778	6.84385	0.60336	5.83536	0.48979	4.69525	0.39567	3.70793	0.3246	2.85277	0.73701	5.89321	0.70129	3.97174	1.76357	9.41175	1.86226	8.29408	2.06579	6.90868
AR01 RHS 135 Deg	5.91186	0.71096	5.14365	0.44056	4.06579	0.36207	3.29656	0.30157	2.55099	0.24077	1.90681	0.85806	4.68194	0.84879	3.35953	1.5215	7.49812	1.72984	6.58937	1.97972	5.47301
CA01 RHS 150 Deg	7.67375	0.63222	6.86371	0.49752	5.93006	0.39688	4.75578	0.3172	3.72119	0.26294	2.86101	0.582	5.91894	0.53872	4.00856	1.6015	9.40752	1.68835	8.38546	1.87801	7.11374
AR01 RHS 150 Deg	6.52377	0.69256	5.62124	0.4416	4.60299	0.35204	3.75501	0.29407	3.02033	0.23862	2.37483	0.82362	5.19857	0.81857	3.91657	1.51663	8.22691	1.72653	7.4162	1.97348	6.4144
CA01 RHS 165 Deg	7.69392	0.64508	6.96475	0.51073	5.95768	0.4047	4.78956	0.33164	3.8356	0.26708	2.9135	0.59155	5.90432	0.54113	4.00493	1.62027	9.47268	1.72269	8.47907	1.92742	7.25384
AR01 RHS 165 Deg	6.74711	0.6363	5.89364	0.38504	4.84907	0.30947	4.01042	0.25824	3.22767	0.2085	2.53892	0.72816	5.34373	0.71556	4.11477	1.44273	8.63717	1.6473	8.01798	1.90208	7.30389
CA01 RHS 180 Deg	7.00582	0.59402	6.27519	0.47746	5.40434	0.37259	4.31515	0.31343	3.42397	0.26812	2.60512	0.53715	5.28032	0.48803	3.46468	1.53054	8.64012	1.62725	7.7829	1.83611	6.79616
AR01 RHS 180 Deg	6.45809	0.61697	5.64551	0.36965	4.59185	0.29881	3.83555	0.25786	3.08194	0.20363	2.33112	0.69739	4.98943	0.69142	3.72823	1.41793	8.33039	1.62457	7.87365	1.89093	7.3529

CA01 RHS - AR01 RHS																					
Angle (Deg)		C1		C2		C3		C4		C5		C6		C7		C11		C12		C13	
	W [mm]	V [mm]	W [mm]	V [mm]	W [mm]	V [mm]	W [mm]	V [mm]	W [mm]	V [mm]	W [mm]	V [mm]	W [mm]	V [mm]	W [mm]	V [mm]	W [mm]	V [mm]	W [mm]	V [mm]	W [mm]
90	0.84	0.06	0.93	0.19	1.25	0.16	0.90	0.12	0.69	0.11	0.49	-0.13	0.20	-0.16	-0.31	0.26	0.82	0.13	0.96	0.07	0.95
105	1.61	0.11	1.74	0.21	1.81	0.17	1.39	0.13	1.13	0.11	0.86	-0.62	0.98	-0.06	0.31	0.31	1.90	0.20	1.73	0.15	1.63
120	1.34	0.04	1.41	0.15	1.51	0.11	1.07	0.08	0.94	0.07	0.69	-0.14	0.74	-0.17	0.08	0.25	1.56	0.15	1.49	0.11	1.15
135	1.12	0.07	1.22	0.16	1.23	0.14	0.94	0.10	0.69	0.09	0.48	-0.09	0.69	-0.12	0.06	0.25	1.18	0.14	0.88	0.09	0.49
150	1.15	-0.06	1.24	0.06	1.33	0.04	1.00	0.02	0.70	0.02	0.49	-0.24	0.72	-0.28	0.09	0.08	1.18	-0.04	0.97	-0.10	0.70
165	0.95	0.01	1.07	0.13	1.11	0.10	0.78	0.07	0.61	0.06	0.37	-0.14	0.56	-0.17	-0.11	0.18	0.84	0.08	0.46	0.03	-0.05
180	0.55	-0.02	0.63	0.11	0.81	0.07	0.48	0.06	0.34	0.06	0.27	-0.16	0.29	-0.20	-0.26	0.11	0.31	0.00	-0.09	-0.05	-0.56